Scuola Universitaria Superiore IUSS Pavia

Study of the pro-inflammatory role of cytokine eNAMPT (Nicotinamide phosphoribosyltransferase) in gastrointestinal disorders and its possible therapeutic use

A Thesis Submitted in Partial Fulfilment of the Requirements
for the Degree of Doctor of Philosophy in

Biomolecular Sciences and Biotechnologies

by

Greta Cascetta

March, 2026

TABLE OF CONTENTS

ABSTRACT

Chronic immune-mediated gastrointestinal disorders such as Autoimmune Atrophic Gastritis (AAG) and Inflammatory Bowel Disease (IBD) arise from complex interactions between genetic susceptibility, environmental triggers, immune dysregulation, and alteration in mucosal homeostasis. Growing evidence identifies extracellular Nicotinamide phosphoribosyltransferase (eNAMPT) as a pivotal pro-inflammatory mediator linking these pathological processes.

This doctoral thesis aims to elucidate the contribution of eNAMPT to the pathogenesis of AAG and IBD, define the molecular regulation of NAMPT through post-translational phosphorylation, characterize its systemic effects on hematopoiesis, and evaluate the therapeutic efficacy of eNAMPT-neutralizing monoclonal antibody ALT-100 in preclinical models of intestinal inflammation.

To investigate the role of eNAMPT in AAG, in collaboration with Professor Di Sabatino from Policlinico San Matteo, gastric biopsies and patient-derived fibroblasts were analyzed. Transcriptomic profiling of gastric corpus biopsies from AAG patients revealed a markedly altered gene expression signature. Functional enrichment indicated that many of dysregulated genes are associated with fibrotic processes and extracellular matrix (ECM) remodeling. Based on these findings, gastric fibroblasts were isolated, characterized, and subjected to RNA sequencing. The analysis identified several differentially expressed genes, similarly, implicated in pro-fibrotic pathways and ECM remodeling. Finally, the impact of eNAMPT was examined; however, eNAMPT treatment elicited only minimal transcriptional and functional changes.

The involvement of eNAMPT in IBD was examined using DNBS- and DSS-induced murine models of Crohn's disease and ulcerative colitis. Recombinant eNAMPT exacerbates disease severity by intensifying mucosal injury, enhancing *lamina propria* infiltration by granulocytes and monocytes, and reshaping circulating myeloid subsets toward pro-inflammatory phenotypes. *Ex vivo* studies further showed that eNAMPT modulates bone marrow-derived hematopoietic stem cells expansion and differentiation, increases colony-forming capacity, and synergizes with cytokines such as GM-CSF to influence lineage commitment and differentiation. These findings indicate that eNAMPT functions not only as a local mucosal cytokine but also as a systemic regulator of immune cell development.

To explore the molecular determinants of NAMPT function, phosphorylation sites were mapped by LC-MS/MS, identifying eight residues with dominant phosphorylation at Ser 199, Ser 200, and Ser 472. Site-directed mutagenesis revealed distinct biological roles for these sites: $NAMPT^{S199A}$ and $NAMPT^{S200A}$ mutants showed impaired dimerization and reduced enzymatic activity, leading

to reduced cell viability and altered subcellular localization. Conversely, the NAMPT^{S472A} mutant retained enzymatic function yet completely lost cytokine-like activity, thus implicating Ser 472 as a critical determinant of receptor engagement and extracellular signaling.

Finally, the therapeutic potential of eNAMPT neutralization was evaluated using ALT-100 (Aqualung Therapeutics®), a humanized monoclonal antibody. In both DNBS and DSS colitis models, ALT-100 treatment ameliorated clinical symptoms and tissue damage. These protective effects highlight eNAMPT as a promising target for immunomodulation in chronic intestinal inflammation.

Collectively, this thesis provides an integrated mechanistic framework positioning eNAMPT at the intersection of mucosal inflammation, hematopoietic regulation, and cytokine signaling and advances the understanding of NAMPT biology, prompting eNAMPT neutralization as a promising therapeutic strategy for AAG and IBD.

ABBREVIATIONS

AAG	Autoimmune Atrophic Gastritis
APCs	Antigen-Presenting Cells
ARDS	Acute Respiratory Distress Syndrome
CD	Crohn's Disease
CCR5	C-C Chemokine Receptor Type 5
cADPRs	ADP-Ribosyl Cyclase
COPD	Chronic Obstructive Pulmonary Disease
DNBS	Dinitrobenzene Sulfonic Acid
DSS	Dextran Sodium Sulfate
EIMs	Extraintestinal Manifestations
ESR	Erythrocyte Sedimentation Rate
GWAS	Genome-Wide Association Studies
HLA	Human Leukocyte Antigen
IBD	Inflammatory Bowel Disease
IEC	Intestinal Epithelial Cell
IFN-γ	Interferon-gamma
IkB-α	Inhibitor of Kappa B alpha
JAK/STAT	Janus Kinase Signal Transducer and Activator of Transcription
MAPK	Mitogen-Activated Protein Kinase
MD-2	Myeloid Differentiation Factor 2
mAb	Monoclonal Antibody
NAD^+	Nicotinamide Adenine Dinucleotide
NAMPT	Nicotinamide Phosphoribosyltransferase
NAPRT	Nicotinic Acid Phosphoribosyltransferase
NF-kB	Nuclear Factor kappa-B
NK	Natural Killer (cell)
NLRP3	NOD-Like Receptor Protein 3
NMN	Nicotinamide Mononucleotide
NMNAT	Nicotinamide Mononucleotide Adenosyl transferase
NOD2	Nucleotide-Binding Oligomerization Domain-Containing Protein
NRK	Nicotinamide Riboside Kinase
NSAIDs	Non-Steroidal Anti-Inflammatory Drugs
PMNs	Polymorphonuclear Neutrophils
PTMs	Post-Translational Modifications
ROS	Reactive Oxygen Species
SIRTs	Sirtuins
SPR	Surface Plasmon Resonance
STAT3	Signal Transducer and Activator of Transcription 3
TFG-β	Transforming Growth Factor beta
Th	T-helper
TLR4	Toll-Like Receptor 4
TNF-α	Tumor Necrosis Factor alpha
TSLP	Thymic Stromal Lymphopoietin
UC	Ulcerative Colitis

1. INTRODUCTION

1.1 DIGESTIVE SYSTEM

The digestive system, also referred to as the alimentary canal, is a continuous, muscular tube extending from the oral cavity to the anus. This system facilitates the passage of ingested food, its digestion, nutrient absorption, and the elimination of waste products. Anatomically, it comprises in sequence: the mouth, the esophagus, and the gastrointestinal tract (GI) along with both primary and accessory digestive organs. Indeed, the term GI specifically encompasses the stomach, the small and large intestine, and the anal canal, as well as accessory organs including the liver, the gallbladder, and pancreas (Fig. 1). These digestive organs, located within the abdominal cavity, are held in place by the peritoneum, a broad serous membranous sac. The peritoneum consists of a layer of simple squamous epithelial cells supported by an underlying connective tissue matrix. It is structurally differentiated into two distinct regions: the parietal peritoneum, which lines the inner surface of the abdominal wall, and the visceral peritoneum, which envelops and supports the abdominal organs. The space enclosed between these two layers, termed the peritoneal cavity, contains a small volume of serous fluid that serves as a lubricant, and serves as a conduit for blood vessels, lymphatics, and nerves.

Functionally, each component of the digestive system plays a crucial and specialized role: the stomach initiates chemical digestion; the small intestine serves as the principal site for nutrient absorption, and the large intestine is responsible for water reclamation and compaction of waste material. Collectively, the GI ensures the provision of essential nutrients and energy required for survival and growth. Nevertheless, its importance extends over digestion. Because of its direct contact with the external environment, through food, drink and even air particles that we ingest, it represents a potential entry point for pathogens and toxins. To counter this, the GI houses a large proportion of the body's immune system, protective secretion as mucous and a diverse microbiota acting as a barrier and a defense system [1,2].

The oral cavity (mouth) constitutes the initial segment of the digestive tract and performs multiple functions that are essential to both digestion and host defense. Its principal roles include the assessment of food quality prior to ingestion and swallowing, mediated by the taste buds present on the tongue; mechanical digestion, achieved through the action of teeth,

tongue and palatal surface; and limited chemical digestion facilitated by the enzymatic components of saliva. Furthermore, the oral cavity contributes to immunological defense and protection through the presence of numerous antimicrobial agents present in saliva and tonsils [3].

The esophagus is a muscular conduit, approximately 25 cm in length in adults, whose primary function is the transport of food from the oral cavity to the stomach with the pharynx acting as a passageway. The esophageal wall comprises two distinct layers of muscle fibers, one arranged longitudinally and the other circularly. The upper one-third of the esophagus consists primarily of skeletal (striated) muscles which are controlled by the voluntary nervous system and allows voluntary initiation of the swallowing process. The middle-third contains a mixture of skeletal and smooth muscle fibers, representing a transitional zone between voluntary and involuntary regulation. The lower one-third is composed predominantly of smooth muscle controlled by the enteric nervous system.

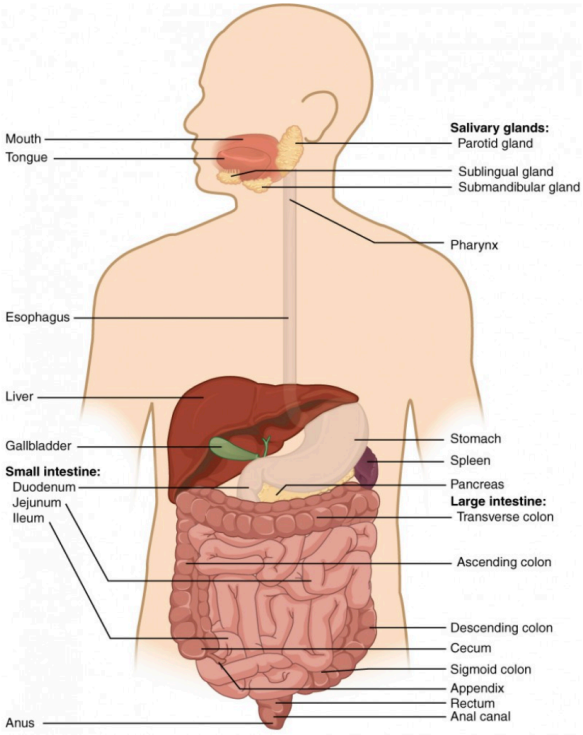

Figure 1. Overview of the human digestive system. Schematic representation of the major organs and accessory structures of the human digestive system. The illustration shows the sequential organization of the alimentary canal from the mouth to the anus, including the pharynx, esophagus, stomach, small intestine (duodenum, jejunum, ileum), and large intestine (cecum, colon, rectum, anal canal). Accessory organs such as the salivary glands, liver, gallbladder, and pancreas are also depicted. These structures collectively contribute to the mechanical and chemical processes of digestion, absorption, and waste elimination (Adapted from OpenStax, Anatomy and Physiology, 2nd edition, 2022).

Peristalsis, a coordinated wave like muscular contraction, allows food passage along the esophagus. During this process, the circular muscle fibers contract behind the bolus to constrict the lumen, while the longitudinal muscle fibers contract ahead of the bolus to shorten and widen the corresponding segment. Notably, the only voluntary phase of swallowing is the buccal phase, which activates primary peristalsis in the upper esophagus. This peristaltic wave then continues downwards under involuntary control, transporting the bolus toward the stomach [4,5].

1.2 THE STOMACH – PHYSIOLOGICAL CHARACTERISTICS

Once food enters the stomach, it undergoes temporary storage, mechanical disruption, and chemical digestion through the combined action of muscular contractions and gastric secretions. The stomach's capacity for food storage derives from its high degree of distensibility and anatomical flexibility, allowing it to expand significantly to accommodate ingested material. Anatomically, the stomach extends approximately from vertebrate T7 to L3, providing substantial volumetric capacity for food retention [6]. The stomach's mechanical processing of food is facilitated by its complex muscular architecture, which consists of three distinct layers: an inner oblique layer, a middle circular layer, and an outer longitudinal layer. The coordinated contraction and relaxation of these muscular layers enable mixing and churning movements, which are essential for chyme formation. Simultaneously, chemical digestion occurs through the activity of gastric glands, which contain parietal cells, chief cells, G cells, foveolar cells, and mucous neck cells, which secrete acids and enzymes necessary for nutrient breakdown [7,8]. The final product of these coordinated mechanical and chemical processes is the chyme, which is gradually released into the small intestine through the pyloric sphincter for further digestion and nutrient absorption.

1.2.1 STOMACH ANATOMY

The stomach represents the most distensible segment of the gastrointestinal tract and is situated intraperitoneally. It occupies the left hypochondriac region, the epigastrium, and partially the umbilical and left lumbar regions. Macroscopically is divided into four regions: the cardia represents the superomedial portion continuous with the esophagus through the cardias; the fundus projects superiorly to the gastroesophageal junction and, together with the left margin of the esophagus forms the angle of His; the body (corpus) constitutes the

largest and most distended part of the organ, delimited by the lesser and greater curvatures, at the level of the angular incisure, the lesser curvature bends sharply to the right, marking the distal boundary of the gastric body; distally the pyloric portion, consisting of the antrum and the pyloric canal, terminates with the pyloric sphincter which opens into the duodenum [9] (Fig. 2A).

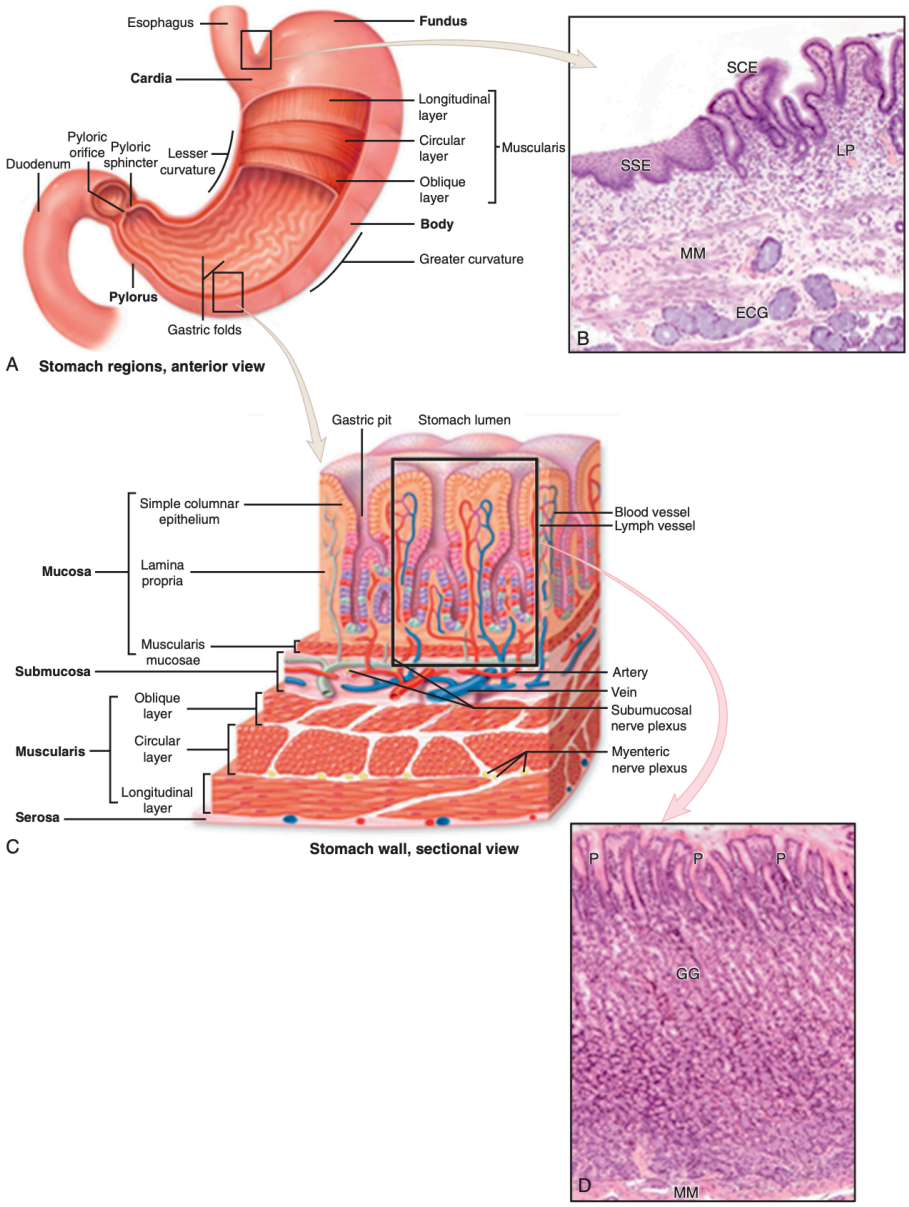

Figure 2. Structural organization and histological features of the stomach. (**A**) Anterior view of the stomach displaying its major anatomical and muscular regions. (**B**) Transition from stratified squamous epithelium (SSE) of the esophagus to simple columnar epithelium (SCE) characteristic of the proximal stomach. (**C**) Transversal section of the stomach wall illustrating its different layers: mucosa, submucosa, *muscularis*, serosa. (**D**) Histological section of the gastric mucosa demonstrating the relationship between the gastric pits (P) and gastric glands (GG), inferiorly delimited by the muscularis mucosae (MM) (Rickesha L. Wilson, Christina E. Stevenson, Anatomy and physiology of the stomach Chapter 56, pages 634-646, 2019).

At the microscopic level, as well as the other components of the alimentary tract, the stomach is organized in four distinct layers, proceeding from the lumen outward: mucosa, submucosa, *muscularis externa*, and serosa (Fig. 2C). The mucosa is lined by simple columnar epithelium comprising mucous secreting cells and is structured into gastric pits. At the base of these pits, stem cells undergo active proliferation to replenish the superficial epithelial cells that are continuously shed into the chyme. This regenerative mechanism ensures rapid replacement of epithelial cells if gastric acid or digestive enzymes breach the protective mucosal barrier, thereby maintaining mucosal integrity [(9)].

Beneath the epithelium extends the *lamina propria*, which contains the gastric glands. Both within the gastric pits and the gland themselves, multiple populations of secretory cells can be identified. The submucosal layer is composed of dense connective tissue and encompasses nerves, blood vessels, and lymphatic vessels, being externally delimited by the *muscularis externa* (Fig. 2D). Finally, the serosal layer consists of several strata of connective tissue that establish continuity with the peritoneum [(9,10)].

1.2.2 CELLULAR AND MOLECULAR BASIS OF GASTRIC FUNCTION

From the anatomo-functional standpoint, the gastric mucosa can be subdivided into two distinct regions: the oxyntic and the antral-pyloric region. The oxyntic region, comprising the proximal two-thirds of the stomach (fundus and corpus), is primarily dedicated to exocrine secretion. Within the oxyntic glands, parietal cells predominate and secrete hydrochloric acid (HCl), bicarbonate ions (HCO_3^-), intrinsic factor, and ghrelin. Chief cells are responsible for the synthesis and release of pepsinogen and leptin, while enterochromaffin-like (ECL) cells produce histamine. Conversely, the antral-pyloric region is mainly involved in endocrine secretion, particularly the release of gastrin by G cells [(11)].

Mucous neck cells, which are ubiquitously distributed throughout the gastric mucosa, are characterized by an apical cytoplasm enriched in hydro-soluble mucins that act as lubricants for gastric contents. Hence, the stomach is not solely an acid-secreting organ but also produces a range of protective regulatory factors. Mucus and bicarbonate form a critical defensive barrier preserving the gastric epithelium from the aggressive acid-peptic environment [(12)]. Moreover, trefoil factors (TFFs), secreted by surface mucous cells, exert anti-inflammatory effects, and promote mucosal restitution following injury [(13,14)].

Ghrelin acts as an orexigenic peptide, stimulating gastric emptying, acid secretion, and histamine release [(15)]. In contrast, leptin functions as a satiety hormone and modulates

immune and inflammatory processes [16]. Pepsinogen, the inactive precursor of pepsin, exists in two molecular forms: type I, secreted exclusively by chief cells in the oxyntic mucosa, and type II, synthesized throughout the entire gastric mucosa [17,18].

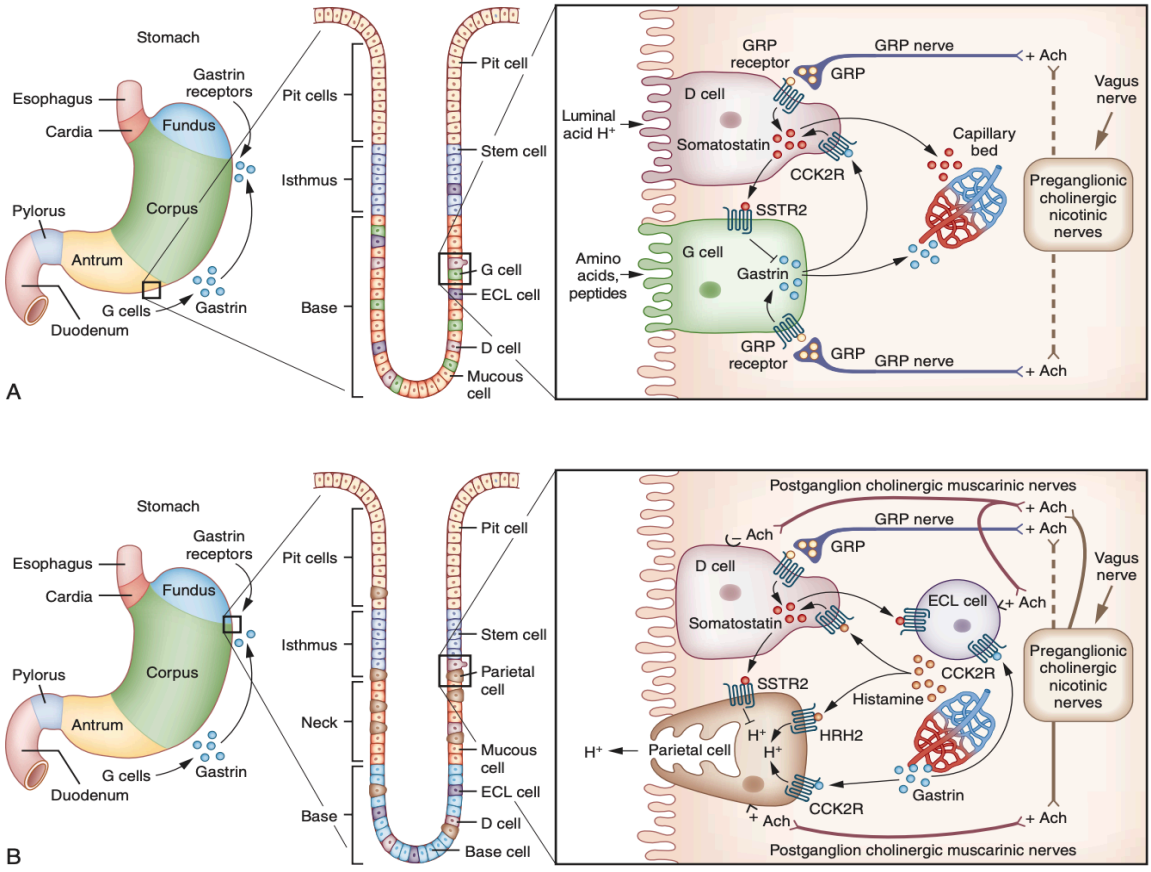

Figure 3. Gastrointestinal hormones. Integrated signaling among D cells, G cells, enterochromaffin-like (ECL) cells, and parietal cells in the antrum and fundus of the stomach regulates gastric acid secretion. (**A**) In the antrum, gastrin-releasing peptide (GRP) stimulates G cells to secrete gastrin, while D cells release somatostatin, which provides inhibitory feedback. (**B**) In the fundus, gastrin enters the circulation and acts on CCK2 receptors located on ECL and parietal cells. Activation of these receptors promotes histamine release from ECL cells and hydrochloric acid secretion from parietal cells, facilitating protein denaturation during digestion (Gerald Litwack, Chapter 7 - Gastrointestinal hormones, Academic Press, 2022).

Intrinsic factor is essential for the absorption of vitamin B_{12} in the distal ileum [19]. Gastrin not only regulates the gastric phase of acid secretion but also exerts trophic effects on parietal and ECL cells; its release is stimulated by dietary proteins and inhibited by gastric acidity and somatostatin [20]. Somatostatin directly modulates acid secretion, being primarily stimulated by antral acidification, while acetylcholine released from vagal efferent suppresses its secretion. Histamine, stored in secretory granules of ECL cells and resident mast cells, is released upon stimulation by gastrin, acetylcholine, or epinephrine, whereas

somatostatin acts as an inhibitory signal (Fig. 3). Collectively, acetylcholine, gastrin, and histamine finely regulate HCl secretion by parietal cells. Hydrochloric acid plays a fundamental role in the absorption of mineral micronutrients. It promotes solubilization of insoluble calcium salts through the formation of calcium chloride, which is readily absorbed in the duodenum and jejunum [21], also facilitates the release of inorganic iron (Fe^{3+}), a process enhanced by the synergistic action of ascorbic acid present in the gastric lumen [22], and is required for the release of vitamin B_{12} [23]. Finally, HCl exerts an antimicrobial function, contributing to the prevention of intestinal colonization by pathogenic environmental microorganisms.

Considering its physiological relevance, the release of HCl into the gastric lumen represents a finely tuned interplay of mediators that, through interaction with their respective receptors in the parietal cell, initiate a cascade of reactions leading to the activation of protein kinases. Gastrin binds to the CCK2R receptor, while acetylcholine interacts with M3 receptors to stimulate phospholipase C via G-protein-mediated mechanism. Phospholipase C converts membrane phospholipids into inositol triphosphate, which induces the release of intracellular calcium (Ca^{2+}) [24,25]. Histamine, through binding to the H2 receptor, activates adenylate cyclase, leading to the production of cyclic adenosine monophosphate (cAMP). The increase in intracellular levels of Ca^{2+} and cAMP results in the activation of protein kinases. Conversely, inhibition of parietal cell secretion by somatostatin occurs through both G-protein-dependent and independent mechanisms, although its suppressive action is thought to be primarily mediated by the inhibition of adenylate cyclase [26].

These kinases trigger a phosphorylation cascade that ultimately terminates activating the H^+/K^+-ATPase proton pump. The H^+/K^+-ATPase (adenosine triphosphatase) is an enzyme composed of a catalytic α-subunit and a glycoprotein β-subunit [27]. The cytoplasmic tail of the β-subunit contains a four-amino acid sequence homologous to tyrosine-based endocytosis signals, which is essential for pump internalization and termination of acid secretion.

Once assembled in the endoplasmic reticulum of the parietal cells, the enzyme is processed in the Golgi apparatus and transported to the plasma membrane as a heterodimeric oligomer [28]. Under resting conditions, proton pumps are stored in intracellular vesicles and translocate to the apical membrane only in response to secretory stimulation [29]. The enzyme utilizes ATP hydrolysis to undergo conformational changes necessary for its secretory function. This process occurs through a phosphorylation-dephosphorylation cycle that alters the orientation of the ion-binding sites [30]. Thus, the parietal cells secrete H^+ ions in

exchange for extracellular K^+ in an electroneutral exchange, maintaining the transmembrane potential difference [31]. Chloride ions (Cl^-) are released into the gastric lumen through specific channels, while dedicated efflux channels maintain low intracellular K^+ concentrations, enabling continuous H^+/K^+ exchange [32].

1.3 THE INTESTINE – PHYSIOLOGICAL CHARACTERISTICS

Following the stomach, the intestine constitutes the subsequent major segment of the gastrointestinal tract, where the processes of digestion, absorption, and waste formation are completed. This organ plays a pivotal role in maintaining metabolic homeostasis through the assimilation of nutrients and the conversion of non-digested residues into material destined for secretion. The intestine is a hollow organ of the digestive system, which exerts both endocrine and exocrine functions producing hormones, enzymes, and alkaline mucinous material [33]. It is anatomically and functionally divided into two principal regions: the small intestine, in which digestion is finalized, and nutrient absorption occurs, and the large intestine, primarily devoted to the reabsorption of water and electrolytes, as well as to the compaction and formation of fecal matter [34,35]. Like other hollow organs of the GI, the intestinal wall is organized into several concentric layers. From the innermost to the outermost, these include the mucosa, comprising the epithelial lining, *lamina propria* and a thin layer of smooth muscle termed the *muscularis mucosae*, followed by the submucosa, the *muscularis externa*, and finally the serosa (Fig. 4). The mucosa is responsible for effective secretion, absorption, and local mucosal motility. Beneath the mucosa lies the submucosa, a dense connective tissue layer that anchors the mucosa to the muscular coat and contains blood and lymphatic vessels and submucosal glands. The *muscularis externa* is typically arranged into inner circular and outer longitudinal layers of smooth muscle whose coordinated contractions produce peristalsis and segmentation, thus promoting the propulsion and mechanical breakdown of luminal contents. The outermost serosa consists of a mesothelial layer supported by loose connective tissue and covers the intraperitoneal segments of the canal [36].

Although the intestine exhibits this fundamental four-layered architecture throughout its length, the small and large intestine display region-specific structural adaptations that reflect their distinct functional roles.

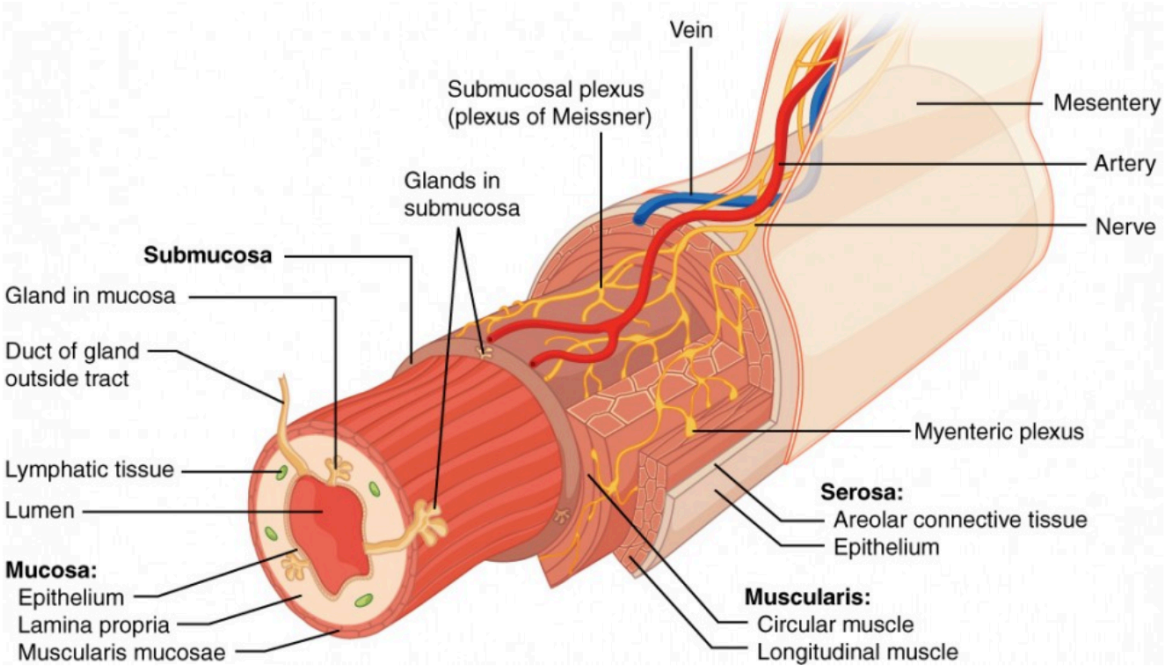

Figure 4. Histological organization of the intestinal wall. The intestinal wall is composed of four principal layers, each with distinct structural and functional roles. From the lumen outward, the intestine is composed of the mucosa, containing epithelium, lamina propria, and *muscularis mucosae*; the submucosa; the *muscularis externa*; and the serosa (Anatomy and Physiology II, module 7: The Digestive System).

1.3.1 ANATOMY AND FUNCTION OF THE SMALL INTESTINE

The small intestine extends from the pylorus to the ileocecal valve, typically measures about 6 to 7 meters in length, and is subdivided into three regions: the duodenum, jejunum, and ileum. It exhibits an exceptionally large absorptive and secretory surface area owing to the presence of circular folds, villi, and epithelial cells equipped with microvilli, which project into the intestinal lumen to maximize efficiency in nutrient uptake and enzymatic activity [34,37]. The duodenum is the initial C-shaped segment of the small intestine, directly continuous with the pylorus and connecting distally to jejunum and ileum. Functionally, the duodenum continues the digestive processes initiated in the stomach by receiving chyme through the pyloric sphincter [38]. Digestion in this segment is facilitated by intestinal enzymes and secretions, as well as by bile from the liver and gallbladder and pancreatic juices delivered via the major and minor duodenal papillae. The papillae are associated with the sphincter of Oddi, which prevents reflux of duodenal contents into the biliary and pancreatic ducts [39]. The jejunum constitutes the second segment of the small intestine,

extending from the duodenojejunal junction to the ileum. It serves as the primary site for the absorption of the end products of carbohydrate, lipid, and protein digestion, including passive calcium uptake. Nutrient absorption is facilitated by numerous fingerlike mucosal projections, the villi, each one to two cells thick, which expand the absorptive surface to approximately 13 m^2. Microvilli on the apical surface of jejunal enterocytes provide the primary site for nutrient uptake [40]. The ileum represents the terminal portion of the small intestine, measuring approximately 3 meters in length and extending from the jejunum to the cecum. While maintaining the same fundamental structural organization as the more proximal segments, the ileum exhibits gradual environmental and morphological transitions, including slower luminal transit, and shorter, broader villi with reduced digestive enzymatic activity. By the time the intestinal contents reach this region, most absorbable nutrients have been depleted, and the ileum assumes specialized absorptive functions, notably the uptake of vitamin B_{12} and the reabsorption of bile acids [41].

1.3.2 ANATOMY AND FUNCTION OF THE LARGE INTESTINE

The unabsorbed and undigested remnants of chyme leaving the ileum pass through the ileocecal junction to enter the large intestine. The large intestine is about 2 meters and comprises the cecum, colon, and rectum and terminates at the anal canal. The colon itself is subdivided into ascending, transverse, descending, and sigmoid portions. The ascending colon functions primarily in the absorption of residual water and electrolytes from indigestible material, thereby contributing to the progressive solidification of fecal matter. The descending colon serves predominantly as a storage segment, retaining feces prior to defecation [42]. Through rhythmic contractions, the sigmoid colon increases intraluminal pressure and facilitates the propulsion of fecal content into the rectum, which acts as a temporary reservoir for feces. Unlike the small intestine, the large intestine lacks villi, reflecting its reduced absorptive function. Instead, it is characterized by deeper intestinal crypts and a higher density of goblet cells, which secrete mucus to ensure effective lubrication and protection of the mucosal surface [37], omental appendices, haustra, and *taeniae coli* (Fig. 5).

The colon exhibits two primary types of motilities: haustral contractions and mass movements. Haustral contractions, triggered by the presence of chyme, slowly advance and mix the contents within individual sacculations, facilitating water and electrolyte absorption. Mass movements are stronger, propelling chyme rapidly toward the rectum [43]. Water

absorption occurs osmotically, driven by active sodium uptake, with potassium and chloride exchanged according to electrochemical gradients. The colon also supports a dense microbial community that ferments undigested material and synthesizes essential vitamins, including vitamin K and several B vitamins [44,45], which are subsequently absorbed. Through these processes, the colon not only completes fluid and electrolyte homeostasis but also contributes to nutrient provision and gut microbial balance.

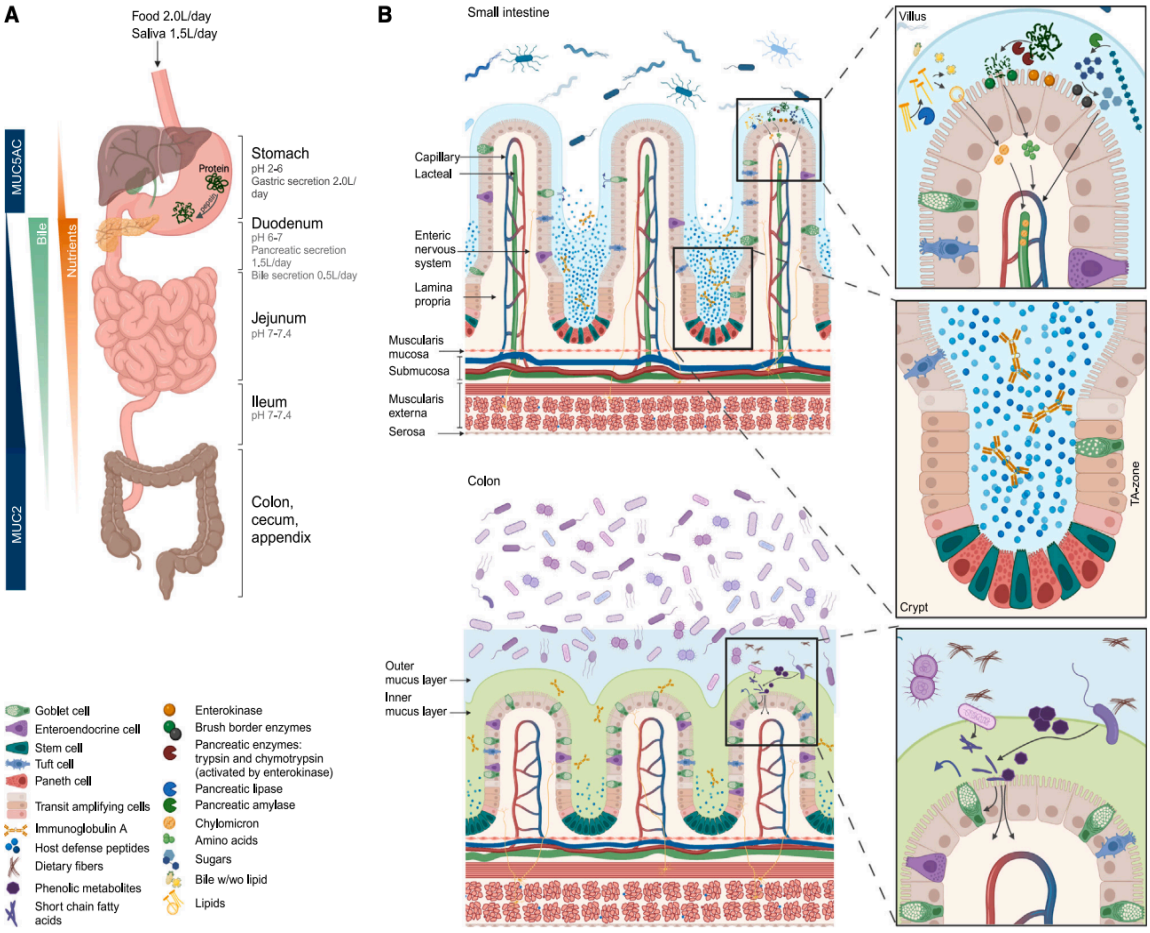

Figure 5. Structural and functional distinctions between the small intestine and colon. (**A**) Overview of the gastrointestinal tract. (**B**) Differences between the small intestine and colon: the small intestine is characterized by villi and a continuous mucus layer that maximize nutrient absorption, with proximal regions specialized for lipid uptake via lacteals and efficient carbohydrate and protein digestion, crypts contain Paneth cells that secrete host defense peptides to maintain epithelial integrity; in contrast, the colon lacks villi, exhibits deeper crypts, and possesses a dense inner mucus layer and a loosely attached outer layer, which provides a niche for mucolytic microbiota (Jensen BAH et al., 2023).

1.4 ROLE OF MICROBIOTA

Over the past two decades, human gastrointestinal (GI) microbiota has emerged as a key determinant of health and disease, profoundly influencing digestion, immunity, and metabolic regulation. Once regarded as a passive collection of commensal organisms, the microbiota is now recognized as a dynamic and metabolically active ecosystem that interacts intimately with the host across distinct anatomical niches of gastrointestinal tract. Although the intestinal microbiota has been extensively studied, growing evidence highlights the unique and underappreciated roles of microbial communities residing in the upper GI tract, including the stomach. These microbial populations differ markedly in composition, density, and functional capacity from those of the distal intestine, yet their contributions to nutrient transformation, immune modulation, and mucosal homeostasis are becoming increasingly evident.

1.4.1 GASTRIC MICROBIOTA

The discovery of *Helicobacter pylori* (*H. Pylori*), first isolated from gastric biopsies in 1982 by Warren and Marshall, revolutionized the understanding of the stomach as a microbiologically active organ. Previously considered sterile due to its high acidity, the stomach is now recognized as a dynamic ecological niche hosting diverse microbial community [46]. Recent studies indicate that gastric mucosa plays a central role in immune regulation, coordinating both innate and adaptive responses to preserve microbial balance and mucosal integrity [47,48,49]. These interactions hold pharmacological relevance, as they influence the host response to drugs, microbial metabolism of xenobiotics, and the efficacy of therapies targeting gastric and systemic diseases.

The gastric microbial load (10^2-10^4 CFU/ml) is markedly lower than that of the intestine (10^{10}-10^{12} CFU/ml) due to the acidic environment, which restricts but does not eliminate bacterial survival [50,51]. While *H. pylori* remains the best-characterized gastric bacterium, the stomach hosts a complex microbiota comprising hundreds of phylotypes [52,53,54,55]. In 2006, Bik and colleagues performed a 16S rRNA-based analysis of human gastric biopsies, identifying *Proteobacteria, Firmicutes, Bacteroides, Actinobacteria,* and *Fusobacteria* as dominant phyla. Despite substantial interindividual variability, the presence of *H. pylori* did not significantly alter the overall microbial composition. Subsequent studies confirmed that *H. pylori* affects species richness and evenness without modifying the broader taxonomic diversity [56,57].

Although similarities between gastric and oronasal microbiota initially suggested a transient community, subsequent sequencing-based investigations revealed a distinct gastric microbial profile, supporting the existence of a resident ecosystem [50,54]. This microbiota likely contributes to nutrient metabolism, mucosal protection, and immunomodulation.

1.4.2 INTESTINAL MICROBIOTA

While the stomach represents a unique but relatively low-density microbial niche, the intestine hosts the most diverse and metabolically active microbial ecosystem in the human body. The intestinal microbiota is composed of arche, eukaryotes, viruses, parasites, and bacteria [58]. Among these, the bacterial community is the most extensively studied, with *Bacteroides* and *Firmicutes* representing the predominant phyla. These microorganisms thrive in the intestinal environment and perform key protective, metabolic, structural, and neuroactive functions [59,60].

The intestinal microbiota is established at birth, evolves in parallel with its host, and is influenced by multiple factors including long-term dietary habits, social and behavioral practices, antibiotic exposure, stress, and pathological conditions [60,61]. Successful colonization of the intestine requires microorganisms to possess specific enzymatic repertoires for nutrient metabolism, surface molecules that facilitate adhesion, and mechanisms to evade bacteriophages and the host immune system [60]. Each compartment of the intestinal tract hosts a distinct microbial community. In the duodenum, *Firmicutes* and *Actinobacteria* are the dominant phyla. In the jejunum, Gram-positive species and facultative anaerobes prevail [62]. Toward the ileum, aerobic species become more abundant, whereas near the ileocecal valve, Gram-negative anaerobes predominate [60]. Along the entire small intestine, both microbial density and diversity progressively increase, reaching their peak in the colon, which is dominated by anaerobic bacteria, primarily *Firmicutes* and *Bacteroidetes* [63]. Intestinal microbiota is essential to host protection through the synthesis of bioactive metabolites, including tryptophan derivatives and polyamines generated from arginine metabolism. These compounds enhance mucosal protection and modulate inflammation [64,65]. Moreover, its structural function is closely linked to its protective role, as both are essential for maintaining intestinal barrier integrity. Certain probiotic strains have been shown to increase the expression of tight junction proteins in intestinal epithelial cells, thereby reducing permeability and preventing the uncontrolled translocation of pathogens or pro-inflammatory molecules into the systemic circulation [66].

1.5 THE GASTRIC AND INTESTINAL IMMUNE SYSTEM

Given the substantial load of microbial antigens in the gastric and intestinal lumen, the host must generate immune responses that are both protective and tolerogenic. Therefore, the mucosal defense system functions as a distinct immunological compartment, largely independent of systemic immunity, capable of protecting the epithelium against pathogens while maintaining tolerance to dietary and commensal antigens.

1.5.1 GASTRIC IMMUNE REGULATION

The relationship between the gastric microbiota and the immune system is reciprocal and complex. Immune activity shapes microbial community composition, while microbial infection can disrupt the equilibrium between inflammatory and tolerogenic responses, contributing to the onset of gastric diseases [67].

The gastric mucosa functions as a specialized immune organ; although the stomach lacks a dedicated mucosa-associated lymphoid tissue (MALT), it contributes actively to immune defense through both innate and adaptive mechanisms (Fig. 6). The gastric mucosa contains abundant $CD4^+$ T cells expressing high levels of integrin α4β7, which facilitates migration to mucosal tissues [68,69,70]. Gastric epithelial cells play a central role in mucosal immunity by interacting directly with macrophages and dendritic cells, promoting T and B cell activation, and secreting cytokines such as IL-6, IL-8, TNF-α, IL-1α/β, GM-CSF, MCP-1 and TFG-β in response to infection or tissue injury [71,72,73]. These epithelial cells also express MHC II molecules, enabling antigen presentation and contributing to the regulation of local immune responses [74,75,76]. Recognition of microbial components occurs through pattern recognition receptors (PRRs) that detect pathogen-associated molecular patterns (PAMPs), initiating signaling cascades leading to cytokine and chemokine production and activation of Th1 and Th2 immune pathways [77,78,79]. Recruitment of macrophages, dendritic cells, and natural killer (NK) cells into the *lamina propria* is mediated by chemokines, while infection also induces $CD8^+$ T cell activation and cytotoxic responses [80,81]. A critical link between innate and adaptive immunity is provided by innate lymphoid cells (ILCs). Studies in human and murine gastric mucosa indicate a predominance of ILC2s, typically associated with allergic and chronic inflammatory responses, whereas ILC1s and ILC3s, important for epithelial repair and antitumor defense, are less represented [82,83,83,83,86].

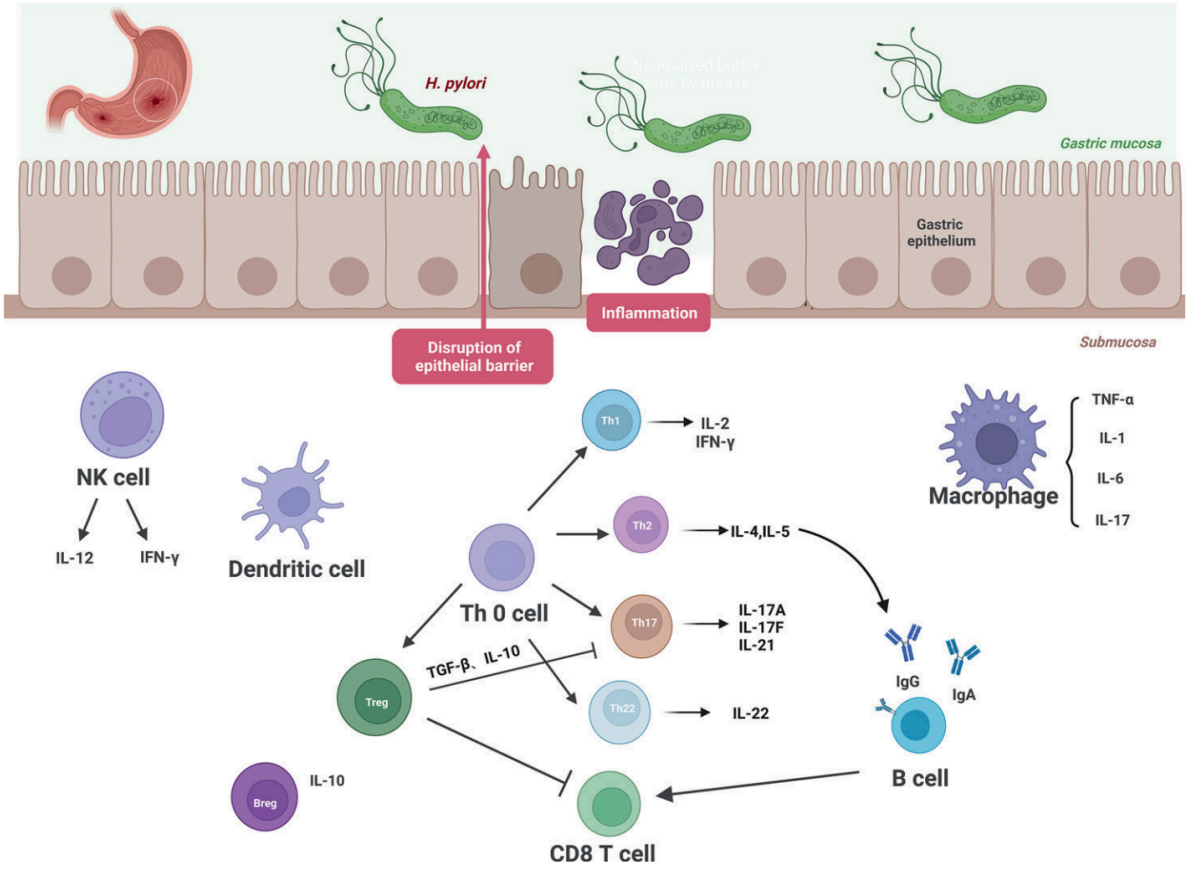

Figure 6. Immune system of gastric mucosa. Innate immunity involves NK cells, macrophages, dendritic cells (DCs), and innate lymphoid cells (ILCs), while adaptive immunity includes $CD4^+$ and $CD8^+$ T cells, differentiating into Th1, Th2, Th17 and Treg subset, and B cells that produce IgA, IgG, and IgM. Gastric epithelial cells also contribute by recognizing pathogen-associated molecular patterns (PAMPs) via pattern recognition receptors (PRRs), releasing cytokines and chemokines, and presenting antigen through MHC II to activate $CD4^+$ T cells (Zhou M. et al.,2024).

1.5.2 THE INTESTINAL BARRIER AND ITS IMMUNOLOGICAL ROLE

The intestinal mucosa represents a highly specialized barrier that prevents microbial translocation while enabling controlled interactions between luminal antigens and the host immune system, thereby preserving epithelial integrity and immunological homeostasis [87,88]. This defense relies on the coordinated action of physical, chemical, and immunological components.

The mucus layer constitutes the first line of defense against luminal microorganisms and antigens. It is primarily composed of mucins secreted by goblet cells and differs along the gastrointestinal tract: in the small intestine, it forms a single gelatinous layer, whereas in the colon it is organized into two strata: an outer, loose layer that supports commensal

colonization and an inner, dense layer that limits microbial contact with the epithelium. It also contains antimicrobial peptides and secretory IgA, which contribute to mucosal protection [89]. Beneath the mucus, the epithelial barrier consists of tightly connected cells joined by tight junctions, adherent junctions, and desmosomes that regulate paracellular permeability and tissue cohesion [88,90]. Among epithelial subtypes, Paneth cells secrete antimicrobial peptides such as defensins and lysozyme, while M cells mediate antigen sampling and presentation to dendritic cells [91]. The *lamina propria* hosts both innate and adaptive immune cells [92]. Recognition of microbe-associated molecular patterns (MAMPs) by PRRs, including TLRs and NLRs, triggers cytokine-driven signaling that coordinates immune responses [88]. Within the innate compartment, dendritic cells capture luminal antigens, migrate to mesenteric lymph nodes, and induce adaptive responses while promoting tolerance toward commensal bacteria [93,94].

The adaptive immune system is mainly composed of T lymphocytes and plasma cells. Tregs secrete IL-10 and TGF-β to maintain tolerance and prevent immune overactivation, whereas effector T cells produce pro-inflammatory cytokines essential for pathogen clearance [95,96]. Plasma cells, derived from B cells, secrete IgA, which neutralizes pathogens and modulates microbiota composition, contributing to immune equilibrium [97] (Fig. 7).

The metabolic and protective functions of the intestinal microbiota are closely interconnected. Undigested carbohydrates are fermented by intestinal microbes, producing short-chain fatty acids (SCFAs) such as acetate, propionate, and butyrate. These metabolites bind to specific receptors (GPR41, GPR43, and GPR109A) on epithelial and immune cells, activating diverse signaling pathways [98]. Butyrate induces the production of TGF-β and IL-10, promotes epithelial repair, activates regulatory T cells (Treg), and suppresses inflammation by inhibiting the NF-kB signaling pathway [60,99]. Acetate enhances the secretion of IgA and mucus, thereby strengthening the mucosal barrier [100], whereas propionate, together with butyrate, activates Tregs and reduces the production of pro-inflammatory cytokines such as IL-6 and IL-12 [101].

Together, these interconnected components ensure effective mucosal defense and immune regulation, maintaining a balance between tolerance and inflammation critical for intestinal homeostasis.

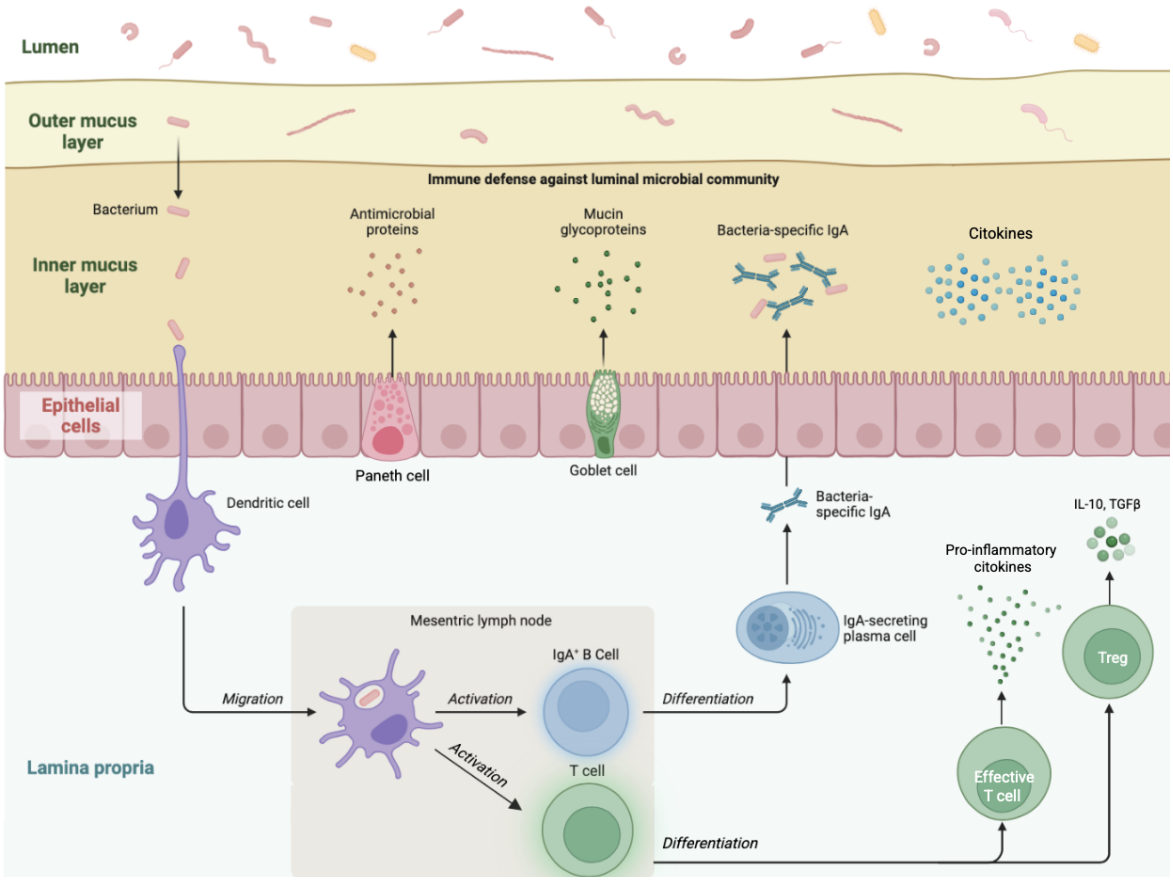

Figure 7. Intestinal mucosal barrier and immune system. The figure illustrates the key components of the intestinal barrier and their roles in immune protection against the luminal microbiota. The mucus layer, composed of mucins from goblet cells and antimicrobial peptides from Paneth cells, prevents microbial adhesion to the epithelium. The epithelial layer includes Paneth cells, which secrete antimicrobial proteins, and goblet cells. In the *lamina propria*, dendritic cells sample luminal antigens and migrate to mesenteric lymph nodes, activating T cells and IgA^+ B cells. These cells differentiate into effector T cells, regulatory T cells (Tregs), and IgA-secreting plasma cells, which release bacteria-specific IgA to maintain microbial balance. Cytokines such as IL-10 and TGF-β regulate immune tolerance, ensuring homeostasis between host defense and commensal microorganism (adapted from Hooper et al., 2010).

1.6 IMMUNOPATHOGENESIS AND CLINICAL PERSPECTIVES IN GASTROINTESTINAL DISEASES

Gastrointestinal diseases represent a heterogeneous group of disorders that affect the structure and function of the digestive system, with significant implication for global morbidity and quality of life. After upper respiratory tract infection, acute gastroenteritis is the most common illness in the United States [102]. These conditions encompass a broad spectrum, ranging from functional disturbances to chronic inflammatory and autoimmune processes that compromise the integrity of gastrointestinal mucosa. Among these disorders, Autoimmune Atrophic Gastritis (AAG) and Inflammatory Bowel Disease (IBD) exemplify chronic, immune mediated conditions of the gastrointestinal tract.

In recent decades, advances in immunology, molecular biology, and microbiome research have greatly enhanced our understanding of the complex interplay between genetic predisposition, environmental factors, and immune responses that support gastrointestinal pathology. Despite these advances, many aspects of the pathogenesis and progression of gastrointestinal disorders remain incompletely understood.

This chapter explores key concepts in gastrointestinal immunopathology, with a focus on reviewing the current state of the art on AAG and IBD.

1.6.1 AUTOIMMUNE ATROPHIC GASTRITIS (AAG)

Since 1973, two major forms of chronic gastritis have been distinguished: Autoimmune Atrophic Gastritis (Type A), restricted to the gastric body, PCA positive, associated with severe achlorhydria, vitamin B_{12} deficiency, hypergastrinemia, and reduced serum pepsinogen I; and Multifocal Atrophic Gastritis (Type B), caused by HP infection, progressing slowly from the antrum and body, characterized by PCA negativity and low gastrin levels.

Autoimmune Atrophic Gastritis (AAG) is a chronic, non-self-limiting inflammatory disorder that affects the oxyntic mucosa, leading to progressive mucosal atrophy [103,104,105,106,107]. This topographic restriction reflects the localization of parietal cells, which constitutes the main target of the autoimmune response [108,109,110]. Specifically, AAG results from immune-mediated destruction of parietal cells triggered by anti-parietal cell antibodies (PCA), which recognize subunits of the gastric H^+/K^+-ATPase proton pump. The inflammatory process appears to be mediated by autoreactive T lymphocytes, although the

exact initiating factor remains unknown [111].

The global prevalence of AAG has been estimated between 0.5% and 4.5% [112], with an annual incidence of approximately 25 new cases per 100.000 individuals [113,114]. Women are affected up to three times more frequently than man, and the disease predominantly occurs in individuals over 60 years of age with reported increased incidence in the 35-45 age range [112,115], and more recently in pediatric patients aged between 8 months and 18 years [116,117,118].

1.6.1.1 AAG SYMPTOMS

A major challenge associated with AAG is its substantial diagnostic delay, as most patients remain asymptomatic until the onset of anemia or neurological manifestations, while others present with nonspecific dyspeptic symptoms. This diagnostic lag contributes to significant impairment in quality of life and the development of irreversible, potentially life-threatening complications [119]. Clinically, AAG manifestations are often nonspecific and mild, especially in early stages prior to the development of micronutrient deficiencies. When present, symptoms primarily involve the gastrointestinal, neurological, hematopoietic, and cardiovascular systems [111].

Gastrointestinal symptoms, the most common complaint, include dyspepsia, non-acid gastroesophageal reflux with heartburn and regurgitation, epigastric pain, bloating, and abdominal distension, all resulting from impaired digestion and motility [120,121,122,123]. Achlorhydria and hypergastrinemia may delay gastric emptying, causing postprandial fullness or early satiety, with potential consequences on eating habits, nutritional status, and small intestinal bacterial overgrowth [124,125].

In 2016, Tenca et al. reported that 58% of AAG patients exhibited psychological alterations, which could evolve into depressive or anxiety-related states. Neurological manifestations primarily result from vitamin B_{12} deficiency. Common findings include myelopathy with or without associated neuropathy, cognitive impairment, optic neuropathy, and paresthesia, all stemming from spongiform degeneration and demyelination within the spinal cord, leading to axonal degeneration and gliosis. Neuropsychiatric symptoms encompass memory decline, personality changes, psychosis, and delirium [126]. Vitamin B_{12} deficiency is also associated with infertility, recurrent spontaneous miscarriage, assisted reproduction failure, pregnancy complications, and neural tube defects in the newborn [127,128,129,130].

Anemia and micronutrient deficiencies cause fatigue, reduced concentration, brittle nails

and hair, and delayed wound healing. In advanced stages, dyspnea, headache, and tachycardia may occur, while in elderly patients, chest pain and palpitations are also reported [131,132].

AAG is also recognized as a preneoplastic condition, associated with an increased risk of developing type I gastric neuroendocrine tumors (NETs), due to persistently elevated gastrin-17 levels, leading first to ECL cell hyperplasia, progressing through dysplasia to neoplasia via a multistep process [133,134,135], and a threefold higher risk of developing gastric adenocarcinomas (GA) [136,137] compared with the general population.

1.6.1.2 ETIOPATHOGENESIS OF AAG

Genetic predisposition plays a relevant role in AAG. Up to 16.5% of patients have a first-degree relative with the disease, and approximately 30% of relatives show circulating PCA [138,139,119]. PCA production follows a hereditary pattern consistent with an incompletely penetrant dominant, non-Mendelian model [140,141].

Two pivotal studies identified specific HLA haplotypes as predisposing factors: HLA-DRB104, DQB103, and DRB103 [142,143]. These class II HLA alleles are involved in the presentation of exogenous antigens to $CD4^+$ T cells, and are associated with other autoimmune disorders, including type I diabetes mellitus, celiac disease, systemic lupus erythematosus, and multiple sclerosis [144].

The primary autoantigen recognized by PCA is the gastric H^+/K^+-ATPase proton pump. Although PCA serve as diagnostic markers, they do not play a direct pathogenic role.

In 1970 Tanaka et al. demonstrated that administration of PCA from AAG patients to rats induced marked parietal cell loss without gastric mucosal inflammation.

Ex vivo studies revealed that the H^+/K^+-ATPase proton pump is also the target of autoreactive Th1 and cytotoxic T cells present in AAG gastric mucosa. Approximately 25% of $CD4^+$ T cell clones from the gastric body of AAG patients proliferated in response to porcine proton pump and produced TNF-α, promoted immunoglobulin production by B cells, expressed perforin-mediated cytotoxicity against antigen-presenting cells, and induced Fas-Fas ligand-mediated apoptosis in target cells [145]. Recently, Troilo et al. reported that 20% of $CD4^+$ T cell clones from AAG gastric mucosa were directed against intrinsic factor, predominantly Th1 or Th17 (94%), producing TNF-α and IL-21 and stimulating immunoglobulin secretion by B cells.

The frequent detection of *Helicobacter pylori* (HP) in individuals with gastric autoimmunity

suggests a potential triggering role [146,111]. According to Amedei et al., in genetically predisposed subjects, HP may activate cross-reactive $CD4^+$ T cells that recognize both gastric ATPase and HP antigens, though not the bacterium's dominant proteins (CagA, VacA, or urease). These cross-reactive peptides induced T-cell proliferation and a Th1 cytokine profile. HP infection also alters the gastric microbiota: reduced bacterial abundance and diversity are observed in HP-related atrophic gastritis, whereas patients with AAG display a microbiota composition more like healthy controls [147].

1.6.1.3 INFLAMMATORY AND IMMUNOMODULATORY CYTOKINES IN AAG

In AAG, aberrant production of cytokines, immune cells, and infiltrating intracellular material contribute to direct injury of gastric parietal cells. The primary immune cells involved include $CD4^+$ and $CD8^+$ T lymphocytes, Th1, Th2, Th17, and Treg subset, B cells, mast cells, dendritic cells, macrophages, and NK cells. Associated cytokines include IL-6, IL-8, IL-9, IL10, IL-13, IL-15, IL-17, IL-21, IL-27, IFN-γ, TNF-α, TSLP, and eNAMPT [148,149] (Fig. 8).

Ex vivo studies on gastric biopsies from AAG patients have demonstrated elevated TNF-α and IL-15 levels compared to healthy controls [150]. TNF-α contributes to epithelial injury and is associated with gastric cancer risk, while IL-15 promotes Ig production, $CD4^+$ and $CD8^+$ T cells proliferation, and NK cells activation, favoring apoptosis [151,152].

Reduced IL-33 levels have also been reported, suggesting a role in atrophy and adenocarcinoma; IL-33 acts as an alarmin with protective effects but can induce IL-13 secretion from ILC2, promoting intestinal metaplasia and M2 macrophage polarization [153,154,155].

IFN-γ is another key mediator of parietal cell atrophy and metaplasia. In murine TxA23 models, IFN-γ knockout prevents metaplasia [156]. IFN-γ, primarily produced by $CD8^+$ T cells, synergizes with IL-17 from Th17 cells to trigger inflammation via ROS and NLRP3 inflammasome activation [157,148]. IL-17A induces apoptosis in gastric organoids, and its neutralization reduces atrophy and metaplasia in murine AAG models [158].

IL-21 also plays a central role in disease progression by regulating T and B cells through JAK/STAT, MAPK, and PI3K pathways.

Comparative studies indicate elevated IL-6 and IL-8 even in *H. pylori* negative atrophic gastritis, with IL-6 mediating epithelial-macrophage interactions in tumorigenesis and IL-8 recruiting neutrophils that induce oxidative stress and mucosal injury [159,160].

Extracellular Nicotinamide phosphoribosyltransferase (eNAMPT), which will be described in detail in chapter 1.8, has recently emerged as a key pro-inflammatory mediator in AAG. Gastric biopsies from AAG patients secrete higher eNAMPT levels, which induce IFN-γ and IL-6 production in organoid cultures, amplifying mucosal immune responses [150]. Conversely, anti-inflammatory mediators protect the gastric mucosa. Treg cells suppress autoimmune responses via IL-10 and TGF-β, reducing disease severity in murine AAG models [161]. IL-10 inhibits inflammatory cytokines synthesis, while TGF-β supports Treg function and suppresses autoreactive T and Th17 cells [162,163,149]. IL-27 exhibits protective effects in murine models, reducing atrophy and metaplasia, but may also enhance INF-γ and IL-17 production [158,148] (Fig. 8).

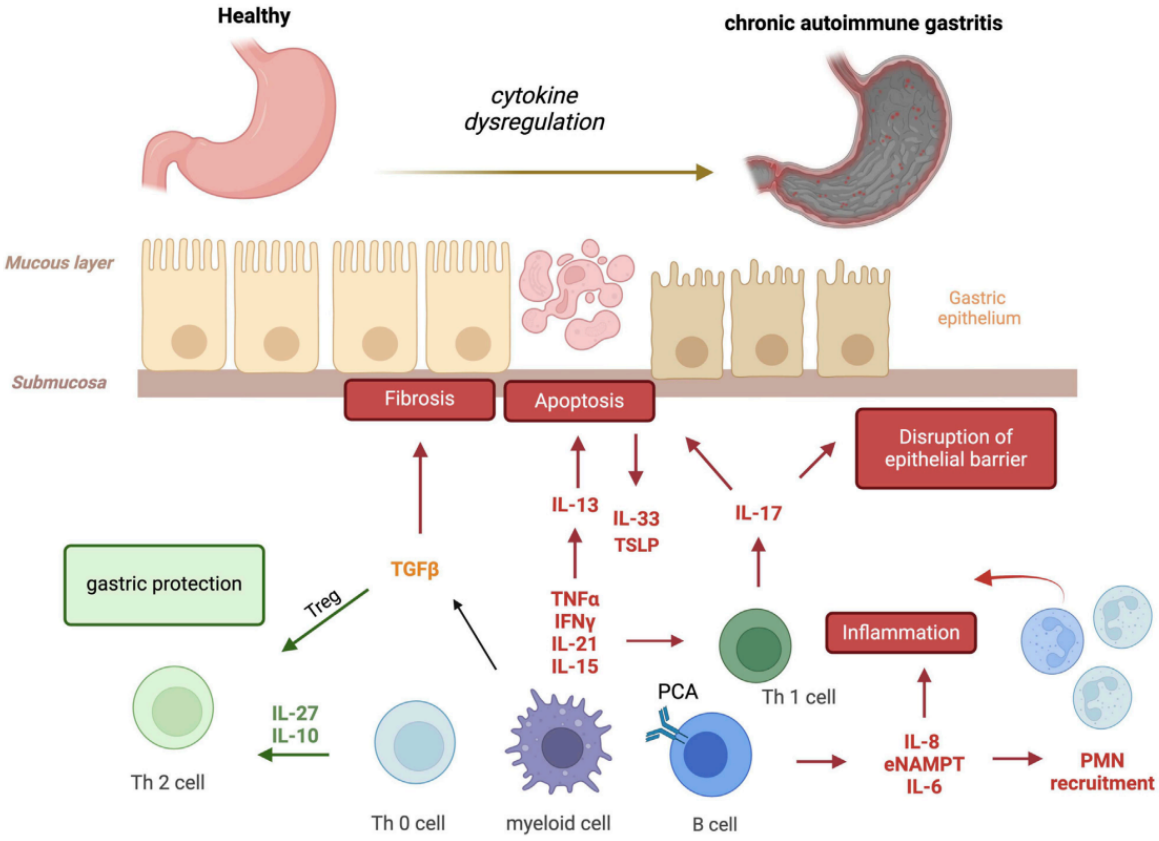

Figure 8. Immune mediators of AAG. Cytokines, immune cells, and infiltrating intracellular components contribute to direct damage to gastric parietal cells. Key immune cells include $CD4^+$ and $CD8^+$ T lymphocytes, Th1, Th2, Th17, Treg, B cells, mast cells, dendritic cells, macrophages, and natural killer cells. Associated cytokines comprise IFN-γ, TNF-α, IL-21, IL-15, TGF-β, IL-27, IL-10, IL-13, IL-33, TSLP, IL-17, IL-8, eNAMPT, IL-6, and PMNs (Cascetta et al., 2024).

Overall, AAG reflects a complex interplay of pro- and anti-inflammatory cytokines that orchestrate mucosal damage, immune regulation, and potential preneoplastic changes, highlighting the critical role of cytokine networks in disease pathogenesis.

1.6.2 INFLAMMATORY BOWEL DISEASE: Ulcerative Colitis and Crohn's Disease

Inflammatory bowel diseases (IBD) comprise a heterogenous group of chronic, relapsing, and progressive disorders of the gastrointestinal tract, mainly represented by Crohn's disease (CD) and ulcerative colitis (UC). These conditions are characterized by persistent intestinal inflammation, alternating period of remission and relapse, mucosal injury, microbial dysbiosis, and various systemic and biochemical abnormalities [164,165]. IBD represents one of the most prevalent gastrointestinal disorders worldwide. Since its initial description in the early twentieth century, both incidence and prevalence of CD ad UC have increased markedly, particularly in industrialized nations such as those in North America, Europe, Australia, and New Zealand [166,167]. According to the Global Burden of Disease (GBD) 2019 report, approximately five million individuals are currently affected by IBD, with around 400.000 new cases diagnosed each year [167]. IBD affects both sexes and may occur at any age, although the peak incidence is typically observed in early adulthood [168]. Mortality rates in IBD vary depending on disease subtypes and comorbidities. Epidemiological studies have shown increased mortality in patients with CD, mainly due to colorectal cancer, cardiovascular and respiratory diseases [169,170], whereas UC does not appear to significantly increase overall mortality [171,172].

1.6.2.1. IBD CLINICAL FEATURES

IBD presents a wide spectrum of intestinal and extraintestinal manifestations, contributing to diagnostic delays and therapeutic challenges [173,174]. The most common intestinal symptoms include chronic diarrhea, abdominal pain, rectal bleeding, and weight loss [175,176]. Symptoms distribution differs between CD and UC: in UC, pain is typically localized in the lower left abdomen, and associated with bloody diarrhea, whereas CD often causes right lower quadrant pain with less frequent rectal bleeding. Intestinal obstruction due to wall thickening is a frequent complication in CD, often accompanied by nutrient malabsorption and nutritional deficiencies [177].

In addition, IBD is considered a systemic condition due to the high prevalence of extraintestinal manifestation (EIMs), reported in 25-40% of patients [167]. These commonly affect the joints, skin, eyes, and hepatobiliary tract, but may also involve the liver, lungs, and pancreas. EIMs can occur either before or after the intestinal onset, preceding gastrointestinal symptoms in about 26% of patients [178]. They may appear concomitantly with intestinal inflammation or independently, often exerting a more profound impact on

quality of life than intestinal symptoms themselves [179]. The presence of EIMs may influence treatment decisions and therapeutic response [180,181], and their frequency seems higher in early-onset disease or in younger individuals, although this association remains debated [182].

1.6.2.2 ETIOLOGY AND PATHOGENESIS OF IBD

The etiology of IBD remains multifactorial and not yet completely understood. Current evidence supports the concept that these disorders result from a complex interplay among genetic susceptibility, environmental influences, intestinal dysbiosis, and immune dysregulation, none of which alone is sufficient to induce disease [183,184].

Genetic predispositions represent one of the major risk factors for IBD development. Genome-wide association studies (GWAS) have identified over 200 genetic loci associated with disease susceptibility [183,184,185], including 30 specifics for CD, 23 for UC, and 28 shared between both [186,168]. In 2001, Ogura et al. identified NOD2 as the first gene associated with CD. Upon ligand binding, NOD2 activates the NF-kB signaling pathway, inducing TNF and IL-12 production, as well as antimicrobial peptides [167]. NOD2 stimulation also promotes autophagy, modulating bacterial clearance and antigen presentation, and supports immune tolerance [187,188,189,168]. Also, mutations in ATG16L1, another key autophagy gene, contribute to immune dysfunction in IBD. The T300A variant, associated with CD, reduces the ability of epithelial and dendritic cells to eliminate intracellular pathogens and present antigens to $CD4^+$ T cells [187]. IL23R, encoding the IL-23 receptor subunit, is also implicated in both UC and CD by modulating Th17-mediated inflammatory responses. The Arg381GIn variant has been identified as protective, reducing receptor signaling and downstream inflammation [188,167]. Finally, HLA gene polymorphisms, such as rs2395185 and rs2097432, have been associated with greater disease severity, need for surgical intervention, and EIM occurrence [190].

In recent years, the increasing prevalence of IBD in industrialized countries highlights the crucial contribution of environmental factors [175]. Smoking remains one of the most significant environmental modifiers: it increases the risk of CD and its extraintestinal complication while exerting a protective effect in UC [179,191,192]. This dual role likely reflects differences in receptor expression along the intestinal tract and the effects of nicotine and carbon monoxide on immune modulation [193].

Dietary habits also influence disease pathogenesis. Diets rich in animal fats, refined

carbohydrates, emulsifiers, and additives, but poor in fibers, vitamins, fruits, and vegetables, can compromise intestinal barrier function, alter microbiota composition, and promote inflammatory processes [194,192,191]. Antibiotic exposure, particularly to metronidazole and fluoroquinolones, has been linked to increased CD risk by reducing microbial diversity and stability [192,191]. Additional environmental contributors include viral infections, psychological stress, use of oral contraceptives and NSAIDs, alcohol consumption, surgeries such as appendectomy and tonsillectomy, and vitamin D deficiency [195,196]. Air pollution, particularly exposure to nitrogen dioxide (NO_2) and sulfur dioxide (SO_2), has also been associated with a higher risk of CD and UC [197].

Loss of intestinal homeostasis is a hallmark of IBD pathogenesis [198]. Patients exhibit reduced commensal bacteria and increased potentially pathogenic species [199,200,201], leading to epithelial barrier dysfunction and enhanced intestinal permeability [202,203]. It remains unclear, however, whether dysbiosis is a cause or a consequence of inflammation [204]. Other microbial domains also contribute to disease pathogenesis. Bacteriophages influence bacterial composition and virulence [167,205], while fungal dysbiosis, characterized by increased *Candida albicans* and reduced *Saccharomyces cerevisiae*, has been reported in both CD and UC [206,207]. Protozoa such as *Blastocystis* and *Diantemoeba fragilis* are decreased, facilitating pathogenic colonization and inflammation [208,209]. Within the Archea domain, *Methanobrevibacter smithii* correlates with remission [210,167].

1.6.2.3 IMMUNE DYSREGULATION IN IBD

Immunological dysregulation plays a central role in IBD pathogenesis. Under physiological conditions, the adaptive immune response maintains tolerance to commensal microbiota while defending against pathogens. In IBD, this balance is disrupted, leading to excessive activation of immune cells and overproduction of pro-inflammatory cytokines [167] (Fig. 9).

The intestinal barrier and antigen-presenting cells (APCs) are key regulators of immune homeostasis. Disruption of epithelial cells (IECs) permits microbial translocation, triggering dendritic cells and macrophages activation with secretion of TNF, INF-γ, and multiple interleukins (IL-1β, IL-6, IL-8, IL-12, IL-18, IL-23) [211,191,167].

IL-1β exacerbates tissue injury and sustains inflammation through IL-17 and IFN-γ release by T cells and innate lymphoid cells [212]. IL-23 induces IFN-γ production via STAT4 activation in memory T cells [213] and stimulates Th17 cytokine synthesis [214]. Together, IL-23 and IFN-γ promote cytotoxic molecules release by NK cells [215,191].

CD is predominantly associated with a Th1-driven immune response characterized by elevated IFN-γ and TNF following IL-12 stimulation, whereas UC exhibits a Th2-type response marked by increased IL-13, IL-4, and IL-5 [216]. Th17 cells contribute to both forms by secreting IL-17A and IL-21 [217]. High mucosal IL-17A levels have been detected in both CD and UC [218,219], promoting monocytes and neutrophils recruitment [220]. Overexpression of IL-21 further confirms Th17 involvement in IBD pathogenesis [221,222].

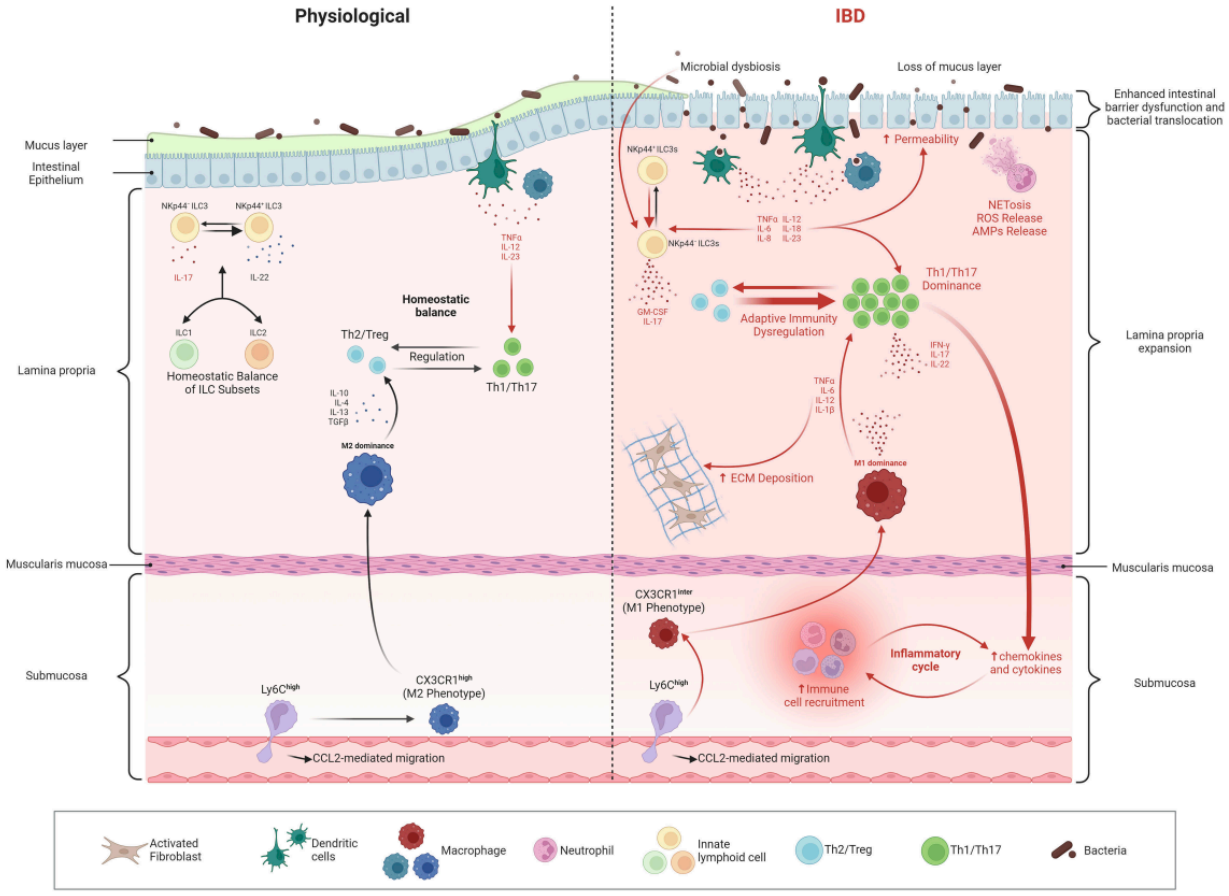

Figure 9. Immune dysregulation in IBD. In the normal gut (left), balanced Th2/Treg and Th1/Th17 responses, anti-inflammatory cytokines (IL-10, TGF-β), and stable ILC subsets maintain epithelial integrity. In IBD (right), microbial dysbiosis, mucus loss, and increased permeability drive dominant Th1/Th17 activity, excessive antigen presentation, and neutrophil NETosis. Macrophages shift to a pro-inflammatory M1 phenotype, promoting fibrosis, while dysregulated ILC3s overproduce IL-17 and IL-22, sustaining epithelial injury and chronic inflammation (de Mattos BR et al., 2015).

1.6.2.4 CROHN'S DISEASE

Crohn's Disease (CD) is a chronic, relapsing inflammatory bowel disease characterized by discontinuous, transmural granulomatous inflammation that can affect any segment of the gastrointestinal tract, from the mouth to the anus, and may also involve extraintestinal organs [223,224]. The disease most frequently affects both the terminal ileum and the colon (approximately 50% of cases), followed by isolated involvement of the small intestine (about 30%) or the colon alone (around 20%). Perianal complications, such as fissures, abscesses, and fistulas, occur in roughly one-quarter of patients, while upper gastrointestinal or extraintestinal manifestations are less common [225] (Fig. 10).

Clinically, three major phenotypes are recognized: inflammatory, stenosing, and penetrating (fistulizing). The inflammatory subtype is defined by mucosal inflammation in the absence of obstructions or fistulas, which may progress to the fibro-stenotic form due to chronic submucosal thickening and fibrosis. Persistent transmural inflammation can also lead to penetrating disease, with fistula formation between intestinal loops or adjacent organs such as the bladder, vagina, or skin. Patients may present overlapping features, and a gradual transition from the inflammatory to the stenosing or penetrating phenotype is common [225].

Crohn's disease patients present chronic diarrhea, abdominal pain, weight loss, fatigue, and low-grade fever. Diagnosis relies on a comprehensive evaluation combining clinical presentation with laboratory, endoscopic, histological, and radiological data.

Among histopathological features, non-caseating granulomas are considered characteristic of CD, although they are identified in less than one-quarter of cases [226,227].

From a pathophysiological perspective, CD results from an inappropriate immune response to intestinal microbiota in genetically predisposed individuals. The inflamed mucosa is infiltrated by $CD4^+$ and $CD8^+$ T cells, B cells, monocytes, and NK cells, guided by integrins and adhesion molecules such as MAdCAM-1. Extracellular matrix remodeling, mediated by MMP-1 and MMP-3, facilitates leukocytes infiltration and tissue injury [228,164]. Cytokines dysregulation plays a central role in disease perpetuation, with increased levels of IL-12, IFN-γ, TNF-α, IL-23, and IL-34 promoting Th1/Th17 immune polarization, whereas IL-25 expression is reduced and inversely correlated with inflammation [229,164].

1.6.2.5 ULCERATIVE COLITIS

Ulcerative colitis (UC) is a chronic inflammatory bowel disease primarily affecting the colon, typically initiating in the rectum and extending continuously to proximal segments

[230,231]. The inflammatory process is confined to the superficial layers of the intestinal wall, namely the mucosa and submucosa, and is histologically characterized by features such as cryptitis and crypt abscesses [168]. A sharp demarcation often separates inflamed mucosa from apparently normal tissue, although microscopic alterations can also be present in macroscopically unaffected areas [232,233]. Unlike CD, ulcerations in UC develop exclusively within inflamed mucosa [234] (Fig. 10). Over time patients may experience complications such as benign strictures, intestinal dysmotility, and anorectal dysfunction [230].

The Montreal classification categorizes UC according to the extent of the inflammation: proctitis (E1) if limited to the rectum, left-sided colitis (E2) if involving up to the rectosigmoid colon, and extensive colitis (E3) if extending beyond the splenic flexure. Population studies report variable disease distribution: proctitis (30-60%), left-sided colitis (16-45%), and extensive colitis (14-35%) [235].

Clinically, UC follows a relapsing-remitting course with periodic exacerbations [236], and disease onset age influences severity, with later-onset cases generally exhibiting milder manifestations [237]. Risk factors for severe disease include age at onset below 40 years, pancolitis, incomplete endoscopic healing during clinical remission, and deep ulcerations [238]. Disease activity is stratified into four stages: remission, mild, moderate, and severe, assessed via clinical indices (Mayo, Lichtiger, SCCAI), endoscopic scores (Mayo, UCEIS), and histological indices (Robarts, Nancy) [234,231].

Although the precise pathogenesis of UC remains incompletely understood, it is widely accepted to result from a complex interplay between host genetic predisposition and environmental factors, triggered by events compromising the intestinal barrier, altering microbiota composition, and inducing aberrant immune responses [165].

UC is distinguished from CD by the central role of colonic epithelial cells and mucosal barrier integrity [231]. Dysregulation involves reduced PPAR-γ expression, defects in endoplasmic reticulum stress responses, alteration in trefoil factors, and goblet cell depletion, contributing to impaired barrier function [239,89]. Immune involvement includes neutrophils accumulation, dendritic cells activation, and innate lymphoid cell-mediated cytokines production, particularly IL-17A, IL-22, and IL-23 [240,241]. Adaptive immunity features a Th2-mediated response, with $CD34^+$ Th9 cells producing IL-9, which inhibits tissue repair and promotes TNF-α expression [242,231].

Clinically, UC patients commonly present diarrhea and hematochezia, as well as tenesmus, fatigue, nocturnal bowel movements, and abdominal cramps, with pain being less pronounced than in CD. Severity correlates with disease extent, and extraintestinal

manifestations occur in approximately one-third of patients, most frequently peripheral arthritis, primary sclerosing cholangitis, and pyoderma gangrenosum [178]. Diagnosis relies on symptom assessment, endoscopic and histological evaluation, and exclusion of alternative etiologies [234]. Stool analysis is recommended to rule out concurrent infections, while blood tests can reveal anemia, leukocytosis, thrombocytosis, hypoalbuminemia, or elevated inflammatory markers [234,243].

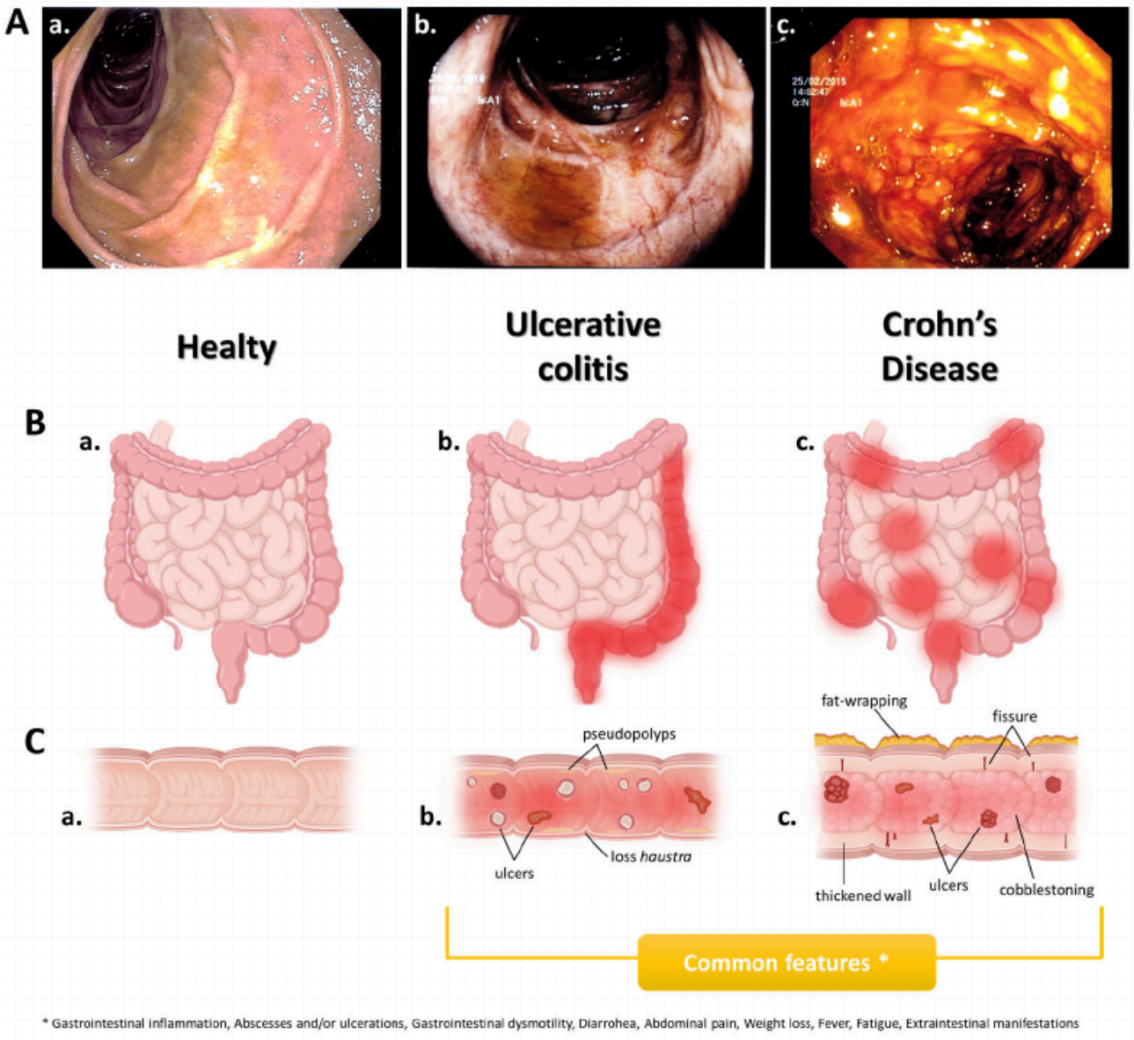

Figure 10. Intestinal morphology in healthy intestine, UC, and CD. Macroscopic and microscopic differences between the healthy intestine and the inflamed mucosa in UC and CD. (**A**) Endoscopic images show normal mucosa with intact folds and vascular pattern (a), diffuse mucosal inflammation with ulceration typical of UC (b), and discontinuous, transmural inflammation with deep ulcers and cobblestoning characteristic of CD (c). (**B**) Schematics illustrate inflammation patterns: continuous and limited to the colon in UC (b) versus segmental, transmural, and anywhere in the GI tract in CD (c), compared to normal bowel (a). (**C**) Cross-sections show structural changes: UC (b) involves mucosa/submucosa with ulceration, pseudo-polyps, and loss of haustra; CD (c) shows transmural inflammation with wall thickening, fissures, fat wrapping, and cobblestoning. Both IBD subtypes commonly cause inflammation, ulceration, diarrhea, abdominal pain, weight loss, fatigue, fever, and extraintestinal complications (Amodeo et al., 2023).

1.6.2.6 BONE MARROW-GUT AXIS IN INTESTINAL INFLAMMATION

Recent studies have revealed a strong link between intestinal inflammation and bone marrow hematopoiesis. Using a DSS-induced murine model of acute colitis, Sezaki et al. demonstrated that acute inflammation triggers the expansion of long-term hematopoietic stem cells (LT-HSCs) and multipotent progenitors (MPP2/MPP3) in the bone marrow. These populations exhibit a myeloid-biased differentiation, leading to increased common myeloid progenitors (CMPs) and reduced common lymphoid progenitors (CLPs) [244,245]. The concurrent accumulation of hematopoietic stem and progenitor cells (HSPCs) in the spleen and peripheral blood suggests activation of extramedullary hematopoiesis.

This response is mediated by innate immune signaling through Toll-like receptors (TLRs) and the interleukin-1 receptor (IL-1R), activated by bacterial components such as LPS from commensal Bacteroides [246,244]. Pro-inflammatory cytokines including GM-CSF, IL-1, interferons, and IL-6 further promote myeloid differentiation at the expense of lymphoid lineages. Importantly, HSPCs migrate from the bone marrow to inflamed mesenteric lymph nodes (MLNs), where they proliferate and differentiate into $Ly6C^+/Ly6G^+$ myeloid cells with immunosuppressive and tissue-repairing functions. Depletion of these cells exacerbates colitis symptoms, highlighting their protective role [247,244].

Overall, intestinal inflammation activates an inter-organ gut-bone marrow communication axis that drives myeloid-biased hematopoiesis to support tissue regeneration. However, chronic inflammation appears to impair HSC self-renewal and disrupt hematopoietic balance, a process that remains incompletely understood [248].

1.7 CURRENT THERAPIES

At present, no specific therapy exists to prevent, reverse, or restore the histopathological alterations characteristic of AAG. Consequently, clinical management primarily focuses on correcting nutritional deficiencies resulting from impaired gastric secretory function. Early diagnosis is of primary importance, as it allows timely initiation of micronutrients supplementation and the establishment of an appropriate endoscopic follow-up to monitor potential neoplastic complications [249,111]. In accordance with the European MAPS (Management of Precancerous Conditions and Lesions in the Stomach) guidelines, endoscopic surveillance with histological confirmation is recommended every 3-5 years, with shorter intervals advised for patients presenting intestinal metaplasia or a family history

of gastric cancer [250].

Similarly, no curative therapy is currently available for inflammatory bowel diseases (IBD), and treatment strategies are aimed at inducing and maintaining remission. The therapeutic goals extend beyond symptom control to include endoscopic healing, prevention of long-term complications, and improvement in patients' quality of life [251]. Pharmacological management relies on several classes of drugs capable of modulating the dysregulated immune response, including aminosalicylates, corticosteroids, immunomodulators, and biological agents [252]. However, treatment response is highly variable and often transient, with loss of efficacy observed after an initial favorable outcome [253,254,255].

1.7.1 THERAPEUTIC APPROACHES IN AAG

Management of AAG primarily relies on lifelong vitamin B_{12} supplementation to correct pernicious anemia and prevent neurological complications. Early intervention is crucial, as delayed treatment may result in irreversible neuronal damage [256]. Iron-deficiency anemia frequently coexists with B_{12} deficiency due to chronic mucosal inflammation and impaired gastric secretion. Oral iron preparations are generally effective and well tolerated, whereas intravenous formulations or transfusions are reserved for severe cases [257,111].

Acid-suppressive therapy with proton pump inhibitors (PPIs) is commonly used to alleviate dyspeptic symptoms but is generally inappropriate in AAG, as it may worsen hypochloridria and exacerbate hypergastrinemia, thereby promoting enterochromaffin-like (ECL) cell hyperplasia [258,259]. H2 receptor antagonists such as famotidine are considered safer alternatives and may also exert anti-inflammatory effects. Adjunctive agents including sucralfate and rebamipide can enhance mucosal protection by stimulating bicarbonate secretion, prostaglandin synthesis, and tissue regeneration, while reducing oxidative stress [260]. Current research is focused on targeted strategies addressing the immunopathogenesis of AAG. Conventional immunosuppressive agents, such as corticosteroids or azathioprine, have shown limited efficacy and are unsuitable for long-term use [261,262]. Novel therapeutic approaches aim to deliver locally acting anti-inflammatory molecules directly to the oxyntic mucosa, thereby reducing inflammation and preventing progression to atrophy and intestinal metaplasia [249]. Advances in gastric stem cell biology suggest that regulating stem cells differentiation and proliferation may contribute to mucosal regeneration and mitigate neoplastic transformation [263,264].

At the molecular level, several proinflammatory cytokines, such as IL-6 TNF-α, INF-γ, IL-

13, IL-17, and eNAMPT, have been implicated in the immune-mediated destruction of parietal cells. These mediators represent promising pharmacological targets for novel immunomodulatory therapies, including monoclonal antibodies designed to inhibit key cytokine pathways [111]. Although no targeted biological treatments are currently available, the development of cytokine- and cell-based interventions represents a major frontier in the management of AAG.

1.7.2 THERAPEUTIC MANAGEMENT OF IBD

Therapeutic management of IBD generally follows either a step-up or top-down strategy. The step-up approach begins with less aggressive agents such as aminosalicylates or corticosteroids, escalating immunosuppressant, biologics, or small molecules in refractory cases or to achieve steroid-free remission. Conversely, the top-down approach recommends early administration of high-efficacy therapies in patients with poor prognostic indicators. The therapeutic choice depends on disease severity, localization, subtype, prior response, and clinical features such as age at onset, extent of intestinal involvement, and extraintestinal manifestations [265,266,267,268] (Fig. 11).

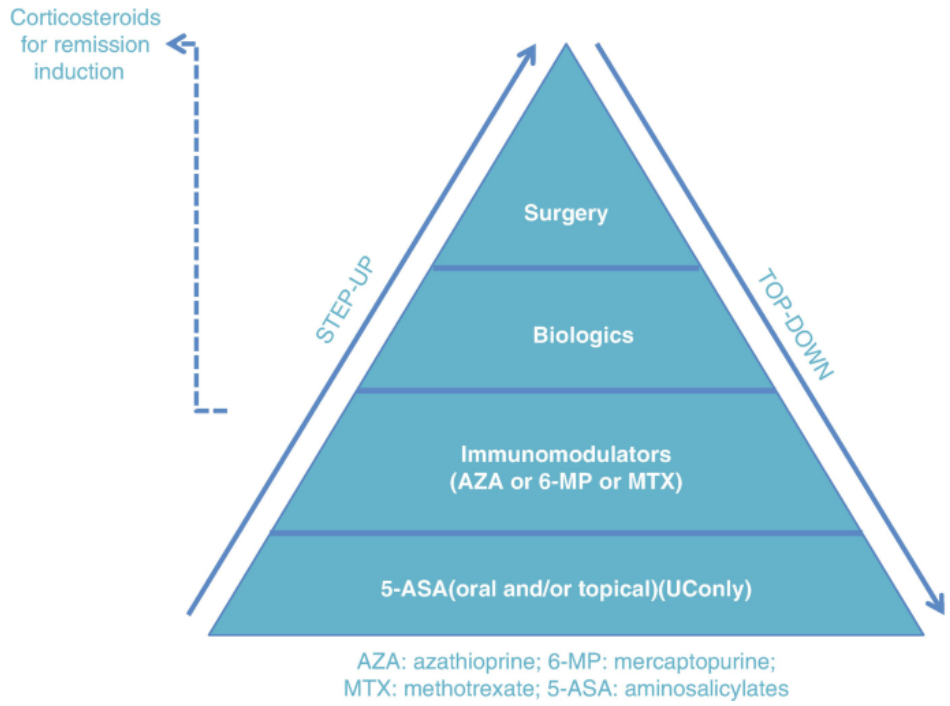

Figure 11. Step-up and top-down therapeutic strategies in inflammatory bowel disease. The diagram illustrates the hierarchical approach to medical and surgical management of inflammatory bowel disease. The step-up strategy progresses upward from less aggressive to more intensive therapies. In contrast, the top-down approach initiates treatment with more potent therapies earlier in the disease course (Gill M. and Bryant R.V., 2019).

Despite substantial advances, a considerable proportion of patients exhibit primary non-response or secondary loss of response, necessitating new treatment options [252].

Emerging strategies, such as small molecule inhibitors, microbiota modulators, apheresis, and cell-based therapies, aim not only to induce and maintain remission but also to achieve mucosal healing by eliminating local inflammation and restoring epithelial integrity [252]. In severe complications or pharmacological failure, colectomy remains indicated, being curative in UC but not in CD [177].

Aminosalicylates, including sulfasalazine and mesalazine (5-ASA), are first line anti-inflammatory agents for mild to moderate UC. Their mechanisms involve inhibition of cyclooxygenase and lipoxygenase pathways, scavenging of reactive oxygen species, suppression of immune cells recruitment and cytokines production, and induction of regulatory T cells via TGF-β [252,269]. Mesalazine is effective in both induction and maintenance of remission [270,271] and reduces colorectal cancer risk by up to 75% [272]. Sulfasalazine has comparable efficacy but greater toxicity [270]. In CD, evidence for 5-ASA efficacy is limited [273], though prolonged use may reduce healthcare utilization and postoperative recurrence [274,275].

Corticosteroids, such as budesonide, act via cytoplasmic glucocorticoid receptors that translocate to the nucleus to repress pro-inflammatory and activate anti-inflammatory genes, with additional membrane receptor effects [276,277]. They are used to induce remission in mesalazine-refractory UC or mild to moderate CD [278], but not for maintenance due to adverse effects including infections, metabolic disorders, and osteoporosis [279,280].

Immunomodulators include thiopurines, methotrexate, and calcineurin inhibitors. Thiopurines inhibit lymphocyte proliferation by interfering with DNA synthesis and Rac1 activation [281]; azathioprine reduces hospitalizations and surgeries in UC and CD but causes myelosuppression and hepatotoxicity [282,283]. Methotrexate suppresses DNA synthesis and cytokines release, inducing remission in up to 72% of CD patients [284], though evidence in UC is limited [285]. Calcineurin inhibitors block NFAT activation and cytokines transcription; cyclosporine A is effective in 80% of acute refractory UC cases [286], while tacrolimus offers greater potency but variable outcomes and nephrotoxicity [287,288].

Biological therapies have transformed IBD management. Anti-TNF-α monoclonal antibodies (i.e. Infliximab, Adalimumab) inhibit TNF-mediated inflammation, reducing hospitalization and surgery [289,290], though 40% of patients are primary non-responders and up to half lose response within one year [291]. IL-12/23 inhibitors (i.e. Ustekinumab, Risankizumab, Mirikizumab) block cytokine signaling via p40 or p19 subunits, attenuating

intestinal inflammation [292,293]. Anti-integrin therapy (i.e. Vedolizumab) prevents lymphocyte adhesion to intestinal mucosa by blocking α4β7-MAdCAM-1 binding, showing excellent safety, even after anti-TNF failure [294,295,296,297].

Small molecules, such as the JAK inhibitor Tofacitinib, modulate cytokine signaling and T-cells activation and are effective in moderate to severe UC, including anti-TNF-resistant cases [298,299].

Given the role of the gut microbiota in IBD, strategies such as antibiotics, prebiotics, probiotics, synbiotics, and postbiotics are being explored [300,301,302,303,304]. Fecal microbiota transplantation (FMT) restores microbial balance and achieves clinical remission in 33% of UC and 52% of CD cases [305]. Additional innovations include apheresis, which removes activated leukocytes [306], and stem cell-based therapies, promoting mucosal regeneration and barrier restoration [252].

Taken together, the therapeutic approaches to AAG and IBD reflect the current limitations in fully understanding their pathogenesis. Ongoing research into targeted immunomodulatory and regenerative strategies holds promise for more effective and personalized treatments in the future. In this evolving landscape, extracellular Nicotinamide phosphoribosyltrasferase (eNAMPT), a proinflammatory cytokine that has emerged as a key mediator of immune activation and tissue damage, finds its way. Its dual role in inflammation and cellular metabolism positions eNAMPT as a promising novel therapeutic target, with early studies demonstrating encouraging results in modulating disease activity and restoring mucosal homeostasis.

1.8 THE PROTEIN NAMPT AND ITS DUAL IDENTITY

The protein Nicotinamide phosphoribosyltrasferase (NAMPT) has been described in literature under three distinct names: Pre-B cell colony-enhancing factor (PBEF), Visfatin, and NAMPT. It was first identified in 1994, following the isolation of its coding gene from a cDNA library derived from human peripheral blood lymphocytes.

Due to its capacity to stimulate the formation of Pre-B cell colonies and to promote B cell maturation in synergy with IL-7 and stem cell factor (SCF), the protein was initially termed PBEF [307].

Subsequent studies revealed that the same protein functions as an insulin-mimetic adipokine secreted predominantly by visceral adipose tissue, exhibiting the ability to bind the insulin receptor at a site distinct from that of insulin itself [308]. This discovery led to its alternative

designation as Visfatin.

At present, NAMPT is the official nomenclature assigned to both the protein and its corresponding gene, as recognized by the Human Genome Organization (HUGO), the Gene Nomenclature Committee, and the Mouse Genomic Nomenclature Committee [308].

The gene encoding NAMPT is located on the long arm of chromosome 7, between regions 7q22.1 and 7q31.33. It comprises 11 exons and 10 introns (Fig. 12), with a coding sequence of 2.357 base pairs [309,310].

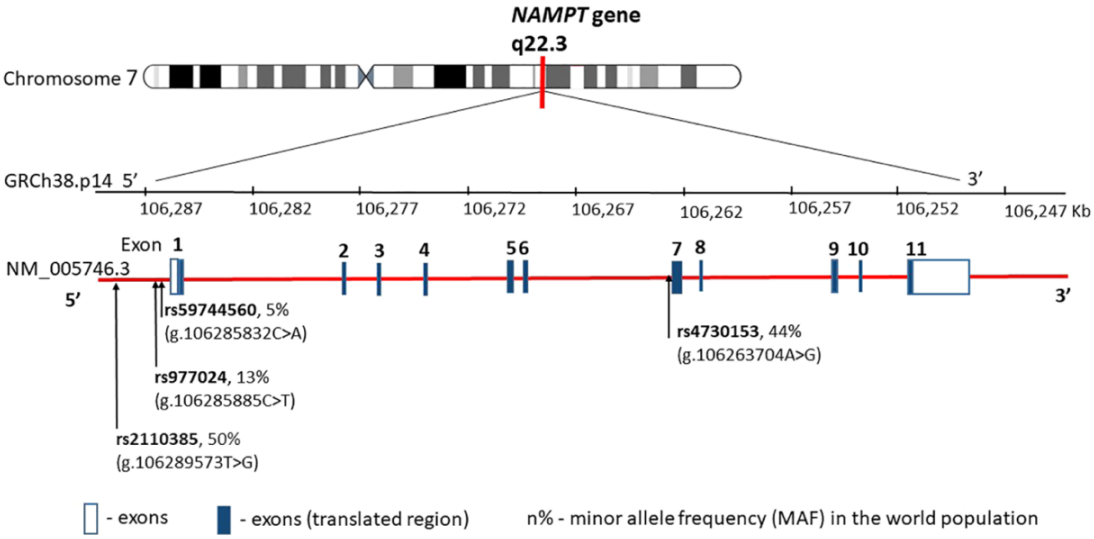

Figure 12. NAMPT Gene. NAMPT gene structure, chromosome location, and variants (Ratajczak-Pawlowska AE et al., 2025).

The NAMPT protein consists of 491 amino acids, has an estimated molecular mass of approximately 52 kDa [309], and exhibits a three-dimensional structure characterized by 19 β-strands and 13 α-helices organized into two distinct domains [311]. The crystal structure of NAMPT, resolved through X-ray crystallography by Kim and colleagues (Fig. 13), classified the enzyme as a member of the class II dimeric phosphoribosyltransferases [311].

In its catalytically active form, NAMPT exists as a homodimer composed of two identical monomeric subunits. Dimerization is essential for the proper assembly of the active site and, consequently, for enzymatic activity [312].

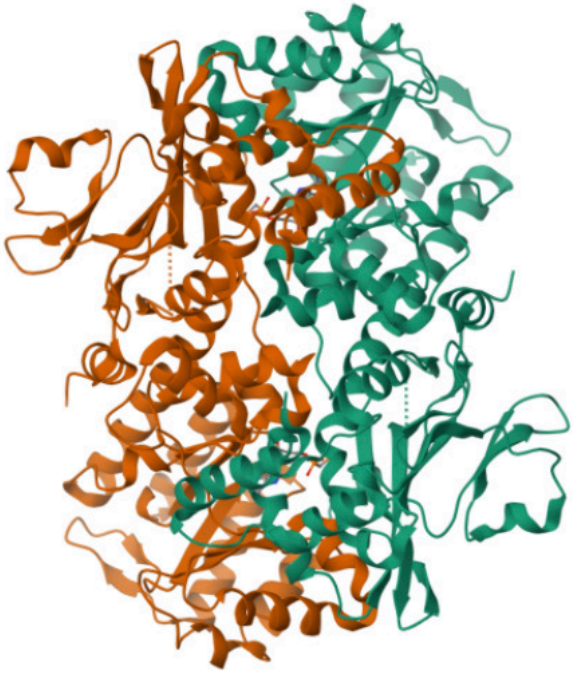

Figure 13. Crystal structure of human NAMPT. Structural representation of NAMPT in its homodimeric state. The two identical monomeric subunits, depicted in orange and green, dimerize to generate the functionally active enzyme (PDB:3DGR, Ho M et al., 2009).

Two major forms of NAMPT have been identified: the intracellular form (iNAMPT) and the extracellular form (eNAMPT). Although these isoforms share the same amino acid sequence, they differ in subcellular localization, regulatory control, and biological function. iNAMPT is primarily localized in cytosol, but it can also be detected in the nucleus and mitochondria [312]. Functionally, iNAMPT contributes to cell proliferation, energy homeostasis, cell survival, and adaptive stress responses. Its enzymatic activity is modulated by intracellular signaling pathways and is tightly coupled to cellular metabolic demands [313,314]. Conversely, eNAMPT is found in the extracellular compartment and is secreted by adipocytes, immune cells, and other cell types, although the mechanism of secretion remains a matter of debate [315]. Several functions have been attributed to eNAMPT, including its proposed ability to activate insulin receptors and stimulate triglyceride accumulation in adipocytes, thereby exerting an insulin-mimetic hypoglycemic effect [308]. In addition, eNAMPT plays a role in modulating inflammatory processes and immune responses [316].

1.8.1 INTRACELLULAR NAMPT (iNAMPT)

The expression of iNAMPT is ubiquitous across all human tissues, underscoring its fundamental role in cellular physiology. Accumulating evidence demonstrates that iNAMPT

is indispensable for organismal viability. Knockout iNAMPT mice exhibit embryonic lethality, confirming the essential requirement of NAMPT for embryonic development and survival [317]. Within mammalian cells, iNAMPT constitutes the rate-limiting enzyme in the nicotinamide adenine dinucleotide (NAD^+) salvage pathway, thereby governing intracellular NAD^+ homeostasis. It catalyzes the reaction between phosphoribosyl pyrophosphate (PRPP) and nicotinamide (NA) to form nicotinamide mononucleotide (NMN) and pyrophosphate (PP), with NMN then further converted to NAD^+ by the action of Nicotinamide mononucleotide adenosyl transferase (NMNAT), which catalyzes the condensation of NMN and ATP [318] (Fig. 14).

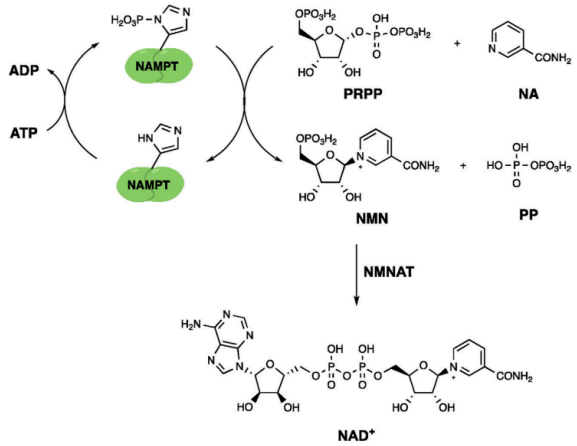

Figure 14. iNAMPT involvement in NAD^+ salvage pathway. iNAMPT mediates the formation of Nicotinamide mononucleotide (NMN) and pyrophosphate (PP) starting from phosphoribosyl pyrophosphate (PRPP) and nicotinamide (NA) in an ATP dependent manner (Siyuan T. et al., 2023).

Through this function, iNAMPT exerts a central regulatory role in multiple NAD^+-dependent biological processes, including energy metabolism, cell proliferation, apoptosis, cellular senescence, and aging, as well as in the activity of several NAD^+-consuming enzymes such as sirtuins (SIRTs), poly (ADP-ribose) polymerases (PARPs), and ADP-ribosyl cyclases (cADPRs) [319,315].

Given its widespread expression, NAMPT contributes critically to both physiological homeostasis and pathophysiology of numerous disorders. However, the degree of tissue dependence on iNAMPT activity is modulated by the relative efficiency of alternative NAD^+ biosynthetic routes, such as those mediated by nicotinic acid phosphoribosyltrasferase (NAPRT) and nicotinamide riboside kinase (NRK) pathways [320]. Importantly, iNAMPT has been implicated in the molecular mechanisms of aging and senescence. Numerous studies have documented an age-associated decline in NAD^+ levels across multiple tissues,

including skeletal muscles, pancreas, liver, and white adipose tissue. A similar reduction in intracellular NAD^+ content has been observed in human cells [321]. This phenomenon appears to arise from alterations in NAD^+ biosynthetic pathways, with compelling evidence indicating a progressive decrease in NAMPT expression during aging [322].

1.8.2 EXTRACELLULAR NAMPT (eNAMPT)

Extracellular NAMPT is a multifunctional protein that acts as an adipokine, a pro-angiogenic factor, and a pro-inflammatory cytokine. Unlike its intracellular isoform, the biological effects of eNAMPT are primarily non-enzymatic and influence multiple physiological and pathological processes.

eNAMPT has been detected in human circulation, as well as in feces and various other biological fluids, including cerebrospinal fluid, saliva, synovial fluid, and seminal plasma.

Initially described as an adipokine regulating systemic metabolism, eNAMPT is secreted by visceral, subcutaneous, and epicardial adipose tissues. Early studies suggested that eNAMPT could lower blood glucose levels through direct activation of the insulin receptor, though these findings were later retracted due to limited reproducibility [308]. Subsequent research has only partially confirmed the insulin-mimetic effects of eNAMPT, leaving its precise role in insulin signaling an open question [323].

Independent of insulin signaling, eNAMPT contributes to pancreatic β-cell viability and metabolic functionality, protecting these cells from lipotoxic apoptosis induced by free fatty acids and maintaining insulin secretion in response to glucose. This effect is largely dependent on eNAMPT enzymatic activity, rather than direct receptor-mediated signaling [324,325]. Thus, eNAMPT plays a critical role in glucose homeostasis and endocrine pancreas function, linking extracellular signals to intracellular metabolic pathways.

In addition to its metabolic functions, eNAMPT exerts pro-angiogenic effects, promoting endothelial cell proliferation, migration, and tubular network formation. These activities are mediated through the MAPK and PI3K/AKT/mTOR signaling pathways, which enhance VEGF expression and secretion as well as VEGFR-2 upregulation in endothelial and epithelial cells. eNAMPT also stimulates the release of pro-angiogenic mediators such as IL-6, CXCL8, FGF2, and MCP-1, and contributes to extracellular matrix remodeling via upregulation of metalloproteinases, facilitating vascular growth and tissue repair [326,327, 328,329]. Beyond angiogenesis, eNAMPT functions as a pro-inflammatory cytokine and damage-associated molecular pattern (DAMP). It activates NF-kB, MAPK, and STAT3

signaling pathways, leading to increased production of cytokines (IL-1β, IL-6, CXCL8, IL-10, TNF-α) and chemokines (CCL2, CCL3, CCL18, CCL20). eNAMPT also acts as a chemoattractant, promoting the recruitment, migration, proliferation, and differentiation of monocytes, B lymphocytes, and neutrophils, and regulates macrophage polarization toward M1 or M2 phenotypes depending on the tissue microenvironment [330,316,331]. In human monocytes, eNAMPT enhances the expression of co-stimulatory molecules (CD40, CD54, CD80), increasing phagocytic capacity, while in macrophages it promotes cell survival via STAT3 activation and inhibition of ER stress-induced apoptosis [332,333].

eNAMPT also contributes to vascular inflammation by upregulating ICAM-1 and VCAM-1 in endothelial cells, facilitating leukocyte adhesion, and activating the NLRP3 inflammasome, resulting in IL-1β release [334,335]. Importantly, these pro-inflammatory and pro-angiogenic effects (Fig. 15) are independent of eNAMPT enzymatic activity and dimerization [336,333]. Clinically, elevated eNAMPT levels have been associated with a wide range of pathological conditions, including metabolic disorders (obesity, diabetes), cardiovascular diseases (atherosclerosis), chronic inflammatory conditions (osteoarthritis, rheumatoid arthritis, IBD), and cancer. These findings underscore the multifactorial role of eNAMPT in disease pathogenesis and support its potential as both a biomarker and a therapeutic target.

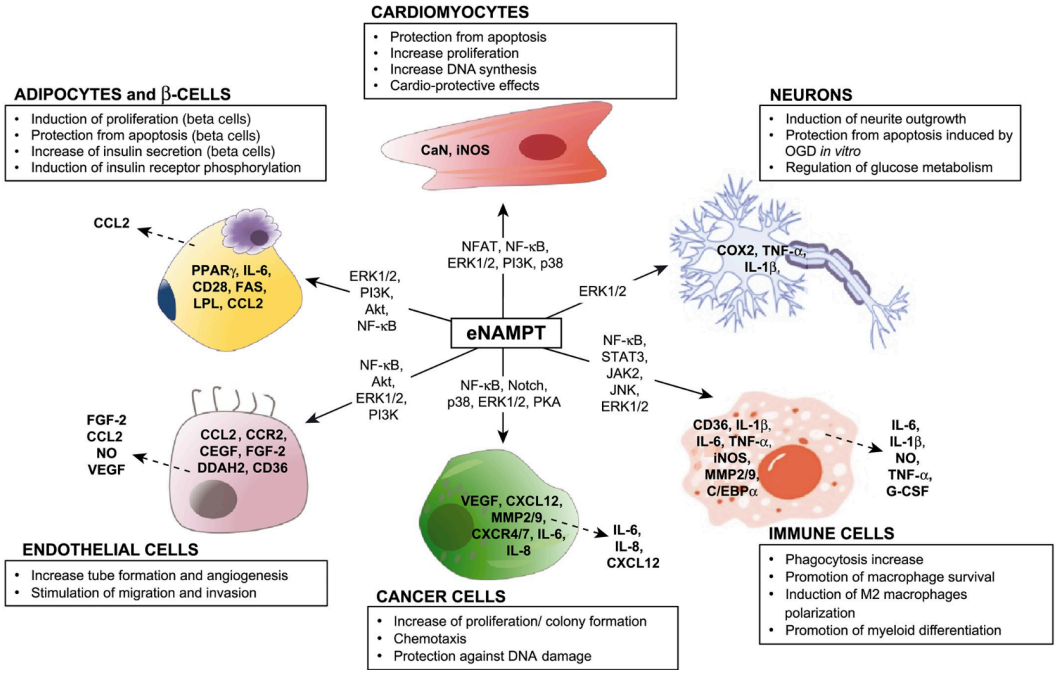

Figure 15. Functional roles of eNAMPT. eNAMPT is released by most of cell types and exerts multifunctional effects in the extracellular environment, acting as an adipokine, a pro-angiogenic factor, and a pro-inflammatory cytokine/DAMP. It can activate downstream intracellular pathways by stimulating a subsequent release of other cytokines (Grolla A et al., 2016).

1.8.3 MECHANISMS REGULATING eNAMPT SECRETION AND MODE OF ACTION

Despite the growing understanding of NAMPT intracellular functions, much remains unclear regarding its mechanism of action in the extracellular space. The complexity of its regulation, combined with the absence of classical secretion signals and the diversity of its biological effects, suggests that eNAMPT operates through unconventional and cell-type specific pathways. Unraveling these mechanisms is essential to fully comprehend the multifaceted role of NAMPT in health and disease.

1.8.3.1 eNAMPT SECRETION

To date, the mechanism underlying NAMPT secretion into the extracellular environment remains only partially elucidated. Initially, it was hypothesized that the release of NAMPT occurred as a passive consequence of cell lysis or death, given that the protein lacks both a signal peptide sequence and caspase-1 cleavage sites [337].

However, subsequent studies refuted this assumption, demonstrating that although eNAMPT levels may increase following such events, its release is in fact a highly regulated and cell type-specific active process [325]. Supporting the notion that NAMPT is secreted through a non-classical pathway, its extracellular release has been shown to be insensitive to ER-Golgi transport inhibitors such as brefeldin A and monensin [325,338].

The potential involvement of lysosomal trafficking has also been investigated, as exposure to chloroquine increases extracellular NAMPT levels; nevertheless, alternative mechanisms such as exosome- or macrovesicle-mediated release appear to contribute only marginally to the overall process [338,336]. Moreover, metabolic and nutritional stress conditions have been shown to significantly influence eNAMPT secretion. Stressful stimuli such as ischemia [339], oxygen-glucose deprivation (OGD) [340], and hypoxia [336] markedly increase eNAMPT release from neurons, glial cells, and melanoma cells. Similarly, oxidative stress and endoplasmic reticulum stress have been associated with enhanced NAMPT secretion [341,342].

Also, inflammatory stimuli have been identified as potent inducers of eNAMPT release. Treatment of activated monocytes with lipopolysaccharide (LPS) and ATP resulted in a robust increase in extracellular NAMPT levels [341]. Similar results have been observed in leukocytes exposed to LPS, in amniotic epithelial cells treated with TNF-α [343], and in cardiomyocytes stimulated with IL-1β [341].

More recently, attention has turned to the role of post-translational modifications in the regulation of NAMPT secretion.

In 2013, Pillai and colleagues demonstrated that treatment with histone deacetylase inhibitors (e.g., trichostatin A) suppresses NAMPT secretion, suggesting that deacetylation represents a critical regulatory event in eNAMPT release [341]. Subsequent studies confirmed that SIRT1-mediated deacetylation of lysine 53 is essential for the export of NAMPT from the intracellular to the extracellular compartment [344].

	Cell type	Modulation of eNAMPT release	Reference
Adipocytes	• 3T3-L1 adipocytes	Increased by Ox-LDL, CTRP3, glucose, rosiglitazone, adipocyte differentiation	(Fukuhara *et al.*, 2005)
			(Tanaka *et al.*, 2007)
	• SGBS adipocytes		(Chen *et al.*, 2013)
			(Derdemezis *et al.*, 2011)
	• Adipocytes derived from healthy donors	Decreased by insulin, PI3K and AKT inhibitors, quercetin	(Li *et al.*, 2014a)
			(Haider *et al.*, 2006a, b)
	• HIB-1B adipocytes		(Haider *et al.*, 2006b)
			(Revollo *et al.*, 2007)
Immune cells	• LPS-activated monocytes	Increased by ATP, LPS	(Schilling and Hauschildt, 2012)
	• Macrophages in visceral adipose tissue		(Curat *et al.*, 2006)
	• Leucocytes		(Friebe *et al.*, 2011)
	• Peripheral blood lymphocytes		(Samal *et al.*, 1994)
Brain cells	• PC12 cells	Increased by $CoCl_2$, ischaemia, OGD	(Kang *et al.*, 2011)
	• Primary neurons		(Jing *et al.*, 2014)
	• Primary glial cells		(Zhao *et al.*, 2014)
Cancer cells	• Hepatoma cells (HepG2, Huh-7)	Increased by anti-CD38 and differentiation in CCL, oxidative stress (H_2O_2), hypoxia	(Samal *et al.*, 1994)
			(Garten *et al.*, 2010)
			(Soncini *et al.*, 2014)
	• Colorectal cancer cells (HCT-116, LS180)		(Ghaemmaghami *et al.*, 2013)
	• Breast cancer cells (MCF10A, MCF7, T47D, MDA-MB-231, BT549, MDA-MB-468)		(Audrito *et al.*, 2015)
	• Melanoma cells (B16, MeWo, HMCB, SkMel28, LB24)		(Lin *et al.*, 2015)
	• Neuroblastoma and glioma cells (SH-SY5Y, SK-N-Be, U87)		
	• Mesothelioma (MSTO)		
	• Prostate cancer cells (DU-145)		(Grolla *et al.*, 2015)
	• Cervical cancer cells (HeLa)		
	• Chronic lymphocytic leukemia lymphocytes		
Other cells	• Fibroblast (COS-7, PA317, CHO)	Increased by LPS, TNF-α, IL-1β, starvation and oxidative stress (H_2O_2), differentiation, glucose, C-peptide	(Samal *et al.*, 1994; Jia *et al.*, 2004)
	• Amniotic epithelial cells		(Ognjanovic *et al.*, 2005)
	• Inflamed HUVECs		(Romacho *et al.*, 2013)
	• Neonatal rat cardiomyocytes		(Pillai *et al.*, 2013)
	• Pancreatic beta cells		(Revollo *et al.*, 2007)
	• Isolated human islets		(Kover *et al.*, 2013)
	• Sebocytes		(Kovacs *et al.*, 2016)
	• Melanocytes		(Grolla *et al.*, 2015)

PubMed was used to retrieve the evidence using 'visfatin' or 'PBEF' as a search string. Only cultured cell lines were considered for this table.

Table 1. Modulation of eNAMPT release in different cell types. This table summarizes the cell types reported to release eNAMPT and the stimuli or conditions that modulate its secretion (Grolla A et al., 2016).

1.8.3.2 eNAMPT POST-TRANSLATIONAL MODIFICATIONS

Post-translational modifications (PTMs) represent a fundamental regulatory layer in protein biology, occurring after translocation to modulate protein stability, localization, activity, and interactions. Through chemical alterations such as phosphorylation, acetylation, ubiquitination, and glycosylation, PTMs enable dynamic and context-dependent control of cellular processes. These modifications are crucial for fine-tuning protein function in response to physiological and environmental changes, thereby playing a central role in maintaining cellular homeostasis and signaling fidelity.

Current knowledge regarding the post-translational modifications of NAMPT remains limited. Nevertheless, several predicted modifications, such as phosphorylation, ubiquitination, and acetylation at specific amino acid residues identified through bioinformatic approaches, are thought to play key regulatory roles in the protein's activity, localization, stability, and expression [345] (Table 2). Among the experimentally confirmed PTMs, two modifications have been functionally characterized: phosphorylation at histidine 247 (H247) and deacetylation at lysine 53 (K53). The SIRT1-mediated deacetylation of K53 has been shown to promote NAMPT expression and the secretion of its extracellular form in adipocytes [344].

PTM	RESIDUE (where known)	Enzyme	FUNCTIONAL EFFECT	REFERENCE
Phosphorylation	Ser 199 Ser 301 Ser 380 His 247	AMPK, MAPKs (putative)	Enzymatic activity and NAD^+ biosynthesis, subcellular localization, secretion	Revollo et al., 2007; Garten et al., 2015; Kim et al., 2015; Burgos et al., 2009
Acetylation/ Deacetylation	Lys53 Lys393	P300/CBP SIRT1	Catalytic efficiency	Revollo et al., 2004; Yoshino et al., 2011; Imai and Yoshino, 2013
Ubiquitination	-	E3 ubiquitin ligases (uspecified)	Proteasomal degradation	Garten et al., 2015; Zhao et al., 2019
SUMOylation	Predicetd lysine residues	SUMO E3 ligases	Subcellular localization	Wang et al., 2018; Zhao et al., 2019
Glycosylation	Predicted Asn motifs	-	Secretion and stability	Audrito et al., 2015; Grolla et al., 2015
S-Nitrosylation / Oxidation	Reactive cysteine residues	Nitric oxide donors, ROS	Alters enzymatic conformation	Romacho et al., 2013; Garten et al., 2015

PubMed was used to retrieve the evidence using 'NAMPT', 'visfatin' or 'PBEF' as a search string.

Table 2. Known PTMs of NAMPT. This table summarizes the known post-translational modifications of NAMPT identified in mammalian systems, highlighting their regulatory enzymes, target residues, and functional consequences.

Supporting these findings, inhibition of histone deacetylases or sirtuins in cardiomyocytes results in reduced intracellular NAMPT levels and a complete blockade of stress-induced eNAMPT release [346]. Phosphorylation at H247 has been associated with NAMPT's ATPase activity, which adds to its canonical phosphoribosyltrasferase function. This modification leads to a substantial increase in catalytic efficiency and substrate affinity, enhancing NAMPT's ability to convert NAM and PRPP into NMN [347]. Mutagenesis studies have confirmed the essential role of H247, as its substitution markedly reduces enzymatic activity [313]. Structural analyses further indicate that phosphorylation at this site promotes a conformational rearrangement that strengthens dimer interaction and increases the enzyme's affinity for PRPP, a prerequisite for efficient NAM binding [348,349].

Collectively, these findings suggest that NAMPT activity and secretion are finely modulated by specific PTMs, which serve as critical molecular switches linking its intracellular enzymatic role to its extracellular signaling functions.

1.8.3.3 eNAMPT PUTATIVE RECEPTORS

The mechanisms regulating the release of extracellular NAMPT are intricately linked to its diverse biological functions. As previously discussed, eNAMPT secretion is a tightly controlled, cell type-specific, and non-classical process, modulated by PTMs and various stress, nutritional or inflammatory stimuli. However, a key unresolved question concerns how eNAMPT exerts its biological effects once secreted. It remains uncertain whether these effects arise from a residual extracellular enzymatic activity or from direct interactions with specific membrane receptors. Given the low extracellular concentrations of NAD^+ precursors and the rapid activation of intracellular signaling cascades such as ERK, STAT3, and NF-kB following eNAMPT exposure, the most plausible hypothesis is that eNAMPT functions primarily as a cytokine-like ligand binding to cell surface receptors [350].

To date, two potential membrane receptors for eNAMPT have been proposed: the C-C chemokine receptor type 5 (CCR5) and the Toll-like receptor (TLR4).

The first evidence of a direct interaction between eNAMPT and CCR5 was provided by Van der Bergh et al. in 2012 through surface plasmon resonance (SPR) analysis. Subsequent studies confirmed this interaction, revealing a structural similarity between eNAMPT and CCL7, a known CCR5 ligand, and suggesting that eNAMPT may function as a CCR5 antagonist [351]. Nevertheless, the involvement of CCR5 as a biologically relevant receptor for eNAMPT remains controversial, as pharmacological inhibition of CCR5 with maraviroc

does not completely abolish eNAMPT-induced cellular effects [331]. In parallel, a possible interaction between eNAMPT and TLR4 has been proposed, mediating NF-kB pathway activation [352]. Supporting this hypothesis, computational analyses revealed a high degree of sequence homology between eNAMPT and MD-2, a known TLR4 ligand in the presence of LPS. Unlike MD-2, however, eNAMPT can directly activate TLR4 even in the absence of bacterial infection or cofactors [352]. Further evidence from Managò et al., in 2019, demonstrated that silencing of TLR4 markedly reduced eNAMPT-induced NF-kB activation, confirming the receptor's functional involvement. Site-directed mutagenesis identified two regions within the N-terminal domain of eNAMPT (β1-β2 loop: aa 41-52, α1-α2 loop: aa 68-77) as critical for receptor binding. This finding was later corroborated by Kim et al., in 2022, who identified an additional interaction site (aa 57-65) within a leucine-rich domain of TLR4 and a potential C-terminal binding site (aa 445-457).

Nevertheless, Colombo et al. have demonstrated that eNAMPT can boost INF-γ macrophage polarization even in the absence of TLR4 [331].

Despite these advances, the identity of biologically relevant eNAMPT receptors remains to be fully established. Recent protein-protein interaction analyses suggest that eNAMPT may engage with multiple surface receptors, extending beyond CCR5 and TLR4 [353].

Together, these finding highlight the dualistic nature of NAMPT: intracellularly, it functions as a key enzymatic regulator of NAD^+ biosynthesis, while extracellularly, it acts as a pleiotropic signaling molecule, modulating processes such as inflammation, angiogenesis, and metabolic regulation through receptor-mediated mechanisms.

1.8.4 eNAMPT INVOLVEMENT IN AAG AND IBD

Given its multifaceted biological roles, numerous chronic and metabolic diseases show increased expression of extracellular NAMPT, including rheumatoid arthritis, osteoarthritis, COPD, diabetes, obesity, atherosclerosis, inflammatory bowel diseases (BD), acute respiratory distress syndrome (ARDS), lupus vasculitis, pulmonary hypertension, and hepatic fibrosis [323,354]. In addition, in 2022, Lenti et al. demonstrated that NAMPT transcripts were significantly elevated in AAG patients compared with healthy controls, suggesting its potential as both biomarker and a therapeutic target.

To date, AAG remains an important unmet medical need, owing to the lack of targeted biological therapies addressing the underlying disease pathogenesis. In recent years, it has been hypothesized that certain pro-inflammatory cytokines, which play a pivotal role in the

progression of AAG, such as eNAMPT, may represent a potential pharmacological target for the development of future immunomodulatory treatments.

Among the various inflammatory conditions involving the extracellular form of NAMPT, chronic inflammatory bowel diseases represent one of the pathological contexts in which its contribution appears particularly relevant. Recent experimental and clinical evidence had highlighted an active role of eNAMPT in the pathogenesis of these disorders, identifying it as a key mediator of the pro-inflammatory cascade.

In particular, prior to my involvement with the group, our research team demonstrated that, in chemically induced murine models of colitis, administration of recombinant eNAMPT exacerbates intestinal pathology by promoting colonic inflammation. It has been demonstrated that this process is associated with increased expression of pro-inflammatory cytokines such as TNF-α and IL-1β and degradation of IkB-α, indicating activation of the NF-kB signaling pathway [355].

Supporting these findings, the group has developed C269, a murine monoclonal antibody capable of neutralizing eNAMPT without affecting intracellular levels. Treatment with C269 in mice with colitis resulted in reduced inflammation in both acute and chronic models, accompanied by decreased colonic infiltration of pro-inflammatory monocytes and neutrophils, reduced activation of pathogenic Th1 cells and cytotoxic T lymphocytes, and diminished production of effector cytokines, including TNF, IL-1, IL-6, IL-17A, IL-23, and IFN-γ [355]. Preclinical data are consistent with clinic observation showing that patients with IBD display elevated circulating levels of eNAMPT, which correlate with adverse disease outcomes. Specifically, in Crohn's disease, serum eNAMPT concentrations are elevated regardless of disease activity, whereas in ulcerative colitis, levels increase significantly only during active disease [332,356]. As observed in other inflammatory disorders, a positive correlation has also been reported between eNAMPT levels and classical inflammatory markers such as IL-6, platelet count, and ESR [356,357].

Furthermore, in IBD, eNAMPT has emerged as a potential predictive and diagnostic biomarker; its serum concentration markedly decreases in patients responding to anti-TNF-α therapy, whereas it remains elevated in non-responders [358]. Notably, eNAMPT levels have also been shown to predict, with high sensitivity and specificity, relapse in active ulcerative colitis [357].

1.9 CURRENT AND EMERGING NAMPT-TARGETED THERAPIES

For all the reasons outlined above, eNAMPT has been extensively investigated for its involvement in the pathophysiology of chronic and metabolic disorders. Numerous strategies have been employed to inhibit NAMPT activity, aiming to modulate its role in inflammation and metabolic regulation. Small-molecule inhibitors and neutralizing monoclonal antibodies, along with more recent approaches such as PROTACs and antisense oligonucleotides, represent the most studied strategies to target NAMPT. Nonetheless, their long-term effects, particularly in chronic inflammatory conditions like intestinal diseases, remain unclear, making it essential to evaluate both sustained efficacy and the potential for adverse effects during prolonged treatment.

1.9.1 NAMPT INHIBITORS

Over the past decades, growing interest in NAMPT has driven the development of inhibitors primarily targeting its intracellular form, investigated for their antitumor potential as well as their immunomodulatory and anti-inflammatory properties [359,325,350]. Prominent compounds in this class include F866, CHS828, GNE617, and OT-82.

FK866, also known as APO866, was the first high-affinity NAMPT inhibitor developed [360]. Despite promising preclinical results, it showed limited clinical efficacy as an antitumor agent and significant myelotoxicity, with dose-limiting thrombocytopenia [361,362]. Similar adverse effects, including potential retinal and cardiac toxicity, have been reported for other inhibitors in this class [363,364].

CHS828, also known as GMX-1778, initially identified as a cytotoxic agent [365], also failed in clinical trials due to minimal therapeutic benefit and severe adverse events, such as diarrhea, vomiting, thrombosis, and myelotoxicity [366,367].

GNE617, an imidazopyridine derivative, exhibited poor water solubility, inhibitory activity against CYP2C9, and formation of toxic metabolites. Targeted structural modifications, including reduced aromaticity and removal of specific substituents, improved its ADMET properties [368].

OT-82, selected via screening in hematopoietic cells, shows high selectivity and promising cytotoxicity. In animal models, it demonstrates good tolerability, with toxicity largely restricted to hematopoietic and lymphoid tissues, and no detectable cardiac, neurological or retinal effects [369]. OT-82 is currently undergoing Phase 1 clinical trials and represents a promising therapeutic approach for certain hematologic malignancies, including acute

myeloid leukemia (AML) and acute lymphoblastic leukemia (ALL).

The resolution of the FK866-NAMPT crystal structure, revealing a narrow, elongated active site formed by head-to-tail dimerization of two protein subunits, enabled the identification of key structural features for effective interaction with NAMPT (Fig. 16).

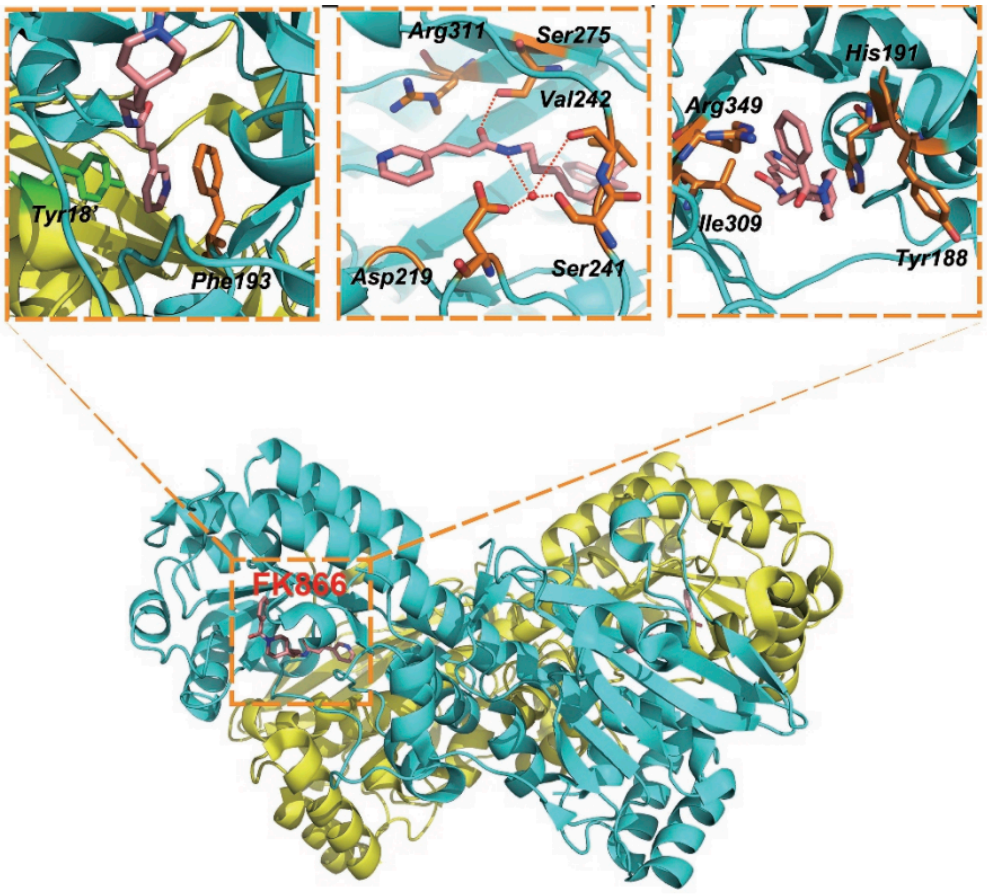

Figure 16. Crystal structure analysis of NAMPT in complex with FK866. Overall view of the dimeric NAMPT structure (shown in cyan and yellow) bound to the inhibitor FK866 (in orange). The inset panels highlight detailed interactions between FK866 and key amino acid residues within the binding pocket. Structural visualization emphasizes the spatial arrangement of critical residues contributing to ligand recognition and binding affinity (Zhang et al., 2017).

This led to a common pharmacophore model guiding rational inhibitor design, consisting of four elements: a head group, typically a pyridine ring or heterocyclic analogue, mimicking nicotinamide and interacting via π and hydrogen bonds; a linker unit, such as an amide or hydrogen-bond acceptor, stabilizing the interaction; a hydrophobic linker, including aromatic or aliphatic chains, spanning the catalytic pocket and engaging nonpolar regions; and a tail group, oriented toward the solvent-exposed region, modifiable to enhance metabolic stability and cellular permeability, ensuring selective targeting of intracellular NAMPT (Fig. 17)[370,371,372].

Figure 17. NAMPT inhibitors pharmacophore. The pharmacophore consists of four key elements: a head group (NAM Mimic), a linker unit (Spacer Group), a hydrophobic linker (Tunnel Binder), and a tail group (Solvent-Exposed Moiety) (Sampath D. et al., 2015).

Using these pharmacophoric elements, increasingly selective and potent NAMPT inhibitors with improved ADMET properties have been developed. These can be classified into three categories: (i) molecules adhering to the pharmacophore model, (ii) structurally alternative molecules, and (iii) hybrid compounds combining NAMPT inhibition with additional pharmacological effects [359].

Despite the substantial advances achieved, a significant limitation remains the limited specificity of these compounds. They exert their activity indiscriminately across different tissues, thereby interfering with NAMPT function also in healthy cells, which may result in systemic toxicity [373,374,375]. Moreover, these inhibitors have been shown to predominantly target the intracellular isoform, iNAMPT, whereas accumulating evidence indicates that, particularly in inflammation and oncological settings, selective inhibition of the extracellular isoform, eNAMPT, would be more advantageous [373].

1.9.2 EMERGING APPROACHES

In recent years, novel therapeutic strategies have emerged with the aim of selectively modulating NAMPT activity without compromising the physiological functions of the organism. Among these, one of the most innovative approaches is represented by the PROTAC (Proteolysis Targeting Chimera) technology, which enables the targeted degradation of the intracellular form of NAMPT through induced proteolysis [376]. The reduction of iNAMPT levels results in a concomitant decrease of the extracellular form, suggesting that PROTAC molecules may simultaneously inhibit both the intracellular enzymatic and extracellular non-enzymatic activities of NAMPT.

Preliminary *in vitro* and *in vivo* studies have reported promising results [377,378], demonstrating superior antitumor efficacy compared with the classical inhibitor FK866.

In addition, these molecules were shown to suppress pro-inflammatory signaling pathways such as NK-kB and MAPK/ERK1/2, which are involved in the DAMP-related functions of eNAMPT [377]. Overall, PROTAC-based degraders represent a promising new generation of molecules capable of overcoming some of the limitations associated with traditional enzymatic inhibitors.

In parallel, antisense oligonucleotides (ASOs) have been developed to block NAMPT synthesis at the transcription level, offering another means of reducing protein expression [348]. This approach holds potential for achieving a fine-tuned downregulation of NAMPT, although its application remains in the early experimental stages.

To further minimize the systemic side effects associated with iNAMPT inhibition, triazolopyridine-based compounds have also been designed. These molecules possess a highly hydrophilic triazole moiety that prevents cellular entry, thereby increasing selectivity for the extracellular form [372]. This structural modification allows for the preferential targeting of the extracellular protein, potentially mitigating the cytotoxicity observed with pan-NAMPT inhibitors.

1.9.3 MONOCLONAL ANTIBODY-BASED APPROACHES

Building on the limitations of small-molecule inhibitors, whose lack of selectivity often results in systemic toxicity; recent research efforts have shifted toward biologic therapies aimed at specifically targeting the extracellular form of NAMPT. In this context, monoclonal antibodies have emerged as a promising class of agents capable of selectively neutralizing eNAMPT while preserving intracellular NAMPT activity.

Given that the pathogenic functions of NAMPT are largely independent of its enzymatic activity, therapeutic strategies targeting the intracellular enzyme have shown limited effect in counteracting its extracellular effects. Monoclonal antibodies (mAbs) therefore represent a more suitable therapeutic option, as they can specifically neutralize extracellular mediators [323]. Starting from this, several research groups, our group included, have investigated this approach through preclinical studies conducted both *in vitro* and *in vivo*, reporting promising results. Among the neutralizing antibodies developed so far, the murine clone C269 demonstrated significant efficacy in chemically induced models of acute and chronic colitis. Treatment with C269 effectively reduced intestinal inflammation by suppressing the expression of inflammatory mediators such as TNF-α, IL-1β, IL-6, and IL-8, without affecting the enzymatic activity of the protein [355].

Among the most advanced and promising candidates is ALT-100, a humanized IgG4 monoclonal antibody developed by Dr. Joe G.N. Garcia and collaborators at Aqualung Therapeutics®. ALT-100 was designed to selectively inhibit the interaction between eNAMPT and its proposed receptor TLR4, thereby preventing the activation of the NK-kB-dependent inflammatory cascade [379]. Due to its cross-reactivity with NAMPT from multiple mammalian species, ALT-100 has been widely employed in *in vivo* studies across different animal models. Preclinical data have demonstrated that ALT-100 exerts broad anti-inflammatory and anti-fibrotic effects, effectively reducing disease severity in several pathological contexts. These include acute lung injury in mice and swine [380,381], pulmonary hypertension in rats [382], radiation-induced pulmonary fibrosis [383], and myocardial infarction, where the antibody mitigated chronic inflammation and cardiac fibrosis, improving ventricular function [384]. Moreover, in a preclinical prostate cancer model, ALT-100 was shown to reduce tumor cell proliferation, invasiveness, and metastatic potential by inhibiting the eNAMPT/TLR4/NF-kB signaling axis [385].

The safety and pharmacokinetic profiles of ALT-100 have been evaluated in a Phase 1 clinical study on health volunteers [386]. The antibody was well tolerated at all administered doses, with no treatment-related serious adverse events or clinically significant changes in vital signs or laboratory parameters. Mild or moderate side effects resolved spontaneously without clinical sequelae. Pharmacokinetic analyses revealed a dose-dependent half-life of up to 27 days, indicating sustained systemic exposure.

Currently, ALT-100 is undergoing Phase 2A clinical trials for the treatment of moderate to severe acute respiratory distress syndrome (ARDS) and ventilator-induced lung injury (VILI), with the goal of reducing the duration of mechanical ventilation and improving clinical outcomes [380]. Importantly, this therapeutic approach differs from conventional anti-cytokine therapies (e.g., anti-TNF-α, anti-IL-1β) by targeting eNAMPT upstream, thereby potentially preventing the onset of the so-called “cytokine storm”. Through this mechanism, ALT-100 aims to control uncontrolled inflammation and progressive fibrosis in severe inflammatory diseases.

In conclusion, monoclonal antibodies targeting eNAMPT represent a promising therapeutic innovation capable of overcoming the limitations of traditional NAMPT inhibitors. By specifically neutralizing the extracellular form, these agents open new avenues for the treatment of inflammatory and fibrotic diseases in which eNAMPT plays a pivotal role, as are AAG and IBD.

2. AIMS

Nicotinamide phosphoribosyltrasferase (NAMPT) is a pleiotropic protein expressed in all cells of the body. In mammals, it exists in two distinct forms: the intracellular form (iNAMPT) and the extracellular form (eNAMPT). iNAMPT functions as a rate-limiting enzyme in the NAD^+ salvage pathway, catalyzing the conversion of nicotinamide into nicotinamide mononucleotide (NMN), a reaction essential for maintaining cellular energy homeostasis. In contrast, eNAMPT acts as a pro-inflammatory cytokine, and its dysregulated expression has been implicated in a wide range of inflammatory disorders.

In autoimmune atrophic gastritis (AAG), a chronic immune-mediated condition characterized by the destruction of gastric parietal cells, eNAMPT is emerging as a key mediator of inflammation. Parietal cell loss reduces gastric acid and intrinsic factor production, impairing micronutrient absorption, and weakening the gastric barrier. Understanding the role of eNAMPT in driving gastric inflammation, as well as its effect on fibroblast activity and extracellular matrix remodeling is crucial, particularly given the absence of effective therapies and the risk of progression to gastric neuroendocrine tumors or adenocarcinoma.

Through a productive collaboration with Dr. Di Sabatino, from Policlinico San Matteo, gastric biopsy samples were obtained from both patients and healthy individuals. Fibroblasts were subsequently isolated from these samples and analyzed to provide deeper insight into eNAMPT's role in AAG.

In addition to AAG, eNAMPT has been implicated in chronic inflammatory bowel diseases (IBD), including Crohn's disease and ulcerative colitis. Elevated eNAMPT levels have been detected in the blood and feces of patients, and circulating levels correlate with disease severity and response to conventional therapies. Although the precise molecular mechanisms remain incompletely understood, eNAMPT is believed to contribute to intestinal inflammation and systemic immune modulation, highlighting its potential as a therapeutic target in IBD. Preclinical murine models, including DSS- and DNBS-chemically induced UC and CD, combined with recombinant eNAMPT administration, have been used to assess the effects of eNAMPT on disease progression and severity. Furthermore, trying to unravel eNAMPT molecular mechanisms at the base of IBD progression, it has been shown that eNAMPT can influence hematopoietic cells differentiation and maturation. E*x vivo* studies on bone-marrow-derived cells allow the investigation of how eNAMPT modulates hematopoietic processes during inflammation,

providing insight into systemic effects beyond the local tissue environment. Understanding these effects is crucial for elucidating the full spectrum of eNAMPT-mediated immune regulation in chronic inflammatory diseases.

PTMs, particularly phosphorylation, provide an additional layer of regulation for NAMPT activity, influencing protein function, enzymatic activity, subcellular localization, secretion, and protein-protein interactions. While some modifications, such as histidine 247 autophosphorylation and lysine 53 deacetylation, have been described, many phosphorylation sites remain unexplored. Characterizing these modifications will provide critical insight into the regulation of eNAMPT activity and its function as an extracellular cytokine in inflammatory conditions.

Finally, this thesis evaluates the therapeutic potential of ALT-100, a humanized monoclonal antibody that neutralizes eNAMPT. Using preclinical models of DNBS-induced Crohn's disease and DSS-induced colitis, the efficacy of ALT-100 is assessed in reversing disease phenotypes and reducing inflammation. Developed by Dr. Joe G.N. Garcia (Aqualung Therapeutics®) and currently in Phase 2A for ARDS treatment, ALT-100 represents a promising candidate for targeted therapy in chronic immune mediated gastrointestinal disorders.

Collectively, this thesis aims to provide: (i) a comprehensive understanding of eNAMPT's contribution to AAG and IBD pathogenesis, (ii) elucidate the molecular regulation of NAMPT through phosphorylation, (iii) characterize its effects on hematopoietic cells, and (iv) evaluate the therapeutic potential of ALT-100, ultimately advancing strategies for the treatment of chronic immune-mediated gastrointestinal diseases.

3. MATERIALS AND METHODS

This chapter describes the experimental approaches and methodological strategies employed throughout the present doctoral research. In the first part, attention is focused on the procedures, models, and analytical techniques used to investigate the pathophysiological mechanisms underlying Autoimmune Atrophic Gastritis. In the second part, the experimental methods used to assess the role of eNAMPT in the progression of Inflammatory Bowel Disease are illustrated, together with the techniques employed to evaluate its effect on hematopoietic stem cells and the therapeutic potential of the ALT-100 monoclonal antibody. Finally, the methodological approaches applied to investigate how NAMPT phosphorylation influences protein localization, enzymatic activity, oligomeric state, and receptor interaction are presented. Collectively, these sections provide a comprehensive overview of the experimental design, ensuring clarity, reproducibility, and contextual understanding of the results discussed in subsequent chapter.

3.1 EXPERIMENTAL APPROACHES IN THE STUDY OF AAG

3.1.1 RNA EXTRACTION FROM GASTRIC BIOPSIES AND FIBROBLASTS

Biopsies, generously provided by Prof. Di Sabatino's group, were sonicated, and total RNA was extracted using the RNeasy Mini Kit (QIAGEN®, Cat.No. 74106) according to the manufacturer's protocol. Cells were lysed in Buffer RLT supplemented with 1% β-mercaptoethanol. An equal volume of 70% ethanol was added to the lysate, and the mixture was applied to RNeasy Mini spin columns. Columns were washed sequentially with Buffer RW1 and Buffer RPE, and a final dry spin was performed. RNA was eluted in 20 µl of RNAse-free water.

After isolation, fibroblasts were cultured in Medium C until reaching confluence. HC derived fibroblasts were treated with recombinant human NAMPT (500 ng/ml, Adipogen®), and RNA extracted as previously described.

RNA concentration and purity were assessed spectrophotometrically at 260 nm using the NanoReady FC-3100. Samples were considered suitable for downstream applications if the A260/A280 ratio was ≥1,8-2,0 and the A260/A230 ratio was ≅ 1,7, indicating minimal contamination.

3.1.2 RNA SEQUENCING FROM BIOPSY SAMPLES

Total RNA from biopsy samples was sequenced by Lexogen (Vienna, Austria). RNA was shipped following the manufacturer's guidelines.

Libraries were prepared using the QuantSeq 3' mRNA-Seq Library Prep Kit (Lexogen®) and sequenced on the Illumina NextSeq 500 platform. Raw sequencing data were normalized to library size. Differential gene expression analysis was performed with DESeq (v2.21) using thresholds of FDR < 0,05 and absolute fold change > 1 to identify differentially expressed genes (DEGs). Functional enrichment of DEGs was conducted using DAVID (v6.8) and Panther Classification System (v12.0) to identify significantly represented biological pathways, processes, and functional categories.

3.1.3 FIBROBLASTS ISOLATION

A protocol for the isolation of fibroblasts from gastric body biopsies was established and optimized in our laboratory. Fibroblasts were isolated from biopsies obtained from healthy controls (HC) and AAG patients. For tissue dissociation, biopsies were incubated in HBSS medium without $Ca^{2+/}Mg^{2+}$, supplemented with 0,04% EDTA and 1% penicillin-streptomycin, under gentle agitation at 37°C for 1 hour. The suspension was filtered through a 100 μm cell strainer, and residual fragments were resuspended in Medium A (RPMI 1640, 10% FBS, 1% L-glutamine, 2% penicillin/streptomycin, 0,25% gentamicin) containing 1mg/ml collagenase A and 50 ng/ml DNase. Enzymatic digestion was performed for 2 hours at 37°C with vigorous agitation. Post-digestion, the cell suspension was filtered, centrifuged at 1500 rpm for 10 minutes, and if necessary, subjected to red blood cell lysis. The pellet was resuspended in Medium C (DMEM + GlutaMAX™, 20% FBS, 1% MEM, 2% penicillin/streptomycin, 0,25% gentamicin, 0,4% amphotericin B), and cell viability was assessed. Cells were seeded according to yield and cultured in Medium C, with medium replacement after 24 hours to enrich fibroblasts. Cultures were maintained at 37°C in a humidified incubator with 5% CO_2.

3.1.4 CELL VIABILITY AND PROLIFERATION ASSAY

Fibroblast's viability and proliferation were assessed using the MTT colorimetric assay, based on the reduction of the yellow tetrazolium salt MTT to insoluble purple formazan crystals by NAD(P)H-dependent cellular oxidoreductases in metabolically active cells. For

the assay, 15.000 cells per well were seeded, and metabolic activity was evaluated at 24, 48, 72 and 96 hours. At each time point, cells were washed with Locke's buffer (140 mM NaCl, 5 mM KCl, 10 mM HEPES, 10 mM glucose, 1,2 mM $MgCl_2$, 2,2 mM $CaCl_2$, pH 4,7). Subsequently, MTT prepared in Locke's buffer was added, and cells were incubated at 37°C in the dark for 2 hours. After incubation, isopropanol containing 0,1 M HCl and 1% Triton X-100 was added, and formazan crystals were solubilized. Absorbance was measured at 575 nm using an INNO-S spectrophotometer.

3.1.5 CELL MIGRATION ASSAY

Fibroblast's migratory capacity was assessed using the wound healing assay. Fibroblasts were seeded and cultured in Medium C until reaching confluence. Once a monolayer was established, a linear scratch was made. HC fibroblasts received recombinant human NAMPT (AdipoGen®) at 500 ng/ml. Images of the wound area were acquired at 0, 24, 48, and 72 hours. Quantitative analysis of wound closure was performed by measuring the residual gap area (%) at each time point using the ImageJ® software.

3.1.6 FIBROBLAST'S PHENOTYPIC CHARACTERIZATION

Fibroblast's phenotypic characterization was performed using immunocytochemistry. Fibroblasts were seeded in Medium C at 10.000 cells per coverslip, previously coated with Poly-L-Lysine (100 μg/ml), and were cultured for 48-72 hours before fixation. Fixation was performed with 4% paraformaldehyde (PFA) in PBS for 15 minutes at 4°C. Cell permeabilization was achieved by incubation with 0,1% Triton X-100 in PBS for 10 minutes at room temperature (RT). Non-specific antibody binding was blocked using 2% BSA. Primary antibody incubation was performed overnight (o/n) at 4°C using anti-Alpha-Smooth Muscle Actin (α-SMA, monoclonal mouse, 2,5 μg/ml; Invitrogen®) in PBS with 0,2% BSA. Coverslips were then incubated with the Alexa Fluor 488-conjugated goat anti-mouse secondary antibody (2 μg/ml; Invitrogen®) for 45 minutes at RT in the dark. Nuclei were counterstained with Hoechst 33342 for 15 minutes. Coverslips were mounted on slides with ProLong™ Gold Antifade Reagent (Invitrogen®), allowed to cure o/n in the dark, and visualized using LEICA TCS SP8 X confocal microscope. Images were analyzed with LAS X Life Science Software.

3.1.7 NAMPT EXPRESSION

NAMPT expression in fibroblasts was evaluated by Western Blot.
Cultured fibroblasts were lysed in RIPA buffer (50 mM Tris-HCl, pH7,2, 150mM NaCl, 0,5 mM EDTA, 0,1% NP-40) supplemented with protease and phosphatase inhibitor cocktail. Lysis was facilitated by mechanical disruption. Following incubation on ice for 15 minutes, lysates were clarified by centrifugation and total protein concentration was determined using the Bradford assay. Proteins were loaded onto 10% polyacrylamide gel and subsequently transferred onto nitrocellulose membrane using the Trans-Blot Turbo Transfer System (BioRad®). Membranes were incubated o/n at 4°C with a mouse anti-NAMPT primary antibody (AdipoGen®) and then with a secondary anti-mouse antibody (BioRad®). Protein bands were detected using the ChemiDoc MP system and analysed with ImageLab Touch software (BioRad®). Band intensities were normalized to two reference proteins: β-actin and α-SMA.

3.1.8 GENE EXPRESSION PROFILING

Gene expression profiling of fibroblasts was performed in collaboration with Prof. Elisabetta Panza (University of Naples "Federico II"). Total RNA from HC- and AAG- derived fibroblasts was reversed-transcribed into cDNA according to the manufacturer's instructions (QIAGEN® RT^2 First Strand Kit). cDNA was then loaded onto an RT^2 Profiler PCR Array plate (QIAGEN®, PAHS-120Z, Cat. No. 330231), containing 96 genes related to inflammatory and fibrotic pathways, along with housekeeping genes and internal quality controls. PCR amplification was carried out using RT^2 SYBR Green qPCR Mastermix (QIAGEN®, Cat. No. 330529) on a CFX Opus 96 thermocycler (BioRad®) under recommended cycling conditions. Ct values were exported and analyzed via QIAGEN® GeneGlobe. Gene expression was normalized to housekeeping genes using ΔCt method, and relative expression changes (ΔΔCt) were calculated as the difference between test and control ΔCt values. Fold changes were computed as 2^(-ΔΔCt), with values > 1 indicating upregulation and < 1 indicating downregulation. Statistical significance was assessed using two-tailed, unpaired Student's t-tests on 2^(-ΔCt), assuming equal variance, with $p < 0,05$ considered significant.

3.2 EXPERIMENTAL APPROACHES IN THE STUDY OF IBD

3.2.1 PRODUCTION OF RECOMBINANT NAMPT

Recombinant NAMPT used in this study was produced in-house using ClearColi BL21 cells, genetically engineered to eliminate the endotoxin activity of LPS on human cells. Bacterial cells were transformed by electroporation with the pET28 plasmid containing the NAMPT coding sequence fused to an N-terminal His-tag and grown in commercial 2xTY medium. Protein expression was induced by the addition of IPTG (0,3 mM). Following bacterial lysis, NAMPT was purified using nickel affinity chromatography, and its purity was confirmed by Western Blot analysis. Endotoxin contamination was assessed and excluded using the ToxinSensor™ Cromogenic LAL Endotoxin Assay Kit (GenScript®).

3.2.2 ANIMAL MODELS

All animal procedures in this study were approved by the Animal Ethics Committee of the University of Pavia (protocol No. 120/2018 DB064.27 dated 07/10/2017;8751/2024). Male BALB/c or C57BL/6 mice aged 8-10 weeks and weighing approximately 25 g were purchased from Charles River Laboratories.

Animals were housed in individually ventilated cages under controlled environmental conditions (temperature 22-25°C; relative humidity 50-60%) with a 12 hours light/dark cycle. Food and water were provided ad libitum throughout the experimental period. Experimental treatment protocols were initiated following a 7-days quarantine and acclimatization period. In accordance with current animal welfare regulations and the principles of the 3Rs, mice were euthanized at the end of the experimental period by cervical dislocation. Death was confirmed by the absence of cardiac activity.

3.2.3 DNBS MODEL

Acute intestinal inflammation was induced by intrarectal administration of dinitrobenzenesulfonic acid (DNBS), which modifies colonic proteins and elicits a Th1-driven immune response via NK-kB activation, producing a pathology resembling Crohn's disease (e.g., severe diarrhea, rectal bleeding, intestinal wall thickening, reduced colon length, and weight loss). DNBS was dissolved in a 1:1 mixture of ethanol and 0,9% NaCl and administered at 2 mg/mouse (moderate disease) or 3 mg/mouse (severe disease), based

on preliminary dose-response studies. Mice were anesthetized with isoflurane (0,5%-3%, maintained at 2%) in an induction chamber, and 100 µl of DNBS solution was delivered into colon using a disposable gavage needle (38 mm, 1,6 mm diameter). Control animals (CTRL) received vehicle only. To prevent reflux, animals were held in a supine Trendelenburg position for 90 ≥ s post-instillation. Animals were monitored for 5 days, during which clinical parameters were evaluated daily.

3.2.4 NAMPT TREATMENT

During the 5-days monitoring period, mice in the treatment group received a daily intraperitoneal (i.p.) injection of 50 µg of recombinant NAMPT dissolved in 100 µl of physiological saline. Control (sham) mice were administered 100 µl of physiological saline alone under the same conditions to exclude potential effects related to injection-induced stress.

3.2.5 ACUTE DSS MODEL

Acute intestinal inflammation was chemically induced in 8-weeks-old C57BL/6 mice by administering 2,5% DSS in drinking water for 7 days, followed by a washout period of three days. Dextran Sulfate Sodium (DSS) disrupt the colonic epithelial barrier, promoting immune cell infiltration and mucosal inflammation producing a pathology resembling ulcerative colitis (e.g., diarrhea, rectal bleeding, reduced colon length, and weight loss). Animals were divided into three experimental groups: sham, DSS, DSS + ALT-100 (1 mg/kg).

3.2.6 CHRONIC DSS MODEL

In collaboration with the Scripps Institute, University of Florida, chronic inflammation was induced in 8-weeks-old C57BL/6 mice by administering 2% DSS in drinking water for 7 days, followed by a 12-days washout period, and a second 7-days DSS cycle. After an additional 3 days washout, mice were sacrificed, for a total duration of 28 days. Throughout the experiment, mice received intraperitoneal injections of the monoclonal antibody ALT-100 every 7 days at doses of 1 mg/kg or 4 mg/kg, according to preliminary data. Two control groups were added: one that received no treatment (sham) and another that was administered

PBS intraperitoneally.

3.2.7 ALT-100 TREATMENT

Concurrently with DNBS- and DSS-induced colitis, animals received subcutaneous (s.c.) injections of the monoclonal antibody (mAb) ALT-100, kindly provided by Dr. Garcia (Aqualung Therapeutics), at two different doses: 1 mg/kg or 4 mg/kg. Control (sham) animals were administered 100 µl of physiological saline or PBS per mouse via the same route.

3.2.8 ISOLATION OF *LAMINA PROPRIA* CELLS

Colons were open longitudinally, cut into 1 cm pieces, and incubated twice in 20 ml HBSS containing 2,5 mM EDTA on a rotating shaker at RT for 20 minutes (35-40 rpm) to remove epithelial cells. After each incubation, tissue fragments were filtered, collected, and transferred to fresh EDTA buffer. Fragments were then transferred to HBSS containing 5 mM $CaCl_2$ to neutralize EDTA prior enzymatic digestion. Tissues were minced into 1 mm pieces and incubated in 10 ml HBSS supplemented with collagenase/dispase (1 mg/ml), DNase (40 µg/ml), and collagenase IV (250 µg/ml) for 40 minutes under rotation (35-40 rpm) at RT. The resulting cell suspension was sequentially filtered through 100 µm and 70 µm strainers, each followed by washing with RPMI-1640. Cells were pelleted by centrifugation (1450 rpm, 8 minutes, 4°C), resuspended in 1 ml FACS buffer (HBSS, 0,5% FBS, 1mM EDTA), and counted. A total of 5 x 10^5 cells were plated per well in round-bottom 96-well plates for antibody staining and subsequent flow cytometric analysis.

3.2.9 ISOLATION OF PERIPHERAL BLOOD CELLS

Peripheral blood was collected from each mouse via intracardiac puncture and immediately mixed with 100 µl of 0,5 M EDTA to prevent coagulation. To lyse red blood cells, 100 µl of whole blood was dispensed into round-bottom 96-well plates and incubated with an equal volume of ACK lysis buffer (150 mM NH_4Cl, 170 mM Tris, pH 7,7). Samples were incubated on ice for 30 minutes and subsequently centrifuged at 1200 rpm for 10 minutes at 4°C. This step was repeated until complete erythrocyte removal, yielding a white cell pellet, which was resuspended in 100 µl of FACS buffer.

3.2.10 ISOLATION OF BONE MARROW CELLS

Bone marrow was isolated from the femur and tibia of both hind limbs. Residual muscle and adipose tissues were removed using PBS-soaked gauze. Femur and tibia were separated by gentle torsion at the knee joint and PBS was flushed through the marrow cavity to extrude the bone marrow. The resulting cell suspension was centrifuged at 1200 rpm for 5 minutes at RT. After supernatant removal, the pellet was resuspended in 1 ml of ACK lysis buffer and incubated for 10 minutes at RT. Subsequently, 5 ml of PBS was added to neutralize the lysis buffer, and the sample was centrifuged again under the same conditions. Following supernatant removal, the pellet was resuspended in 1 ml of FACS buffer. A total of 5 x 10^5 cells were plated per well in round-bottom 96-well plates for antibody staining and subsequent flow cytometric analysis.

3.2.11 FLOW CYTOMETRY (FACS)

Before staining, isolated cells from *lamina propria*, bone marrow, and blood were subjected to nonspecific binding blocking with 10 µl of Fc-blocking solution (10% v/v in FACS Buffer) on ice for 5 minutes, except for hematopoietic stem cell precursors. Cells were then incubated with 50 µl of antibody cocktail in a 1:1 mixture of FACS buffer and Brilliant Stain Buffer (BD Horizon®) for 30 minutes on ice in the dark. Following staining, cells were washed twice with 100 µl FACS buffer (1200 rpm, 5 minutes, RT), fixed with 1% PFA for 15 minutes on ice, and washed twice more. Specific anti-mouse antibodies (Table 3) were used to identify hematopoietic progenitors, myeloid cells, T cells, and B cells. Antibodies included CD34, Sca-1, CD117, CD86, CD206, CD45 B220, F4/80, Ly6G, CD3, CD4, CD8 (1:100); Ly6C and CD11b (1:200); Lineage cocktail (20 µl/sample); and Vitality dye (1:1000). Data were acquired using a BD FACSLyric™ Flow Cytometer (BD Biosciences®) at the Centro Grandi Strumenti (CGS), University of Pavia.

Cell Type	Antibody	Fluorochrome	Laser (nm)
B Cells	CD45 B220	FITC	488
	Vitality dye	APC-Cy7	640
T Cells	CD45	FITC	488
	CD3	PerCP-Cy5.5	488
	CD8	V500-C	405
	CD4	APC	640
	Vitality dye	APC-Cy7	640
Hematopoietic Precursors	Lineage cocktail	APC	640
	Sca-1	BV786	405
	CD34	PE	488
	CD117	V450	405
	CD16	FITC	488
	Vitality dye	APC-Cy7	640
Myeloid Cells	CD45	FITC	488
	CD11b	APC	640
	Ly6G	V500-C	405
	Ly6C	PE-Cy7	488
	F4/80	APC	640
	CD86	PerCP-Cy5.5	488
	CD206	PE	488
	Vitality dye	APC-Cy7	640

Table 3. Summary of the antibody panels used for FACS analysis. The table lists the specific anti-mouse antibodies, corresponding fluorochromes, and excitation lasers (nm) employed to identify distinct immune cell populations, including B cells, T cells, hematopoietic precursors, and myeloid cells.

3.2.12 IMMUNOHISTOCHEMICAL ANALYSIS (IHC)

For immunohistochemical analysis, following removal of sigmoid portion, colons were rolled into histology cassettes, with the proximal end oriented toward the center of the spiral. The cassettes containing the samples were fixed in 20% formalin for 24 hours at RT. After fixation, samples were transferred to 80% ethanol and submitted to Cogentech (IFOM, Milan) for IHC analyses.

3.2.13 COLONY-FORMING UNIT (CFU) ASSAY

To assess the clonogenic potential of hematopoietic stem and progenitor cells (HSPCs), we established and optimized a colony-forming unit (CFU) assay using MethoCult™ semisolid medium (STEMCELL™ Technologies).

The protocol was first optimized using bone marrow cells isolated from healthy untreated mice (sham controls). Various conditions were tested to achieve optimal colony growth and medium stability. The final protocol employed 50.000 cells per 35 mm culture dish, which provided an even cellular distribution and prevented medium desiccation during incubation. Following optimization, the CFU assay was applied to bone marrow cells isolated from 4 experimental groups: (i) healthy untreated mice (controls), (ii) mice with moderate DNBS-induced intestinal inflammation, (iii) DNBS-treated mice receiving recombinant NAMPT, and (iv) mice with severe DNBS-induced inflammation. The aim was to assess the clonogenic capacity of bone marrow cells in the presence or absence of stimulatory factors, specifically: recombinant NAMPT (500 ng/ml), IL-6 (10 ng/ml), and hematopoietic cytokines (G-CSF 20 ng/ml, GM-CSF 50 ng/ml) alone or in combination. Cells were incubated at 37°C in a 5% CO_2 atmosphere for 7 days. At the end of the incubation period, hematopoietic colonies were counted.

3.2.14 STATISTICAL ANALYSIS

Flow cytometry data were analyzed using FlowJo software (license code 107152-100). Statistical analyses were performed with GraphPad Prism software. Prior to assessing statistical significance, a normality test was conducted to determine data distribution. Based on the results, either a Student's t-test, a paired t-test, or a non-parametric Wilcoxon-Mann-Whitney test was applied, as appropriate. Data were considered statistically significant for p-values < 0,05 (*), 0,01 (**), 0,001 (***).

3.3 EXPERIMENTAL APPROACHES IN THE STUDY OF PTMs

3.3.1 CELL CULTURE

For *in vitro* experiments, murine melanoma B16 cells were used. These adherent cells were cultured in DMEM with high glucose, supplemented with 10% FBS, 1% penicillin-streptomycin, and 1% L-glutamine at 37°C in a humidified atmosphere containing 5% CO_2.

3.3.2 GENERATION OF MUTANT CELL LINES

Four mutant B16 murine melanoma cell lines were generated through lentiviral transduction, designed to over-express either wild-type (WT) NAMPT or its mutated variants. The murine NAMPT gene was amplified using the following primers:

FW: 5'-CGAGATCTAATGCTGCGGCAGAAGCC;

RW: 5'-CGGTCGACCTAATGAGGTGCCACGTCCTG.

The amplified product was cloned (BglII/SalI) into the pEGFP-C1 vector. Subsequently, the NAMPT-GFP fusion was subcloned (Xbal/SalI) into the bicistronic pLV-IRES-GFP vector. Correct insertion and sequence integrity were verified by DNA sequencing. The mutant forms of NAMPT (NAMPT S199A, NAMPT S200A, NAMPT S472A) were generated from the NAMPT WT construct using site-directed mutagenesis (QuikChange XL II kit, Agilent Stratagene). The primer sequences used for mutagenesis are reported in table 4:

Mutation	**FW Primer (5'→3')**	**RW Primer (5'→3')**
S199A	TGGTTACAGAGGAGTCG CTTCGCAAGAGACTGC	GCAGTCTCTTGCGAAGCGA CTCCTCTGTAACCA
S200A	CAGTCTCTTGCGCAGAGA CTCCTCTGTAACCAAAGT	ACTTTGGTTACAGAGGAG TCTCTGCGCAAGAGACTG
S472A	TTTTTCTGACTTCATCAAA TGCGTAGCTTTTTGTCACCTTCCC	TGGTTACAGAGGAGTC GCTGCGCAAGAGACTGCTGG

Table 4. Primers used for the generation of NAMPT mutant constructs. Forward and reverse primers designed for site-directed mutagenesis to obtain NAMPT S199A, NAMPT S200A, NAMPT S472A variants.

B16 cells were stably engineered to express NAMPT fused to GFP at the N-terminal region.

3.3.3 IDENTIFICATION OF PHOSPHORYLATION SITES

To obtain purified murine NAMPT, immunoprecipitation was performed using GFP-Trap agarose beads. For phosphosite identification, B16 cells were serum-starved for 4 hours, then lysed in RIPA buffer supplemented with protease and phosphatase inhibitor cocktail. Lysates were centrifuged at 13.000 rpm for 10 minutes at 4°C, and the resulting supernatant incubated o/n at 4°C with GFP-Trap agarose beads. After incubation, the beads were pelleted, washed four times with cold IP buffer, and bound proteins were eluted with 0,2 M glycine (pH 2.5). Phosphorylated peptides were identified by the group of Prof. Wohlschlegel (UCLA) using LC-MS/MS analysis. The samples were analysed with a Dionex Ultimate 3000 ultra-high-pressure liquid chromatography system (Thermo Scientific®) coupled to an Orbitrap Fusion™ Tribrid™ mass spectrometer (Thermo Scientific®) equipped with a Phoenix Nimbus ion source (Phoenix S&T®).

3.3.4 MUTANTS PURIFICATON

For the production and purification of recombinant mutated NAMPT proteins, the same methodological approach described previously in paragraph 3.2.1 was employed. Briefly, protein variants were expressed in ClearColi and subsequently purified through affinity chromatography. The identical purification strategy allowed for direct comparison of the biochemical and biophysical properties between the WT and mutated NAMPT forms.

3.3.5 ENZYMATIC ACTIVITY ASSAY

The enzymatic activity of WT and mutated recombinant NAMPT was evaluated via its role in NADH synthesis in the presence of ATP and substrates. NADH production was measured spectrophotometrically at 340 nm. The reaction was performed in HEPES buffer containing NAM (30 mM), PRPP (50 mM), ATP (12,5 mM), ADH/BSA, $MgCl_2$ (1M), DTT (100 mM), 1 μg NMNAT, and 1 μg NAMPT. Absorbance was recorded using Synergy HT spectrophotometer (BioTek®).

3.3.6 CELL VIABILITY ASSAY

Mutant cell lines viability was assessed using the MTT assay as described in paragraph 3.1.4. 25.000 cells were seeded and cultured in complete DMEM. Cell growth was evaluated at 0,

24, 48, and 72 hours. At each time point, cells were washed with Locke's buffer and then incubated with MTT solution. Formazan crystals were solubilized and absorbance was read at 575 nm using a Synergy HT spectrophotometer (BioTek®).

3.3.7 CELLULAR LOCALIZATION

Cellular localization of WT and mutated NAMPT was assessed by immunofluorescence as previously described in paragraph 3.1.6. Briefly, 20.000 cells were seeded and growth in DMEM for two days. Cells were washed, fixed and permeabilized with 80% ethanol. Nuclei were stained with Hoechst and coverslips were mounted with Mowiol® 4-88 (Calbiochem®). Images were acquired using a Carl Zeiss™ Axio Vert.A1 FL-LED microscope.

3.3.8 ASSESSMENT OF NAMPT EXPRESSION AND RELEASE

To evaluate whether the introduced mutations affected NAMPT expression and release, Western Blot assays were performed. For analysis, 250.000 cells were seeded in complete DMEM and cultured for 24 hours without reaching confluence. The medium was then replaced with serum-free DMEM to induce nutrient deprivation. To assess NAMPT release, the supernatant was collected and concentrated using Amicon® Ultra centrifugal filters with a 30 kDa cut-off by repeated centrifugation at 8.000 rpm, 4°C, for 8 minutes. Samples were loaded onto 10% polyacrylamide gels. For intracellular NAMPT analysis, cells were lysed as previously described in paragraph 3.1.7 and protein quantified. 50 μg of protein were loaded on 10% polyacrylamide gels. After electrophoresis, proteins were transferred to nitrocellulose membranes, and Western Blot analysis was performed as previously described. Anti-NAMPT and anti-actin antibodies were used.

3.3.9 BLUE NATIVE GEL ELECTROPHORESIS

To determine the oligomeric state of the various NAMPT mutant forms, we established and performed native gel electrophoresis protocol in the presence of Coomassie Blue G-250. To facilitate the migration of non-denatured proteins, a 6% polyacrylamide gel in the absence of denaturing agents was used. Dry wells were loaded with 50 μg of protein and filled with cathode buffer (0,15 mM Bis-Tris, 5mM Tricine, 0,002% Coomassie Blue G-250, pH 7). Cathode buffer was also added to gel support, while the remainder of the running cassette was filled with anode buffer (5 mM Bis-Tris, pH 7). Electrophoresis was performed at 140V

for 4 hours. Protein bands were then transferred on nitrocellulose membranes and Western Blot was performed as previously described.

3.3.10 GEL FILTRATION CHROMATOGRAPHY

Protein samples were concentrated to 3 mg/ml using 30 kDa Amicon® Ultra centrifugal filters pre-equilibrated with storage buffer (50 mM NaH_2PO_4, 0,5 mM β-mercaptoethanol), and centrifuged at 3.000 rpm for 10 minutes at 4°C. WT and mutant NAMPT proteins at the desired concentration were analyzed by size-exclusion chromatography to assess their aggregation state. Separations were performed on an analytical Superdex® 200 Increase 5/150 GL column equilibrated with 0,05 M K_2HPO_4 buffer (pH 7,2). Samples (20 µl) were injected and eluted at 0,2 ml/min under 1,5 MPa column pressure.

3.3.11 EVALUATION OF PRO-INFLAMMATORY CYTOKINE ROLE OF MUTANT NAMPT FORMS

Murine peritoneal macrophages (PECs) were isolated from C57BL/6 mice by inducing inflammation through intraperitoneal injection of 1 ml 3% (w/v) thioglycolate. After 5 days, mice were euthanized, PECs were collected by peritoneal lavage with PBS, centrifuged at 1.200 rpm for 8 minutes, and treated with ACK red blood cell lysis buffer. Cell number was determined using Türk's reagent, and 3 x 10^6 cells were seeded and incubated at 37°C for 1 hour in complete RPMI medium. After cellular adhesion cells were treated with recombinant WT or mutated NAMPT (500 ng/ml), alone or combined with IFN-γ (200 U/ml), for 3 hours in serum-free RPMI medium. Cells were then lysed, total RNA was extracted and reverse-transcribed into cDNA, and qPCR was performed using the CFX Opus 96 system (BioRad®) to evaluate pro-inflammatory gene expression (IL-6, IL-1β, CXCL10).

4. RESULTS

4.1 THE ROLE OF NAMPT IN AUTOIMMUNE ATROPHIC GASTRITIS

4.1.1 DIFFERENTIAL GENE EXPRESSION IN AAG BIOPSIES

Our primary objective was to identify gene expression differences in patients with Autoimmune Atrophic Gastritis to uncover novel pathways involved in disease pathogenesis and potential therapeutic targets. To this end, in collaboration with Prof. Antonio Di Sabatino, gastric body biopsies were obtained from healthy controls (HC, n=10) and AAG patients (AAG, n=10). After RNA extraction, samples were subjected to gene expression profiling by bulk RNA sequencing (Lexogen), and data analysis was performed by Dr. Ilaria Massaiu (Istituto Cardiologico Monzino). Transcriptomic analysis revealed a marked alteration in gene expression profiles in AAG samples compared with healthy controls, with 858 genes significantly upregulated and 577 genes downregulated in AAG patients (Fig. 18).

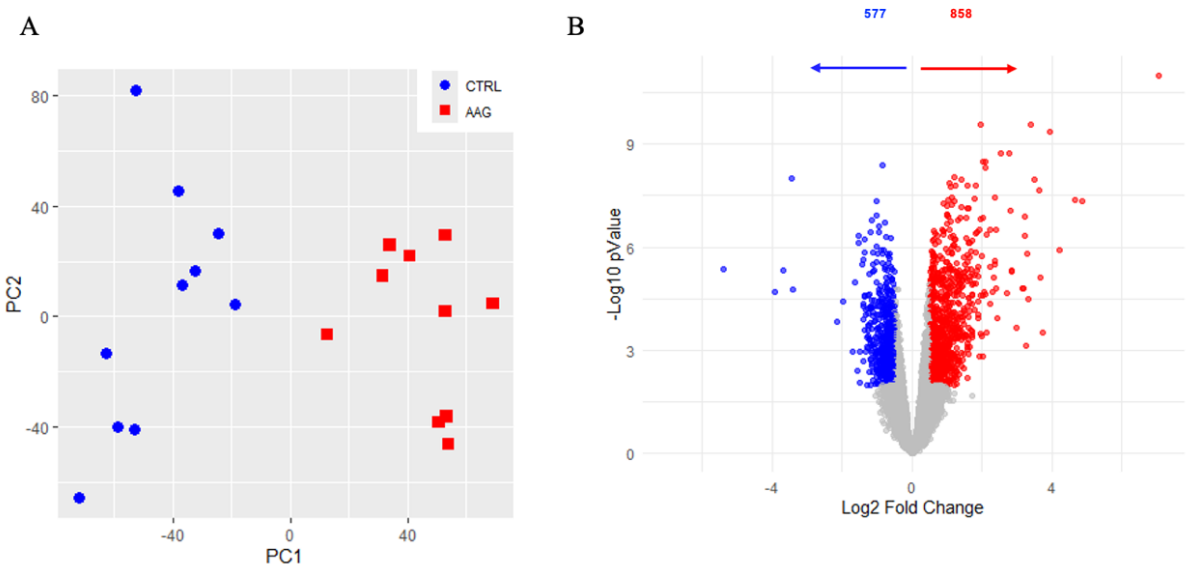

Figure 18. Gene expression in AAG biopsies. (**A**) Principal Component Analysis (PCA) between HC (blue) and AAG (red) samples. (**B**) Volcano plot showing differentially expressed genes between AAG patients and healthy controls (HC). Differentially expressed genes (DEGs) were defined as those with p< 0,05 and logFC > 0,5.

Detailed transcriptomic analysis identified several genes potentially involved in fibrosis, extracellular matrix remodeling, and chronic inflammatory response, key processes in the pathophysiology of AAG (Fig. 19). Among the upregulated genes (Fig. 19A), ONECUT3, BPIFB1, MUC6, MUC5B, and SLC28A2 were prominent, associated with intestinal

metaplasia, mucin production, and ion channel regulation. Conversely, several genes essential for gastric function were markedly downregulated (Fig. 19B), including PGA5, PGA3, CHIA, and PSAPL1 consistent with the loss of parietal cell activity. With respect to tissue remodeling and fibrotic mechanisms, INHBB, IL1B, and IL11 were significantly downregulated. This reduced expression may reflect a disruption in the balance between pro- and anti-fibrotic signaling during AAG progression. Additionally, SERPINB8 and TTC7B, both downregulated, have been associated with cell differentiation, tumor suppression, and tissue remodeling processes.

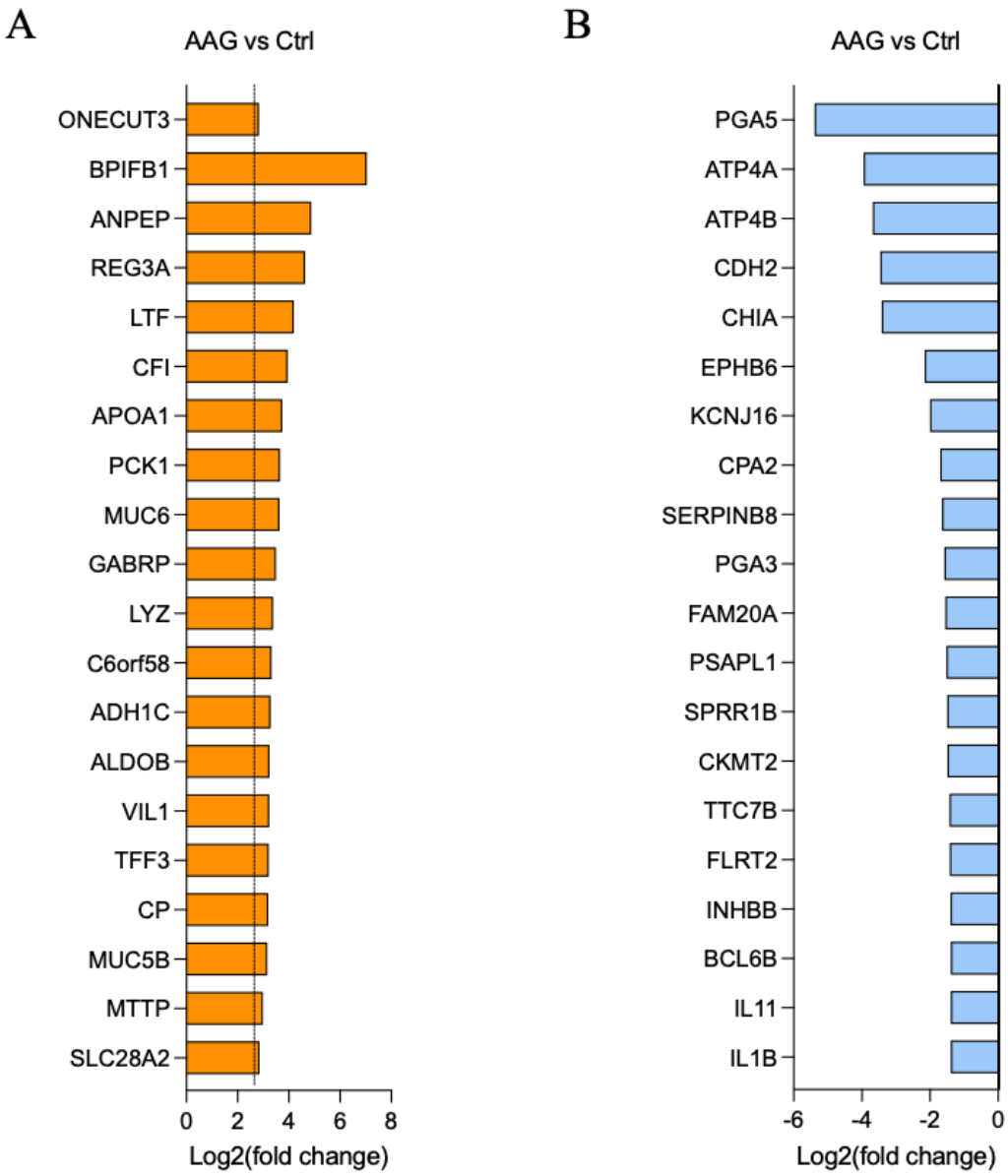

Figure 19. AAG gene expression profile. (**A**) Up-regulated, and (**B**) down-regulated genes in AAG *vs* HC.

Collectively, these findings indicate that AAG is characterized by a pronounced dysregulation of genes involved in cell differentiation, immune responses, and tissue remodeling, with potential implications for gastric fibrosis and intestinal metaplasia.

To gain an overview of the biological processes altered in AAG, Gene Set Enrichment Analysis (GSEA) was performed by comparing gene expression profiles from gastric biopsies of AAG patients and healthy controls (HC) (Fig. 20). The analysis revealed significant enrichment of immune- and inflammation- related pathways in AAG samples, including humoral and organ-specific immune responses and chronic inflammatory processes (Fig. 20A). Molecular function analysis further highlighted increased activity of genes encoding structural extracellular matrix (ECM) proteins, consistent with enhanced matrix deposition and remodeling (Fig. 20B).

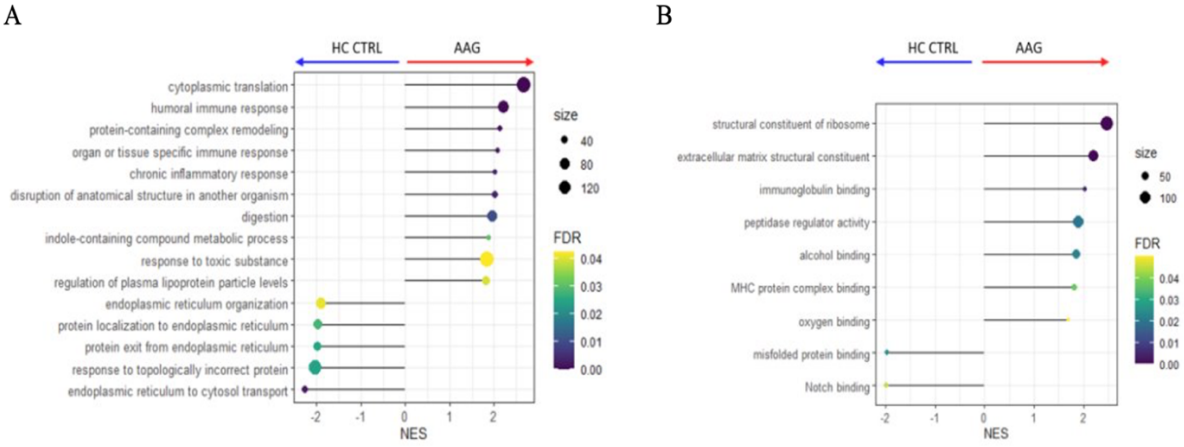

Figure 20. Gene Set Enrichment Analysis (GSEA). (**A**) Main dysregulated biological processes, and (**B**) principal deregulated molecular functions in AAG. The size of each dot indicates the number of genes involved in the pathway, while the color represents the false discovery rate (FDR) value.

These findings suggest aberrant activation of tissue remodeling mechanisms, prompting further investigation into the role of resident mesenchymal cells, particularly gastric fibroblasts, in AAG pathogenesis.

4.1.2 ROLE OF FIBROBLASTS IN AAG PROGRESSION

To investigate the potential involvement of fibroblasts in the pathogenesis of AAG, this study aimed to optimize a protocol for the isolation of fibroblasts from gastric body biopsies. This approach enabled the establishment of primary fibroblast cultures from both AAG patients and HCs (Fig. 21), which were subsequently used for morphological, functional, and immunocytochemical characterization studies.

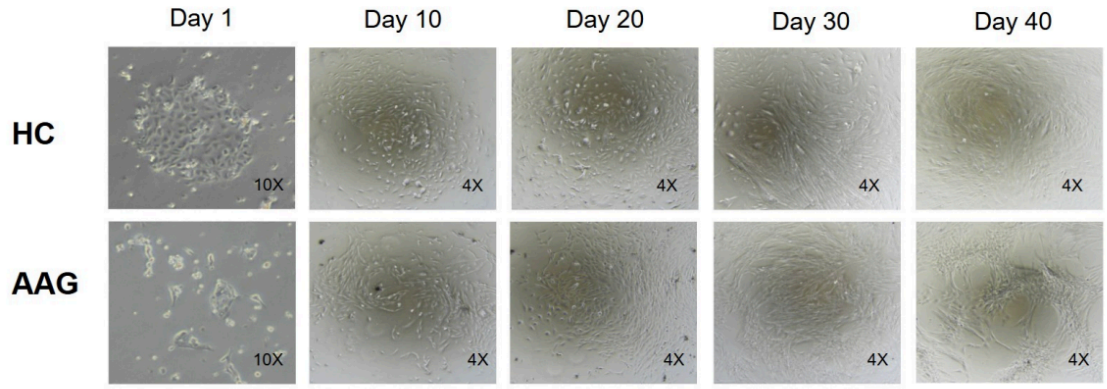

Figure 21. Fibroblasts derived from gastric bodies of AAG and HC growth. Representative images of in *vitro* growth of gastric fibroblasts from HC (top) and AAG (bottom) at 1, 10, 20, 30, and 40 days after isolation. Images were acquired at 10x and 4x magnification.

Immunocytochemical analysis using an anti-α-smooth muscle actin (α-SMA) antibody was performed to confirm fibroblast identity. Confocal microscopy revealed α-SMA expression in most cells from both groups, with AAG-derived fibroblasts showing more intense and homogeneous staining (Fig. 22A).

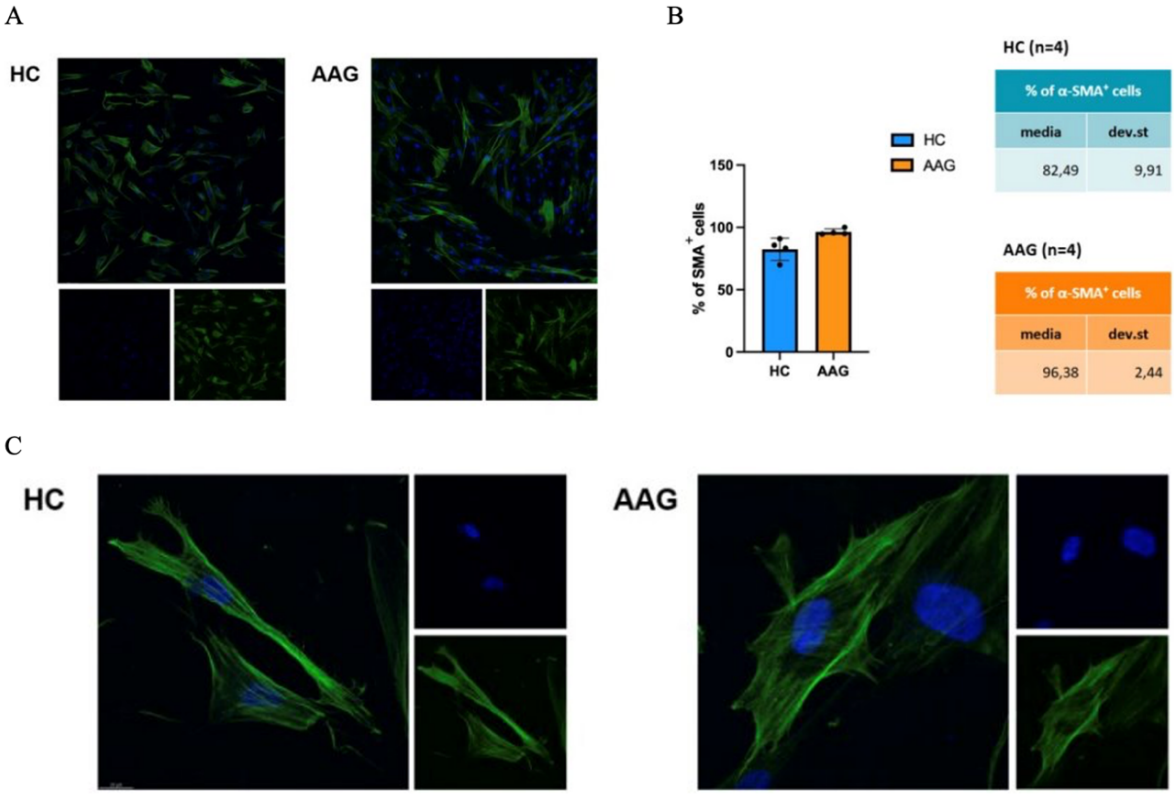

Figure 22. Phenotypic characterization of fibroblasts. (**A**) Representative images showing α-SMA expression in fibroblasts derived from HC and AAG patients. Lower panels display individual channels for DAPI (nuclei) and FITC (α-SMA). (**B**) Quantification of α-SMA$^+$ cells in HC and AAG derived fibroblasts. (**C**) High-magnification images highlighting cell morphology and actin cytoskeletal organization in the two groups. Images obtained using a LEICA TCS SP8 X confocal microscope, 40x objective.

Quantitative analysis indicated a higher proportion of α-SMA$^+$ cells in AAG fibroblasts (96.38%) compared with HC fibroblasts (82.49%) (Fig. 22B), suggesting a more activated phenotype consistent with enhanced tissue remodeling and fibrotic potential.

To better quantify α-SMA protein expression, Western Blot analysis was performed followed by densitometric quantification using ImageJ software (Fig. 23).

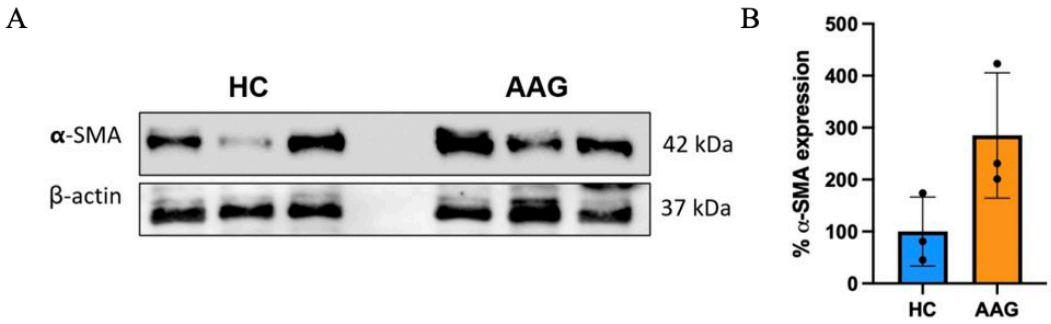

Figure 23. α-SMA protein expression quantification. (**A**) Western Blot analysis for α-SMA performed on HC and AAG-derived fibroblasts. (**B**) Densitometric quantification. Data are shown as mean ± SD.

Although some biological variability was observed, densitometric analysis revealed higher α-SMA expression in AAG-derived fibroblasts compared with HC, consistent with immunocytochemical findings. AAG fibroblasts tended to express increased levels of α-SMA, indicating a more pronounced contractile and activated phenotype than those from HC.

To assess the proliferative capacity of fibroblasts, an MTT assay was performed at different time points (24, 48, 72, and 96 hours) (Fig. 24).

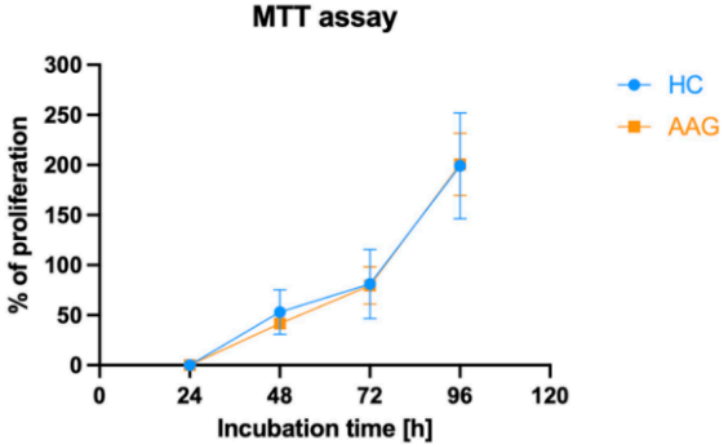

Figure 24. Fibroblast proliferation. MTT assay showing comparison between proliferation of HC- and AAG- derived fibroblasts.

The results, expressed as the percentage of proliferation relative to t_0, showed a progressive increase in cell growth in both groups. However, no significant differences in proliferation rates were observed between AAG- and HC-derived fibroblasts.

To assess potential differences in migratory capacity between HC and AAG fibroblasts, a wound healing assay was performed, monitoring wound closure at 0, 24, 48, and 72 hours (Fig. 25). Both groups exhibited a progressive reduction of the wound area over time, indicative of active cell migration. AAG-derived fibroblasts displayed an enhanced migratory ability, resulting in a faster wound closure compared to HC fibroblasts.

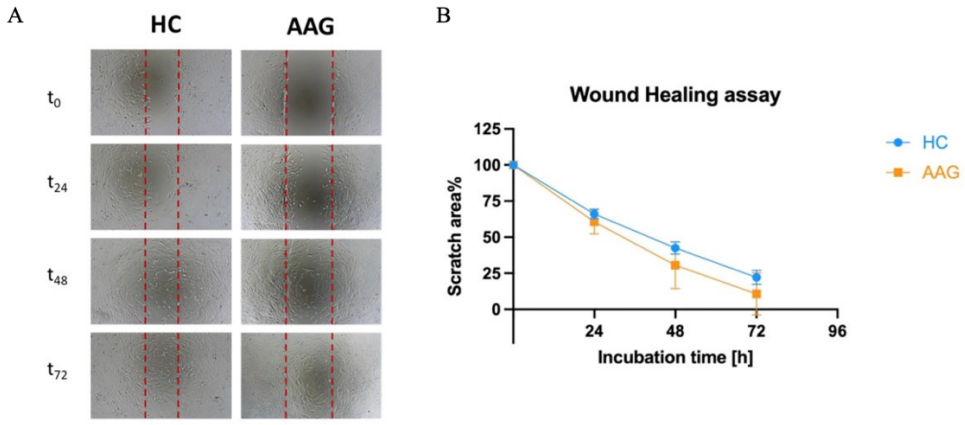

Figure 25. Fibroblast migration capacity. Wound healing assay. (**A**) Representative 4x images of HC and AAG fibroblasts migration. (**B**) Quantification of the residual scratch area at 24, 48, and 72 hours relative to time 0. Data are presented as mean ± SD.

To further investigate the transcriptional behavior of fibroblasts, RNA sequence analysis and an RNA array were performed using RNA extracted from HC- and AAG- isolated fibroblasts.

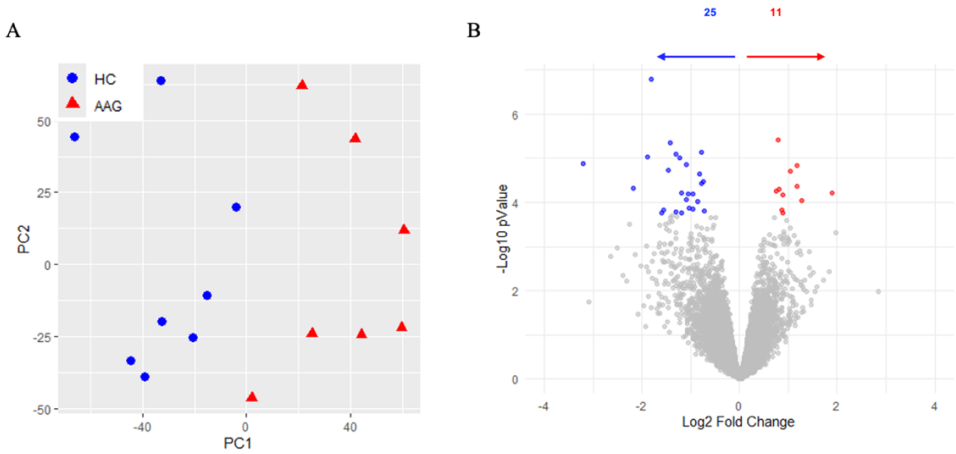

Figure 26. Gene expression in AAG fibroblasts. (**A**) Principal Component Analysis (PCA) between HC (blue) and AAG (red) samples. (**B**) Volcano plot showing differentially expressed genes between AAG- and HC- isolated fibroblasts. Differentially expressed genes (DEGs) were defined as those with p< 0,05 and logFC > 0,5.

Transcriptomic analysis revealed a moderate alteration in gene expression profiles in AAG-isolated fibroblast compared with healthy controls, with 11 genes significantly upregulated and 25 genes downregulated in AAG patients (Fig. 26).

More detailed analyses revealed that most of the differentially expressed genes in AAG-derived fibroblasts are involved in cytoskeletal remodeling. For instance, among up-regulated genes, SYNE2, KIF20B, and KIF1B encode for a nesprin protein that links the nucleus to the cytoskeleton, and for two kinesin proteins involved in microtubule dynamics and transport (Fig. 27A). The GSEA confirms the upregulation of several genes involved in cytoskeletal remodeling (Fig. 27B).

A

Up-regulated genes

gene	logFC	FDR
SYNE2	1.90	2.79E-02
DGKH	1.28	3.60E-02
ZBTB20	1.18	2.79E-02
MKI67	1.17	1.47E-02
ZFHX3	1.04	1.68E-02
USP38	0.89	4.99E-02
KIF20B	0.88	2.88E-02
KATNBL1	0.86	4.92E-02
KIF1B	0.80	2.79E-02
FOXC2	0.79	1.44E-02
UBE2C	0.75	2.79E-02

Down-regulated genes

gene	logFC	FDR
CTSS	-3.20	1.47E-02
MUC20-OT1	-2.18	2.79E-02
GAS7	-1.88	1.44E-02
PAMR1	-1.81	1.62E-03
NEAT1	-1.59	4.99E-02
DIO2	-1.57	4.92E-02
MT-CO3	-1.46	1.68E-02
MT-ND4	-1.43	1.44E-02
PLAT	-1.31	4.99E-02
MT-ND2	-1.30	1.44E-02
MT-ND5	-1.23	1.44E-02
DNM3OS	-1.19	2.79E-02
MT-CO2	-1.18	4.99E-02
MT-CYB	-1.10	3.55E-02
MT-CO1	-1.10	1.47E-02
MT-ND3	-1.05	2.79E-02
AHSA2P	-1.04	4.79E-02
COL27A1	-0.96	4.92E-02
FBLN5	-0.96	2.79E-02
C1S	-0.87	3.62E-02

B

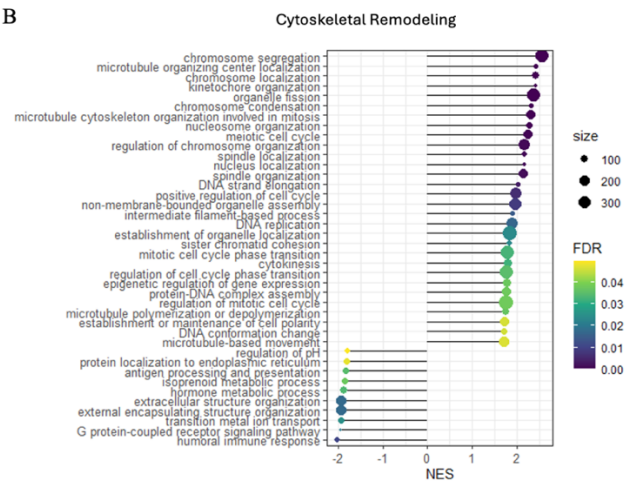

Figure 27. Differential gene expression in AAG fibroblasts. (**A**) Up- and down-regulated genes in AAG-isolated fibroblasts compared with HC controls. (**B**) Heatmap of genes involved in cytoskeletal remodeling. The size of each dot indicates the number of genes involved in the pathway, while the color represents the false discovery rate (FDR) value.

These data show that AAG-derived fibroblasts show morphological alterations and upregulation of cytoskeletal organization pathways.

Moreover, analyzing a panel of genes involved in fibrotic and inflammatory processes (Fig. 28), we observed that AAG-derived fibroblasts exhibited upregulation of several genes with potential immunoregulatory activity, including IFNG, IL10, IL4, IL13, and BMP7. PDGFA and PDGFB levels were markedly increased in AAG fibroblasts, suggesting enhanced activation of pathways associated with fibroblast-to-cancer-associated fibroblast (CAF) transition and acquisition of a pro-tumorigenic phenotype.

Notably, FASLG expression was also elevated, indicating potential modulation of fibroblast interaction with immune and stromal cells. Additionally, SERPINA1 expression was increased, consistent with its reported role in promoting fibroblast-to-myofibroblast

differentiation and cell migration. Conversely, a downregulation of genes involved in extracellular matrix remodeling (MMP2, MMP3, MMP14, PLAT, PLAU) and TGF-β signaling (TGFBR2, TGIF1) was observed, suggesting an altered regulatory balance between pro-fibrotic and matrix-degradative pathways in AAG fibroblasts.

These findings suggest that fibroblasts derived from AAG mucosa acquire a distinct transcriptional phenotype characterized by anti-inflammatory features and a myofibroblast-like transition, resembling cancer-associated fibroblasts rather than conventionally activated fibroblasts. This alternatively activated state may represent a compensatory mechanism aimed at limiting chronic tissue damage in the context of persistent lymphocytic infiltration and glandular destruction.

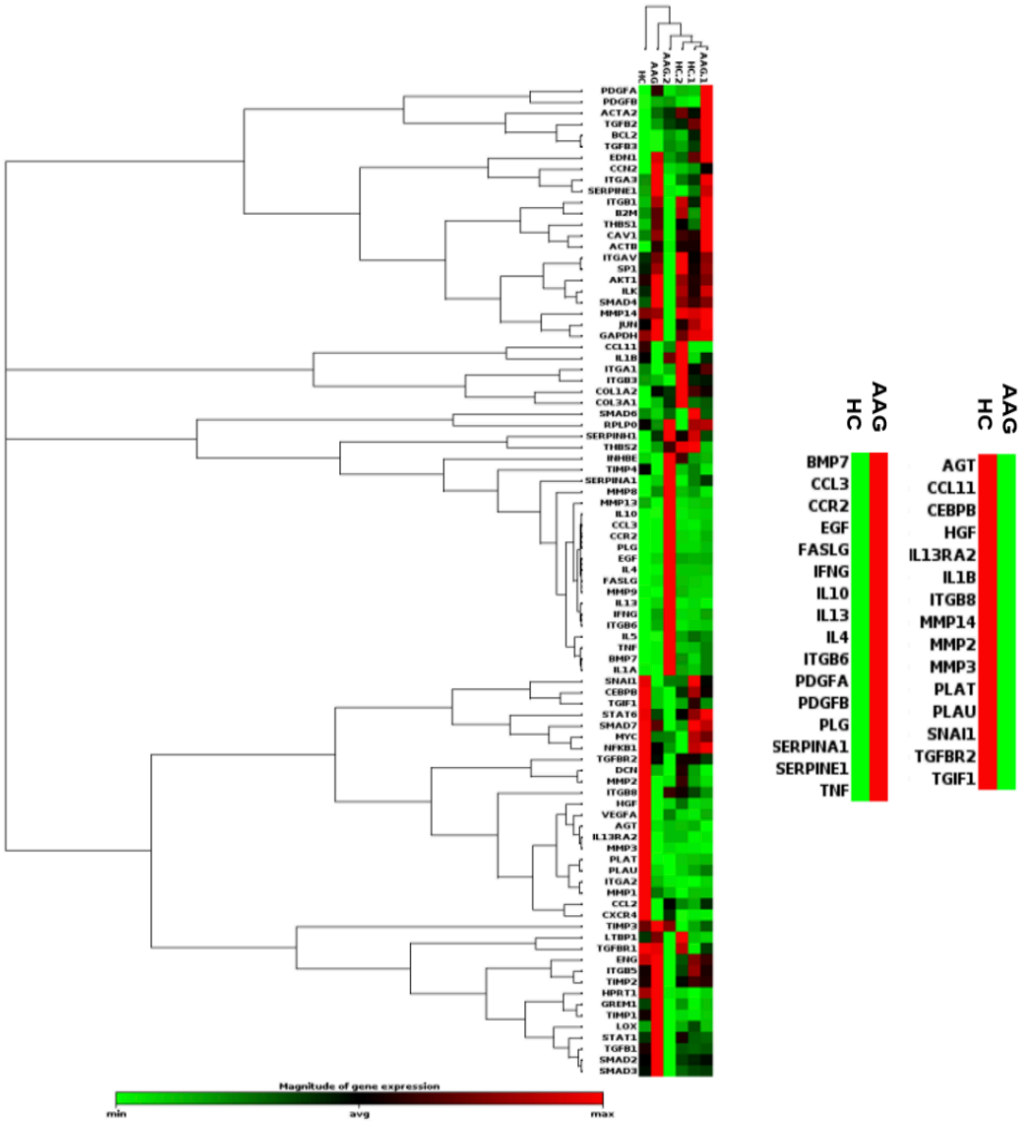

Figure 28. Transcriptional profile of HC and AAG fibroblasts. Heatmap of RNA array analysis performed using a panel of genes involved in fibrosis and inflammation. In green downregulated genes, in red upregulated genes. On the left main differentially expressed genes.

Data on AAG fibroblasts altered ECM were further confirmed through RT-PCR analyses (Fig. 29).

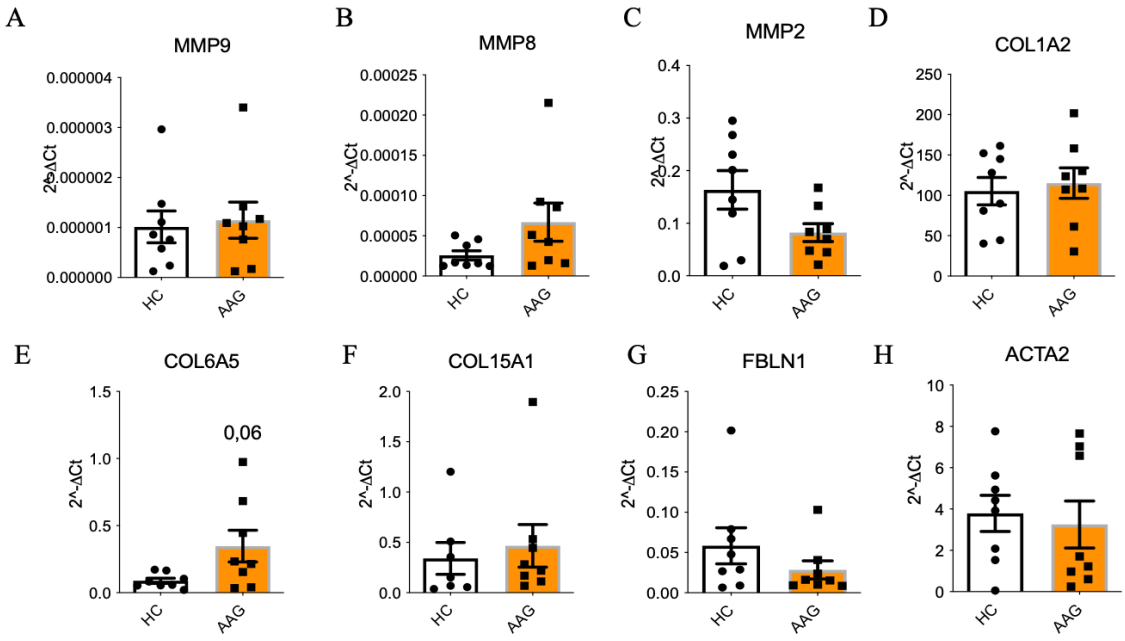

Figure 29. Expression profiles of ECM genes in AAG-isolated fibroblasts. (**A-H**) RT-PCR quantification of MMP9 (**A**), MMP8 (**B**), MMP2 (**C**), COL1A2 (**D**), COL6A5 (**E**), COL15A1 (**F**), FBLN1 (**G**), and ACTA2 (**H**) expression in HC and AAG fibroblasts. Data are expressed as mean ± SD.

RT-PCR analysis shows that fibroblasts isolated from AAG patients exhibit reduced expression of MMP2, FBLN1, and ACTA2, indicating decreased ECM remodeling and fibroblast contractility, and increased expression of MMP8, COL1A2, COL6A5, and COL15A1, suggesting altered collagen deposition and ECM composition compared to healthy controls.

These data demonstrate that fibroblasts from AAG patients may exhibit a dysfunctional phenotype with reduced ECM degradation and remodeling and altered ECM deposition. This pattern could contribute to gastric tissue atrophy by impairing normal tissue turnover and repair while promoting an abnormal ECM environment. This may reflect fibroblast adaptation to chronic inflammation or autoimmune signaling.

4.1.3 NAMPT INVOLVEMENT IN AAG

In 2022, in collaboration with Prof. Lenti, it was demonstrated that NAMPT is overexpressed in gastric body biopsies from patients with Autoimmune Atrophic Gastritis and that its extracellular form (eNAMPT) is released at significantly higher levels.

Moreover, eNAMPT was shown to exert a pro-inflammatory effect on the gastric mucosa, comparable to other well-characterized cytokines. Specifically, treatment of healthy control gastric biopsies with recombinant eNAMPT resulted in a significant upregulation of INF-γ and IL-6 expression [150].

To further elucidate the role of NAMPT in modulating the transcriptional profile of the gastric mucosa, bulk RNA sequencing was performed on gastric body biopsies from HCs treated with recombinant NAMPT (500 ng/ml, 24 hours) (Fig. 30).

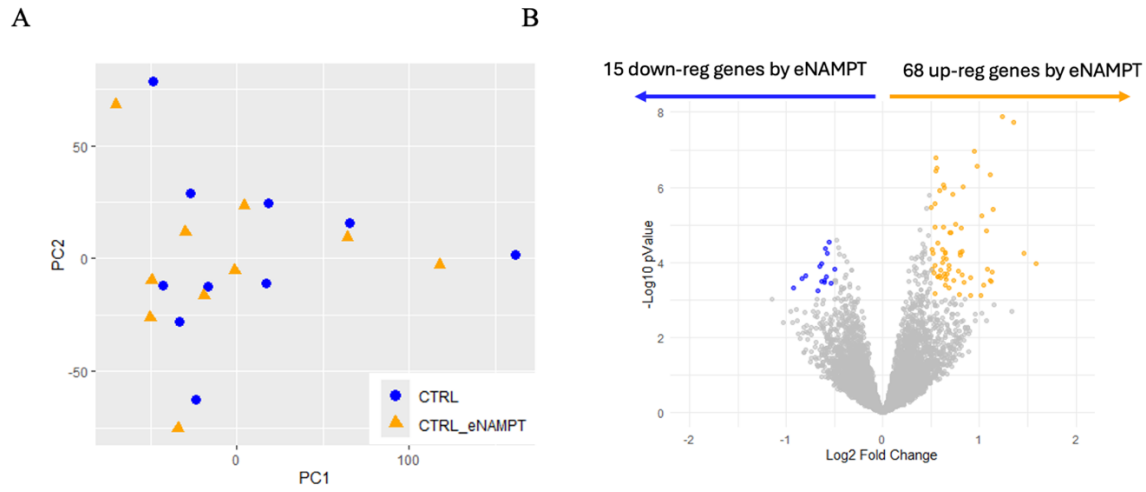

Figure 30. Gene expression in HC biopsies treated with NAMPT. (**A**) PCA and (**B**) Volcano plot of HC biopsies treated with recombinant NAMPT (orange) compared to untreated control biopsies (blue).

The PCA plot shows that the two groups do not form clearly separated clusters, indicating that eNAMPT induces only modest global transcriptional changes in HC biopsies. The partial overlap of the two conditions suggests that only a limited subset of genes is affected (Fig. 30A). Despite the absence of a strong separation at the whole-transcriptome level, differential expression analysis reveals a specific but relatively small gene-expression signature driven by eNAMPT treatment. Volcano plot analysis revealed that, in total, 83 genes were significantly modulated by eNAMPT: 68 genes were upregulated (orange), and 15 genes were downregulated (blue) (Fig. 30B). The distribution of significant genes illustrates that eNAMPT triggers a selective transcriptional response, rather than a broad inflammatory activation. This indicates a potential immunomodulatory effect of eNAMPT within the inflammatory context of AAG.

Figure 31 lists the top up- (Fig. 31A) and down-regulated (Fig. 31B) genes in HC biopsies after NAMPT treatment. Many of significantly upregulated genes are associated with extracellular matrix (ECM) organization (MXRA5, FBLN1, and LUM), immune activation

(CCL11), and endothelial-stromal interaction (ICAM1, SELE, and EDIL3), suggesting that eNAMPT induces a mild pro-remodeling and pro-inflammatory response. Notably, several down-regulated genes are markers of epithelial differentiation (IHH), mucin production (REG4, MUC4, and PLLP), and gastric homeostasis, indicating a partial suppression of epithelial-associated programs. These findings support the hypothesis that eNAMPT acts on stromal and endothelial compartments of the stomach, with more limited effect on epithelial cells.

A

gene	logFC	FDR
MXRA5	1.59	1.60E-02
MRC2	1.47	1.17E-02
FBLN1	1.36	8.41E-05
ICAM1	1.23	8.41E-05
LUM	1.14	2.04E-03
KRT15	1.13	2.02E-02
PCLO	1.12	2.62E-02
DCN	1.11	5.48E-04
SOD3	1.11	2.57E-02
PTN	1.08	1.92E-02
SELE	1.08	5.29E-03
EDIL3	1.04	3.10E-02
MGP	1.03	2.77E-03
BCL2A1	1.01	4.73E-02
COL3A1	0.98	4.80E-04
COL1A2	0.94	3.37E-04
CFD	0.91	2.36E-02
NEGR1	0.91	4.80E-02
CCL11	0.84	2.65E-02
POSTN	0.83	8.88E-04

B

gene	logFC	FDR
REG4	-0.93	3.42E-02
MUC4	-0.84	2.37E-02
IHH	-0.80	2.29E-02
ASPHD2	-0.68	3.84E-02
PRR15	-0.66	1.72E-02
SLC4A2	-0.64	1.59E-02
IL11	-0.63	2.62E-02
LINC01559	-0.61	2.57E-02
TNFRSF1B	-0.60	2.67E-02
PLLP	-0.59	1.12E-02
MYEOV	-0.58	2.29E-02
AKR1C3	-0.58	1.17E-02
OAS1	-0.56	8.69E-03
IL1B	-0.54	2.76E-02
ECM1	-0.50	1.92E-02

Figure 31. Gene expression profile in HC biopsies treated with NAMPT. Main (**A**) up-regulated and (**B**) down-regulated genes in HC biopsies treated with NAMPT compared to untreated HC samples.

A Gene Ontology Enrichment Analysis (GO) was also performed. In HC samples treated with NAMPT compared to untreated controls, GO revealed enrichment of pathways associated with extracellular structure organization, external encapsulating structure organization, cytoplasmic translation, humoral immune response, and chronic inflammatory response (Fig. 32A). In addition, Cell Type Enrichment Analysis (CTEA) showed a reduction in the presence of endothelial cells, pericytes, and macrophages (Fig. 32B). Together these findings suggest that NAMPT presence exerts coordinated effects on both molecular pathways and cell type dynamics in the stomach.

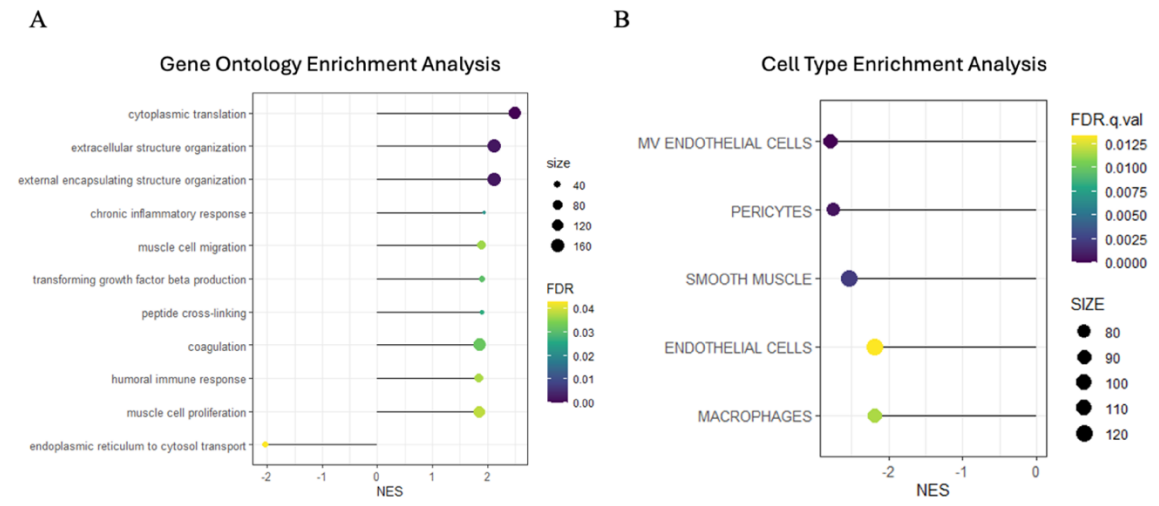

Figure 32. GO and CTE analysis on HC biopsies treated with NAMPT. (**A**) Main biological processes altered in NAMPT-treated HC biopsies compared to untreated controls. (**B**) Main cell types altered in NAMPT-treated HC biopsies compared to untreated controls. The size of each dot indicates the number of genes involved in the pathway, while the color represents the false discovery rate (FDR) value.

4.1.4 NAMPT EXPRESSION IN FIBROBLASTS

In parallel with the biopsy analyses, NAMPT expression was evaluated in isolated HC and AAG fibroblasts by Western Blot and RT-PCR (Fig. 33).

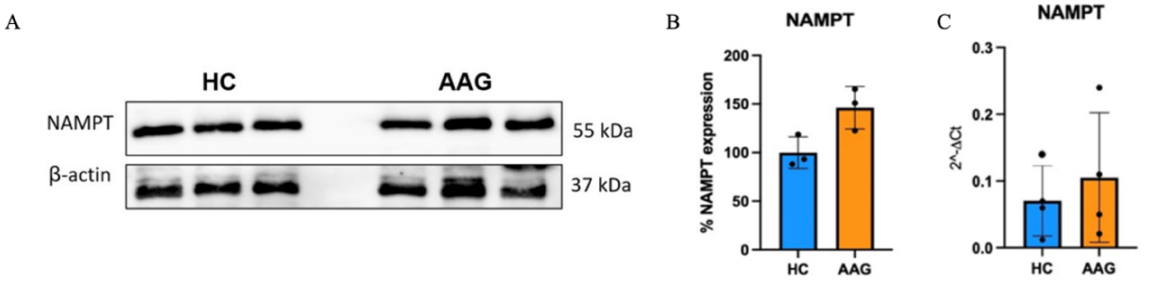

Figure 33. NAMPT expression in HC and AAG fibroblasts. (**A**) Western Blot analysis of NAMPT expression in HC and AAG fibroblasts. (**B**) Densitometric quantification using ImageJ. (**C**) RT-PCR quantification of NAMPT expression in HC and AAG fibroblasts. Data are expressed as mean ± SD.

Data showed moderate increased levels on NAMPT expression, both at transcription and expression levels. Therefore, NAMPT treatment effects were also evaluated on fibroblast cell migratory capacity using the wound healing assay (Fig. 34). Fibroblasts isolated from HC were treated with recombinant NAMPT monitoring wound closure at 0, 24, 48, and 72 hours.

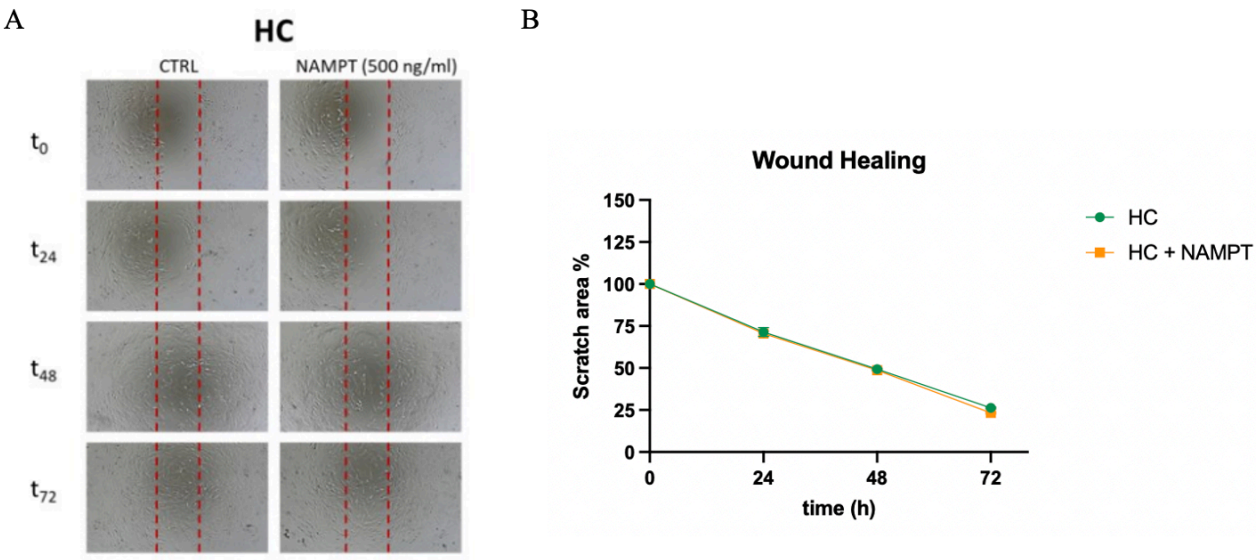

Figure 34. HC and AAG fibroblasts migratory activity after treatment. (**A**) Representative 4x images of wound healing assay. (**B**) Quantification of the residual scratch area at 24, 48, and 72 hours relative to time 0. Data are presented as mean ± SD.

The results showed no significant differences in migration between treated and untreated fibroblasts, suggesting a low sensitivity of these cells to the direct effects of NAMPT *in vitro*.

4.2 THE ROLE OF NAMPT IN INFLAMMATORY BOWEL DISEASE

4.2.1 THE CYTOKINE eNAMPT IN THE PROGRESSION OF IBD

To explore the role of the cytokine eNAMPT in the intestinal inflammatory response, an *in vivo* study was conducted using a murine model of Crohn's disease. Male BALB/c mice were randomly allocated into 5 experimental groups: a healthy control group (sham), a healthy group treated with recombinant eNAMPT (sham + eNAMPT), a group with moderate Crohn's disease induced by 2 mg/mouse of DNBS (moderate DNBS), a group with moderate Crohn's disease treated with eNAMPT (moderate DNBS + eNAMPT), and a group with severe Crohn's disease induced by 3 mg/mouse of DNBS (severe DNBS).

In the DNBS-treated groups, intestinal inflammation was induced by intrarectal administration of DNBS at two different doses, reproducing moderate and severe forms of the disease, respectively. In groups receiving eNAMPT (50 µg/mouse), the recombinant protein was administered intraperitoneally once daily for 4 consecutive days (Fig. 35A). At the end of the treatment period, changes in body weight and colon length were assessed to monitor the progression of the inflammatory response and to evaluate the potential contribution of eNAMPT to disease development (Fig. 35B-C).

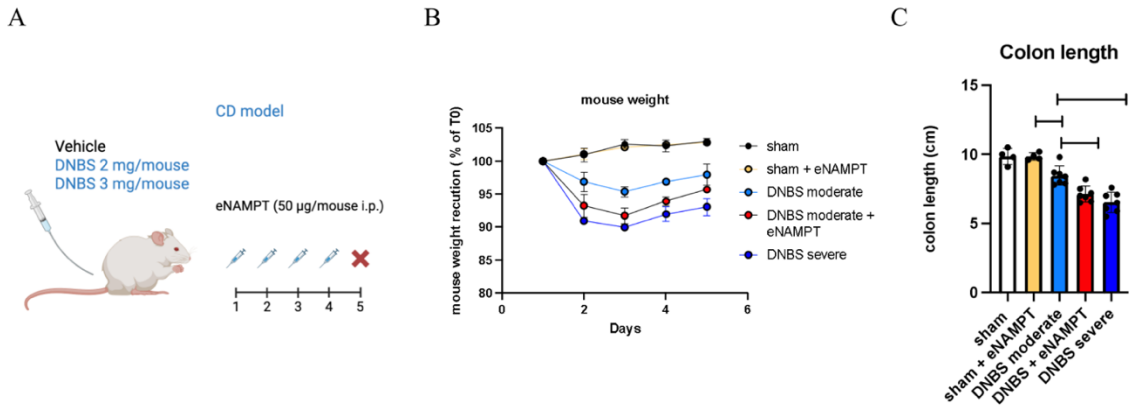

Figure 35. Experimental design and effects of eNAMPT treatment in a murine model of CD. (**A**) Schematic of the experimental protocol. CD was induced by intrarectal administration of DNBS (2 or 3 mg/mouse) to generate moderate and severe disease respectively. Recombinant eNAMPT (50 µg/mouse) was administered i.p. for 4 consecutive days. (**B**) Body weight variation over time, expressed as percentage of baseline (t_0). (**C**) Colon length at the end of the treatment. Data are shown as mean ± SEM, n=2.

The results showed that administration of eNAMPT to mice with moderate Crohn's disease (moderate DNBS + eNAMPT) led to a marked reduction in body weight compared with

healthy controls (sham), healthy mice treated with eNAMPT (sham + eNAMPT), and untreated mice with moderate disease (moderate DNBS). The extent of weight loss in this group was comparable to that observed in animals with severe disease (severe DNBS), suggesting a role for eNAMPT in promoting disease progression under inflammatory conditions (Fig. 35B).

Consistently, colon length in mice with moderate disease treated with eNAMPT (moderate DNBS + eNAMPT) was significantly reduced compared with the other experimental groups, and approached values observed in animals with severe disease (Fig. 35C). This finding supports the hypothesis that elevated levels of eNAMPT, resulting from intraperitoneal administration of the recombinant protein, may exacerbate disease severity in the presence of intestinal inflammation. Conversely, administration of eNAMPT to healthy animals did not produce significant changes in either body weight or colon length, indicating that eNAMPT alone is not sufficient to induce pathological alterations in the absence of pre-existing inflammation.

4.2.2 EFFECT OF eNAMPT TREATMENT AT TISSUE LEVEL

To investigate the effects of exogenous eNAMPT administration at the tissue level, colon samples were collected from all experimental groups and analyzed by immunohistochemistry (IHC) by Cogentech (IFOM, Milan). Histological evaluation was performed using hematoxylin and eosin (HE), Picrosirius Red, and Masson's trichrome staining (Fig. 36A).

HE staining revealed well-preserved tissue architecture in colons from both healthy controls (sham) and healthy mice treated with recombinant eNAMPT (sham + eNAMPT), confirming that eNAMPT administration alone does not induce epithelial or structural damage. These findings are consistent with the absence of phenotypic changes in body weight and colon length in these groups. In contrast, DNBS-treated mice with moderate Crohn's like inflammation (DNBS) exhibited marked epithelial disruption and mucosal injury, which are further aggravated by eNAMPT treatment (DNBS + eNAMPT). These observations indicate that eNAMPT amplifies the intestinal inflammatory response under pathological conditions. Picrosirius Red staining revealed increased fibroblast activation and collagen accumulation in colons from DNBS-treated mice (DNBS). Effect further enhanced in DNBS + eNAMPT mice, suggesting that eNAMPT promotes fibrotic remodeling during intestinal inflammation. No collagen deposition was detected in healthy animals (sham or

sham + eNAMPT), confirming that eNAMPT alone does not activate fibroblasts in the absence of an inflammatory trigger.

Masson's trichrome staining confirmed a significant increase in collagen deposition in DNBS-treated mice, which was further accentuated by eNAMPT administration. These findings collectively indicate that eNAMPT enhances the pro-fibrotic response characteristic of chronic intestinal inflammation.

A

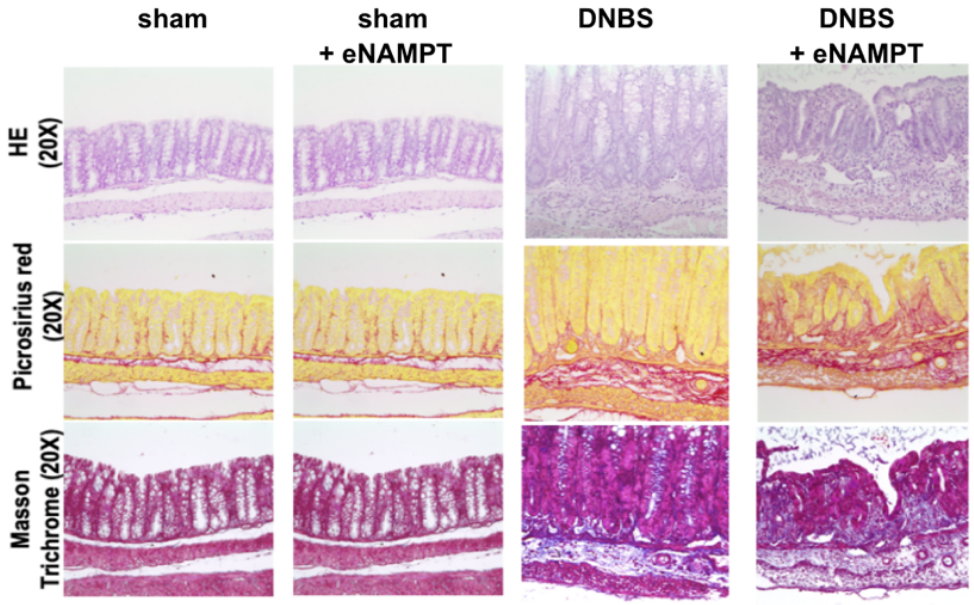

B

GROUPS	DISTORTION OF GLANDULAR ARCHITECTURE	CHORION INFLAMMATORY INFILTRATION	SUPPRESSION OF MUCOSECRETORY ACTIVITY	REGENERATIVE/ DISPLASTIC ALTERATIONS	GLANDULAR ATROPHY	FIBROSIS	SCORE
SHAM	0	0	0	0	0	0	0
SHAM + eNAMPT	0	0	0	0	0	0	0
DNBS	2	2	1	1	0	2	8
DNBS + eNAMPT	2	3	2	2	0	3	12

Legend: 0= Absent 1=Mild 2=Moderate 3=Discrete 4=Severe

Figure 36. Histological evaluation of colonic tissue following eNAMPT treatment. (**A**) Representative histological sections of colon from healthy controls (sham), eNAMPT-treated healthy mice (sham + eNAMPT), DNBS-treated (DNBS), and DNBS + eNAMPT-treated mice. Samples were stained with hematoxylin and eosin (HE), Picrosirius Red, and Masson's trichrome (20x magnification). (**B**) Semiquantitative histopathological scoring of tissue damage.

A semiquantitative histological scoring system (0-4 per parameter) was applied to assess tissue damage based on glandular architectural distortion, inflammatory cell infiltration, mucin secretion, regenerative dysplasia, glandular atrophy, and fibrosis (Fig. 36B). As expected, colons from healthy mice treated with eNAMPT (sham + eNAMPT) showed no histological alterations, maintaining a total score of 0, identical to untreated controls. Whereas, in mice with moderate DNBS-induced disease, the total histological score reached

8, reflecting substantial mucosal damage associated with inflammation and fibrosis. DNBS-treated mice receiving eNAMPT displayed a marked worsening of histopathology, with increased inflammatory infiltration (score 2 → 3), reduced mucin secretion (1 → 2), appearance of dysplastic regenerative changes (1 → 2), and enhanced fibrosis (2 → 3). Overall, these alterations increased the total histological score from 8 to 12, demonstrating that recombinant eNAMPT administration exacerbates intestinal injury and contributes to disease progression.

4.2.3 INFLAMMATORY INFILTRATE IN *LAMINA PROPRIA* OF DNBS-INDUCED MICE

To determine whether the exacerbation of clinical symptoms observed following exogenous eNAMPT administration was associated with an enhanced local immune response, the inflammatory infiltrate within the intestinal *lamina propria* was analyzed through flow cytometry. Flow cytometric analysis included the characterization of several immune cell subtypes. Among these were B lymphocytes, identified by surface expression of CD45 B220 ($CD45^+B220^+$) (Fig. 37A), and T lymphocytes, identified by the expression of CD45 and CD3 ($CD45^+CD3^+$) and further classified into T helper cells (Th; $CD45^+CD3^+CD4^+$) (Fig. 37B), and cytotoxic T cells ($CD45^+CD3^+CD8^+$) (Fig. 37C).

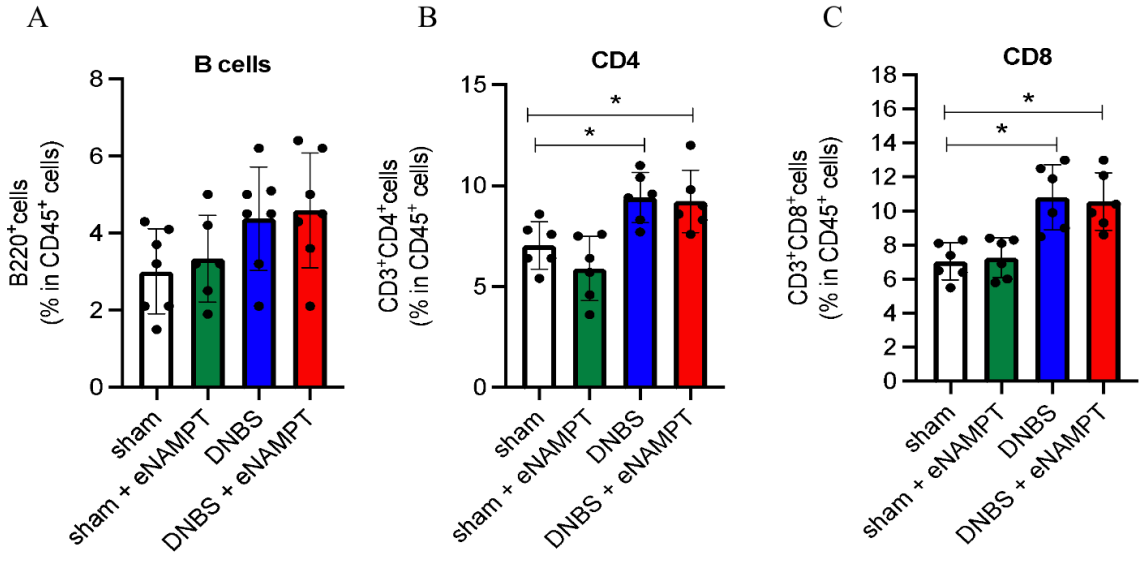

Figure 37. FACS analysis of lymphocyte populations in *lamina propria*. Quantification of (**A**) B cells ($CD45^+B220^+$), (**B**) $CD4^+$ T cells ($CD45^+CD3^+CD4^+$), and (**C**) $CD8^+$ T cells ($CD45^+CD3^+CD8^+$) in the *lamina propria* of sham, sham + eNAMPT, DNBS, and DNBS + eNAMPT mice. Data are presented as mean ± SD, n=2.

The analysis revealed no significant differences in the composition of the inflammatory infiltrate between healthy control mice (sham) and healthy mice treated with recombinant eNAMPT (sham + eNAMPT). In contrast, DNBS-treated mice with moderate Crohn's like disease (moderate DNBS) showed an increased proportion of both $CD4^+$ and $CD8^+$ T cells in the *lamina propria*. However, when DNBS-treated mice were administered recombinant eNAMPT (moderate DNBS + eNAMPT), no further significant increase in either $CD4^+$ or $CD8^+$ T cell populations was detected. Similarly, no significant changes in the frequency of B cells were observed in any DNBS-treated groups, suggesting that B lymphocytes are not substantially involved in disease progression and are not influenced by eNAMPT treatment. The analysis also included evaluation of the myeloid compartment, identified by co-expression of CD45 and CD11b ($CD45^+CD11b^+$). Within this population, specific subtypes were distinguished based on surface markers: monocytes ($CD45^+CD11b^+Ly6C^+$), granulocytes ($CD45^+CD11b^+Ly6G^+$), and macrophages ($CD45^+CD11b^+F4/80^+$). Macrophages were further classified into two distinct phenotypes: M1 macrophages, characterized by expression of CD86, and M2 macrophages, identified by expression of CD206 (Fig. 38A-E).

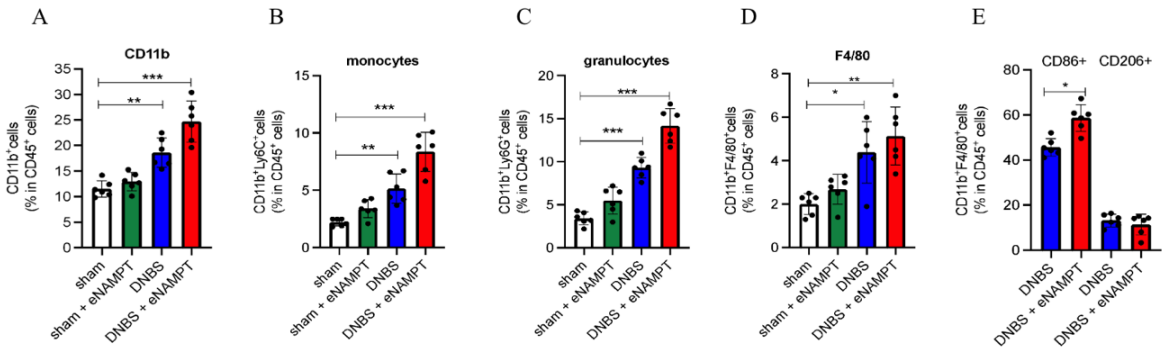

Figure 38. FACS analysis of myeloid cell populations in the *lamina propria*. Quantification of (**A**) total myeloid cells ($CD45^+CD11b^+$), (**B**) monocytes ($CD45^+CD11b^+Ly6C^+$), (**C**) granulocytes ($CD45^+CD11b^+Ly6G^+$), (**D**) macrophages ($CD45^+CD11b^+F4/80^+$), and (**E**) M1 ($CD86^+$) or M2 ($CD206^+$) macrophages in the *lamina propria*. Data are presented as mean ± SD, n=2.

Results indicate that treatment with cytokine eNAMPT in mice with moderate Crohn's disease (DNBS + eNAMPT) markedly promotes the accumulation of myeloid cells in the intestinal *lamina propria* compared with animals exhibiting moderate inflammation induced by DNBS alone. This increase predominantly involves monocytes, granulocytes, and macrophages. Furthermore, the expansion of the myeloid compartment is associated with a shift in macrophage polarization, characterized by a significant rise in the pro-inflammatory

CD86^{+} (M1) macrophage population and a concomitant decrease in the anti-inflammatory CD206^{+} (M2) subset. In contrast, healthy mice treated with eNAMPT (sham + eNAMPT) exhibited slight, non-significant increases in monocyte and granulocyte levels, confirming that the pro-inflammatory effect of eNAMPT becomes evident only in the presence of pre-existing intestinal inflammation.

4.2.4 SYSTEMIC EFFECT OF eNAMPT ON CIRCULATING MYELOID POPULATIONS

The systemic impact of the cytokine eNAMPT was examined. The analysis initially focused on myeloid cells, particularly monocytes and granulocytes (Fig. 39A-C).

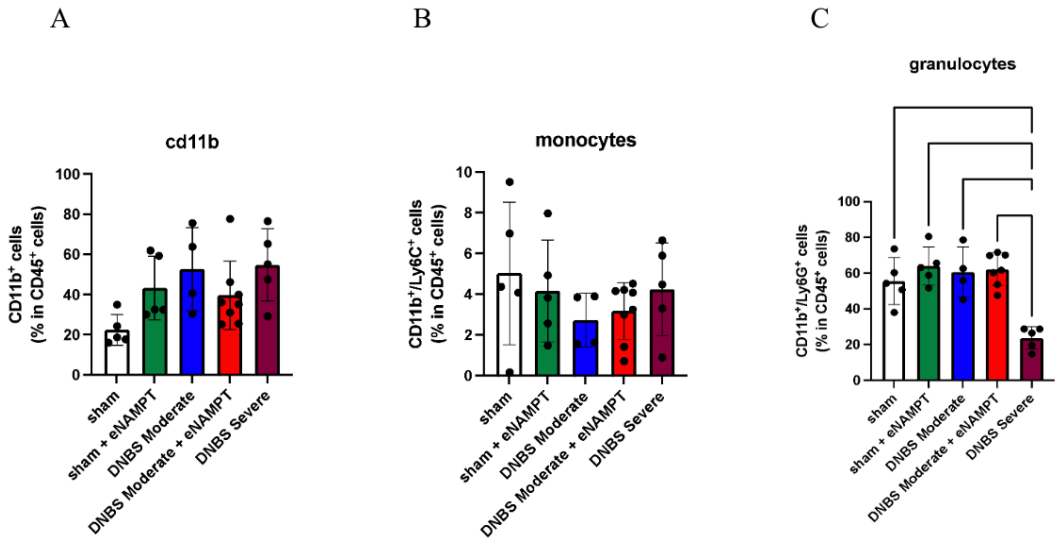

Figure 39. FACS analysis of circulating myeloid populations. (**A**) Percentage of total myeloid cells (CD11b^{+}) within CD45^{+} circulating leukocytes. (**B**) percentage of circulating monocytes (CD11b^{+}Ly6C^{+}) and (**C**) granulocytes (CD11b^{+}Ly6G^{+}) in the peripheral blood. Data are expressed as mean ± SD, n=2.

Since no significant differences were observed in the overall proportions of these populations among the experimental groups, further investigation concentrated on specific myeloid subpopulations distinguished by the expression levels of Ly6G, namely Ly6G^{high} and Ly6G^{low} cells, to better characterize potential shifts in cell maturation states.

Flow cytometry analysis revealed marked alterations in circulating myeloid subsets (Fig. 40F). In untreated healthy controls (sham), the peripheral blood was characterized by a predominance of mature Ly6G^{high} granulocytes, accompanied by a smaller proportion of

Ly6G^{low} immature cells (Fig. 40A). In contrast, exogenous administration of recombinant NAMPT in healthy mice (sham + eNAMPT) led to an increase in Ly6G^{high} granulocytes, and a substantial expansion of the Ly6G^{low} immature population (Fig. 40B). Mice with moderate inflammation induced by DNBS (DNBS moderate) exhibited a pronounced expansion of Ly6G^{high} granulocytes, consistent with an acute inflammatory response, while Ly6G^{low} populations remained relatively low (Fig. 40C). However, in DNBS-treated animals receiving recombinant NAMPT (DNBS + eNAMPT), peripheral blood analysis revealed significant changes: mature Ly6G^{high} granulocytes were markedly reduced, and Ly6G^{low} immature cells increased dramatically (Fig. 40D). A similar pattern was observed in mice with severe disease (DNBS severe) (Fig. 40E).

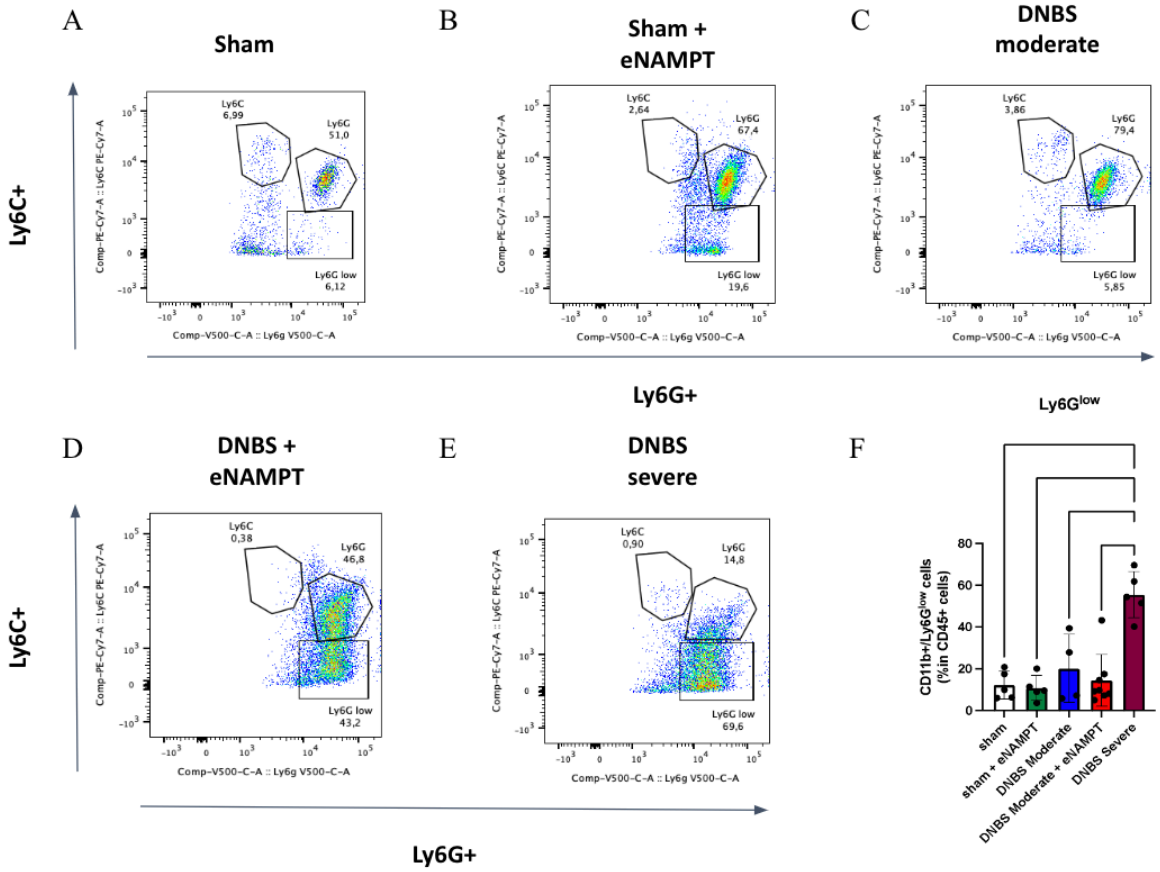

Figure 40. FACS analysis of eNAMPT effect on mature and immature granulocyte populations. Representative FACS dot plots showing Ly6G (Ly6g^{high} or Ly6G^{low}) expression profiles in circulating myeloid cells from (**A**) sham, (**B**) sham + eNAMPT, (**C**) DNBS moderate, (**D**) DNBS + eNAMPT, and (**E**) DNBS severe mice. (**F**) Quantification of Ly6G^{low} cells across experimental groups. Data are shown as mean ± SD, n=2.

Taken together, these findings suggest that eNAMPT may interfere with myeloid cell maturation during intestinal inflammation, reducing the generation of mature effector cells (Ly6G^{high}) and promoting the accumulation of immature myeloid forms (Ly6G^{low}).

4.2.5 EFFECT OF eNAMPT IN HEMATOPOIESIS AND CELL DIFFERENTIATION

We next investigated the potential role of eNAMPT in regulating hematopoietic processes within the bone marrow. Flow cytometry analyses were used to evaluate the presence of mature myeloid population (Fig. 41), hematopoietic stem cells (Fig. 42), and hematopoietic progenitors (Fig. 43). Flowcytometry analyses revealed that in untreated healthy mice (sham), the most abundant population consisted of mature granulocytes (Ly6G^{high}), followed by immature Ly6G^{low} cells and monocytes (Ly6C^{+}) (Fig. 41A). Comparison with the sham + eNAMPT group indicated that eNAMPT treatment reshaped myeloid composition within the bone marrow, promoting granulocytic expansion while markedly reducing the monocytic compartment (Fig. 41B). In mice with moderate colitis, a mild increase in Ly6C^{+} monocytes and slight decrease in Ly6G^{high} granulocytes were observed relative to healthy controls (Fig. 41C). Notably, as seen in peripheral blood, administration of recombinant eNAMPT (DNBS + eNAMPT) induced a pronounced expansion of the immature Ly6G^{low} population within the bone marrow. The overall cellular composition in this group closely resembled that of animals with severe disease (DNBS severe) (Fig. 41D-E), suggesting that eNAMPT contributes to hematopoietic remodeling toward an immunophenotypic profile characteristic of advanced disease stages.

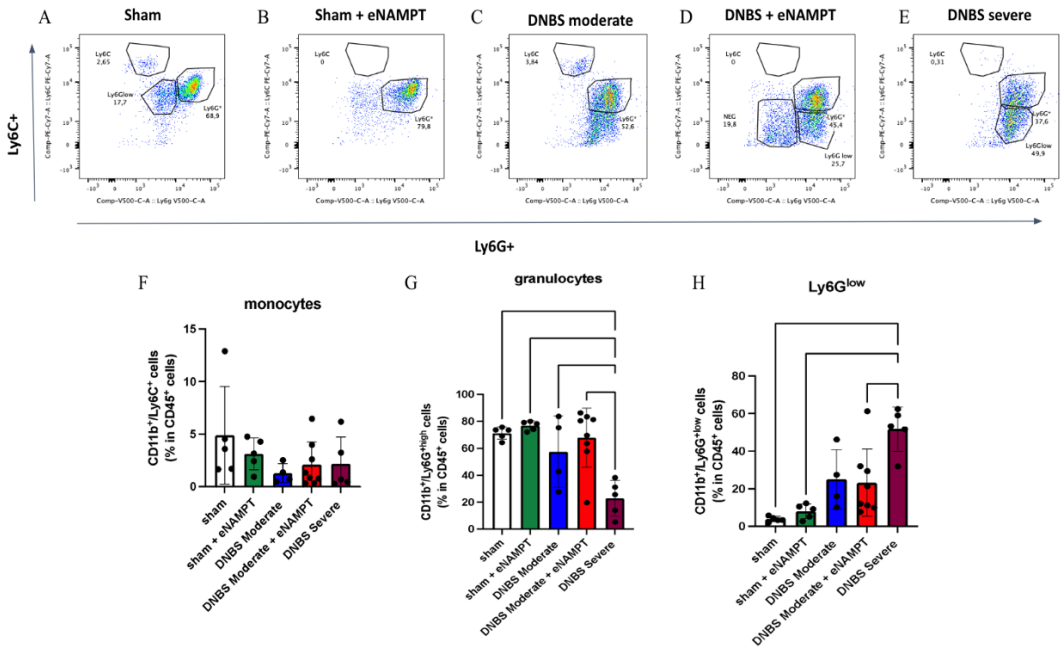

Figure 41. FACS analyses of mature myeloid populations in the bone marrow. Representative dot plots (**A-E**) show the distribution of Ly6C^{+} monocytes, Ly6G^{high} granulocytes, and Ly6G^{low} immature granulocytes in bone marrow for (**A**) sham, (**B**) sham + eNAMPT, (**C**) DNBS moderate, (**D**) DNBS + eNAMPT, and (**E**) DNBS severe mice. Quantification of the relative proportion of (**F**) Ly6C^{+} monocytes, (**G**) Ly6G^{high} granulocytes, and (**H**) Ly6G^{low} immature granulocytes among CD45^{+}CD11b^{+} cells is presented for all experimental groups. Data are expressed as mean ± SD, n=2.

Given the increase in immature cellular components and the concomitant reduction of mature myeloid populations observed in bone marrow analyses, we next examined hematopoietic stem and progenitor cells (Fig. 42 and 43) to assess whether elevated eNAMPT levels exert an upstream effect on hematopoiesis.

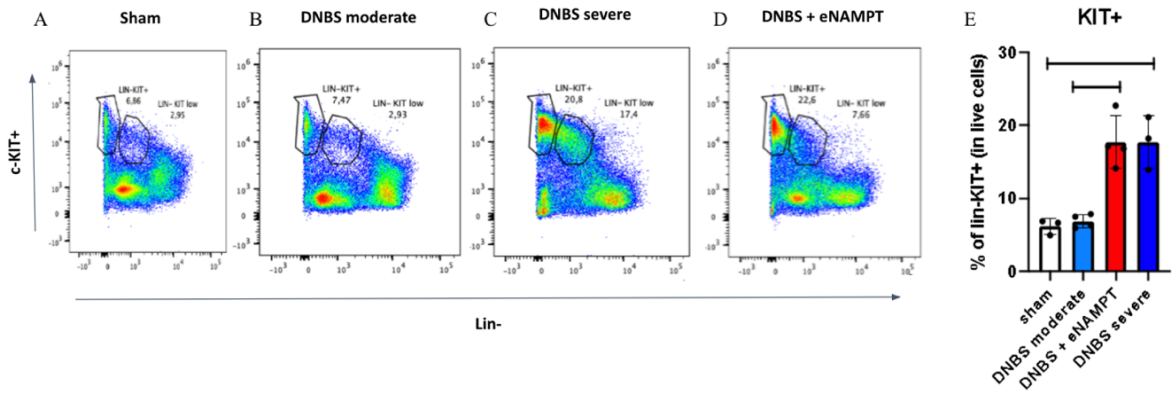

Figure 42. FACS analyses of immature populations in the bone marrow. Representative flow cytometry dot plots showing hematopoietic stem cells in bone marrow from (**A**) sham, (**B**) DNBS moderate, (**C**) DNBS severe, and (**D**) DNBS + eNAMPT mice. (**E**) Quantification of HSCs within the live cells is indicated in each plot. Data are shown as mean ± SD, n=2.

Flow cytometric analyses revealed comparable frequencies of Lin$^-$c-KIT$^+$ cells in the bone marrow of untreated healthy mice (sham) and mice with DNBS-induced moderate Crohn's-like inflammation (moderate DNBS). In contrast, mice with DNBS-induced moderate intestinal inflammation treated with eNAMPT (DNBS + eNAMPT) displayed a significant expansion of the Lin$^-$c-KIT$^+$ compartment compared with the moderate DNBS group. Notably, the proportion of Lin$^-$c-KIT$^+$ cells in DNBS + eNAMPT was comparable to that observed in mice with severe DNBS-induced inflammation, supporting a link between eNAMPT elevation and hematopoietic activation under inflammatory conditions (Fig. 42E). To further characterize hematopoietic progenitor dynamics, multiple bone marrow subpopulations were analyzed, including megakaryocyte-erythroid progenitor (MEPs, CD34$^-$CD16/32$^-$), common myeloid progenitors (CMPs, CD34$^+$CD16/32$^-$), and granulocyte-monocyte progenitors (GMPs, CD34$^+$CD16/32$^+$) (Fig. 43). Flow cytometric analyses revealed a general increase in hematopoietic progenitor cells (LSK, Lin-Sca-1$^+$c-KIT$^+$) in the bone marrow of DNBS-severe mice, whereas this expansion was not observed in DNBS-treated mice with moderate inflammation (Fig. 43E). However, more accurate analyses showed a significant reduction in the frequency of MEPs in the bone marrow of mice with DNBS-induced moderate inflammation treated with eNAMPT (DNBS + eNAMPT) compared with the moderate DNBS group (Fig. 43F). In contrast, the proportion

of CMPs remained largely unchanged between the two groups (Fig. 43G), suggesting that eNAMPT does not substantially affect this intermediate progenitor population. Notably, a marked increase in GMP frequency was observed in DNBS + eNAMPT mice, indicating a selective expansion of granulocyte-monocyte progenitors (Fig. 43H). This pattern closely mirrored that observed in the severe DNBS model, suggesting that elevated eNAMPT levels can mimic, at the hematopoietic level, the inflammatory response associated with a more acute pathological condition, promoting an unbalanced proliferation toward granulocytes and monocytes, which are subsequently released into the bloodstream and recruited to the site of inflammation, where they accumulate.

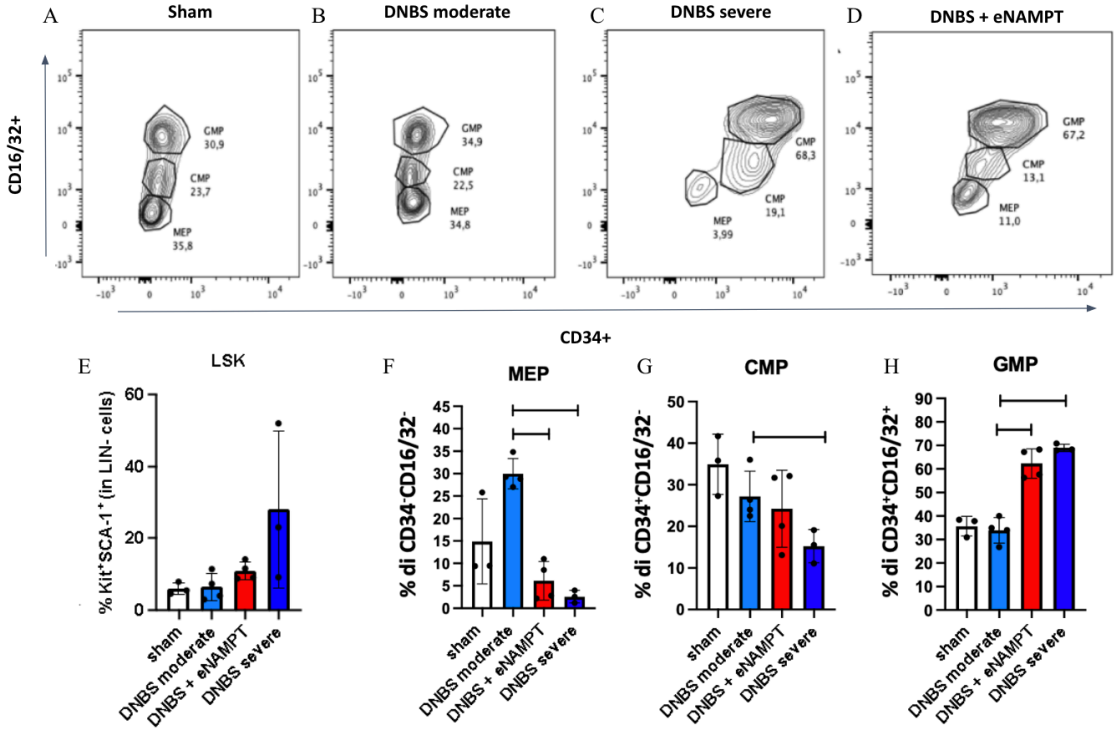

Figure 43. FACS analyses of hematopoietic progenitor cells in the bone marrow. Representative dot plots of FACS analyses showing hematopoietic progenitors in bone marrow from (**A**) sham, (**B**) DNBS moderate, (**C**) DNBS severe, and (**D**) DNBS + eNAMPT mice. (**E**) Quantification of total progenitors within Lin^- cells, and (**F**) MEPs within $CD34^-CD16/32^-$ cells, and (**G**) CMPs, (**H**) GMPs within $CD34^+CD16/32^-$ cells. Data are shown as mean ± SD, n=2.

4.2.6 EFFECT OF eNAMPT ON HEMATOPOIETIC STEM CELLS GROWTH *EX VIVO*

Given the involvement of cytokine eNAMPT in modulating bone marrow cells differentiation and maturation during inflammation, we developed and validated an experimental protocol for *ex vivo* studies to further characterize and elucidate the effects of eNAMPT on the hematopoietic process.

Once optimized, the protocol was applied to assess the growth and differentiation potential

of hematopoietic stem cells isolated from the bone marrow of untreated healthy mice (sham) and in the presence of different cytokines (Fig. 44).

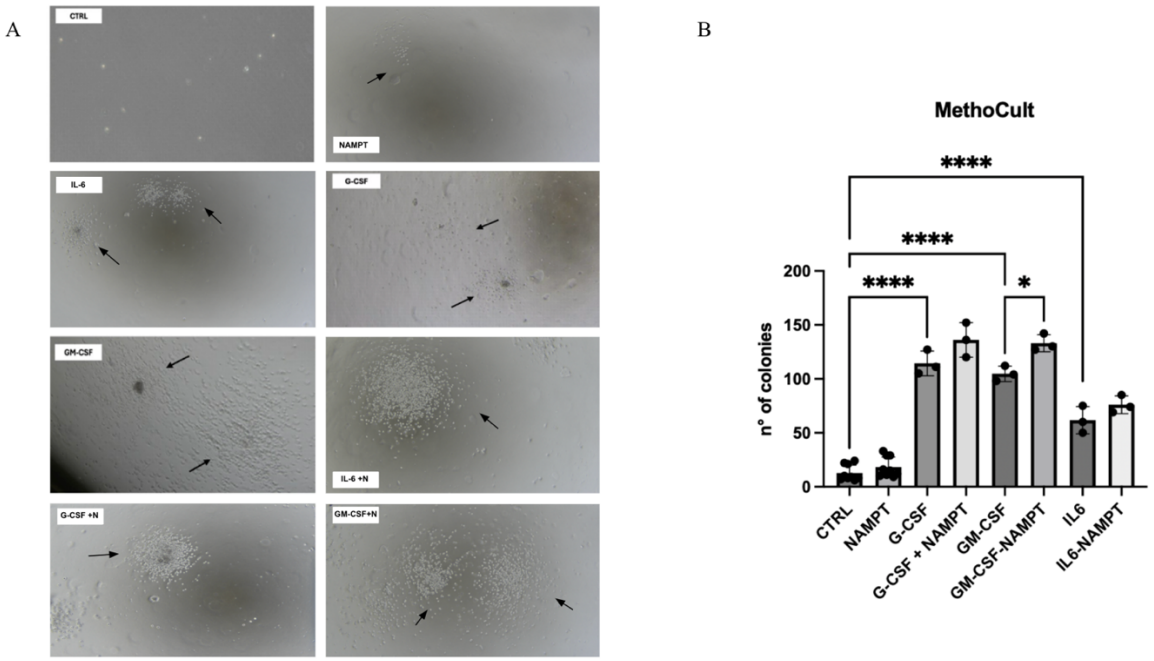

Figure 44. Effect of cytokines on bone marrow-derived colony formation. (**A**) Representative images of bone marrow-derived cells cultured under different conditions: untreated control (CTRL), NAMPT, IL-6, G-CSF, GM-CSF treated, and the combination of each cytokine with NAMPT (IL-6 + NAMPT, G-CSF + NAMPT, GM-CSF + NAMPT). Colony formation is indicated by black arrows. (**B**) Quantification of colony formation under each experimental condition. Data are expressed as the mean ± SEM of independent experiments, n=3.

Compared with the control condition (CTRL), in which no cytokine stimulation was applied, treatment with IL-6, G-CSF or GM-CSF resulted in significant increase in the number of colonies formed. In contrast, NAMPT alone was unable to promote cell differentiation, as no substantial changes in colony counts were observed. However, when NAMPT was combined with either IL-6 or G-CSF a slight enhancement in colony formation was detected. In addition, when combined with GM-CSF, the enhancement in colony formation was more marked and statistically significative, indicating a synergistic effect between recombinant NAMPT and these hematopoietic growth factors.

Therefore, the experiment was repeated in the DNBS-induced Crohn's disease model. Bone marrow-derived cells isolated from 4 distinct groups of animals: untreated healthy mice (sham), mice with DNBS-induced moderate Crohn's disease (moderate DNBS), mice with DNBS-induced severe Crohn's disease (severe DNBS) were cultured either in the absence of stimulating factors or in the presence of G-CSF or GM-CSF (Fig. 45).

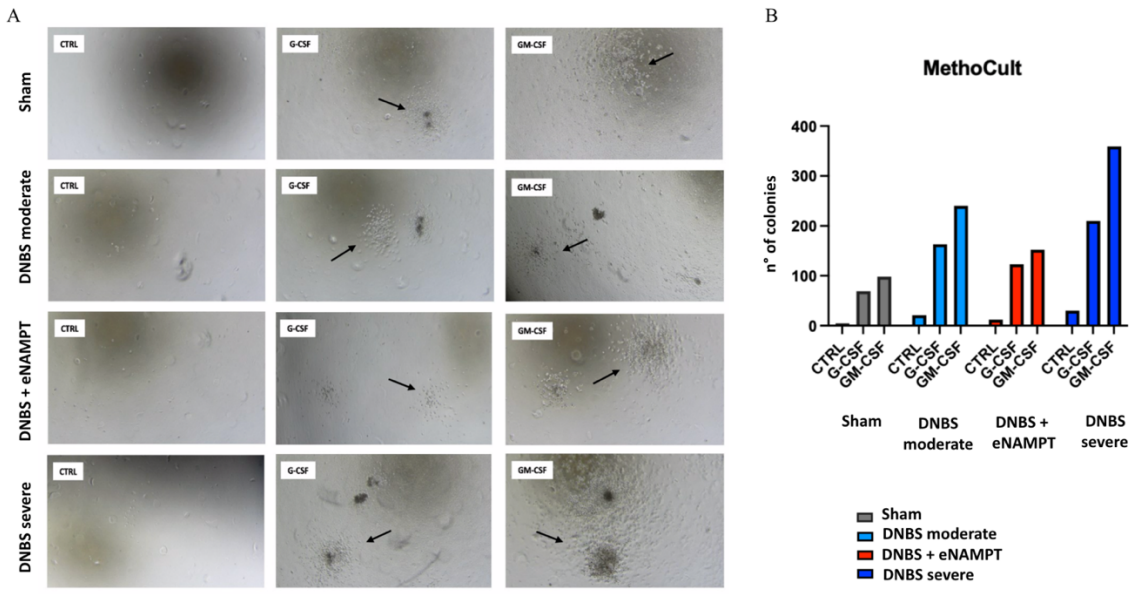

Figure 45. Effect of colony stimulating-factors on bone marrow-derived cells in a DNBS-induced Crohn's disease model. (**A**) Representative images of bone marrow-derived cells isolated from sham, DNBS moderate, DNBS + eNAMPT, and DNBS severe mice cultured under different conditions: untreated control (CTRL), G-CSF, or GM-CSF treatment. Colony formation is indicated by black arrows. (**B**) Quantification of the number of colonies formed under each condition.

Data show that hematopoietic stem cells derived from all the experimental groups responded to cytokine stimulation by generating colonies. However, when HCSs isolated from moderate and severe DNBS mice were compared with HCSs isolated from healthy (sham) mice, a significant increase in colony formation was observed. In contrast, when treated with eNAMPT, HCSs derived from DNBS mice showed a reduced colony formation capacity. Taken together, these findings suggest that intestinal inflammation promotes expansion of the hematopoietic stem cell compartment, leading to enhanced hematopoietic activity; however, elevated levels of eNAMPT may drive excessive proliferation, ultimately resulting in exhaustion of bone marrow hematopoietic stem cells.

4.2.7 EFFECT OF ALT-100 TREATMENT IN MURINE CD PROGRESSION

To evaluate the therapeutic role of the humanized monoclonal antibody ALT-100 in alleviating IBD symptoms, acute intestinal inflammation was chemically induced in 8-weeks-old BALB/c mice by i.r. administration of DNBS at a dose of 3 mg/mouse. Animals were divided into three experimental groups: sham, DNBS, DNBS + ALT-100 (1 mg/kg). At the end of the treatment period, changes in body weight and colon length were assessed to monitor the progression of the inflammatory response and to evaluate the potential effect

of ALT-100 to disease improvement (Fig. 46).

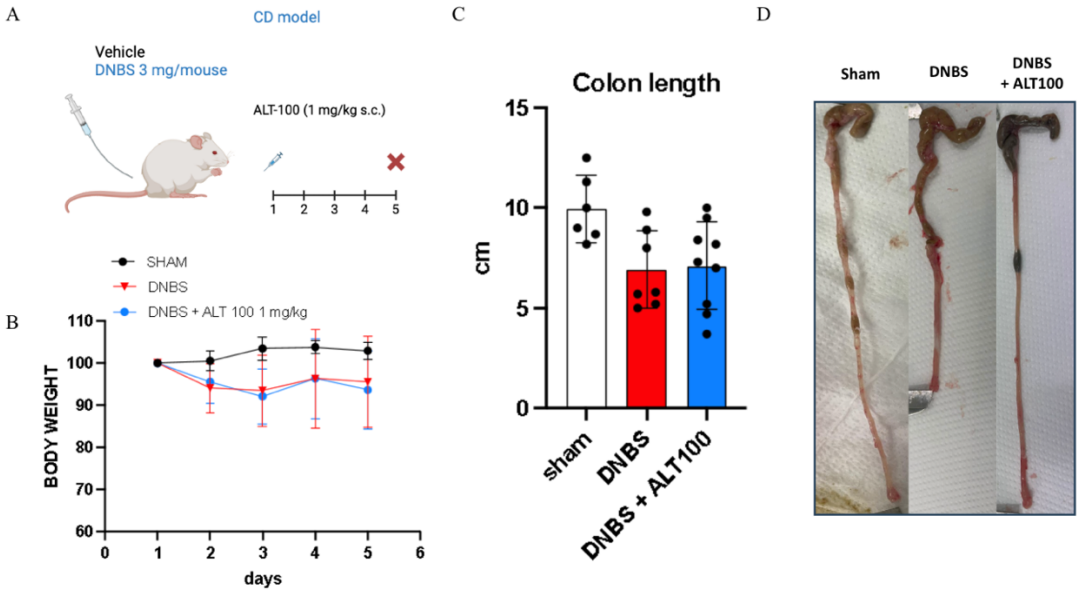

Figure 46. Experimental design and evaluation of ALT-100 treatment in a DNBS model. (**A**) Schematic representation of the experimental model. (**B**) Body weight evaluation during treatment of experimental groups (sham, DNBS, DNBS + ALT). (**C**) Colon length measurements at the end of treatment. (**D**) Representative images of colons collected at the end of the treatment. Data are shown as mean ± SD, n=2.

Results showed that treatment with ALT-100 did not lead to a recovery in body weight compared with DNBS-treated mice (Fig. 46B). However, colon length in ALT-100-treated mice appeared partially restored relative to DNBS mice, reaching values comparable to those observed in healthy controls (Fig. 46C-D). These data suggest that the humanized anti-NAMPT antibody is effective in reducing some of the symptoms associated with CD in an acute DNBS-induced model.

4.2.8 EFFECT OF ALT-100 TREATMENT AT TISSUE LEVEL

Next, we evaluated eNAMPT neutralization by ALT-100 effect at tissue level through IHC analyses. Histological features were assessed using three staining techniques (Cogentech, IFOM, Milan): hematoxylin and eosin (HE), Picrosirius Red, and Masson's trichrome (Fig. 47A). HE staining revealed that after ALT-100 treatment, epithelial damage present in DNBS-treated mice was notably reduced; Picrosirius Red showed a substantial reduction of collagen deposition in DNBS + ALT-100 mice; Masson's trichrome staining confirmed that DNBS-induced colons displayed elevated collagen deposition and increased fibrotic

formation, which was markedly attenuated in DNBS mice treated with ALT-100. Together, these findings demonstrate that treatment with the humanized anti-eNAMPT antibody ALT-100 can mitigate the profibrotic processes typically associated with chronic inflammatory bowel disease.

A

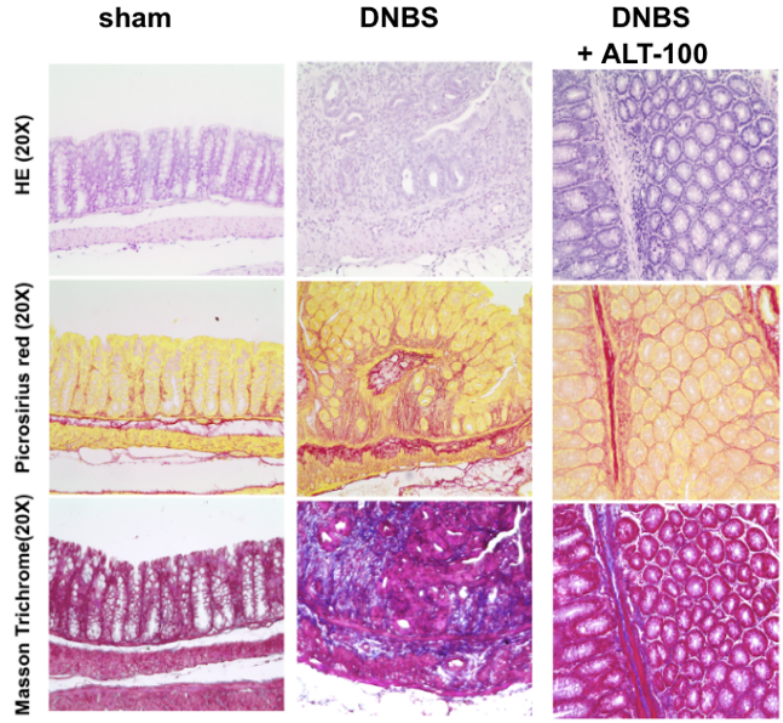

B

GROUPS	DISTORTION OF GLANDULAR ARCHITECTURE	CHORION INFLAMMATORY INFILTRATION	SUPPRESSION OF MUCOSECRETORY ACTIVITY	REGENERATIVE/ DISPLASTIC ALTERATIONS	GLANDULAR ATROPHY	FIBROSIS	SCORE
DNBS	2	2	1	1	0	2	8
DNBS + ALT-100 1mg/kg	0	2	0	0	0	1	3
Legend:	0=Absent	1= Mild	2= Moderate	3= Discrete	4= Severe		

Figure 47. IHC evaluation of ALT-100 treatment. (**A**) Representative images of colon sections from sham, DNBS, and DNBS + ALT-100 (1 mg/kg) mice stained with Hematoxylin and Eosin (HE), Picrosirius Red, and Masson's trichrome (20x magnification). (**B**) Semiquantitative histopathological scoring of tissue damage.

A semiquantitative histological scoring system (0-4 per parameter) was applied to assess tissue damage based on glandular architectural distortion, inflammatory cell infiltration, mucin secretion, regenerative dysplasia, glandular atrophy, and fibrosis (Fig. 47B). In the DNBS-induced murine model of Crohn's disease, inflammation and fibrosis yielded a total histological score of 8. Treatment with the humanized monoclonal antibody ALT-100 markedly improved tissue morphology. ALT-100 restored glandular structure, muco-secretory activity, and epithelial integrity (all scores 0). Fibrosis was also reduced (2 → 1).

Overall, ALT-100 administration significantly alleviated DNBS-induced intestinal damage, lowering the total histological score from 8 to 3, demonstrating its protective and anti-fibrotic effects.

4.2.9 EEFECT OF ALT-100 TREATMENT ON THE INFLAMMATORY INFILTRATE

The effect of ALT-100 on the inflammatory infiltrate within the colon was also investigated. *Lamina propria* cells were isolated and analyzed by flow cytometry. Given that previous data showed that eNAMPT exerts its effect primarily on the myeloid cell compartment, the immune populations analyzed included total myeloid cells ($CD45^+CD11b^+$), specifically monocytes ($Ly6C^+$) and granulocytes ($LY6G^+$) (Fig. 48).

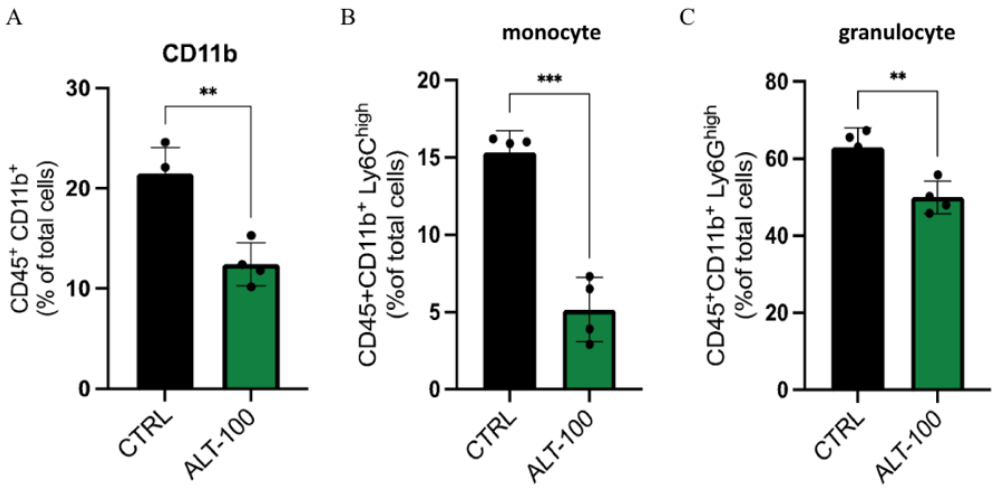

Figure 48. Flow cytometric analysis of ALT-100 effect in *lamina propria*. Quantification of (**A**) total myeloid cells ($CD45^+CD11b^+$), (**B**) monocytes ($Ly6C^+$), and (**C**) granulocytes ($Ly6G^+$) within total myeloid cells, in colon from DNBS untreated (CTRL) and ALT-100 treated mice. Data are shown as mean ± SD, n=2.

Flow cytometric analyses revealed that treatment with ALT-100 (1 mg/kg) significantly reduced the percentage of total myeloid cells in the *lamina propria* (Fig. 48A). Similarly, both monocytes ($CD45^+CD11b^+Ly6C^+$) and granulocytes ($CD45^+CD11b^+Ly6G^+$) were notably decreased following ALT-100 administration (Fig. 48B-C). This demonstrates that the humanized anti-eNAMPT monoclonal antibody ALT-100 effectively reduces the accumulation of myeloid cells, particularly monocytes and granulocytes, within the inflamed colon.

4.2.10 EFFECT OF ALT-100 ON INFLAMMATORY CELLS RECRUITMENT

After demonstrating that ALT-100 modulates the myeloid compartment within the colonic *lamina propria*, its effect was investigated also at the systemic level. To this end, mature circulating cells were analyzed in peripheral blood (Fig. 49).

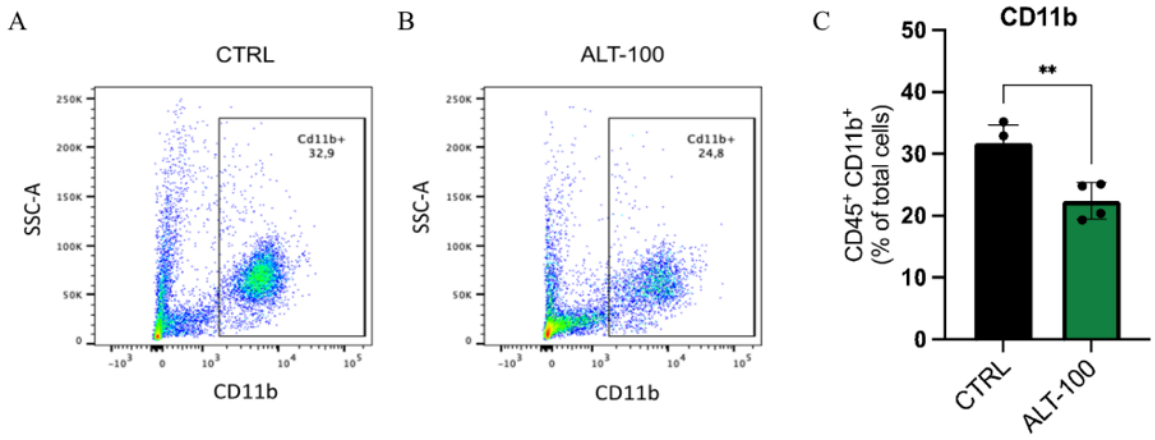

Figure 49. Flow cytometric analysis of ALT-100 effect in blood circulation. Representative dot plots of FACS analysis (**A**) and (**B**), showing mature myeloid population ($C45^+CD11b^+$) in blood of respectively DNBS untreated (CTRL) and ALT-100 treated mice, and (**C**) quantification. Data are shown as mean ± SD, n=2.

Flow cytometric analysis of blood cell populations following administration of the monoclonal antibody ALT-100 (1 mg/kg) revealed a significant reduction in the percentage of myeloid cells. These data are consistent with the findings obtained in the *lamina propria*, supporting the hypothesis that ALT-100 reduces the recruitment of myeloid cells into the inflamed compartment.

4.2.11 EFFECT OF ALT-100 ON INFALLAMTORY CELLS DIFFERENTIATION

Following the observations that ALT-100 reduces myeloid cells infiltration at the inflammatory site in Crohn's like DNBS-induced model, and reduces also myeloid recruitment at systemic level, we investigated whether this effect was due to an impaired recruitment or altered myeloid differentiation in the bone marrow. Bone marrow cells from DNBS-induced mice, treated or untreated with ALT-100 (1 mg/kg), were analyzed by flow cytometry (Fig. 50). ALT-100 treatment significantly decreased hematopoietic progenitors ($Lin^-c\text{-}KIT^+$) (Fig. 50A). Similarly, the proportion of hematopoietic stem cells (LSK, $Lin^-Sca\text{-}1^+c\text{-}KIT^+$) decreased (Fig. 50B). Consistently, mature myeloid cells ($CD45^+CD11b^+$) in the bone marrow were reduced (Fig. 50C).

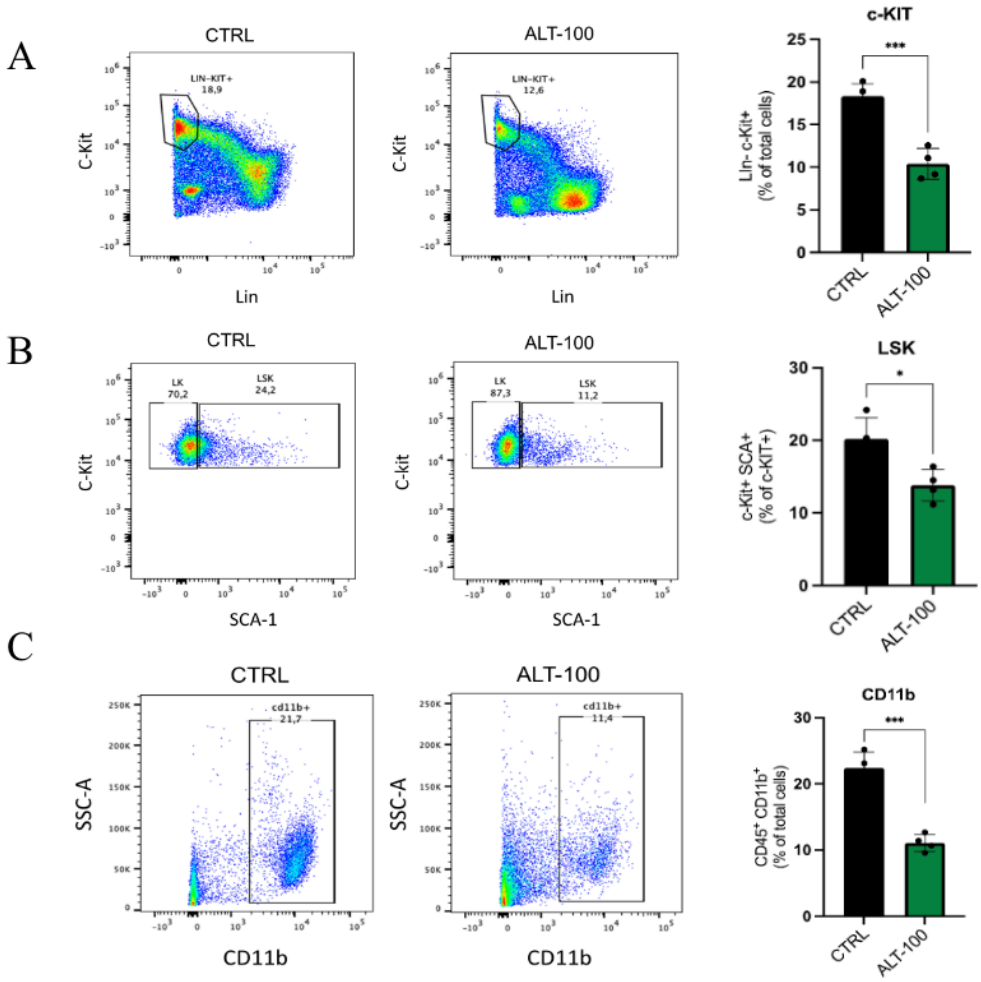

Figure 50. Flow cytometric analysis of ALT-100 effect in bone marrow. Representative dot plots and relative quantification of (**A**) hematopoietic progenitors ($Lin^-c\text{-}KIT^+$), (**B**) hematopoietic stem cells (LSK, $Lin^-Sca\text{-}1^+KIT^+$), and (**C**) mature myeloid cells ($CD45^+CD11b^+$) in the bone marrow of DNBS untreated (CTRL) and ALT-100 treated mice. Data are shown as mean ± SD, n=2.

Overall, these findings indicate that ALT-100 not only modulates the composition of the local inflammatory infiltrate by reducing the myeloid component but also exerts systemic effects by modulating hematopoietic differentiation. Specifically, ALT-100 reduces progenitors and HCSs proliferation and myeloid output, thereby contributing to the attenuation of inflammatory myelopoiesis in DNBS-induce Crohn's like disease.

4.2.12 EFFECT OF ALT-100 ON FIBROTIC PROCESS

Finally, since intestinal fibrosis represents a common complication of CD, and previous data suggested a modulatory role of ALT-100 on the fibrotic process, the expression of genes involved in fibrosis and inflammation were analyzed through an RNA array analysis.

The analysis involved RNA extracted from colon of untreated (sham) mice, sham mice treated with eNAMPT (sham + eNAMPT), untreated DNBS-induced mice (DNBS), and DNBS-induced mice treated with ALT-100 (DNBS + ALT-100) (Fig. 51A). Moreover, the expression of two pro-fibrotic genes (MMP and TFG-β) was examined through RT-PCR (Fig. 51B-C).

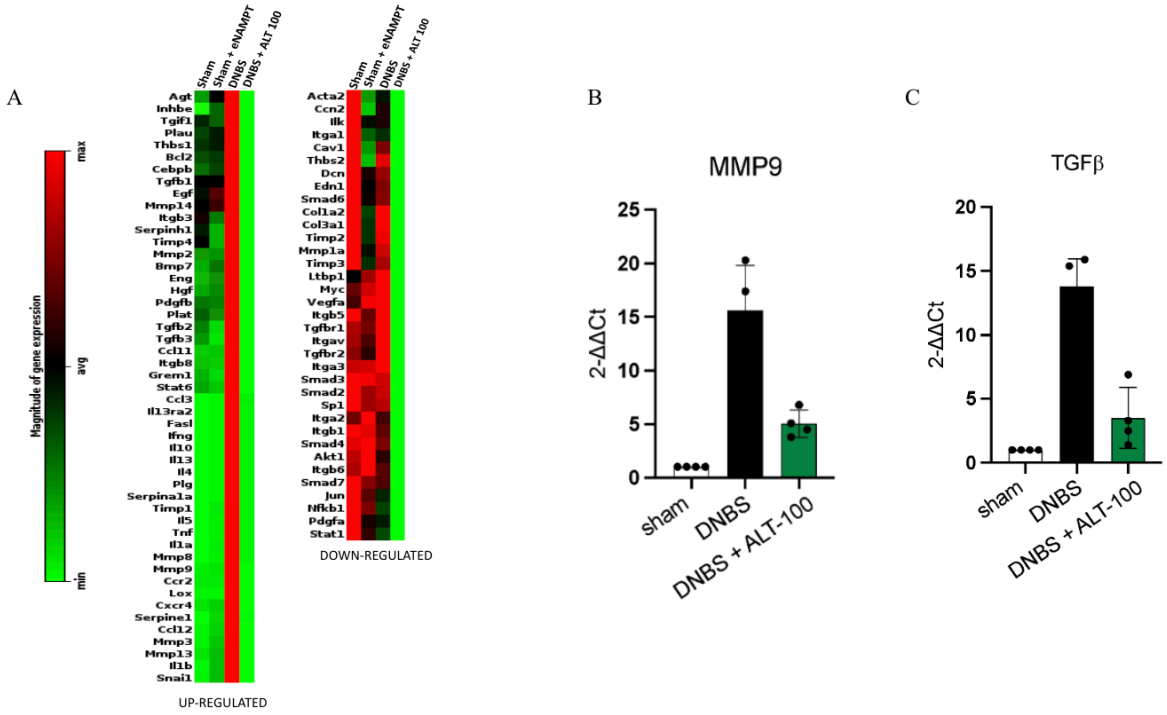

Figure 51. ALT-100 effect on pro-fibrotic process. (**A**) Heatmap of RNA array analysis performed using a panel of genes involved in fibrosis. In green down-regulated genes, in red up-regulated genes. Gene expression quantification of (**B**) MMP9 and (**C**) TGF-β through RT-PCR after ALT-100 treatment.

RNA array analysis was performed to evaluate the expression of a panel of fibrosis-associated genes. The heatmap illustrates a broad downregulation of several pro-fibrotic genes in ALT-100 treated samples compared to untreated DNBS controls. Notably, a marked reduction was observed in members of the MMP family (including MMP3, MMP9, MMP8, MMP13, and MMP14) and in genes belonging to the TGF-β signaling pathway (TGFB1, TGFB2, TGFB3, BMP7, TGFBR1, TGFBR2), both of which are key mediators of extracellular matrix remodeling and fibrogenesis. We analyzed through RT-PCR the expression levels of MMP9 and TGF-β. As shown in figure 51, both MMP9 (B) and TGF-β (C) expression levels were markedly increased in the colons of DNBS-treated mice compared with healthy controls (sham). Treatment with the ALT-100 antibody (DNBS + ALT-100) significantly reduced the expression of these pro-fibrotic genes compared to

untreated DNBS mice, restoring levels close to those observed in healthy animals, although still slightly elevated, consistent with IHC analyses. Overall, these results confirm that ALT-100 exerts a strong anti-fibrotic effect by suppressing the transcriptional activation of key mediators involved in the fibrotic response.

4.2.13 EFFECT Of ALT-100 TREATMENT IN MURINE COLITIS PROGRESSION

To further validate the efficacy of ALT-100 in ameliorating inflammatory bowel disease symptoms, we employed an additional model of IBD, the DSS-induced colitis model. Both acute and chronic treatment protocols were used to comprehensively assess the therapeutic potential of ALT-100 in different stages of intestinal inflammation.

Acute intestinal inflammation was chemically induced in 8-weeks-old C57BL/6 mice by administering 2,5% DSS in drinking water for 7 days, followed by a washout period of 3 days. Animals were divided into 3 experimental groups: sham, DSS, DSS + ALT-100 (1 mg/kg). At the end of the treatment period, changes in body weight and colon length were assessed to monitor the progression of the inflammatory response and to evaluate the potential effect of ALT-100 to disease improvement (Fig. 52).

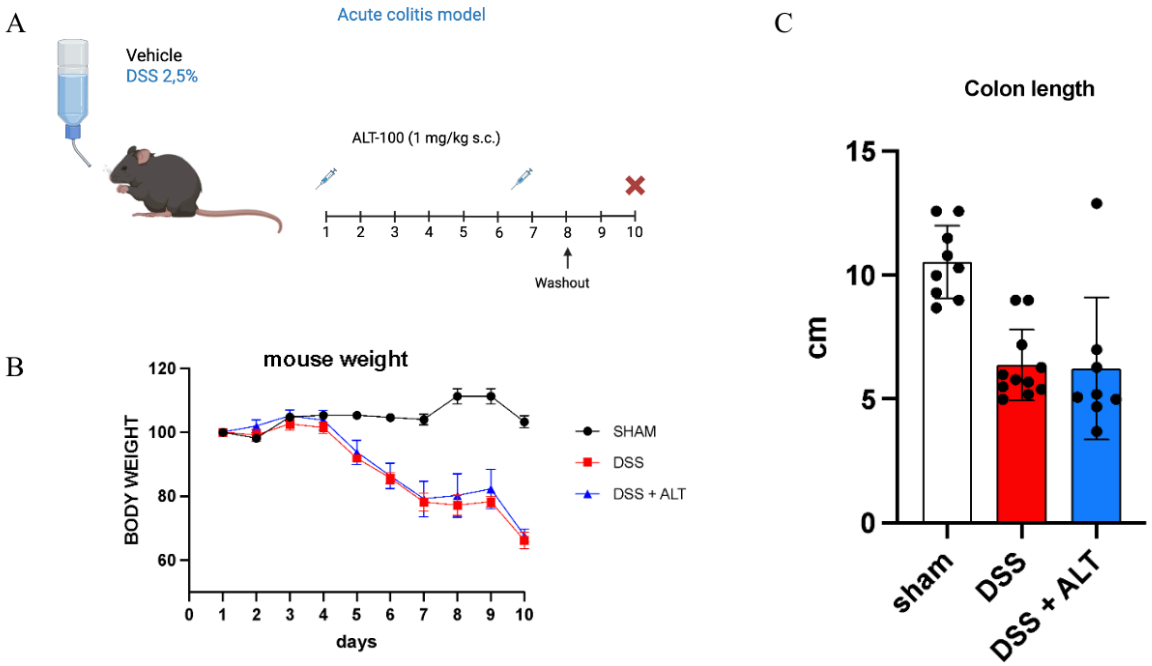

Figure 52. Experimental design and evaluation of ALT-100 treatment in an acute DSS model. (**A**) Schematic representation of the experimental model. (**B**) Body weight evaluation during treatment of experimental groups (sham, DSS, DSS + ALT). (**C**) Colon length measurements at the end of treatment. Data are shown as mean ± SD, n=2.

In contrast with the DNBS model, in the acute DSS-induced colitis model, results showed that treatment with ALT-100 did not lead to a recovery in body weight compared with DSS-treated mice (Fig. 52B) or colon length (Fig. 52C). This lack of efficacy may be attributable to the predominant activity of ALT-100 on fibrotic processes, which are less prominent in the DSS model compared to the DNBS-induced model. Consequently, the relative short treatment period during the acute inflammatory phase may have been insufficient for ALT-100 to exert its therapeutic effects.

To further investigate this hypothesis, the efficacy of ALT-100 was subsequently evaluated in a chronic DSS model with higher ALT-100 dosage. In collaboration with the Scripps Institute, University of Florida, chronic inflammation was induced in 8-weeks-old C57BL/6 mice by administering 2% DSS in drinking water for 7 days, followed by a 12-days washout period, and a second 7-days DSS cycle. After an additional 3 days washout, mice were sacrificed, for a total duration of 28 days. Animals were divided into 4 experimental groups: sham, DSS + PBS, DSS + ALT-100 (1 mg/kg), and DSS + ALT-100 (4 mg/kg). At the end of the treatment period, changes in body weight and colon length were assessed to monitor the progression of the inflammatory response and to evaluate the potential effect of ALT-100 to disease improvement (Fig. 53).

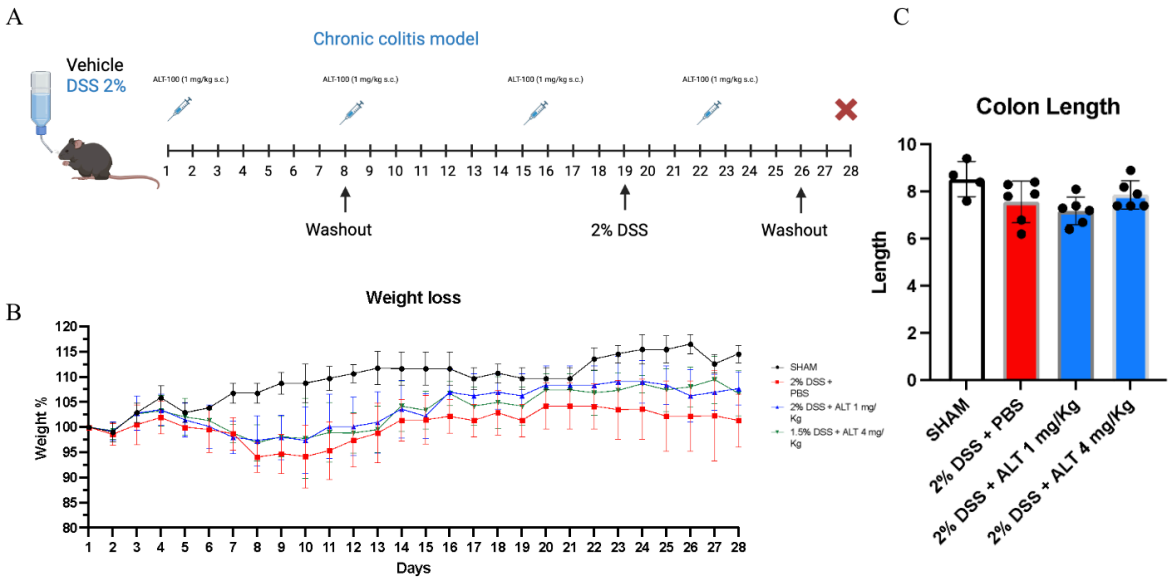

Figure 53. Experimental design and evaluation of ALT-100 treatment in a chronic DSS model. (**A**) Schematic representation of the experimental model. (**B**) Body weight evaluation during treatment of experimental groups (sham, DSS + PBS, DSS + ALT 1 mg/kg, DSS + ALT-100 4 mg/kg). (**C**) Colon length measurements at the end of treatment. Data are shown as mean ± SD, n=2.

Results showed that DSS administration induced a progressive weight loss in vehicle-treated mice, while ALT-100 treatment mitigates this effect. Although the reduction in weight loss was not markedly pronounced, a trend toward recovery of normal body weight was observed in ALT-100-treated groups (1 and 4 mg/kg) compared with DSS + PBS controls (Fig. 53B). Measurement of colon length at the endpoint revealed that ALT-100 at both doses partially restored colon length, suggesting a protective effect against DSS-induced tissue damage (Fig. 53C). Overall, these findings indicate that ALT-100 exerts beneficial effects in the chronic DSS model of colitis, promoting recovery of body weight and preservation of colon architecture, consistent with its therapeutic potential in chronic intestinal inflammation.

4.3 THE ROLE OF NAMPT PHOSPHORILATIONS

4.3.1 IDENTIFICATION OF NAMPT PHOSPHORYLATION SITES

The identification of phosphorylation sites within the NAMPT protein was performed in collaboration with the research group of Professor Wohlschlegel at the UCLA, Los Angeles. To this end, a stable murine cell line (B16) was generated to overexpress NAMPT fused at its N-terminus with the GFP. The recombinant NAMPT-GFP protein was subsequently immunoprecipitated using anti-GFP beads and analyzed by liquid chromatography-tandem mass spectrometry (LC-MS/MS) employing a data-dependent acquisition (DDA) strategy combined with parallel reaction monitoring (Fig. 54A). This approach enabled the identification of potential phosphorylation sites covering approximately 78% of the NAMPT protein sequence (Fig. 54B). The remaining uncharacterized region, in white, was likely inaccessible due to steric hindrance imposed by the N-terminal GFP.

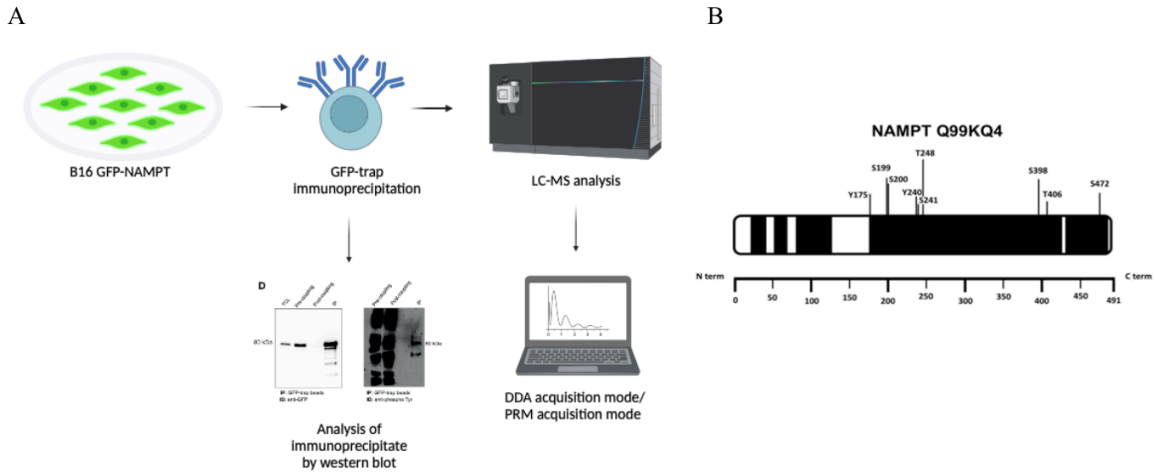

Figure 54. Identification of NAMPT phosphorylation sites. (**A**) Schematic representation of the experimental workflow for the IP and analysis of NAMPT. (**B**) Sequence analysis of NAMPT: black indicates regions of the analyzed sequence, in white the portion not covered by the analysis.

These analyses led to the identification of 8 distinct phosphorylation sites on the NAMPT protein, which are summarized in table 5. The values of the normalized peak areas are proportional to the degree of phosphorylation of the corresponding residue. These data clearly indicate that serine residue 199 (7,66 ± 0,55) and 200 (6,05 ± 1,57) are the most highly phosphorylated sites on NAMPT.

The experimentally identified phosphorylation sites were subsequently compared with those predicted using a bioinformatic approach (https://www.phosphosite.org/). Bioinformatic analyses revealed a total of 27 potential phosphorylation sites 4 threonines, 10 serines, and

13 tyrosines. Among these, serine 472 was predicted as one of the most likely phosphorylated ones.

NAMPT MODIFIED PEPTIDES	PHOSPHORYLATED AMINO ACID	m/z	CHARGE	NORMALIZED AREA (area average ± SD)
Y [+80] LLETSGNLDGLETK	Y175	598,9448	3	0,32 ± 0,05
GVS [+80] SQETAGIGASAHLVNFK	S199	684,9965	3	7,66 ± 0,55
GVSS [+80] QETAGIGASAHLVNFK	S200	684,9965	3	6,05 ± 1,57
DPVPGY [+80] SVPAAEHSTITAWGK	Y240	755,0192	3	3,88 ± 0,39
DPVPGYS [+80] VPAAEHSTITAWGK	S241	755,0192	3	3,91 ± 0,46
DLLNC [+57] S [+80]FK	S398	538,7278	2	0,35 ± 0,06
C [+57] SYVVT [+80] NGLGVNVFKDPVADPNK	T406	644,0581	4	2,55 ± 0,15
SYS [+80] FDEVRK	S472	605,7606	2	1,03 ± 0,19

Table 5. NAMPT phosphorylated sites identified by LC-MS/MS. The table reports the modified peptides, the corresponding phosphorylated amino acid residue, their mass-to-charge ratios (m/z), charge state, and normalized peak area (mean ± SD). Normalized area values are proportional to the phosphorylation degree. In red boxes, amino acid residues identified for future analyses.

Based on these, we focused our investigation on residues S199, S200 and S472. To investigate the functional relevance of the identified phosphorylation sites, site-directed mutagenesis was performed to substitute the serine residues with alanine, thereby preventing phosphorylation.

4.3.2 ENZYMATIC CHARACTERIZATION OF NAMPT MUTANT FORMS

Three recombinant NAMPT variants were generated: NAMPT^{S199A}, NAMPT^{S200A}, and NAMPT^{S472A}. The mutant proteins were expressed in *E.coli* using pET28 plasmids and an indirect in vitro enzymatic assay was performed to assess their capacity to catalyze the formation of nicotinamide mononucleotide (NMN) (Fig. 55). Results showed that the NAMPT^{S472A} mutant displayed enzymatic activity comparable to the wild-type protein (NAMPT WT), whereas the NAMPT^{S199A} and NAMPT^{200A} exhibited a complete loss of activity. Thus, only the S472A substitution did not affect NAMPT's ability to synthesize NMN, while mutations at S199 and S200 impaired enzymatic function *in vitro*. Given that NAMPT is active exclusively as a homodimer, and that residues S199 and S200 are located at the dimer interface, unlike S472 which lies on the outer surface, the loss of activity in the S199A and S200A mutants may results from impaired dimer formation.

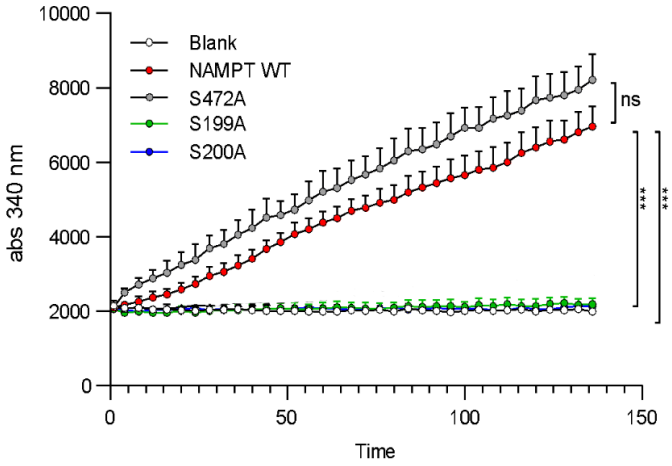

Figure 55. Evaluation of enzymatic activity of NAMPT mutants *in vitro*. *In vitro* enzymatic activity of recombinant NAMPT WT (red), NAMPT^{S199A} (green), NAMPT^{S200A} (blue), and NAMPT^{S472} (grey) proteins, measured as absorbance at 340 nm over time.

4.3.3 EVALUATION OF RECOMBINANT NAMPT OLIGOMERIC STATE

To investigate the oligomeric state of recombinant mutants, a native PAGE followed by Western Blot analysis and a size-exclusion chromatography (SEC) were performed (Fig. 56).

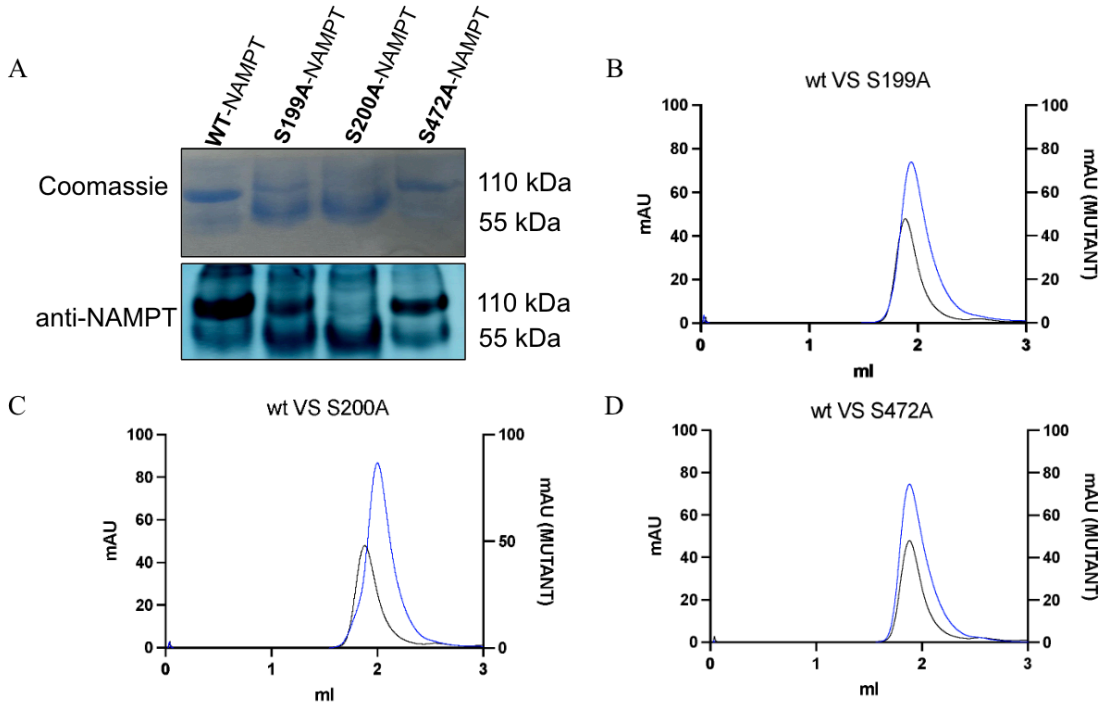

Figure 56. Analyses of NAMPT phospho-mutants oligomeric state. (**A**) Native PAGE followed by Coomassie staining and WB using anti-NAMPT antibody. (**B-D**) Analytical size-exclusion chromatography (SEC) profiles comparing NAMPT WT (black) with (**B**) NAMPT^{S199A}, (**C**) NAMPT^{S200A} and, (**D**) NAMPTS^{472A} mutants (blue).

Native PAGE followed by Western Blot analysis with anti-NAMPT antibody (Fig. 56A) revealed that NAMPT WT and NAMPT^{S472A} predominantly exist as a dimer (110 kDa), whereas NAMPT^{S200A} in mainly monomeric (55 kDa), and NAMPT^{S199A} exists as both monomer and dimer. To confirm these findings, SEC was performed on recombinant NAMPT proteins (S199A, S200A, S472A) (Fig. 56B-C-D). The elution profile of NAMPT WT was superimposed to the elution profiles of NAMPT mutants. Supporting Native PAGE results, NAMPT^{S472A} showed an identical elution volume (1,9 ml) to that of NAMPT WT, consistent with a dimeric state, while NAMPT^{S200A} eluted later (2,1 ml), indicating a monomeric form. NAMPT^{S199A} displayed an intermediate elution profile (2 ml), suggesting coexistence of both species. Overall, these results indicate that mutations at S199 and S200 impair NAMPT dimerization, correlating with loss of enzymatic activity, whereas S472A retains dimeric capacity and an enzymatic activity.

4.3.4 EFFECT OF NAMPT MUTATIONS ON CELL VIABILITY

To investigate the impact of NAMPT phosphorylation on cell viability, 5 stable B16 cell lines were generated via lentiviral infection: B16 Scramble, expressing GFP only, B16 GFP-NAMPT WT, B16 GFP-NAMPT^{S199A}, B16 GFP-NAMPT^{S200A}, and B16 GFP-NAMPT^{S472A}. Cell viability was assessed using the MTT assay at different time points (0, 18, 24, and 48 hours) to monitor proliferation dynamics over time (Fig. 57).

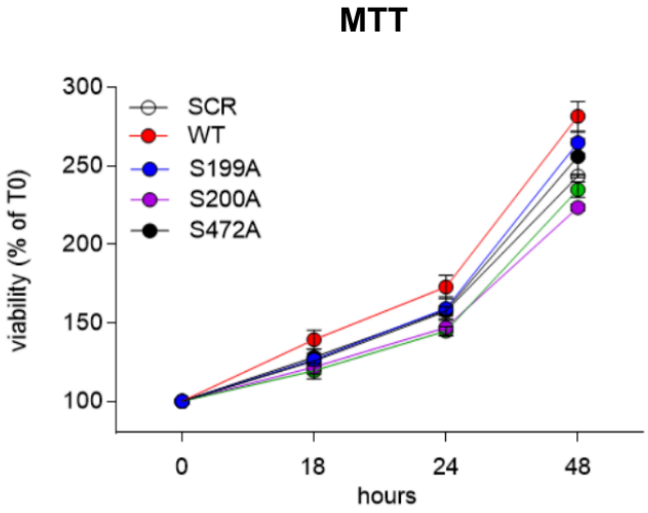

Figure 57. Analysis of cell viability in B16 cell lines expressing WT or mutant forms of GFP-NAMPT. Cell viability assessed by MTT assay in B16 cell lines expressing GFP only (SCR), GFP-NAMPT WT, or the mutant forms GFP-NAMPT^{S199A}, GFP-NAMPT^{S200A}, and GFP-NAMPT^{S472A} at 0, 18, 24, and 48 hours. Data are expressed as percentage of viability relative to time 0.

NAMPT WT B16 cells exhibited a slightly enhanced proliferation compared with the S199A and S472A mutants, indicating that phosphorylation at Ser 199 and Ser 472 does not significantly affect NAMPT's role in supporting cell growth. On the contrary, WT and SCR B16 cell lines exhibited enhanced proliferation compared with the S200A mutant, consistent with impaired enzymatic activity. Data highlight functional similarity between NAMPT WT and NAMPT^{S472A} and indicate that mutations impairing NAMPT enzymatic activity negatively affect cell viability.

4.3.5 INVESTIGATION OF THE SUBCELLULAR LOCALIZATION OF NAMPT MUTANTS

Another aspect investigated was the subcellular localization of the NAMPT mutant proteins. As described in the introduction, WT NAMPT is distributed in both the cytosolic and nuclear compartments. However, the mechanism governing NAMPT translocation between these cellular regions remains unclear. Therefore, we aimed to assess whether phosphorylation at residues S199, S200, or S472 may play a key role in this process. NAMPT localization was analyzed by fluorescence microscopy, taking advantage of the N-terminal GFP, and nuclei were stained with Hoechst (Fig. 58).

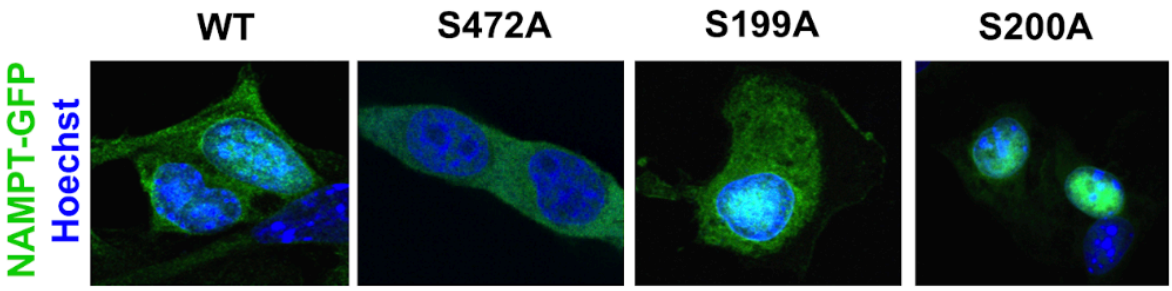

Figure 58. Fluorescence microscopy images of NAMPT mutant forms subcellular localization. Fluorescence microscopy images of B16 cells expressing GFP-NAMPT WT, GFP-NAMPT^{S199A}, GFP-NAMPT^{S200A}, and GFP-NAMPT^{S472A}. NAMPT localization is visualized in green (GFP), while cell nuclei are stained in blue with Hoechst dye.

GFP-NAMPT WT fluorescence was detected in both the cytoplasm and nucleus, consistent with previous reports. Similarly, GFP-NAMPT^{S472A} and GFP-NAMPT^{S199A} were present in both compartments, whereas GFP-NAMPT^{S200A} appeared predominantly nuclear. These preliminary observations suggest that the S200A mutation may alter NAMPT subcellular distribution, implying a potential regulatory role for phosphorylation at this residue in cytoplasm-to-nucleus transport.

4.3.6 EXPRESSION AND SECRETION ANALYSES OF NAMPT MUTANT FORMS

To assess the effect of phosphorylation on NAMPT expression and secretion, B16 cell lines expressing GFP-NAMPT WT or its mutant forms (S199A, S200A, S472A) were cultured in serum-free medium for 4 hours to induce protein release under nutrient deprivation conditions. Intracellular and extracellular protein fractions were analyzed by SDS-PAGE and Western Blot (Fig. 59).

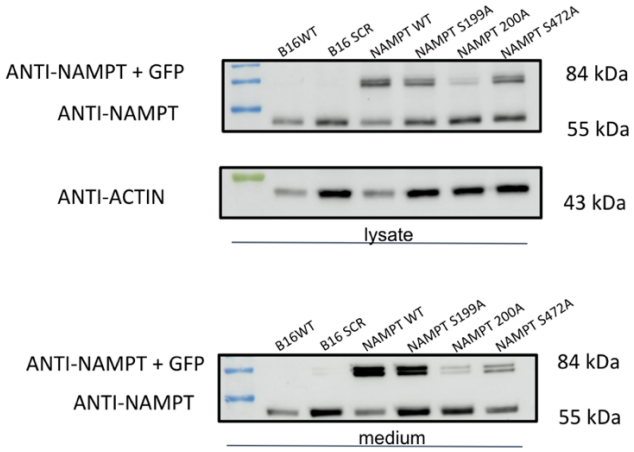

Figure 59. Western Blot analysis of NAMPT mutant forms expression and secretion. Western Blot analysis of GFP-NAMPT WT, GFP-NAMPT^{S199A}, GFP-NAMPT^{S200A}, and GFP-NAMPT^{S472A} obtained from cell lysate or supernatant (medium).

GFP-NAMPT WT and GFP-NAMPT^{S472A} exhibited similar expression levels, whereas GFP-NAMPT^{S199A} and GFP-NAMPT^{S200A} showed reduced expression. This decrease is likely related to impaired dimerization and enzymatic activity, leading to negative selection in culture. Despite these differences, all mutant forms were secreted at comparable levels, indicating that phosphorylation at residues S199, S200, or S472 does not significantly affect extracellular NAMPT release.

4.3.7 ASSESSMENT OF THE CYTOKINE-LIKE ACTIVITY OF NAMPT MUTANTS

Extracellular NAMPT (eNAMPT) has been widely recognized as a pro-inflammatory cytokine, although the molecular mechanism underlying its activity and the identity of its receptor(s) remain unclear. To investigate the cytokine-like activity of the NAMPT mutant forms, murine peritoneal macrophages (PECs) were treated for 4 hours with recombinant NAMPT WT, GFP-NAMPT^{S199A}, GFP-NAMPT^{S200A}, and GFP-NAMPT^{S472A}, either alone or in combination with IFN-γ. Following treatment total RNA was extracted and the

expression of pro-inflammatory genes (IL-6, IL-1β, and CXCL10) was assessed by RT-PCR (Fig. 60). According to results, NAMPT^{S199A} exhibited markedly reduced cytokine-like activity compared with NAMPT WT. While NAMPT WT significantly increased the expression of IL-6, IL-1β, and CXCL10 in murine peritoneal macrophages, this effect was notably diminished with NAMPT^{S199A}.

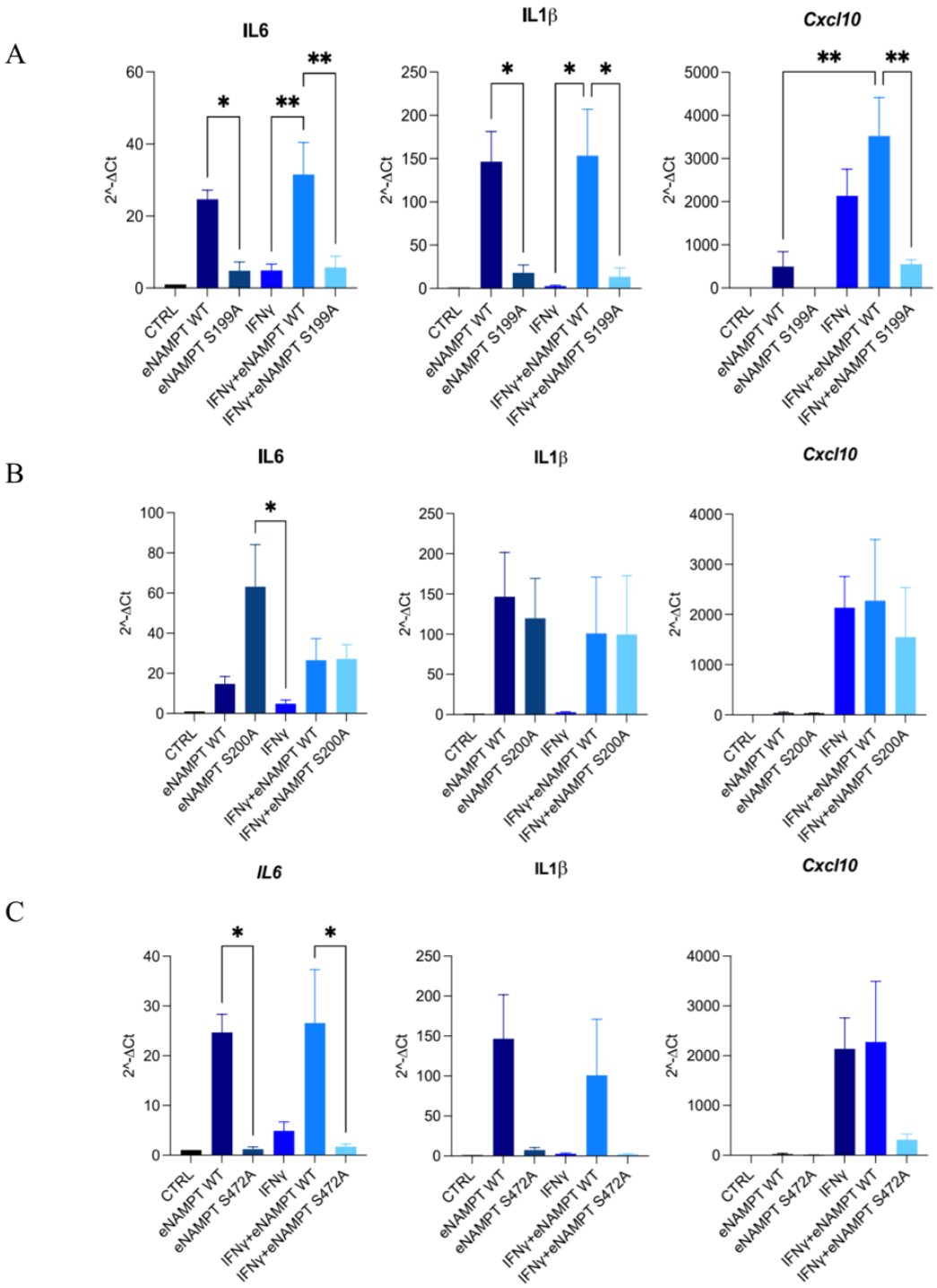

Figure 60. Analysis of NAMPT mutant forms cytokine activity. RT-PCR shows expression of pro-inflammatory genes (IL-6, IL-1β, and CXCL10) after (**A**) NAMPT^{S199A}, (**B**) NAMPT^{S200A}, or (**C**) NAMPT^{S472A} treatment, alone or in combination with IFN-γ.

Treatment with NAMPT^{S200A} resulted in a higher induction of IL-6 compared to NAMPT WT or IFN-γ alone, while IL-1β and CXCL10 levels remained similar to those elicited by the WT protein. NAMPT^{S200A} also maintained synergistic activity with IFN-γ. These findings suggest that eNAMPT pro-inflammatory function may be partially independent of its enzymatic activity or dimerization state. Conversely, NAMPT^{S472A} completely lost cytokine activity, as no upregulation of IL-6, IL-1β or CXCL10 was observed, either alone or in combination with IFN-γ. Despite retaining enzymatic activity comparable to the wild type, this mutant appears unable to trigger inflammatory signaling, likely due to impaired interaction with its receptor. Given that Ser 472 is located on the protein's outer surface, its phosphorylation may be essential for receptor binding and cytokine function.

To conclude, table 6 summarizes the functional and cellular consequences of site-directed mutagenesis of NAMPT at residues S199, S200, and S472, compared with the wild-type protein.

NAMPT MUTATED SITE	OLIGOMERIC STATE	ENZIMATIC ACTIVITY	PROLIFERATION	SUBCELLULAR LOCALIZATION	SECRETION	CITOKINE ACTIVITY
WT	DIMER	ACTIVE	NORMAL	CYTOSOL/NUCLEUS	YES	YES
S199A	MONOMER/DIMER	INACTIVE	NORMAL	CYTOSOL/NUCLEUS	YES	NO
S200A	MONOMER	INACTIVE	REDUCED	NUCLEUS	YES	YES
S472A	DIMER	ACTIVE	NORMAL	CYTOSOL/NUCLEUS	YES	NO

Table 6. Functional, Structural, and Cellular Characterization of NAMPT Mutants.

Collectively, the data highlight distinct functional signatures for each mutation. While the S199A and S200A substitutions lead to loss of enzymatic activity and altered oligomerization, they differ markedly in their effects on cellular proliferation and cytokine-like signaling. In contrast, the S472A mutant retains wild-type-like enzymatic activity and localization but lacks cytokine activity, suggesting that this residue plays a specific role in mediating extracellular signaling rather than enzymatic function.

5. DISCUSSION

In this thesis, we investigated the multifaceted contribution of NAMPT to immune-mediated gastrointestinal diseases, such as AAG and IBD, integrating transcriptomic, cellular, *in vivo*, and molecular approaches.

Through RNA sequencing of gastric biopsies, we delineated distinct transcriptional profiles distinguishing Autoimmune Atrophic Gastritis (AAG) patients from healthy controls (HC), revealing a coordinated dysregulation of inflammatory pathways, immune-cell recruitment signatures, and alterations in epithelial and stromal homeostasis. Although NAMPT emerged as an upregulated inflammatory mediator within AAG tissues [(150)], its direct influence on the global transcriptional landscape appeared moderate, suggesting that NAMPT contributes to AAG pathogenesis primarily through targeted immunomodulatory functions rather than broad transcriptional reprogramming. Complementary RNA-seq analyses of patient-derived gastric fibroblasts further demonstrated that AAG fibroblasts exhibit a disease-specific transcriptional signature marked by disrupted extracellular matrix organization, cytoskeletal architecture, and pathways associated with tissue remodeling. Notably, NAMPT expression increased only moderately in AAG-derived fibroblast at both the protein and gene level, and eNAMPT treatment of HC fibroblasts produced only minimal functional effects. These findings suggest that although NAMPT contributes to AAG progression, its pathological actions are likely mediated through other cellular compartments, potentially epithelial populations, rather than through stromal fibroblasts alone.

Extending the investigation to Inflammatory Bowel Disease (IBD), *in vivo* analyses revealed that eNAMPT significantly exacerbates disease severity in DNBS-induced Crohn-like disease. For instance, elevated eNAMPT levels intensified mucosal injury, promoted expansion and recruitment of inflammatory myeloid subpopulations such as mature and immature granulocytes ($Ly6G^+$) within the *lamina propria*, and altered circulating and bone marrow-derived progenitors' populations, inducing the expansion of GMPs. This establishes eNAMPT as both a local amplifier of intestinal inflammation and a systemic modulator of hematopoiesis. Furthermore, the capacity of NAMPT to modulate the proliferation of stem cells derived from mouse bone marrow has been validated by *ex vivo* studies, in which eNAMPT was found to act synergistically with multiple growth factors, including G-CSF and GM-CSF, thereby enhancing colony formation. Importantly, therapeutic neutralization of eNAMPT with the humanized monoclonal antibody ALT-100 (Aqualung Therapeutics®)

attenuated clinical symptoms in both a DNBS-induced Crohn-like murine model and in a chronic DSS-induced colitis model. Moreover, ALT-100 was able to restore histological disease parameters, reduced immune-cell infiltration, and preserved tissue architecture in the DNBS-induced Crohn model, underscoring the translational feasibility of targeting eNAMPT in intestinal inflammation.

At the molecular level, phosphosite mutagenesis studies delineated phosphorylation as a critical regulatory mechanism governing NAMPT's dual enzymatic and cytokine-like activity. Ser 199 and Ser 200 were identified as essential residues for proper dimerization and enzymatic function, whereas Ser 472 was shown to be indispensable for extracellular cytokine activity possibly through receptor engagement, despite preserving intracellular catalytic capacity. These findings demonstrate that NAMPT's metabolic and pro-inflammatory functions are modulated by discrete post-translational modifications, and phosphorylation could represent a key element in understanding mechanisms behind eNAMPT release and activity.

Collectively, this work advances the conceptualization of NAMPT as a key mediator of gastrointestinal immune pathology. By integrating patient-derived transcriptomics, cell biology, immune profiling, *in vivo* modeling, and molecular dissection of NAMPT regulation, this thesis provides a comprehensive framework for understanding NAMPT-mediated disease mechanisms and supports the development of eNAMPT-targeted therapeutic strategies in AAG, IBD, and related immune-mediated disorders.

6. REFERENCES

1. Langkamp-Henken B, Glezer JA, Kudsk KA. Immunologic structure and function of the gastrointestinal tract. Nutr Clin Pract. 1992 Jun;7(3):100-8. doi: 10.1177/0115426592007003100. PMID: 1289681.

2. James SP. The gastrointestinal mucosal immune system. Dig Dis. 1993;11(3):146-56. doi: 10.1159/000171407. PMID: 8370141.

3. Asad R, Shahzad MA, Knawal S, Bano S, Javed M, Anwar A, Shah SSUD. Evaluation of Antimicrobial Peptides in Saliva as Potential Therapeutic Agents Against Oral Pathogens in Pakistan. Cureus. 2024 Nov 15;16(11):e73758. doi: 10.7759/cureus.73758. PMID: 39677072; PMCID: PMC11646478.

4. Vegesna AK, Chuang KY, Besetty R, Phillips SJ, Braverman AS, Barbe MF, Ruggieri MR, Miller LS. Circular smooth muscle contributes to esophageal shortening during peristalsis. World J Gastroenterol. 2012 Aug 28;18(32):4317-22. doi: 10.3748/wjg.v18.i32.4317. PMID: 22969194; PMCID: PMC3436046.

5. Nicosia MA, Brasseur JG, Liu JB, Miller LS. Local longitudinal muscle shortening of the human esophagus from high-frequency ultrasonography. Am J Physiol Gastrointest Liver Physiol. 2001 Oct;281(4):G1022-33. doi: 10.1152/ajpgi.2001.281.4.G1022. PMID: 11557523.

6. Karnul AM, Murthy CK. A Study of Variations of the Stomach in Adults and Growth of the Fetal Stomach. Cureus. 2022 Aug 28;14(8):e28517. doi: 10.7759/cureus.28517. PMID: 36185902; PMCID: PMC9515405.

7. Flemström G, Isenberg JI. Gastroduodenal mucosal alkaline secretion and mucosal protection. News Physiol Sci. 2001 Feb;16:23-8. doi: 10.1152/physiologyonline.2001.16.1.23. PMID: 11390942.

8. Qin J, Pei X. Isolation of Human Gastric Epithelial Cells from Gastric Surgical Tissue and Gastric Biopsies for Primary Culture. Methods Mol Biol. 2018;1817:115-121. doi: 10.1007/978-1-4939-8600-2_12. PMID: 29959708.

9. Chaudhry SR, Liman MNP, Omole AE, et al. Anatomy, Abdomen and Pelvis: Stomach. [Updated 2024 Jul 17]. In: StatPearls [Internet]. Treasure Island (FL): StatPearls Publishing; 2025 Jan-. Available from:

10. Pangtey B, Kaul JM, Mishra S. Histogenesis of Muscularis Mucosa and Muscularis Externa of Stomach: A Human Foetal Study. J Clin Diagn Res. 2017 Aug;11(8):AC01-AC03. doi: 10.7860/JCDR/2017/26219.10323. Epub 2017 Aug 1. PMID: 28969103; PMCID: PMC5620743.

11. Di Mario F, Goni E. Gastric acid secretion: changes during a century. Best Pract Res Clin Gastroenterol. 2014 Dec;28(6):953-65. doi: 10.1016/j.bpg.2014.10.006. Epub 2014 Oct 30. PMID: 25439063.

12. Johansson ME, Sjövall H, Hansson GC. The gastrointestinal mucus system in health and disease. Nat Rev Gastroenterol Hepatol. 2013 Jun;10(6):352-61. doi: 10.1038/nrgastro.2013.35. Epub 2013 Mar 12. PMID: 23478383; PMCID: PMC3758667.

13. Allen A, Flemström G. Gastroduodenal mucus bicarbonate barrier: protection against acid and pepsin. Am J Physiol Cell Physiol. 2005 Jan;288(1):C1-19. doi: 10.1152/ajpcell.00102.2004. PMID: 15591243.

14. Tu S, Chi AL, Lim S, Cui G, Dubeykovskaya Z, Ai W, Fleming JV, Takaishi S, Wang TC. Gastrin regulates the TFF2 promoter through gastrin-responsive cis-acting elements and multiple signaling pathways. Am J Physiol Gastrointest Liver Physiol. 2007 Jun;292(6):G1726-37. doi: 10.1152/ajpgi.00348.2006. Epub 2007 Mar 1. PMID: 17332476.

15. Klok MD, Jakobsdottir S, Drent ML. The role of leptin and ghrelin in the regulation of food intake and body weight in humans: a review. Obes Rev. 2007 Jan;8(1):21-34. doi: 10.1111/j.1467-789X.2006.00270.x. PMID: 17212793.

16. Sobhani I, Bado A, Vissuzaine C, Buyse M, Kermorgant S, Laigneau JP, Attoub S, Lehy T, Henin D, Mignon M, Lewin MJ. Leptin

secretion and leptin receptor in the human stomach. Gut. 2000 Aug;47(2):178-83. doi: 10.1136/gut.47.2.178. PMID: 10896907; PMCID: PMC1727985.

17. Samloff IM. Cellular localization of group I pepsinogens in human gastric mucosa by immunofluorescence. Gastroenterology. 1971 Aug;61(2):185-8. PMID: 4935210.

18. Samloff IM, Liebman WM. Cellular localization of the group II pepsinogens in human stomach and duodenum by immunofluorescence. Gastroenterology. 1973 Jul;65(1):36-42. PMID: 4124404.

19. Wilhelm SM, Kale-Pradhan PB. Effects of proton pump inhibitors on vitamin B12. Maturitas. 2014 Sep;79(1):1-2. doi: 10.1016/j.maturitas.2014.06.005. Epub 2014 Jun 14. PMID: 24996485.

20. Berson SA, Yllow RS. Nature of immunoreactive gastrin extracted from tissues of gastrointestinal tract. Gastroenterology. 1971 Feb;60(2):215-22. PMID: 5549263.

21. Sipponen P, Härkönen M. Hypochlorhydric stomach: a risk condition for calcium malabsorption and osteoporosis? Scand J Gastroenterol. 2010;45(2):133-8. doi: 10.3109/00365520903434117. PMID: 19958055.

22. Bezwoda W, Charlton R, Bothwell T, Torrance J, Mayet F. The importance of gastric hydrochloric acid in the absorption of nonheme food iron. J Lab Clin Med. 1978 Jul;92(1):108-16. PMID: 26726.

23. Kozyraki R, Cases O. Vitamin B12 absorption: mammalian physiology and acquired and inherited disorders. Biochimie. 2013 May;95(5):1002-7. doi: 10.1016/j.biochi.2012.11.004. Epub 2012 Nov 20. PMID: 23178706.

24. Johnson LR, ed. Physiology of the Gastrointestinal Tract - The gastric H, K-ATPase: Regulation and structure/function of the acid pump of the stomach, 3rd ed.. New York: Raven Press; 1994:1119-1138.

25. Engevik AC, Kaji I, Goldenring JR. The Physiology of the Gastric Parietal Cell. Physiol Rev. 2020 Apr 1;100(2):573-602. doi: 10.1152/physrev.00016.2019. Epub 2019 Oct 31. PMID: 31670611; PMCID: PMC7327232.

26. Walsh JH, Dockray GJ, ed. Gut Peptides: Biochemistry and Physiology - Gut somatostatin, New York: Raven Press; 1994:123-145.

27. Maeda M, Oshiman K, Tamura S, Futai M. Human gastric (H+ + K+)-ATPase gene. Similarity to (Na+ + K+)-ATPase genes in exon/intron organization but difference in control region. J Biol Chem. 1990 Jun 5;265(16):9027-32. PMID: 2160952.

28. Engevik AC, Feng R, Yang L, Zavros Y. The acid-secreting parietal cell as an endocrine source of Sonic Hedgehog during gastric repair. Endocrinology. 2013 Dec;154(12):4627-39. doi: 10.1210/en.2013-1483. Epub 2013 Oct 3. PMID: 24092639; PMCID: PMC3836061.

29. Sawaguchi A, Aoyama F, Ide S, Suganuma T. The cryofixation of isolated rat gastric mucosa provides new insights into the functional transformation of gastric parietal cells: an in vitro experimental model study. Arch Histol Cytol. 2005 Sep;68(3):151-60. doi: 10.1679/aohc.68.151. PMID: 16276021.

30. Wallmark B, Stewart HB, Rabon E, Saccomani G, Sachs G. The catalytic cycle of gastric (H+ + K+)-ATPase. J Biol Chem. 1980 Jun 10;255(11):5313-9. PMID: 6102997.

31. G. Sachs, B. Wallmark, G. Saccomam, E. Rabon, H.B. Stewart, D.R. Dibona, T. Berglindh, Chapter 8 The ATP-Dependent Component of Gastric Acid Secretion, Editor(s): Arnost Kleinzeller, Felix Bronner, Clifford L. Slayman, Current Topics in Membranes and Transport, Academic Press, Volume 16, 1982, Pages 135-159, ISSN 0070-2161, ISBN 9780121533168, .

32. Heitzmann D, Warth R. No potassium, no acid: K+ channels and gastric acid secretion. Physiology (Bethesda). 2007 Oct;22:335-41. doi: 10.1152/physiol.00016.2007. PMID: 17928547.

33. Götze H, Adelson JW, Hadorn HB, Portmann R, Troesch V. Hormone-elicited enzyme release by the small intestinal wall. Gut. 1972 Jun;13(6):471-6. doi: 10.1136/gut.13.6.471. PMID: 5040834; PMCID: PMC1412199.

34. Fish EM, Shumway KR, Burns B. Physiology, Small Bowel. 2024 Jan 31. In: StatPearls [Internet]. Treasure Island (FL): StatPearls Publishing; 2025 Jan–. PMID: 30335296.

35. Azzouz LL, Sharma S. Physiology, Large Intestine. 2023 Jul 31. In: StatPearls [Internet]. Treasure Island (FL): StatPearls Publishing; 2025 Jan–. PMID: 29939634.

36. Salva MN, Gupta C, Pandey AK, Kumar N, Kotian SR, Kalthur SG. Histogenesis and Histomorphometric study of Human Fetal Small Intestine. Ethiop J Health Sci. 2019 Nov;29(6):689-696. doi: 10.4314/ejhs.v29i6.5. PMID: 31741639; PMCID: PMC6842717.

37. Martini E, Krug SM, Siegmund B, Neurath MF, Becker C. Mend Your Fences: The Epithelial Barrier and its Relationship With Mucosal Immunity in Inflammatory Bowel Disease. Cell Mol Gastroenterol Hepatol. 2017 Mar 23;4(1):33-46. doi: 10.1016/j.jcmgh.2017.03.007. PMID: 28560287; PMCID: PMC5439240.

38. Hundt M, Wu CY, Young M. Anatomy, Abdomen and Pelvis: Biliary Ducts. 2023 Jul 15. In: StatPearls [Internet]. Treasure Island (FL): StatPearls Publishing; 2025 Jan–. PMID: 29083810.

39. Portincasa P, Di Ciaula A, Wang HH, Palasciano G, van Erpecum KJ, Moschetta A, Wang DQ. Coordinate regulation of gallbladder motor function in the gut-liver axis. Hepatology. 2008 Jun;47(6):2112-26. doi: 10.1002/hep.22204. PMID: 18506897.

40. David N. Alter, Chapter 32 - Clinical chemistry of the gastrointestinal disorders, Editor(s): William Clarke, Mark A. Marzinke, Contemporary Practice in Clinical Chemistry (Fourth Edition), Academic Press, 2020, Pages 561-572, ISBN 9780128154991, .

41. Megan S. Kennedy, Eugene B. Chang, Chapter One - The microbiome: Composition and locations,

42. Vishy Mahadevan, Anatomy of the caecum, appendix and colon, Surgery (Oxford), Volume 38, Issue 1, 2020, Pages 1-6, ISSN 0263-9319, .

43. Corsetti, M., Costa, M., Bassotti, G. et al. First translational consensus on terminology and definitions of colonic motility in animals and humans studied by manometric and other techniques. Nat Rev Gastroenterol Hepatol 16, 559–579 (2019).

44. Smajdor, J., Jedlińska, K., Porada, R. et al. The impact of gut bacteria producing long chain homologs of vitamin K2 on colorectal carcinogenesis. Cancer Cell Int 23, 268 (2023).

45. Tarracchini C, Lugli GA, Mancabelli L, van Sinderen D, Turroni F, Ventura M, Milani C. Exploring the vitamin biosynthesis landscape of the human gut microbiota. mSystems. 2024 Oct 22;9(10):e0092924. doi: 10.1128/msystems.00929-24. Epub 2024 Sep 17. PMID: 39287373; PMCID: PMC11494892.

46. Emilie Bessède, Francis Mégraud, Microbiota and gastric cancer, Seminars in Cancer Biology, Volume 86, Part 3, 2022, Pages 11-17, ISSN 1044-579X, .

47. Kim DH, Wang Y, Jung H, Field RL, Zhang X, Liu TC, Ma C, Fraser JS, Brestoff JR, Van Dyken SJ. A type 2 immune circuit in the stomach controls mammalian adaptation to dietary chitin. Science. 2023 Sep 8;381(6662):1092-1098. doi: 10.1126/science.add5649. Epub 2023 Sep 7. PMID: 37676935; PMCID: PMC10865997.

48. Satoh-Takayama N, Kato T, Motomura Y, Kageyama T, Taguchi-Atarashi N, Kinoshita-Daitoku R, Kuroda E, Di Santo JP, Mimuro H, Moro K, Ohno H. Bacteria-Induced Group 2 Innate Lymphoid Cells in the Stomach Provide Immune Protection through Induction of IgA. Immunity. 2020 Apr 14;52(4):635-649.e4. doi: 10.1016/j.immuni.2020.03.002. Epub 2020 Apr 1. PMID: 32240600.

49. Yan Y, Satoh-Takayama N. New perspectives on gastric disorders: the relationship between innate lymphoid cells and microbes in the stomach. Cell Mol Life Sci. 2025 Mar 13;82(1):113. doi: 10.1007/s00018-025-05632-w. PMID: 40074935; PMCID: PMC11904066.

50. Delgado S, Cabrera-Rubio R, Mira A, Suárez A, Mayo B. Microbiological survey of the human gastric ecosystem using culturing and pyrosequencing methods. Microb Ecol. 2013 Apr;65(3):763-72. doi: 10.1007/s00248-013-0192-5. Epub 2013 Feb 10. PMID: 23397369.

51. Theisen J, Nehra D, Citron D, Johansson J, Hagen JA, Crookes PF, DeMeester SR, Bremner CG, DeMeester TR, Peters JH. Suppression of gastric acid secretion in patients with gastroesophageal reflux disease results in gastric bacterial overgrowth and deconjugation of bile acids. J Gastrointest Surg. 2000 Jan-Feb;4(1):50-4. doi: 10.1016/s1091-255x(00)80032-3. PMID: 10631362.

52. Li XX, Wong GL, To KF, Wong VW, Lai LH, Chow DK, Lau JY, Sung JJ, Ding C. Bacterial microbiota profiling in gastritis without Helicobacter pylori infection or non-steroidal anti-inflammatory drug use. PLoS One. 2009 Nov 24;4(11):e7985. doi: 10.1371/journal.pone.0007985. PMID: 19956741; PMCID: PMC2776972.

53. Bik EM, Eckburg PB, Gill SR, Nelson KE, Purdom EA, Francois F, Perez-Perez G, Blaser MJ, Relman DA. Molecular analysis of the bacterial microbiota in the human stomach. Proc Natl Acad Sci U S A. 2006 Jan 17;103(3):732-7. doi: 10.1073/pnas.0506655103. Epub 2006 Jan 4. PMID: 16407106; PMCID: PMC1334644.

54. Andersson AF, Lindberg M, Jakobsson H, Bäckhed F, Nyrén P, Engstrand L. Comparative analysis of human gut microbiota by barcoded pyrosequencing. PLoS One. 2008 Jul 30;3(7):e2836. doi: 10.1371/journal.pone.0002836. PMID: 18665274; PMCID: PMC2475661.

55. Ianiro G, Molina-Infante J, Gasbarrini A. Gastric Microbiota. Helicobacter. 2015 Sep;20 Suppl 1:68-71. doi: 10.1111/hel.12260. PMID: 26372828.

56. Khosravi Y, Dieye Y, Poh BH, Ng CG, Loke MF, Goh KL, Vadivelu J. Culturable bacterial microbiota of the stomach of Helicobacter pylori positive and negative gastric disease patients. ScientificWorldJournal. 2014;2014:610421. doi: 10.1155/2014/610421. Epub 2014 Jul 3. PMID: 25105162; PMCID: PMC4106172.

57. Schulz C, Schütte K, Koch N, Vilchez-Vargas R, Wos-Oxley ML, Oxley APA, Vital M, Malfertheiner P, Pieper DH. The active bacterial assemblages of the upper GI tract in individuals with and without Helicobacter infection. Gut. 2018 Feb;67(2):216-225. doi: 10.1136/gutjnl-2016-312904. Epub 2016 Dec 5. PMID: 27920199.

58. Lozupone CA, Stombaugh JI, Gordon JI, Jansson JK, Knight R. Diversity, stability and resilience of the human gut microbiota. Nature. 2012 Sep 13;489(7415):220-30. doi: 10.1038/nature11550. PMID: 22972295; PMCID: PMC3577372.

59. Bäckhed F, Ley RE, Sonnenburg JL, Peterson DA, Gordon JI. Host-bacterial mutualism in the human intestine. Science. 2005 Mar 25;307(5717):1915-20. doi: 10.1126/science.1104816. PMID: 15790844.

60. Adak A, Khan MR. An insight into gut microbiota and its functionalities. Cell Mol Life Sci. 2019 Feb;76(3):473-493. doi: 10.1007/s00018-018-2943-4. Epub 2018 Oct 13. PMID: 30317530; PMCID: PMC11105460.

61. Davenport ER, Cusanovich DA, Michelini K, Barreiro LB, Ober C, Gilad Y. Genome-Wide Association Studies of the Human Gut Microbiota. PLoS One. 2015 Nov 3;10(11):e0140301. doi: 10.1371/journal.pone.0140301. PMID: 26528553; PMCID: PMC4631601.

62. El Aidy S, van den Bogert B, Kleerebezem M. The small intestine microbiota, nutritional modulation and relevance for health. Curr Opin Biotechnol. 2015 Apr;32:14-20. doi: 10.1016/j.copbio.2014.09.005. Epub 2014 Oct 8. PMID: 25308830.

63. Eckburg PB, Bik EM, Bernstein CN, Purdom E, Dethlefsen L, Sargent M, Gill SR, Nelson KE, Relman DA. Diversity of the human intestinal microbial flora. Science. 2005 Jun 10;308(5728):1635-8. doi: 10.1126/science.1110591. Epub 2005 Apr 14. PMID: 15831718; PMCID: PMC1395357.

64. Hubbard TD, Murray IA, Bisson WH, Lahoti TS, Gowda K, Amin SG, Patterson AD, Perdew GH. Adaptation of the human aryl hydrocarbon receptor to sense microbiota-derived indoles. Sci Rep. 2015 Aug 3;5:12689. doi: 10.1038/srep12689. PMID: 26235394; PMCID: PMC4522678.

65. Kibe R, Kurihara S, Sakai Y, Suzuki H, Ooga T, Sawaki E, Muramatsu K, Nakamura A, Yamashita A, Kitada Y, Kakeyama M, Benno Y, Matsumoto M. Upregulation of colonic luminal polyamines produced by intestinal microbiota delays senescence in mice. Sci Rep. 2014 Apr 1;4:4548. doi: 10.1038/srep04548. PMID: 24686447; PMCID: PMC4070089.

66. Putaala H, Salusjärvi T, Nordström M, Saarinen M, Ouwehand AC, Bech Hansen E, Rautonen N. Effect of four probiotic strains and Escherichia coli O157:H7 on tight junction integrity and cyclo-oxygenase expression. Res Microbiol. 2008 Nov-Dec;159(9-10):692-8. doi: 10.1016/j.resmic.2008.08.002. Epub 2008 Aug 22. PMID: 18783733.

67. Yan Y, Satoh-Takayama N. New perspectives on gastric disorders: the relationship between innate lymphoid cells and microbes in the stomach. Cell Mol Life Sci. 2025 Mar 13;82(1):113. doi: 10.1007/s00018-025-05632-w. PMID: 40074935; PMCID: PMC11904066.

68. Michetti M, Kelly CP, Kraehenbuhl JP, Bouzourene H, Michetti P. Gastric mucosal alpha(4)beta(7)-integrin-positive CD4 T lymphocytes and immune protection against helicobacter infection in mice. Gastroenterology. 2000 Jul;119(1):109-18. doi: 10.1053/gast.2000.8548. PMID: 10889160.

69. Shiu J, Blanchard TG. Dendritic cell function in the host response to Helicobacter pylori infection of the gastric mucosa. Pathog Dis. 2013 Feb;67(1):46-53. doi: 10.1111/2049-632X.12014. Epub 2013 Jan 22. PMID: 23620119.

70. Bimczok D, Kao JY, Zhang M, Cochrun S, Mannon P, Peter S, Wilcox CM, Mönkemüller KE, Harris PR, Grams JM, Stahl RD, Smith PD, Smythies LE. Human gastric epithelial cells contribute to gastric immune regulation by providing retinoic acid to dendritic cells. Mucosal Immunol. 2015 May;8(3):533-44. doi: 10.1038/mi.2014.86. Epub 2014 Sep 24. PMID: 25249167; PMCID: PMC4372513.

71. Gall A, Gaudet RG, Gray-Owen SD, Salama NR. TIFA Signaling in Gastric Epithelial Cells Initiates the cag Type 4 Secretion System-Dependent Innate Immune Response to Helicobacter pylori Infection. mBio. 2017 Aug 15;8(4):e01168-17. doi: 10.1128/mBio.01168-17. PMID: 28811347; PMCID: PMC5559637.

72. Barrera C, Espejo R, Reyes VE. Differential glycosylation of MHC class II molecules on gastric epithelial cells: implications in local immune responses. Hum Immunol. 2002 May;63(5):384-93. doi: 10.1016/s0198-8859(02)00386-5. PMID: 11975982.

73. Beswick EJ, Pinchuk IV, Minch K, Suarez G, Sierra JC, Yamaoka Y, Reyes VE. The Helicobacter pylori urease B subunit binds to CD74 on gastric epithelial cells and induces NF-kappaB activation and interleukin-8 production. Infect Immun. 2006 Feb;74(2):1148-55. doi: 10.1128/IAI.74.2.1148-1155.2006. PMID: 16428763; PMCID: PMC1360328.

74. Suerbaum S, Michetti P. Helicobacter pylori infection. N Engl J Med. 2002 Oct 10;347(15):1175-86. doi: 10.1056/NEJMra020542. PMID: 12374879.

75. Tanahashi T, Kita M, Kodama T, Yamaoka Y, Sawai N, Ohno T, Mitsufuji S, Wei YP, Kashima K, Imanishi J. Cytokine expression and production by purified Helicobacter pylori urease in human gastric epithelial cells. Infect Immun. 2000 Feb;68(2):664-71. doi: 10.1128/IAI.68.2.664-671.2000. PMID: 10639431; PMCID: PMC97190.

76. Jung HC, Kim JM, Song IS, Kim CY. Helicobacter pylori induces an array of pro-inflammatory cytokines in human gastric epithelial cells: quantification of mRNA for interleukin-8, -1 alpha/beta, granulocyte-macrophage colony-stimulating factor, monocyte chemoattractant protein-1 and tumour necrosis factor-alpha. J Gastroenterol Hepatol. 1997 Jul;12(7):473-80. doi: 10.1111/j.1440-1746.1997.tb00469.x. PMID: 9257236.

77. Chaudhary PM, Ferguson C, Nguyen V, Nguyen O, Massa HF, Eby M, Jasmin A, Trask BJ, Hood L, Nelson PS. Cloning and characterization of two Toll/Interleukin-1 receptor-like genes TIL3 and TIL4: evidence for a multi-gene receptor family in humans. Blood. 1998 Jun 1;91(11):4020-7. PMID: 9596645.

78. Takeda K, Akira S. Toll-like receptors. Curr Protoc Immunol. 2015 Apr 1;109:14.12.1-14.12.10. doi: 10.1002/0471142735.im1412s109. PMID: 25845562.

79. Gobert AP, Wilson KT. Human and Helicobacter pylori Interactions Determine the Outcome of Gastric Diseases. Curr Top Microbiol Immunol. 2017;400:27-52. doi: 10.1007/978-3-319-50520-6_2. PMID: 28124148; PMCID: PMC5316293.

80. Azem J, Svennerholm AM, Lundin BS. B cells pulsed with Helicobacter pylori antigen efficiently activate memory CD8+ T cells from H. pylori-infected individuals. Clin Immunol. 2006 Feb-Mar;118(2-3):284-91. doi: 10.1016/j.clim.2005.09.011. Epub 2005 Dec 1. PMID: 16324887.

81. Kronsteiner B, Bassaganya-Riera J, Philipson C, Viladomiu M, Carbo A, Pedragosa M, Vento S, Hontecillas R. Helicobacter pylori infection in a pig model is dominated by Th1 and cytotoxic CD8+ T cell responses. Infect Immun. 2013 Oct;81(10):3803-13. doi: 10.1128/IAI.00660-13. Epub 2013 Jul 29. PMID: 23897614; PMCID: PMC3811743.

82. Baker JR Jr, Farazuddin M, Wong PT, O'Konek JJ. The unfulfilled potential of mucosal immunization. J Allergy Clin Immunol. 2022 Jul;150(1):1-11. doi: 10.1016/j.jaci.2022.05.002. Epub 2022 May 13. PMID: 35569567; PMCID: PMC9098804.

83. Ohno H, Satoh-Takayama N. Stomach microbiota, Helicobacter pylori, and group 2 innate lymphoid cells. Exp Mol Med. 2020 Sep;52(9):1377-1382. doi: 10.1038/s12276-020-00485-8. Epub 2020 Sep 10. PMID: 32908209; PMCID: PMC8080604.

84. Salimi M, Wang R, Yao X, Li X, Wang X, Hu Y, Chang X, Fan P, Dong T, Ogg G. Activated innate lymphoid cell populations accumulate in human tumour tissues. BMC Cancer. 2018 Mar 27;18(1):341. doi: 10.1186/s12885-018-4262-4. PMID: 29587679; PMCID: PMC5870240.

85. Meyer AR, Engevik AC, Madorsky T, Belmont E, Stier MT, Norlander AE, Pilkinton MA, McDonnell WJ, Weis JA, Jang B, Mallal SA, Peebles RS Jr, Goldenring JR. Group 2 Innate Lymphoid Cells Coordinate Damage Response in the Stomach. Gastroenterology. 2020 Dec;159(6):2077-2091.e8. doi: 10.1053/j.gastro.2020.08.051. Epub 2020 Sep 4. PMID: 32891625; PMCID: PMC7726005.

86. Fu W, Wang W, Zhang J, Zhao Y, Chen K, Wang Y, Zhang J, Xiong Y, Guo X, Ding S. Dynamic change of circulating innate and adaptive lymphocytes subtypes during a cascade of gastric lesions. J Leukoc Biol. 2022 Oct;112(4):931-938. doi: 10.1002/JLB.5MA0422-505R. Epub 2022 Jun 3. PMID: 35657091.

87. Martini E, Krug SM, Siegmund B, Neurath MF, Becker C. Mend Your Fences: The Epithelial Barrier and its Relationship With Mucosal Immunity in Inflammatory Bowel Disease. Cell Mol Gastroenterol Hepatol. 2017 Mar 23;4(1):33-46. doi: 10.1016/j.jcmgh.2017.03.007. PMID: 28560287; PMCID: PMC5439240.

88. Peterson LW, Artis D. Intestinal epithelial cells: regulators of barrier function and immune homeostasis. Nat Rev Immunol. 2014 Mar;14(3):141-53. doi: 10.1038/nri3608. PMID: 24566914.

89. Johansson ME, Hansson GC. Immunological aspects of intestinal mucus and mucins. Nat Rev Immunol. 2016 Oct;16(10):639-49. doi: 10.1038/nri.2016.88. Epub 2016 Aug 8. PMID: 27498766; PMCID: PMC6435297.

90. Schlegel N, Boerner K, Waschke J. Targeting desmosomal adhesion and signalling for intestinal barrier stabilization in inflammatory bowel diseases-Lessons from experimental models and patients. Acta Physiol (Oxf). 2021 Jan;231(1):e13492. doi: 10.1111/apha.13492. Epub 2020 May 22. PMID: 32419327.

91. Wallaeys C, Garcia-Gonzalez N, Libert C. Paneth cells as the cornerstones of intestinal and organismal health: a primer. EMBO Mol Med. 2023 Feb 8;15(2):e16427. doi: 10.15252/emmm.202216427. Epub 2022 Dec 27. PMID: 36573340; PMCID: PMC9906427.

92. Turner JR. Intestinal mucosal barrier function in health and disease. Nat Rev Immunol. 2009 Nov;9(11):799-809. doi: 10.1038/nri2653. PMID: 19855405.

93. Pabst O, Bernhardt G. The puzzle of intestinal lamina propria dendritic cells and macrophages. Eur J Immunol. 2010 Aug;40(8):2107-11. doi: 10.1002/eji.201040557. PMID: 20853495.

94. Kinnebrew MA, Pamer EG. Innate immune signaling in defense against intestinal microbes. Immunol Rev. 2012 Jan;245(1):113-31. doi: 10.1111/j.1600-065X.2011.01081.x. PMID: 22168416; PMCID: PMC4624287.

95. Izcue A, Coombes JL, Powrie F. Regulatory T cells suppress systemic and mucosal immune activation to control intestinal inflammation. Immunol Rev. 2006 Aug;212:256-71. doi: 10.1111/j.0105-2896.2006.00423.x. PMID: 16903919.

96. Maynard CL, Weaver CT. Intestinal effector T cells in health and disease. Immunity. 2009 Sep 18;31(3):389-400. doi: 10.1016/j.immuni.2009.08.012. PMID: 19766082; PMCID: PMC3109492.

97. Kato LM, Kawamoto S, Maruya M, Fagarasan S. The role of the adaptive immune system in regulation of gut microbiota. Immunol Rev. 2014 Jul;260(1):67-75. doi: 10.1111/imr.12185. PMID: 24942682.

98. Rooks MG, Garrett WS. Gut microbiota, metabolites and host immunity. Nat Rev Immunol. 2016 May 27;16(6):341-52. doi: 10.1038/nri.2016.42. PMID: 27231050; PMCID: PMC5541232.

99. Macia L, Tan J, Vieira AT, Leach K, Stanley D, Luong S, Maruya M, Ian McKenzie C, Hijikata A, Wong C, Binge L, Thorburn AN, Chevalier N, Ang C, Marino E, Robert R, Offermanns S, Teixeira MM, Moore RJ, Flavell RA, Fagarasan S, Mackay CR. Metabolite-sensing receptors GPR43 and GPR109A facilitate dietary fibre-induced gut homeostasis through regulation of the inflammasome. Nat Commun. 2015 Apr 1;6:6734. doi: 10.1038/ncomms7734. PMID: 25828455.

100. Wu W, Sun M, Chen F, Cao AT, Liu H, Zhao Y, Huang X, Xiao Y, Yao S, Zhao Q, Liu Z, Cong Y. Microbiota metabolite short-chain fatty acid acetate promotes intestinal IgA response to microbiota which is mediated by GPR43. Mucosal Immunol. 2017 Jul;10(4):946-956. doi: 10.1038/mi.2016.114. Epub 2016 Dec 14. PMID: 27966553; PMCID: PMC5471141.

101. Morrison DJ, Preston T. Formation of short chain fatty acids by the gut microbiota and their impact on human metabolism. Gut Microbes. 2016 May 3;7(3):189-200. doi: 10.1080/19490976.2015.1134082. Epub 2016 Mar 10. PMID: 26963409; PMCID: PMC4939913.

102. James, D. (2015). Diseases of the Small and Large Bowel. In: Paulman, P., Taylor, R. (eds) Family Medicine. Springer, Cham.

103. Solcia E, Rindi G, Fiocca R, Villani L, Buffa R, Ambrosiani L, Capella C. Distinct patterns of chronic gastritis associated with carcinoid and cancer and their role in tumorigenesis. Yale J Biol Med. 1992 Nov-Dec;65(6):793-804; discussion 827-9. PMID: 1341079; PMCID: PMC2589778.

104. Neumann WL, Coss E, Rugge M, Genta RM. Autoimmune atrophic gastritis--pathogenesis, pathology and management. Nat Rev Gastroenterol Hepatol. 2013 Sep;10(9):529-41. doi: 10.1038/nrgastro.2013.101. Epub 2013 Jun 18. PMID: 23774773.

105. Di Sabatino A, Lenti MV, Giuffrida P, Vanoli A, Corazza GR. New insights into immune mechanisms underlying autoimmune diseases of the gastrointestinal tract. Autoimmun Rev. 2015 Dec;14(12):1161-9. doi: 10.1016/j.autrev.2015.08.004. Epub 2015 Aug 12. PMID: 26275585.

106. Hunt RH, Camilleri M, Crowe SE, El-Omar EM, Fox JG, Kuipers EJ, Malfertheiner P, McColl KE, Pritchard DM, Rugge M, Sonnenberg A, Sugano K, Tack J. The stomach in health and disease. Gut. 2015 Oct;64(10):1650-68. doi: 10.1136/gutjnl-2014-307595. Epub 2015 Sep 4. PMID: 26342014; PMCID: PMC4835810.

107. Rugge M, Pennelli G, Pilozzi E, Fassan M, Ingravallo G, Russo VM, Di Mario F; Gruppo Italiano Patologi Apparato Digerente (GIPAD); Società Italiana di Anatomia Patologica e Citopatologia Diagnostica/International Academy of Pathology, Italian division (SIAPEC/IAP). Gastritis: the histology report. Dig Liver Dis. 2011 Mar;43 Suppl 4:S373-84. doi: 10.1016/S1590-8658(11)60593-8. PMID: 21459343.

108. Graham DY, Rugge M. Clinical practice: diagnosis and evaluation of dyspepsia. J Clin Gastroenterol. 2010 Mar;44(3):167-72. doi: 10.1097/MCG.0b013e3181c64c69. PMID: 20009950; PMCID: PMC2828509.

109. Sugano K, Tack J, Kuipers EJ, Graham DY, El-Omar EM, Miura S, Haruma K, Asaka M, Uemura N, Malfertheiner P; faculty members of Kyoto Global Consensus Conference. Kyoto global consensus report on Helicobacter pylori gastritis. Gut. 2015 Sep;64(9):1353-67. doi: 10.1136/gutjnl-2015-309252. Epub 2015 Jul 17. PMID: 26187502; PMCID: PMC4552923.

110. Fox JG, Wang TC. Inflammation, atrophy, and gastric cancer. J Clin Invest. 2007 Jan;117(1):60-9. doi: 10.1172/JCI30111. PMID: 17200707; PMCID: PMC1716216.

111. Lenti MV, Rugge M, Lahner E, Miceli E, Toh BH, Genta RM, De Block C, Hershko C, Di Sabatino A. Autoimmune gastritis. Nat Rev Dis Primers. 2020 Jul 9;6(1):56. doi: 10.1038/s41572-020-0187-8. PMID: 32647173.

112. Massironi S, Zilli A, Elvevi A, Invernizzi P. The changing face of chronic autoimmune atrophic gastritis: an updated comprehensive perspective. Autoimmun Rev. 2019 Mar;18(3):215-222. doi: 10.1016/j.autrev.2018.08.011. Epub 2019 Jan 11. PMID: 30639639.

113. Centanni M, Marignani M, Gargano L, Corleto VD, Casini A, Delle Fave G, Andreoli M, Annibale B. Atrophic body gastritis in patients with autoimmune thyroid disease: an underdiagnosed association. Arch Intern Med. 1999 Aug 9-23;159(15):1726-30. doi: 10.1001/archinte.159.15.1726. PMID: 10448775.

114. Briani C, Dalla Torre C, Citton V, Manara R, Pompanin S, Binotto G, Adami F. Cobalamin deficiency: clinical picture and radiological findings. Nutrients. 2013 Nov 15;5(11):4521-39. doi: 10.3390/nu5114521. PMID: 24248213; PMCID: PMC3847746.

115. Miceli E, Vanoli A, Lenti MV, Klersy C, Di Stefano M, Luinetti O, Caccia Dominioni C, Pisati M, Staiani M, Gentile A, Capuano F, Arpa G, Paulli M, Corazza GR, Di Sabatino A. Natural history of autoimmune atrophic gastritis: a prospective, single centre, long-term experience. Aliment Pharmacol Ther. 2019 Dec;50(11-12):1172-1180. doi: 10.1111/apt.15540. Epub 2019 Oct 17. PMID: 31621927.

116. Pogoriler J, Kamin D, Goldsmith JD. Pediatric non-Helicobacter pylori atrophic gastritis: a case series. Am J Surg Pathol. 2015 Jun;39(6):786-92. doi: 10.1097/PAS.0000000000000378. PMID: 25602795.

117. Saglietti C, Sciarra A, Abdelrahman K, Schneider V, Karpate A, Nydegger A, Sempoux C. Autoimmune Gastritis in the Pediatric Age: An Underestimated Condition Report of Two Cases and Review. Front Pediatr. 2018 May 1;6:123. doi: 10.3389/fped.2018.00123. PMID: 29765934; PMCID: PMC5939145.

118. Calcaterra V, Montalbano C, Miceli E, Luinetti O, Albertini R, Vinci F, Regalbuto C, Larizza D. Anti-gastric parietal cell antibodies for autoimmune gastritis screening in juvenile autoimmune thyroid disease. J Endocrinol Invest. 2020 Jan;43(1):81-86. doi: 10.1007/s40618-019-01081-y. Epub 2019 Jul 1. PMID: 31264142.

119. Lenti MV, Miceli E, Cococcia S, Klersy C, Staiani M, Guglielmi F, Giuffrida P, Vanoli A, Luinetti O, De Grazia F, Di Stefano M, Corazza GR, Di Sabatino A. Determinants of diagnostic delay in autoimmune atrophic gastritis. Aliment Pharmacol Ther. 2019 Jul;50(2):167-175. doi: 10.1111/apt.15317. Epub 2019 May 22. PMID: 31115910.

120. Kalkan Ç, Soykan I, Soydal Ç, Özkan E, Kalkan E. Assessment of Gastric Emptying in Patients with Autoimmune Gastritis. Dig Dis Sci. 2016 Jun;61(6):1597-602. doi: 10.1007/s10620-015-4021-1. Epub 2016 Jan 2. PMID: 26725066.

121. Carabotti M, Esposito G, Lahner E, Pilozzi E, Conti L, Ranazzi G, Severi C, Bellini M, Annibale B. Gastroesophageal reflux symptoms and microscopic esophagitis in a cohort of consecutive patients affected by atrophic body gastritis: a pilot study. Scand J Gastroenterol. 2019 Jan;54(1):35-40. doi: 10.1080/00365521.2018.1553062. Epub 2019 Jan 13. PMID: 30638085.

122. Carabotti M, Lahner E, Esposito G, Sacchi MC, Severi C, Annibale B. Upper gastrointestinal symptoms in autoimmune gastritis: A cross-sectional study. Medicine (Baltimore). 2017 Jan;96(1):e5784. doi: 10.1097/MD.0000000000005784. PMID: 28072728; PMCID: PMC5228688.

123. Iwai W, Abe Y, Iijima K, Koike T, Uno K, Asano N, Imatani A, Shimosegawa T. Gastric hypochlorhydria is associated with an exacerbation of dyspeptic symptoms in female patients. J Gastroenterol. 2013 Feb;48(2):214-21. doi: 10.1007/s00535-012-0634-8. Epub

2012 Jul 25. PMID: 22829345.

124. Singh S, Chakole S, Agrawal S, Shetty N, Prasad R, Lohakare T, Wanjari M, Yelne S. A Comprehensive Review of Upper Gastrointestinal Symptom Management in Autoimmune Gastritis: Current Insights and Future Directions. Cureus. 2023 Aug 13;15(8):e43418. doi: 10.7759/cureus.43418. PMID: 37706145; PMCID: PMC10496934.

125. Russell RM, Krasinski SD, Samloff IM, Jacob RA, Hartz SC, Brovender SR. Folic acid malabsorption in atrophic gastritis. Possible compensation by bacterial folate synthesis. Gastroenterology. 1986 Dec;91(6):1476-82. doi: 10.1016/0016-5085(86)90204-0. PMID: 3770372.

126. Kumar N. Neurologic presentations of nutritional deficiencies. Neurol Clin. 2010 Feb;28(1):107-70. doi: 10.1016/j.ncl.2009.09.006. PMID: 19932379.

127. Bennett M. Vitamin B12 deficiency, infertility and recurrent fetal loss. J Reprod Med. 2001 Mar;46(3):209-12. PMID: 11304860.

128. Reznikoff-Etiévant MF, Zittoun J, Vaylet C, Pernet P, Milliez J. Low Vitamin B(12) level as a risk factor for very early recurrent abortion. Eur J Obstet Gynecol Reprod Biol. 2002 Sep 10;104(2):156-9. doi: 10.1016/s0301-2115(02)00100-8. PMID: 12206930.

129. Refsum H. Folate, vitamin B12 and homocysteine in relation to birth defects and pregnancy outcome. Br J Nutr. 2001 May;85 Suppl 2:S109-13. PMID: 11509098.

130. Gaskins AJ, Chiu YH, Williams PL, Ford JB, Toth TL, Hauser R, Chavarro JE; EARTH Study Team. Association between serum folate and vitamin B-12 and outcomes of assisted reproductive technologies. Am J Clin Nutr. 2015 Oct;102(4):943-50. doi: 10.3945/ajcn.115.112185. Epub 2015 Sep 9. PMID: 26354529; PMCID: PMC4588741.

131. Green R, Allen LH, Bjørke-Monsen AL, Brito A, Guéant JL, Miller JW, Molloy AM, Nexo E, Stabler S, Toh BH, Ueland PM, Yajnik C. Vitamin B12 deficiency. Nat Rev Dis Primers. 2017 Jun 29;3:17040. doi: 10.1038/nrdp.2017.40. Erratum in: Nat Rev Dis Primers. 2017 Jul 20;3:17054. doi: 10.1038/nrdp.2017.54. PMID: 28660890.

132. Yang GT, Zhao HY, Kong Y, Sun NN, Dong AQ. Correlation between serum vitamin B12 level and peripheral neuropathy in atrophic gastritis. World J Gastroenterol. 2018 Mar 28;24(12):1343-1352. doi: 10.3748/wjg.v24.i12.1343. PMID: 29599609; PMCID: PMC5871829.

133. Mahmud N, Stashek K, Katona BW, Tondon R, Shroff SG, Roses R, Furth EE, Metz DC. The incidence of neoplasia in patients with autoimmune metaplastic atrophic gastritis: a renewed call for surveillance. Ann Gastroenterol. 2019 Jan-Feb;32(1):67-72. doi: 10.20524/aog.2018.0325. Epub 2018 Nov 8. PMID: 30598594; PMCID: PMC6302190.

134. Vannella L, Sbrozzi-Vanni A, Lahner E, Bordi C, Pilozzi E, Corleto VD, Osborn JF, Delle Fave G, Annibale B. Development of type I gastric carcinoid in patients with chronic atrophic gastritis. Aliment Pharmacol Ther. 2011 Jun;33(12):1361-9. doi: 10.1111/j.1365-2036.2011.04659.x. Epub 2011 Apr 15. PMID: 21492197.

135. Zhang H, Jin Z, Cui R, Ding S, Huang Y, Zhou L. Autoimmune metaplastic atrophic gastritis in chinese: a study of 320 patients at a large tertiary medical center. Scand J Gastroenterol. 2017 Feb;52(2):150-156. doi: 10.1080/00365521.2016.1236397. Epub 2016 Sep 27. PMID: 27652682.

136. Massironi S, Zilli A, Elvevi A, Invernizzi P. The changing face of chronic autoimmune atrophic gastritis: an updated comprehensive perspective. Autoimmun Rev. 2019 Mar;18(3):215-222. doi: 10.1016/j.autrev.2018.08.011. Epub 2019 Jan 11. PMID: 30639639.

137. Annibale B, Azzoni C, Corleto VD, di Giulio E, Caruana P, D'Ambra G, Bordi C, Delle Fave G. Atrophic body gastritis patients with enterochromaffin-like cell dysplasia are at increased risk for the development of type I gastric carcinoid. Eur J Gastroenterol Hepatol. 2001 Dec;13(12):1449-56. doi: 10.1097/00042737-200112000-00008. PMID: 11742193.

138. Whittingham S, Ungar B, Mackay IR, Mathews JD. The genetic factor in pernicious anaemia. A family study in patients with gastritis. Lancet. 1969 May 10;1(7602):951-4. doi: 10.1016/s0140-6736(69)91856-x. PMID: 4180811.

139. Veldek TE, Abels J, Anders GJ, Arends A, Hoedemaeker PJ, Nieweg HO. A Family Study Of Pernicious Anemia By An Immunologic Method. J Lab Clin Med. 1964 Aug;64:177-87. PMID: 14202781.

140. Baxter AG, Jordan MA, Silveira PA, Wilson WE, Van Driel IR. Genetic control of susceptibility to autoimmune gastritis. Int Rev Immunol. 2005 Jan-Apr;24(1-2):55-62. doi: 10.1080/08830180590884404. PMID: 15763989.

141. Wangel AG, Callender ST, Spray GH, Wright R. A famiy study of pernicious anaemia. I. Autoantibodies, achlorhydria, serum pepsinogen and vitamin B12. Br J Haematol. 1968 Feb;14(2):161-81. doi: 10.1111/j.1365-2141.1968.tb01485.x. PMID: 4865547.

142. Oksanen AM, Haimila KE, Rautelin HI, Partanen JA. Immunogenetic characteristics of patients with autoimmune gastritis. World J Gastroenterol. 2010 Jan 21;16(3):354-8. doi: 10.3748/wjg.v16.i3.354. PMID: 20082482; PMCID: PMC2807957.

143. Lahner E, Spoletini M, Buzzetti R, Corleto VD, Vannella L, Petrone A, Annibale B. HLA-DRB1*03 and DRB1*04 are associated with atrophic gastritis in an Italian population. Dig Liver Dis. 2010 Dec;42(12):854-9. doi: 10.1016/j.dld.2010.04.011. Epub 2010 Jun 2. PMID: 20627832.

144. Kulski, J.K., Suzuki, S. & Shiina, T. Human leukocyte antigen super-locus: nexus of genomic supergenes, SNPs, indels, transcripts, and haplotypes. Hum Genome Var 9, 49 (2022).

145. D'Elios MM, Bergman MP, Azzurri A, Amedei A, Benagiano M, De Pont JJ, Cianchi F, Vandenbroucke-Grauls CM, Romagnani S, Appelmelk BJ, Del Prete G. H(+),K(+)-atpase (proton pump) is the target autoantigen of Th1-type cytotoxic T cells in autoimmune gastritis. Gastroenterology. 2001 Feb;120(2):377-86. doi: 10.1053/gast.2001.21187. PMID: 11159878.

146. Presotto F, Sabini B, Cecchetto A, Plebani M, De Lazzari F, Pedini B, Betterle C. Helicobacter pylori infection and gastric autoimmune diseases: is there a link? Helicobacter. 2003 Dec;8(6):578-84. doi: 10.1111/j.1523-5378.2003.00187.x. PMID: 14632671.

147. Parsons BN, Ijaz UZ, D'Amore R, Burkitt MD, Eccles R, Lenzi L, Duckworth CA, Moore AR, Tiszlavicz L, Varro A, Hall N, Pritchard DM. Comparison of the human gastric microbiota in hypochlorhydric states arising as a result of Helicobacter pylori-induced atrophic gastritis, autoimmune atrophic gastritis and proton pump inhibitor use. PLoS Pathog. 2017 Nov 2;13(11):e1006653. doi: 10.1371/journal.ppat.1006653. PMID: 29095917; PMCID: PMC5667734.

148. Zhang Z, Zhu T, Zhang L, Xing Y, Yan Z, Li Q. Critical influence of cytokines and immune cells in autoimmune gastritis. Autoimmunity. 2023 Dec;56(1):2174531. doi: 10.1080/08916934.2023.2174531. PMID: 36762543.

149. Cascetta G, Colombo G, Eremita G, Garcia JGN, Lenti MV, Di Sabatino A, Travelli C. Pro- and anti-inflammatory cytokines: the hidden keys to autoimmune gastritis therapy. Front Pharmacol. 2024 Aug 13;15:1450558. doi: 10.3389/fphar.2024.1450558. PMID: 39193325; PMCID: PMC11347309.

150. Lenti MV, Facciotti F, Miceli E, Vanoli A, Fornasa G, Lahner E, Spadoni I, Giuffrida P, Arpa G, Pasini A, Rovedatti L, Caprioli F, Travelli C, Lattanzi G, Conti L, Klersy C, Vecchi M, Paulli M, Annibale B, Corazza GR, Rescigno M, Di Sabatino A. Mucosal Overexpression of Thymic Stromal Lymphopoietin and Proinflammatory Cytokines in Patients With Autoimmune Atrophic Gastritis. Clin Transl Gastroenterol. 2022 Jul 1;13(7):e00510. doi: 10.14309/ctg.0000000000000510. Epub 2022 Jun 13. PMID: 35905420; PMCID: PMC10476748.

151. Parameswaran N, Patial S. Tumor necrosis factor-α signaling in macrophages. Crit Rev Eukaryot Gene Expr. 2010;20(2):87-103. doi: 10.1615/critreveukargeneexpr.v20.i2.10. PMID: 21133840; PMCID: PMC3066460.

152. Budagian V, Bulanova E, Paus R, Bulfone-Paus S. IL-15/IL-15 receptor biology: a guided tour through an expanding universe. Cytokine Growth Factor Rev. 2006 Aug;17(4):259-80. doi: 10.1016/j.cytogfr.2006.05.001. Epub 2006 Jun 30. PMID: 16815076.

153. Noto CN, Hoft SG, Bockerstett KA, Jackson NM, Ford EL, Vest LS, DiPaolo RJ. IL13 Acts Directly on Gastric Epithelial Cells to Promote Metaplasia Development During Chronic Gastritis. Cell Mol Gastroenterol Hepatol. 2022;13(2):623-642. doi: 10.1016/j.jcmgh.2021.09.012. Epub 2021 Sep 26. PMID: 34587523; PMCID: PMC8715193.

154. Petersen CP, Meyer AR, De Salvo C, Choi E, Schlegel C, Petersen A, Engevik AC, Prasad N, Levy SE, Peebles RS, Pizarro TT, Goldenring JR. A signalling cascade of IL-33 to IL-13 regulates metaplasia in the mouse stomach. Gut. 2018 May;67(5):805-817. doi: 10.1136/gutjnl-2016-312779. Epub 2017 Feb 14. PMID: 28196875; PMCID: PMC5681443.

155. Privitera G, Williams JJ, De Salvo C. The Importance of Th2 Immune Responses in Mediating the Progression of Gastritis-Associated Metaplasia to Gastric Cancer. Cancers (Basel). 2024 Jan 25;16(3):522. doi: 10.3390/cancers16030522. PMID: 38339273; PMCID: PMC10854712.

156. Osaki LH, Bockerstett KA, Wong CF, Ford EL, Madison BB, DiPaolo RJ, Mills JC. Interferon-γ directly induces gastric epithelial cell death and is required for progression to metaplasia. J Pathol. 2019 Apr;247(4):513-523. doi: 10.1002/path.5214. Epub 2019 Jan 24. PMID: 30511397; PMCID: PMC6402979.

157. Hu Z, Chai J. Structural Mechanisms in NLR Inflammasome Assembly and Signaling. Curr Top Microbiol Immunol. 2016;397:23-42. doi: 10.1007/978-3-319-41171-2_2. PMID: 27460803.

158. Bockerstett KA, Lewis SA, Wolf KJ, Noto CN, Jackson NM, Ford EL, Ahn TH, DiPaolo RJ. Single-cell transcriptional analyses of spasmolytic polypeptide-expressing metaplasia arising from acute drug injury and chronic inflammation in the stomach. Gut. 2020 Jun;69(6):1027-1038. doi: 10.1136/gutjnl-2019-318930. Epub 2019 Sep 3. PMID: 31481545; PMCID: PMC7282188.

159. Yang XT, Niu PQ, Li XF, Sun MM, Wei W, Chen YQ, Zheng JY. Differential cytokine expression in gastric tissues highlights helicobacter pylori's role in gastritis. Sci Rep. 2024 Apr 1;14(1):7683. doi: 10.1038/s41598-024-58407-x. PMID: 38561502; PMCID: PMC10984929.

160. Yu B, de Vos D, Guo X, Peng S, Xie W, Peppelenbosch MP, Fu Y, Fuhler GM. IL-6 facilitates cross-talk between epithelial cells and tumor- associated macrophages in Helicobacter pylori-linked gastric carcinogenesis. Neoplasia. 2024 Apr;50:100981. doi: 10.1016/j.neo.2024.100981. Epub 2024 Feb 28. PMID: 38422751; PMCID: PMC10912637.

161. Stummvoll GH, DiPaolo RJ, Huter EN, Davidson TS, Glass D, Ward JM, Shevach EM. Th1, Th2, and Th17 effector T cell-induced autoimmune gastritis differs in pathological pattern and in susceptibility to suppression by regulatory T cells. J Immunol. 2008 Aug 1;181(3):1908-16. doi: 10.4049/jimmunol.181.3.1908. PMID: 18641328; PMCID: PMC2561289.

162. Huter EN, Stummvoll GH, DiPaolo RJ, Glass DD, Shevach EM. Cutting edge: antigen-specific TGF beta-induced regulatory T cells suppress Th17-mediated autoimmune disease. J Immunol. 2008 Dec 15;181(12):8209-13. doi: 10.4049/jimmunol.181.12.8209. PMID: 19050237; PMCID: PMC2788513.

163. Tong Y, Wang R, Liu X, Tian M, Wang Y, Cui Y, Zou W, Zhao Y. Zuojin Pill ameliorates chronic atrophic gastritis induced by MNNG through TGF-β1/PI3K/Akt axis. J Ethnopharmacol. 2021 May 10;271:113893. doi: 10.1016/j.jep.2021.113893. Epub 2021 Jan 29. PMID: 33524511.

164. Petagna L, Antonelli A, Ganini C, Bellato V, Campanelli M, Divizia A, Efrati C, Franceschilli M, Guida AM, Ingallinella S, Montagnese F, Sensi B, Siragusa L, Sica GS. Pathophysiology of Crohn's disease inflammation and recurrence. Biol Direct. 2020 Nov 7;15(1):23. doi: 10.1186/s13062-020-00280-5. PMID: 33160400; PMCID: PMC7648997.

165. Mulder DJ, Noble AJ, Justinich CJ, Duffin JM. A tale of two diseases: the history of inflammatory bowel disease. J Crohns Colitis. 2014 May;8(5):341-8. doi: 10.1016/j.crohns.2013.09.009. Epub 2013 Oct 3. PMID: 24094598.

166. Ng SC, Shi HY, Hamidi N, Underwood FE, Tang W, Benchimol EI, Panaccione R, Ghosh S, Wu JCY, Chan FKL, Sung JJY, Kaplan GG. Worldwide incidence and prevalence of inflammatory bowel disease in the 21st century: a systematic review of population-based

studies. Lancet. 2017 Dec 23;390(10114):2769-2778. doi: 10.1016/S0140-6736(17)32448-0. Epub 2017 Oct 16. Erratum in: Lancet. 2020 Oct 3;396(10256):e56. doi: 10.1016/S0140-6736(20)32028-6. PMID: 29050646.

167. Diez-Martin E, Hernandez-Suarez L, Muñoz-Villafranca C, Martin-Souto L, Astigarraga E, Ramirez-Garcia A, Barreda-Gómez G. Inflammatory Bowel Disease: A Comprehensive Analysis of Molecular Bases, Predictive Biomarkers, Diagnostic Methods, and Therapeutic Options. Int J Mol Sci. 2024 Jun 27;25(13):7062. doi: 10.3390/ijms25137062. PMID: 39000169; PMCID: PMC11241012.

168. Khor B, Gardet A, Xavier RJ. Genetics and pathogenesis of inflammatory bowel disease. Nature. 2011 Jun 15;474(7351):307-17. doi: 10.1038/nature10209. PMID: 21677747; PMCID: PMC3204665.

169. Canavan C, Abrams KR, Mayberry J. Meta-analysis: colorectal and small bowel cancer risk in patients with Crohn's disease. Aliment Pharmacol Ther. 2006 Apr 15;23(8):1097-104. doi: 10.1111/j.1365-2036.2006.02854.x. PMID: 16611269.

170. Jess T, Gamborg M, Matzen P, Munkholm P, Sørensen TI. Increased risk of intestinal cancer in Crohn's disease: a meta-analysis of population-based cohort studies. Am J Gastroenterol. 2005 Dec;100(12):2724-9. doi: 10.1111/j.1572-0241.2005.00287.x. PMID: 16393226.

171. Hutfless SM, Weng X, Liu L, Allison J, Herrinton LJ. Mortality by medication use among patients with inflammatory bowel disease, 1996-2003. Gastroenterology. 2007 Dec;133(6):1779-86. doi: 10.1053/j.gastro.2007.09.022. Epub 2007 Sep 26. PMID: 18054550.

172. Höie O, Schouten LJ, Wolters FL, Solberg IC, Riis L, Mouzas IA, Politi P, Odes S, Langholz E, Vatn M, Stockbrügger RW, Moum B; European Collaborative Study Group of Inflammatory Bowel Disease (EC-IBD). Ulcerative colitis: no rise in mortality in a European-wide population based cohort 10 years after diagnosis. Gut. 2007 Apr;56(4):497-503. doi: 10.1136/gut.2006.101519. Epub 2006 Oct 6. PMID: 17028127; PMCID: PMC1856843.

173. Scheurlen KM, Parks MA, Macleod A, Galandiuk S. Unmet Challenges in Patients with Crohn's Disease. J Clin Med. 2023 Aug 27;12(17):5595. doi: 10.3390/jcm12175595. PMID: 37685662; PMCID: PMC10488639.

174. Sorrentino D, Nguyen VQ, Chitnavis MV. Capturing the Biologic Onset of Inflammatory Bowel Diseases: Impact on Translational and Clinical Science. Cells. 2019 Jun 6;8(6):548. doi: 10.3390/cells8060548. PMID: 31174359; PMCID: PMC6627618.

175. Wang R, Li Z, Liu S, Zhang D. Global, regional and national burden of inflammatory bowel disease in 204 countries and territories from 1990 to 2019: a systematic analysis based on the Global Burden of Disease Study 2019. BMJ Open. 2023 Mar 28;13(3):e065186. doi: 10.1136/bmjopen-2022-065186. PMID: 36977543; PMCID: PMC10069527.

176. Chen X, Xiang X, Xia W, Li X, Wang S, Ye S, Tian L, Zhao L, Ai F, Shen Z, Nie K, Deng M, Wang X. Evolving Trends and Burden of Inflammatory Bowel Disease in Asia, 1990-2019: A Comprehensive Analysis Based on the Global Burden of Disease Study. J Epidemiol Glob Health. 2023 Dec;13(4):725-739. doi: 10.1007/s44197-023-00145-w. Epub 2023 Sep 1. PMID: 37653213; PMCID: PMC10686927.

177. Fakhoury M, Negrulj R, Mooranian A, Al-Salami H. Inflammatory bowel disease: clinical aspects and treatments. J Inflamm Res. 2014 Jun 23;7:113-20. doi: 10.2147/JIR.S65979. PMID: 25075198; PMCID: PMC4106026.

178. Vavricka SR, Rogler G, Gantenbein C, Spoerri M, Prinz Vavricka M, Navarini AA, French LE, Safroneeva E, Fournier N, Straumann A, Froehlich F, Fried M, Michetti P, Seibold F, Lakatos PL, Peyrin-Biroulet L, Schoepfer AM. Chronological Order of Appearance of Extraintestinal Manifestations Relative to the Time of IBD Diagnosis in the Swiss Inflammatory Bowel Disease Cohort. Inflamm Bowel Dis. 2015 Aug;21(8):1794-800. doi: 10.1097/MIB.0000000000000429. PMID: 26020601.

179. Rogler G, Singh A, Kavanaugh A, Rubin DT. Extraintestinal Manifestations of Inflammatory Bowel Disease: Current Concepts, Treatment, and Implications for Disease Management. Gastroenterology. 2021 Oct;161(4):1118-1132. doi: 10.1053/j.gastro.2021.07.042. Epub 2021 Aug 3. PMID: 34358489; PMCID: PMC8564770.

180. Garber A, Regueiro M. Extraintestinal Manifestations of Inflammatory Bowel Disease: Epidemiology, Etiopathogenesis, and Management. Curr Gastroenterol Rep. 2019 May 16;21(7):31. doi: 10.1007/s11894-019-0698-1. PMID: 31098819.

181. Su CG, Judge TA, Lichtenstein GR. Extraintestinal manifestations of inflammatory bowel disease. Gastroenterol Clin North Am. 2002 Mar;31(1):307-27. doi: 10.1016/s0889-8553(01)00019-x. PMID: 12122740.

182. Jang HJ, Kang B, Choe BH. The difference in extraintestinal manifestations of inflammatory bowel disease for children and adults. Transl Pediatr. 2019 Jan;8(1):4-15. doi: 10.21037/tp.2019.01.06. PMID: 30881893; PMCID: PMC6382501.

183. Flynn S, Eisenstein S. Inflammatory Bowel Disease Presentation and Diagnosis. Surg Clin North Am. 2019 Dec;99(6):1051-1062. doi: 10.1016/j.suc.2019.08.001. Epub 2019 Sep 11. PMID: 31676047.

184. Jung S, Ye BD, Lee HS, Baek J, Kim G, Park D, Park SH, Yang SK, Han B, Liu J, Song K. Identification of Three Novel Susceptibility Loci for Inflammatory Bowel Disease in Koreans in an Extended Genome-Wide Association Study. J Crohns Colitis. 2021 Nov 8;15(11):1898-1907. doi: 10.1093/ecco-jcc/jjab060. PMID: 33853113.

185. Mentella MC, Scaldaferri F, Pizzoferrato M, Gasbarrini A, Miggiano GAD. Nutrition, IBD and Gut Microbiota: A Review. Nutrients. 2020 Mar 29;12(4):944. doi: 10.3390/nu12040944. PMID: 32235316; PMCID: PMC7230231.

186. Jostins L, Ripke S, Weersma RK, Duerr RH, McGovern DP, Hui KY, Lee JC, Schumm LP, Sharma Y, Anderson CA, Essers J, Mitrovic M, Ning K, Cleynen I, Theatre E, Spain SL, Raychaudhuri S, Goyette P, Wei Z, Abraham C, Achkar JP, Ahmad T, Amininejad L, Ananthakrishnan AN, Andersen V, Andrews JM, Baidoo L, Balschun T, Bampton PA, Bitton A, Boucher G, Brand S, Büning C, Cohain A, Cichon S, D'Amato M, De Jong D, Devaney KL, Dubinsky M, Edwards C, Ellinghaus D, Ferguson LR, Franchimont D, Fransen K, Gearry R, Georges M, Gieger C, Glas J, Haritunians T, Hart A, Hawkey C, Hedl M, Hu X, Karlsen TH, Kupcinskas L, Kugathasan S, Latiano A, Laukens D, Lawrance IC, Lees CW, Louis E, Mahy G, Mansfield J, Morgan AR, Mowat C, Newman W, Palmieri O, Ponsioen CY, Potocnik U, Prescott NJ, Regueiro M, Rotter JI, Russell RK, Sanderson JD, Sans M, Satsangi J, Schreiber S, Simms LA, Sventoraityte J, Targan SR, Taylor KD, Tremelling M, Verspaget HW, De Vos M, Wijmenga C, Wilson DC, Winkelmann J, Xavier RJ, Zeissig S, Zhang B, Zhang CK, Zhao H; International IBD Genetics Consortium (IIBDGC); Silverberg MS, Annese V, Hakonarson H, Brant SR, Radford-Smith G, Mathew CG, Rioux JD, Schadt EE, Daly MJ, Franke A, Parkes M, Vermeire S, Barrett JC, Cho JH. Host-microbe interactions have shaped the genetic architecture of inflammatory bowel disease. Nature. 2012 Nov 1;491(7422):119-24. doi: 10.1038/nature11582. PMID: 23128233; PMCID: PMC3491803.

187. Cooney R, Baker J, Brain O, Danis B, Pichulik T, Allan P, Ferguson DJ, Campbell BJ, Jewell D, Simmons A. NOD2 stimulation induces autophagy in dendritic cells influencing bacterial handling and antigen presentation. Nat Med. 2010 Jan;16(1):90-7. doi: 10.1038/nm.2069. Epub 2009 Dec 6. PMID: 19966812.

188. Travassos LH, Carneiro LA, Ramjeet M, Hussey S, Kim YG, Magalhães JG, Yuan L, Soares F, Chea E, Le Bourhis L, Boneca IG, Allaoui A, Jones NL, Nuñez G, Girardin SE, Philpott DJ. Nod1 and Nod2 direct autophagy by recruiting ATG16L1 to the plasma membrane at the site of bacterial entry. Nat Immunol. 2010 Jan;11(1):55-62. doi: 10.1038/ni.1823. Epub 2009 Nov 8. PMID: 19898471.

189. Shaw MH, Kamada N, Warner N, Kim YG, Nuñez G. The ever-expanding function of NOD2: autophagy, viral recognition, and T cell activation. Trends Immunol. 2011 Feb;32(2):73-9. doi: 10.1016/j.it.2010.12.007. Epub 2011 Jan 19. PMID: 21251876; PMCID: PMC3056277.

190. Salvador-Martín S, Zapata-Cobo P, Velasco M, Palomino LM, Clemente S, Segarra O, Sánchez C, Tolín M, Moreno-Álvarez A, Fernández-Lorenzo A, Pérez-Moneo B, Loverdos I, Navas López VM, Millán A, Magallares L, Torres-Peral R, García-Romero R, Pujol-Muncunill G, Merino-Bohorquez V, Rodríguez A, Salcedo E, López-Cauce B, Marín-Jiménez I, Menchén L, Laserna-Mendieta E, Lucendo AJ, Sanjurjo-Sáez M, López-Fernández LA. Association between HLA DNA Variants and Long-Term Response to Anti-TNF Drugs in a Spanish Pediatric Inflammatory Bowel Disease Cohort. Int J Mol Sci. 2023 Jan 16;24(2):1797. doi: 10.3390/ijms24021797. PMID: 36675312; PMCID: PMC9861004.

191. Chen Y, Cui W, Li X, Yang H. Interaction Between Commensal Bacteria, Immune Response and the Intestinal Barrier in

Inflammatory Bowel Disease. Front Immunol. 2021 Nov 11;12:761981. doi: 10.3389/fimmu.2021.761981. PMID: 34858414; PMCID: PMC8632219.

192. Singh N, Bernstein CN. Environmental risk factors for inflammatory bowel disease. United European Gastroenterol J. 2022 Dec;10(10):1047-1053. doi: 10.1002/ueg2.12319. Epub 2022 Oct 19. PMID: 36262056; PMCID: PMC9752273.

193. Berkowitz L, Schultz BM, Salazar GA, Pardo-Roa C, Sebastián VP, Álvarez-Lobos MM, Bueno SM. Impact of Cigarette Smoking on the Gastrointestinal Tract Inflammation: Opposing Effects in Crohn's Disease and Ulcerative Colitis. Front Immunol. 2018 Jan 30;9:74. doi: 10.3389/fimmu.2018.00074. PMID: 29441064; PMCID: PMC5797634.

194. Younis N, Zarif R, Mahfouz R. Inflammatory bowel disease: between genetics and microbiota. Mol Biol Rep. 2020 Apr;47(4):3053-3063. doi: 10.1007/s11033-020-05318-5. Epub 2020 Feb 21. PMID: 32086718.

195. Van der Sloot KWJ, Weersma RK, Alizadeh BZ, Dijkstra G. Identification of Environmental Risk Factors Associated With the Development of Inflammatory Bowel Disease. J Crohns Colitis. 2020 Dec 2;14(12):1662-1671. doi: 10.1093/ecco-jcc/jjaa114. PMID: 32572465.

196. Ho SM, Lewis JD, Mayer EA, Plevy SE, Chuang E, Rappaport SM, Croitoru K, Korzenik JR, Krischer J, Hyams JS, Judson R, Kellis M, Jerrett M, Miller GW, Grant ML, Shtraizent N, Honig G, Hurtado-Lorenzo A, Wu GD. Challenges in IBD Research: Environmental Triggers. Inflamm Bowel Dis. 2019 May 16;25(Suppl 2):S13-S23. doi: 10.1093/ibd/izz076. Erratum in: Inflamm Bowel Dis. 2019 Nov 14;25(12):e171. doi: 10.1093/ibd/izz125. PMID: 31095702; PMCID: PMC6787673.

197. Ogura Y, Bonen DK, Inohara N, Nicolae DL, Chen FF, Ramos R, Britton H, Moran T, Karaliuskas R, Duerr RH, Achkar JP, Brant SR, Bayless TM, Kirschner BS, Hanauer SB, Nuñez G, Cho JH. A frameshift mutation in NOD2 associated with susceptibility to Crohn's disease. Nature. 2001 May 31;411(6837):603-6. doi: 10.1038/35079114. PMID: 11385577.

198. Qiu P, Ishimoto T, Fu L, Zhang J, Zhang Z, Liu Y. The Gut Microbiota in Inflammatory Bowel Disease. Front Cell Infect Microbiol. 2022 Feb 22;12:733992. doi: 10.3389/fcimb.2022.733992. PMID: 35273921; PMCID: PMC8902753.

199. Chelakkot C, Ghim J, Ryu SH. Mechanisms regulating intestinal barrier integrity and its pathological implications. Exp Mol Med. 2018 Aug 16;50(8):1-9. doi: 10.1038/s12276-018-0126-x. PMID: 30115904; PMCID: PMC6095905.

200. Vich Vila A, Imhann F, Collij V, Jankipersadsing SA, Gurry T, Mujagic Z, Kurilshikov A, Bonder MJ, Jiang X, Tigchelaar EF, Dekens J, Peters V, Voskuil MD, Visschedijk MC, van Dullemen HM, Keszthelyi D, Swertz MA, Franke L, Alberts R, Festen EAM, Dijkstra G, Masclee AAM, Hofker MH, Xavier RJ, Alm EJ, Fu J, Wijmenga C, Jonkers DMAE, Zhernakova A, Weersma RK. Gut microbiota composition and functional changes in inflammatory bowel disease and irritable bowel syndrome. Sci Transl Med. 2018 Dec 19;10(472):eaap8914. doi: 10.1126/scitranslmed.aap8914. PMID: 30567928.

201. Lloyd-Price J, Arze C, Ananthakrishnan AN, Schirmer M, Avila-Pacheco J, Poon TW, Andrews E, Ajami NJ, Bonham KS, Brislawn CJ, Casero D, Courtney H, Gonzalez A, Graeber TG, Hall AB, Lake K, Landers CJ, Mallick H, Plichta DR, Prasad M, Rahnavard G, Sauk J, Shungin D, Vázquez-Baeza Y, White RA 3rd; IBDMDB Investigators; Braun J, Denson LA, Jansson JK, Knight R, Kugathasan S, McGovern DPB, Petrosino JF, Stappenbeck TS, Winter HS, Clish CB, Franzosa EA, Vlamakis H, Xavier RJ, Huttenhower C. Multi-omics of the gut microbial ecosystem in inflammatory bowel diseases. Nature. 2019 May;569(7758):655-662. doi: 10.1038/s41586-019-1237-9. Epub 2019 May 29. PMID: 31142855; PMCID: PMC6650278.

202. Coyne MJ, Comstock LE. Type VI Secretion Systems and the Gut Microbiota. Microbiol Spectr. 2019 Mar;7(2):10.1128/microbiolspec.psib-0009-2018. doi: 10.1128/microbiolspec.PSIB-0009-2018. PMID: 30825301; PMCID: PMC6404974.

203. Llewellyn SR, Britton GJ, Contijoch EJ, Vennaro OH, Mortha A, Colombel JF, Grinspan A, Clemente JC, Merad M, Faith JJ. Interactions Between Diet and the Intestinal Microbiota Alter Intestinal Permeability and Colitis Severity in Mice. 2018 Mar;154(4):1037-1046.e2. doi: 10.1053/j.gastro.2017.11.030. Epub 2017 Nov 23. PMID: 29174952; PMCID: PMC5847454.

204. Khan I, Ullah N, Zha L, Bai Y, Khan A, Zhao T, Che T, Zhang C. Alteration of Gut Microbiota in Inflammatory Bowel Disease (IBD): Cause or Consequence? IBD Treatment Targeting the Gut Microbiome. Pathogens. 2019 Aug 13;8(3):126. doi: 10.3390/pathogens8030126. PMID: 31412603; PMCID: PMC6789542.

205. Cao Z, Sugimura N, Burgermeister E, Ebert MP, Zuo T, Lan P. The gut virome: A new microbiome component in health and disease. EBioMedicine. 2022 Jul;81:104113. doi: 10.1016/j.ebiom.2022.104113. Epub 2022 Jun 23. PMID: 35753153; PMCID: PMC9240800.

206. Sokol H, Leducq V, Aschard H, Pham HP, Jegou S, Landman C, Cohen D, Liguori G, Bourrier A, Nion-Larmurier I, Cosnes J, Seksik P, Langella P, Skurnik D, Richard ML, Beaugerie L. Fungal microbiota dysbiosis in IBD. Gut. 2017 Jun;66(6):1039-1048. doi: 10.1136/gutjnl-2015-310746. Epub 2016 Feb 3. PMID: 26843508; PMCID: PMC5532459.

207. Beheshti-Maal A, Shahrokh S, Ansari S, Mirsamadi ES, Yadegar A, Mirjalali H, Zali MR. Gut mycobiome: The probable determinative role of fungi in IBD patients. Mycoses. 2021 May;64(5):468-476. doi: 10.1111/myc.13238. Epub 2021 Feb 3. PMID: 33421192.

208. Dubik M, Pilecki B, Moeller JB. Commensal Intestinal Protozoa-Underestimated Members of the Gut Microbial Community. Biology (Basel). 2022 Nov 30;11(12):1742. doi: 10.3390/biology11121742. PMID: 36552252; PMCID: PMC9774987.

209. Petersen AM, Stensvold CR, Mirsepasi H, Engberg J, Friis-Møller A, Porsbo LJ, Hammerum AM, Nordgaard-Lassen I, Nielsen HV, Krogfelt KA. Active ulcerative colitis associated with low prevalence of Blastocystis and Dientamoeba fragilis infection. Scand J Gastroenterol. 2013 May;48(5):638-9. doi: 10.3109/00365521.2013.780094. Epub 2013 Mar 25. PMID: 23528075.

210. Mafra D, Ribeiro M, Fonseca L, Regis B, Cardozo LFMF, Fragoso Dos Santos H, Emiliano de Jesus H, Schultz J, Shiels PG, Stenvinkel P, Rosado A. Archaea from the gut microbiota of humans: Could be linked to chronic diseases? Anaerobe. 2022 Oct;77:102629. doi: 10.1016/j.anaerobe.2022.102629. Epub 2022 Aug 17. PMID: 35985606.

211. Guan Q. A Comprehensive Review and Update on the Pathogenesis of Inflammatory Bowel Disease. J Immunol Res. 2019 Dec 1;2019:7247238. doi: 10.1155/2019/7247238. PMID: 31886308; PMCID: PMC6914932.

212. Aggeletopoulou I, Kalafateli M, Tsounis EP, Triantos C. Exploring the role of IL-1β in inflammatory bowel disease pathogenesis. Front Med (Lausanne). 2024 Jan 22;11:1307394. doi: 10.3389/fmed.2024.1307394. PMID: 38323035; PMCID: PMC10845338.

213. de Mattos BR, Garcia MP, Nogueira JB, Paiatto LN, Albuquerque CG, Souza CL, Fernandes LG, Tamashiro WM, Simioni PU. Inflammatory Bowel Disease: An Overview of Immune Mechanisms and Biological Treatments. Mediators Inflamm. 2015;2015:493012. doi: 10.1155/2015/493012. Epub 2015 Aug 3. PMID: 26339135; PMCID: PMC4539174.

214. Takatori H, Kanno Y, Watford WT, Tato CM, Weiss G, Ivanov II, Littman DR, O'Shea JJ. Lymphoid tissue inducer-like cells are an innate source of IL-17 and IL-22. J Exp Med. 2009 Jan 16;206(1):35-41. doi: 10.1084/jem.20072713. Epub 2008 Dec 29. PMID: 19114665; PMCID: PMC2626689.

215. Poggi A, Benelli R, Venè R, Costa D, Ferrari N, Tosetti F, Zocchi MR. Human Gut-Associated Natural Killer Cells in Health and Disease. Front Immunol. 2019 May 3;10:961. doi: 10.3389/fimmu.2019.00961. PMID: 31130953; PMCID: PMC6509241.

216. Tindemans I, Joosse ME, Samsom JN. Dissecting the Heterogeneity in T-Cell Mediated Inflammation in IBD. Cells. 2020 Jan 2;9(1):110. doi: 10.3390/cells9010110. PMID: 31906479; PMCID: PMC7016883.

217. Zhou L, Ivanov II, Spolski R, Min R, Shenderov K, Egawa T, Levy DE, Leonard WJ, Littman DR. IL-6 programs T(H)-17 cell differentiation by promoting sequential engagement of the IL-21 and IL-23 pathways. Nat Immunol. 2007 Sep;8(9):967-74. doi: 10.1038/ni1488. Epub 2007 Jun 20. PMID: 17581537.

218. Kobayashi T, Okamoto S, Hisamatsu T, Kamada N, Chinen H, Saito R, Kitazume MT, Nakazawa A, Sugita A, Koganei K, Isobe K, Hibi T. IL23 differentially regulates the Th1/Th17 balance in ulcerative colitis and Crohn's disease. Gut. 2008 Dec;57(12):1682-9. doi:

10.1136/gut.2007.135053. Epub 2008 Jul 24. PMID: 18653729.

219. Sugihara T, Kobori A, Imaeda H, Tsujikawa T, Amagase K, Takeuchi K, Fujiyama Y, Andoh A. The increased mucosal mRNA expressions of complement C3 and interleukin-17 in inflammatory bowel disease. Clin Exp Immunol. 2010 Jun;160(3):386-93. doi: 10.1111/j.1365-2249.2010.04093.x. Epub 2010 Jan 19. PMID: 20089077; PMCID: PMC2883109.

220. Flannigan KL, Ngo VL, Geem D, Harusato A, Hirota SA, Parkos CA, Lukacs NW, Nusrat A, Gaboriau-Routhiau V, Cerf-Bensussan N, Gewirtz AT, Denning TL. IL-17A-mediated neutrophil recruitment limits expansion of segmented filamentous bacteria. Mucosal Immunol. 2017 May;10(3):673-684. doi: 10.1038/mi.2016.80. Epub 2016 Sep 14. PMID: 27624780; PMCID: PMC5350071.

221. Domínguez-Fernández C, Egiguren-Ortiz J, Razquin J, Gómez-Galán M, De Las Heras-García L, Paredes-Rodríguez E, Astigarraga E, Miguélez C, Barreda-Gómez G. Review of Technological Challenges in Personalised Medicine and Early Diagnosis of Neurodegenerative Disorders. Int J Mol Sci. 2023 Feb 7;24(4):3321. doi: 10.3390/ijms24043321. PMID: 36834733; PMCID: PMC9968142.

222. Pap D, Veres-Székely A, Szebeni B, Vannay Á. PARK7/DJ-1 as a Therapeutic Target in Gut-Brain Axis Diseases. Int J Mol Sci. 2022 Jun 14;23(12):6626. doi: 10.3390/ijms23126626. PMID: 35743072; PMCID: PMC9223539.

223. Feuerstein JD, Cheifetz AS. Crohn Disease: Epidemiology, Diagnosis, and Management. Mayo Clin Proc. 2017 Jul;92(7):1088-1103. doi: 10.1016/j.mayocp.2017.04.010. Epub 2017 Jun 7. PMID: 28601423.

224. Baumgart DC, Sandborn WJ. Crohn's disease. Lancet. 2012 Nov 3;380(9853):1590-605. doi: 10.1016/S0140-6736(12)60026-9. Epub 2012 Aug 20. Erratum in: Lancet. 2013 Jan 19;381(9862):204. PMID: 22914295.

225. Cheifetz AS. Management of active Crohn disease. JAMA. 2013 May 22;309(20):2150-8. doi: 10.1001/jama.2013.4466. PMID: 23695484; PMCID: PMC5877483.

226. Heresbach D, Alexandre JL, Branger B, Bretagne JF, Cruchant E, Dabadie A, Dartois-Hoguin M, Girardot PM, Jouanolle H, Kerneis J, Le Verger JC, Louvain V, Politis J, Richecoeur M, Robaszkiewicz M, Seyrig JA; ABERMAD (Association Bretonne d'Etude et de Recherche sur les Maladies de l'Appareil Digestif). Frequency and significance of granulomas in a cohort of incident cases of Crohn's disease. Gut. 2005 Feb;54(2):215-22. doi: 10.1136/gut.2004.041715. PMID: 15647184; PMCID: PMC1774855.

227. Dambha F, Tanner J, Carroll N. Diagnostic imaging in Crohn's disease: what is the new gold standard? Best Pract Res Clin Gastroenterol. 2014;28(3):421-436.

228. Papadakis KA. Chemokines in inflammatory bowel disease. Curr Allergy Asthma Rep. 2004 Jan;4(1):83-9. doi: 10.1007/s11882-004-0048-7. PMID: 14680627.

229. de Souza HS, Fiocchi C. Immunopathogenesis of IBD: current state of the art. Nat Rev Gastroenterol Hepatol. 2016 Jan;13(1):13-27. doi: 10.1038/nrgastro.2015.186. Epub 2015 Dec 2. PMID: 26627550.

230. Torres J, Mehandru S, Colombel JF, Peyrin-Biroulet L. Crohn's disease. Lancet. 2017 Apr 29;389(10080):1741-1755. doi: 10.1016/S0140-6736(16)31711-1. Epub 2016 Dec 1. PMID: 27914655.

231. Ungaro R, Mehandru S, Allen PB, Peyrin-Biroulet L, Colombel JF. Ulcerative colitis. Lancet. 2017 Apr 29;389(10080):1756-1770. doi: 10.1016/S0140-6736(16)32126-2. Epub 2016 Dec 1. PMID: 27914657; PMCID: PMC6487890.

232. Kornbluth A, Sachar DB; Practice Parameters Committee of the American College of Gastroenterology. Ulcerative colitis practice guidelines in adults: American College Of Gastroenterology, Practice Parameters Committee. Am J Gastroenterol. 2010 Mar;105(3):501-23; quiz 524. doi: 10.1038/ajg.2009.727. Epub 2010 Jan 12. Erratum in: Am J Gastroenterol. 2010 Mar;105(3):500. PMID: 20068560.

233. Annese V, Daperno M, Rutter MD, Amiot A, Bossuyt P, East J, Ferrante M, Götz M, Katsanos KH, Kießlich R, Ordás I, Repici A,

Rosa B, Sebastian S, Kucharzik T, Eliakim R; European Crohn's and Colitis Organisation. European evidence based consensus for endoscopy in inflammatory bowel disease. J Crohns Colitis. 2013 Dec;7(12):982-1018. doi: 10.1016/j.crohns.2013.09.016. Epub 2013 Nov 1. PMID: 24184171.

234. Dignass A, Eliakim R, Magro F, Maaser C, Chowers Y, Geboes K, Mantzaris G, Reinisch W, Colombel JF, Vermeire S, Travis S, Lindsay JO, Van Assche G. Second European evidence-based consensus on the diagnosis and management of ulcerative colitis part 1: definitions and diagnosis. J Crohns Colitis. 2012 Dec;6(10):965-90. doi: 10.1016/j.crohns.2012.09.003. Epub 2012 Oct 3. PMID: 23040452.

235. Magro F, Rodrigues A, Vieira AI, Portela F, Cremers I, Cotter J, Correia L, Duarte MA, Tavares ML, Lago P, Ministro P, Peixe P, Lopes S, Garcia EB. Review of the disease course among adult ulcerative colitis population-based longitudinal cohorts. Inflamm Bowel Dis. 2012 Mar;18(3):573-83. doi: 10.1002/ibd.21815. Epub 2011 Jul 26. PMID: 21793126.

236. Cosnes J, Gower-Rousseau C, Seksik P, Cortot A. Epidemiology and natural history of inflammatory bowel diseases. Gastroenterology. 2011 May;140(6):1785-94. doi: 10.1053/j.gastro.2011.01.055. PMID: 21530745.

237. Charpentier C, Salleron J, Savoye G, Fumery M, Merle V, Laberenne JE, Vasseur F, Dupas JL, Cortot A, Dauchet L, Peyrin-Biroulet L, Lerebours E, Colombel JF, Gower-Rousseau C. Natural history of elderly-onset inflammatory bowel disease: a population-based cohort study. Gut. 2014 Mar;63(3):423-32. doi: 10.1136/gutjnl-2012-303864. Epub 2013 Feb 13. PMID: 23408350.

238. Reinisch W, Reinink AR, Higgins PD. Factors associated with poor outcomes in adults with newly diagnosed ulcerative colitis. Clin Gastroenterol Hepatol. 2015 Apr;13(4):635-42. doi: 10.1016/j.cgh.2014.03.037. Epub 2014 Jun 2. PMID: 24887059.

239. Jiang C, Ting AT, Seed B. PPAR-gamma agonists inhibit production of monocyte inflammatory cytokines. Nature. 1998 Jan 1;391(6662):82-6. doi: 10.1038/34184. PMID: 9422509.

240. Buonocore S, Ahern PP, Uhlig HH, Ivanov II, Littman DR, Maloy KJ, Powrie F. Innate lymphoid cells drive interleukin-23-dependent innate intestinal pathology. Nature. 2010 Apr 29;464(7293):1371-5. doi: 10.1038/nature08949. PMID: 20393462; PMCID: PMC3796764.

241. Fuss IJ, Heller F, Boirivant M, Leon F, Yoshida M, Fichtner-Feigl S, Yang Z, Exley M, Kitani A, Blumberg RS, Mannon P, Strober W. Nonclassical CD1d-restricted NK T cells that produce IL-13 characterize

242. Gerlach K, Hwang Y, Nikolaev A, Atreya R, Dornhoff H, Steiner S, Lehr HA, Wirtz S, Vieth M, Waisman A, Rosenbauer F, McKenzie AN, Weigmann B, Neurath MF. TH9 cells that express the transcription factor PU.1 drive T cell-mediated colitis via IL-9 receptor signaling in intestinal epithelial cells. Nat Immunol. 2014 Jul;15(7):676-86. doi: 10.1038/ni.2920. Epub 2014 Jun 8. Erratum in: Nat Immunol. 2015 Feb;16(2):214. PMID: 24908389.

243. Ho GT, Mowat C, Goddard CJ, Fennell JM, Shah NB, Prescott RJ, Satsangi J. Predicting the outcome of severe ulcerative colitis: development of a novel risk score to aid early selection of patients for second-line medical therapy or surgery. Aliment Pharmacol Ther. 2004 May 15;19(10):1079-87. doi: 10.1111/j.1365-2036.2004.01945.x. PMID: 15142197.

244. Sezaki M, Hayashi Y, Nakato G, Wang Y, Nakata S, Biswas S, Morishima T, Fakruddin M, Moon J, Ahn S, Kim P, Miyamoto Y, Baba H, Fukuda S, Takizawa H. Hematopoietic stem and progenitor cells integrate microbial signals to promote post-inflammation gut tissue repair. EMBO J. 2022 Nov 17;41(22):e110712. doi: 10.15252/embj.2022110712. Epub 2022 Oct 18. PMID: 36254590; PMCID: PMC9670188.

245. Liu X, Zhang H, Shi G, Zheng X, Chang J, Lin Q, Tian Z, Yang H. The impact of gut microbial signals on hematopoietic stem cells and the bone marrow microenvironment. Front Immunol. 2024 Feb 13;15:1338178. doi: 10.3389/fimmu.2024.1338178. PMID: 38415259; PMCID: PMC10896826.

246. Burberry A, Zeng MY, Ding L, Wicks I, Inohara N, Morrison SJ, Núñez G. Infection mobilizes hematopoietic stem cells through

cooperative NOD-like receptor and Toll-like receptor signaling. Cell Host Microbe. 2014 Jun 11;15(6):779-91. doi: 10.1016/j.chom.2014.05.004. Epub 2014 May 29. PMID: 24882704; PMCID: PMC4085166.

247. Gabrilovich DI, Nagaraj S. Myeloid-derived suppressor cells as regulators of the immune system. Nat Rev Immunol. 2009 Mar;9(3):162-74. doi: 10.1038/nri2506. PMID: 19197294; PMCID: PMC2828349.

248. Wirtz S, Popp V, Kindermann M, Gerlach K, Weigmann B, Fichtner-Feigl S, Neurath MF. Chemically induced mouse models of acute and chronic intestinal inflammation. Nat Protoc. 2017 Jul;12(7):1295-1309. doi: 10.1038/nprot.2017.044. Epub 2017 Jun 1. PMID: 28569761.

249. Castellana C, Eusebi LH, Dajti E, Iascone V, Vestito A, Fusaroli P, Fuccio L, D'Errico A, Zagari RM. Autoimmune Atrophic Gastritis: A Clinical Review. Cancers (Basel). 2024 Mar 28;16(7):1310. doi: 10.3390/cancers16071310. PMID: 38610988; PMCID: PMC11010983.

250. Pimentel-Nunes P, Libânio D, Marcos-Pinto R, Areia M, Leja M, Esposito G, Garrido M, Kikuste I, Megraud F, Matysiak-Budnik T, Annibale B, Dumonceau JM, Barros R, Fléjou JF, Carneiro F, van Hooft JE, Kuipers EJ, Dinis-Ribeiro M. Management of epithelial precancerous conditions and lesions in the stomach (MAPS II): European Society of Gastrointestinal Endoscopy (ESGE), European Helicobacter and Microbiota Study Group (EHMSG), European Society of Pathology (ESP), and Sociedade Portuguesa de Endoscopia Digestiva (SPED) guideline update 2019. Endoscopy. 2019 Apr;51(4):365-388. doi: 10.1055/a-0859-1883. Epub 2019 Mar 6. PMID: 30841008.

251. Turner D, Ricciuto A, Lewis A, D'Amico F, Dhaliwal J, Griffiths AM, Bettenworth D, Sandborn WJ, Sands BE, Reinisch W, Schölmerich J, Bemelman W, Danese S, Mary JY, Rubin D, Colombel JF, Peyrin-Biroulet L, Dotan I, Abreu MT, Dignass A; International Organization for the Study of IBD. STRIDE-II: An Update on the Selecting Therapeutic Targets in Inflammatory Bowel Disease (STRIDE) Initiative of the International Organization for the Study of IBD (IOIBD): Determining Therapeutic Goals for Treat-to-Target strategies in IBD. Gastroenterology. 2021 Apr;160(5):1570-1583. doi: 10.1053/j.gastro.2020.12.031. Epub 2021 Feb 19. PMID: 33359090.

252. Cai Z, Wang S, Li J. Treatment of Inflammatory Bowel Disease: A Comprehensive Review. Front Med (Lausanne). 2021 Dec 20;8:765474. doi: 10.3389/fmed.2021.765474. PMID: 34988090; PMCID: PMC8720971.

253. Li J, Wang F, Zhang HJ, Sheng JQ, Yan WF, Ma MX, Fan RY, Gu F, Li CF, Chen DF, Zheng P, Gu YP, Cao Q, Yang H, Qian JM, Hu PJ, Xia B. Corticosteroid therapy in ulcerative colitis: Clinical response and predictors. World J Gastroenterol. 2015 Mar 14;21(10):3005-15. doi: 10.3748/wjg.v21.i10.3005. PMID: 25780299; PMCID: PMC4356921.

254. Timmer A, Patton PH, Chande N, McDonald JW, MacDonald JK. Azathioprine and 6-mercaptopurine for maintenance of remission in ulcerative colitis. Cochrane Database Syst Rev. 2016 May 18;2016(5):CD000478. doi: 10.1002/14651858.CD000478.pub4. Update in: Cochrane Database Syst Rev. 2025 Feb 27;2:CD000478. doi: 10.1002/14651858.CD000478.pub5. PMID: 27192092; PMCID: PMC7034525.

255. Sandborn WJ, Su C, Sands BE, D'Haens GR, Vermeire S, Schreiber S, Danese S, Feagan BG, Reinisch W, Niezychowski W, Friedman G, Lawendy N, Yu D, Woodworth D, Mukherjee A, Zhang H, Healey P, Panés J; OCTAVE Induction 1, OCTAVE Induction 2, and OCTAVE Sustain Investigators. Tofacitinib as Induction and Maintenance Therapy for Ulcerative Colitis. N Engl J Med. 2017 May 4;376(18):1723-1736. doi: 10.1056/NEJMoa1606910. PMID: 28467869.

256. Lahner E, Annibale B. Pernicious anemia: new insights from a gastroenterological point of view. World J Gastroenterol. 2009 Nov 7;15(41):5121-8. doi: 10.3748/wjg.15.5121. PMID: 19891010; PMCID: PMC2773890.

257. Pisani A, Riccio E, Sabbatini M, Andreucci M, Del Rio A, Visciano B. Effect of oral liposomal iron versus intravenous iron for treatment of iron deficiency anaemia in CKD patients: a randomized trial. Nephrol Dial Transplant. 2015 Apr;30(4):645-52. doi: 10.1093/ndt/gfu357. Epub 2014 Nov 13. PMID: 25395392.

258. Lahner E, Zagari RM, Zullo A, Di Sabatino A, Meggio A, Cesaro P, Lenti MV, Annibale B, Corazza GR. Chronic atrophic gastritis: Natural history, diagnosis and therapeutic management. A position paper by the Italian Society of Hospital Gastroenterologists and Digestive Endoscopists [AIGO], the Italian Society of Digestive Endoscopy [SIED], the Italian Society of Gastroenterology [SIGE], and the Italian Society of Internal Medicine [SIMI]. Dig Liver Dis. 2019 Dec;51(12):1621-1632. doi: 10.1016/j.dld.2019.09.016. Epub 2019 Oct 19. PMID: 31635944.

259. Taylor L, McCaddon A, Wolffenbuttel BHR. Creating a Framework for Treating Autoimmune Gastritis-The Case for Replacing Lost Acid. Nutrients. 2024 Feb 27;16(5):662. doi: 10.3390/nu16050662. PMID: 38474790; PMCID: PMC10934127.

260. Haruma K, Ito M. Review article: clinical significance of mucosal-protective agents: acid, inflammation, carcinogenesis and rebamipide. Aliment Pharmacol Ther. 2003 Jul;18 Suppl 1:153-9. doi: 10.1046/j.1365-2036.18.s1.17.x. PMID: 12925154.

261. Strickland RG, Fisher JM, Lewin K, Taylor KB. The response to prednisolone in atrophic gastritis: a possible effect on non-intrinsic factor-mediated vitamin B 12 absorption. Gut. 1973 Jan;14(1):13-9. doi: 10.1136/gut.14.1.13. PMID: 4571069; PMCID: PMC1412575.

262. Jorge AD, Sanchez D. The effect of azathioprine on gastric mucosal histology and acid secretion in chronic gastritis. Gut. 1973 Feb;14(2):104-6. doi: 10.1136/gut.14.2.104. PMID: 4696531; PMCID: PMC1412565.

263. Arnold, K., Sarkar, A., Yram, M. A., Polo, J. M., Bronson, R., Sengupta, S., et al. (2011). Sox2+ adult stem and progenitor cells are important for tissue regeneration and survival of mice. Cell Stem Cell 9, 317–329. doi: 10.1016/j.stem.2011.09.001

264. Nienhüser, H., Kim, W., Malagola, E., Ruan, T., Valenti, G., Middelhoff, M., et al. (2020). Mist1+ gastric isthmus stem cells are regulated by Wnt5a and expand in response to injury and inflammation in mice. Gut doi: 10.1136/gutjnl-2020-320742

265. Harbord M, Eliakim R, Bettenworth D, Karmiris K, Katsanos K, Kopylov U, Kucharzik T, Molnár T, Raine T, Sebastian S, de Sousa HT, Dignass A, Carbonnel F; European Crohn's and Colitis Organisation [ECCO]. Third European Evidence-based Consensus on Diagnosis and Management of Ulcerative Colitis. Part 2: Current Management. J Crohns Colitis. 2017 Jul 1;11(7):769-784. doi: 10.1093/ecco-jcc/jjx009. Erratum in: J Crohns Colitis. 2017 Dec 4;11(12):1512. doi: 10.1093/ecco-jcc/jjx105. Erratum in: J Crohns Colitis. 2023 Jan 27;17(1):149. doi: 10.1093/ecco-jcc/jjac104. PMID: 28513805.

266. Berg DR, Colombel JF, Ungaro R. The Role of Early Biologic Therapy in Inflammatory Bowel Disease. Inflamm Bowel Dis. 2019 Nov 14;25(12):1896-1905. doi: 10.1093/ibd/izz059. PMID: 30934053; PMCID: PMC7185690.

267. Torres J, Bonovas S, Doherty G, Kucharzik T, Gisbert JP, Raine T, Adamina M, Armuzzi A, Bachmann O, Bager P, Biancone L, Bokemeyer B, Bossuyt P, Burisch J, Collins P, El-Hussuna A, Ellul P, Frei-Lanter C, Furfaro F, Gingert C, Gionchetti P, Gomollon F, González-Lorenzo M, Gordon H, Hlavaty T, Juillerat P, Katsanos K, Kopylov U, Krustins E, Lytras T, Maaser C, Magro F, Marshall JK, Myrelid P, Pellino G, Rosa I, Sabino J, Savarino E, Spinelli A, Stassen L, Uzzan M, Vavricka S, Verstockt B, Warusavitarne J, Zmora O, Fiorino G. ECCO Guidelines on Therapeutics in Crohn's Disease: Medical Treatment. J Crohns Colitis. 2020 Jan 1;14(1):4-22. doi: 10.1093/ecco-jcc/jjz180. PMID: 31711158.

268. D'Ugo S, Romano F, Sibio S, Bagaglini G, Sensi B, Biancone L, Monteleone G, Sica GS. Impact of surgery on quality of life in Crohn's disease: short- and mid-term follow-up. Updates Surg. 2020 Sep;72(3):773-780. doi: 10.1007/s13304-020-00738-1. Epub 2020 Mar 17. PMID: 32185677.

269. Elhag DA, Kumar M, Saadaoui M, Akobeng AK, Al-Mudahka F, Elawad M, Al Khodor S. Inflammatory Bowel Disease Treatments and Predictive Biomarkers of Therapeutic Response. Int J Mol Sci. 2022 Jun 23;23(13):6966. doi: 10.3390/ijms23136966. PMID: 35805965; PMCID: PMC9266456.

270. Murray A, Nguyen TM, Parker CE, Feagan BG, MacDonald JK. Oral 5-aminosalicylic acid for induction of remission in ulcerative colitis. Cochrane Database Syst Rev. 2020 Aug 12;8(8):CD000543. doi: 10.1002/14651858.CD000543.pub5. PMID: 32786164; PMCID: PMC8189994.

271. Ford AC, Khan KJ, Sandborn WJ, Hanauer SB, Moayyedi P. Efficacy of topical 5-aminosalicylates in preventing relapse of quiescent ulcerative colitis: a meta-analysis. Clin Gastroenterol Hepatol. 2012 May;10(5):513-9. doi: 10.1016/j.cgh.2011.10.043. Epub 2011 Nov 12. PMID: 22083024.

272. Eaden J, Abrams K, Ekbom A, Jackson E, Mayberry J. Colorectal cancer prevention in ulcerative colitis: a case-control study. Aliment Pharmacol Ther. 2000 Feb;14(2):145-53. doi: 10.1046/j.1365-2036.2000.00698.x. PMID: 10651654.

273. Akobeng AK, Zhang D, Gordon M, MacDonald JK. Oral 5-aminosalicylic acid for maintenance of medically-induced remission in Crohn's disease. Cochrane Database Syst Rev. 2016 Sep 28;9(9):CD003715. doi: 10.1002/14651858.CD003715.pub3. PMID: 27681657; PMCID: PMC6457838.

274. Hart A, Ng SC, Watkins J, Paridaens K, Edwards JO, Fullarton JR, Sonderegger YLY, Ghatnekar O, Ghosh S. The use of 5-aminosalicylates in Crohn's disease: a retrospective study using the UK Clinical Practice Research Datalink. Ann Gastroenterol. 2020 Sep-Oct;33(5):500-507. doi: 10.20524/aog.2020.0521. Epub 2020 Jun 22. PMID: 32879597; PMCID: PMC7406809.

275. Gjuladin-Hellon T, Gordon M, Iheozor-Ejiofor Z, Akobeng AK. Oral 5-aminosalicylic acid for maintenance of surgically-induced remission in Crohn's disease. Cochrane Database Syst Rev. 2019 Jun 20;6(6):CD008414. doi: 10.1002/14651858.CD008414.pub3. PMID: 31220875; PMCID: PMC6586553.

276. Hayashi R, Wada H, Ito K, Adcock IM. Effects of glucocorticoids on gene transcription. Eur J Pharmacol. 2004 Oct 1;500(1-3):51-62. doi: 10.1016/j.ejphar.2004.07.011. PMID: 15464020.

277. Lichtenstein GR, Abreu MT, Cohen R, Tremaine W; American Gastroenterological Association. American Gastroenterological Association Institute technical review on corticosteroids, immunomodulators, and infliximab in inflammatory bowel disease. Gastroenterology. 2006 Mar;130(3):940-87. doi: 10.1053/j.gastro.2006.01.048. PMID: 16530532.

278. Barrett K, Saxena S, Pollok R. Using corticosteroids appropriately in inflammatory bowel disease: a guide for primary care. Br J Gen Pract. 2018 Oct;68(675):497-498. doi: 10.3399/bjgp18X699341. PMID: 30262630; PMCID: PMC6146008.

279. Curkovic I, Egbring M, Kullak-Ublick GA. Risks of inflammatory bowel disease treatment with glucocorticosteroids and aminosalicylates. Dig Dis. 2013;31(3-4):368-73. doi: 10.1159/000354699. Epub 2013 Nov 14. PMID: 24246990.

280. Coward S, Kuenzig ME, Hazlewood G, Clement F, McBrien K, Holmes R, Panaccione R, Ghosh S, Seow CH, Rezaie A, Kaplan GG. Comparative Effectiveness of Mesalamine, Sulfasalazine, Corticosteroids, and Budesonide for the Induction of Remission in Crohn's Disease: A Bayesian Network Meta-analysis. Inflamm Bowel Dis. 2017 Mar;23(3):461-472. doi: 10.1097/MIB.0000000000001023. Erratum in: Inflamm Bowel Dis. 2017 May 1;23(5):E25. doi: 10.1097/MIB.0000000000001151. Corrected and republished in: Inflamm Bowel Dis. 2017 May 1;23(5):E26-E37. doi: 10.1097/MIB.0000000000001158. PMID: 28146003.

281. Shin JY, Wey M, Umutesi HG, Sun X, Simecka J, Heo J. Thiopurine Prodrugs Mediate Immunosuppressive Effects by Interfering with Rac1 Protein Function. J Biol Chem. 2016 Jun 24;291(26):13699-714. doi: 10.1074/jbc.M115.694422. Epub 2016 May 9. PMID: 27189938; PMCID: PMC4919453.

282. Jharap B, Seinen ML, de Boer NK, van Ginkel JR, Linskens RK, Kneppelhout JC, Mulder CJ, van Bodegraven AA. Thiopurine therapy in inflammatory bowel disease patients: analyses of two 8-year intercept cohorts. Inflamm Bowel Dis. 2010 Sep;16(9):1541-9. doi: 10.1002/ibd.21221. PMID: 20155846.

283. Gisbert JP, Niño P, Cara C, Rodrigo L. Comparative effectiveness of azathioprine in Crohn's disease and ulcerative colitis: prospective, long-term, follow-up study of 394 patients. Aliment Pharmacol Ther. 2008 Jul;28(2):228-38. doi: 10.1111/j.1365-2036.2008.03732.x. Epub 2008 May 12. PMID: 18485129.

284. Lémann M, Chamiot-Prieur C, Mesnard B, Halphen M, Messing B, Rambaud JC, Gendre JP, Colombel JF, Modigliani R. Methotrexate for the treatment of refractory Crohn's disease. Aliment Pharmacol Ther. 1996 Jun;10(3):309-14. doi: 10.1111/j.0953-

0673.1996.00309.x. PMID: 8791956.

285. Chande N, Wang Y, MacDonald JK, McDonald JW. Methotrexate for induction of remission in ulcerative colitis. Cochrane Database Syst Rev. 2014 Aug 27;2014(8):CD006618. doi: 10.1002/14651858.CD006618.pub3. PMID: 25162749; PMCID: PMC6486224.

286. Lichtiger S, Present DH, Kornbluth A, Gelernt I, Bauer J, Galler G, Michelassi F, Hanauer S. Cyclosporine in severe ulcerative colitis refractory to steroid therapy. N Engl J Med. 1994 Jun 30;330(26):1841-5. doi: 10.1056/NEJM199406303302601. PMID: 8196726.

287. Yamamoto S, Nakase H, Mikami S, Inoue S, Yoshino T, Takeda Y, Kasahara K, Ueno S, Uza N, Kitamura H, Tamaki H, Matsuura M, Inui K, Chiba T. Long-term effect of tacrolimus therapy in patients with refractory ulcerative colitis. Aliment Pharmacol Ther. 2008 Sep 1;28(5):589-97. doi: 10.1111/j.1365-2036.2008.03764.x. Epub 2008 Jun 28. PMID: 18549460.

288. Iida T, Nojima M, Nakase H. Therapeutic Efficacy and Adverse Events of Tacrolimus in Patients with Crohn's Disease: Systematic Review and Meta-Analysis. Dig Dis Sci. 2019 Oct;64(10):2945-2954. doi: 10.1007/s10620-019-05619-1. Epub 2019 Apr 13. PMID: 30982208.

289. Sandborn WJ, Rutgeerts P, Feagan BG, Reinisch W, Olson A, Johanns J, Lu J, Horgan K, Rachmilewitz D, Hanauer SB, Lichtenstein GR, de Villiers WJ, Present D, Sands BE, Colombel JF. Confronto del tasso di colectomia dopo il trattamento della colite ulcerosa con placebo o infliximab. Gastroenterologia. 2009 Ott;137(4):1250-60; quiz 1520. doi: 10.1053/j.gastro.2009.06.061. Epub 2009 28 luglio. PMID: 19596014.

290. Present DH, Rutgeerts P, Targan S, Hanauer SB, Mayer L, van Hogezand RA, Podolsky DK, Sands BE, Braakman T, DeWoody KL, Schaible TF, van Deventer SJ. Infliximab for the treatment of fistulas in patients with Crohn's disease. N Engl J Med. 1999 May 6;340(18):1398-405. doi: 10.1056/NEJM199905063401804. PMID: 10228190.

291. Ben-Horin S, Kopylov U, Chowers Y. Optimizing anti-TNF treatments in inflammatory bowel disease. Autoimmun Rev. 2014 Jan;13(1):24-30. doi: 10.1016/j.autrev.2013.06.002. Epub 2013 Jun 19. PMID: 23792214.

292. Feagan BG, Sandborn WJ, D'Haens G, Panés J, Kaser A, Ferrante M, Louis E, Franchimont D, Dewit O, Seidler U, Kim KJ, Neurath MF, Schreiber S, Scholl P, Pamulapati C, Lalovic B, Visvanathan S, Padula SJ, Herichova I, Soaita A, Hall DB, Böcher WO. Induction therapy with the selective interleukin-23 inhibitor risankizumab in patients with moderate-to-severe Crohn's disease: a randomised, double-blind, placebo-controlled phase 2 study. Lancet. 2017 Apr 29;389(10080):1699-1709. doi: 10.1016/S0140-6736(17)30570-6. Epub 2017 Apr 12. PMID: 28411872.

293. Almradi A, Hanzel J, Sedano R, Parker CE, Feagan BG, Ma C, Jairath V. Clinical Trials of IL-12/IL-23 Inhibitors in Inflammatory Bowel Disease. BioDrugs. 2020 Dec;34(6):713-721. doi: 10.1007/s40259-020-00451-w. PMID: 33105016.

294. Wyant T, Fedyk E, Abhyankar B. An Overview of the Mechanism of Action of the Monoclonal Antibody Vedolizumab. J Crohns Colitis. 2016 Dec;10(12):1437-1444. doi: 10.1093/ecco-jcc/jjw092. Epub 2016 Jun 1. PMID: 27252400.

295. Feagan BG, Rutgeerts P, Sands BE, Hanauer S, Colombel JF, Sandborn WJ, Van Assche G, Axler J, Kim HJ, Danese S, Fox I, Milch C, Sankoh S, Wyant T, Xu J, Parikh A; GEMINI 1 Study Group. Vedolizumab as induction and maintenance therapy for ulcerative colitis. N Engl J Med. 2013 Aug 22;369(8):699-710. doi: 10.1056/NEJMoa1215734. PMID: 23964932.

296. Colombel JF, Sands BE, Rutgeerts P, Sandborn W, Danese S, D'Haens G, Panaccione R, Loftus EV Jr, Sankoh S, Fox I, Parikh A, Milch C, Abhyankar B, Feagan BG. The safety of vedolizumab for ulcerative colitis and Crohn's disease. Gut. 2017 May;66(5):839-851. doi: 10.1136/gutjnl-2015-311079. Epub 2016 Feb 18. PMID: 26893500; PMCID: PMC5531223.

297. Scribano ML. Vedolizumab for inflammatory bowel disease: From randomized controlled trials to real-life evidence. World J Gastroenterol. 2018 Jun 21;24(23):2457-2467. doi: 10.3748/wjg.v24.i23.2457. PMID: 29930467; PMCID: PMC6010939.

298. Tran V, Shammas RM, Sauk JS, Padua D. Evaluating tofacitinib citrate in the treatment of moderate-to-severe active ulcerative

colitis: design, development and positioning of therapy. Clin Exp Gastroenterol. 2019 May 2;12:179-191. doi: 10.2147/CEG.S150908. PMID: 31118734; PMCID: PMC6507103.

299. Honap S, Pavlidis P, Ray S, Sharma E, Anderson S, Sanderson JD, Mawdsley J, Samaan MA, Irving PM. Tofacitinib in Acute Severe Ulcerative Colitis-A Real-World Tertiary Center Experience. Inflamm Bowel Dis. 2020 Oct 23;26(11):e147-e149. doi: 10.1093/ibd/izaa157. PMID: 32566937.

300. Khan KJ, Ullman TA, Ford AC, Abreu MT, Abadir A, Marshall JK, Talley NJ, Moayyedi P. Terapia antibiotica nella malattia infiammatoria intestinale: una revisione sistematica e una meta-analisi. Am J Gastroenterol. 2011 Apr;106(4):661-73. doi: 10.1038/ajg.2011.72. Epub 2011 15 marzo. Erratum in: Am J Gastroenterolo. Maggio 2011;106(5):1014. Abadir, A [corretto in Abadir, Amir]. PMID: 21407187.

301. Nguyen LH, Örtqvist AK, Cao Y, Simon TG, Roelstraete B, Song M, Joshi AD, Staller K, Chan AT, Khalili H, Olén O, Ludvigsson JF. Antibiotic use and the development of inflammatory bowel disease: a national case-control study in Sweden. Lancet Gastroenterol Hepatol. 2020 Nov;5(11):986-995. doi: 10.1016/S2468-1253(20)30267-3. Epub 2020 Aug 17. PMID: 32818437; PMCID: PMC8034612.

302. Mardini HE, Grigorian AY. Probiotic mix VSL#3 is effective adjunctive therapy for mild to moderately active ulcerative colitis: a meta-analysis. Inflamm Bowel Dis. 2014 Sep;20(9):1562-7. doi: 10.1097/MIB.0000000000000084. PMID: 24918321.

303. Zhang XF, Guan XX, Tang YJ, Sun JF, Wang XK, Wang WD, Fan JM. Clinical effects and gut microbiota changes of using probiotics, prebiotics or synbiotics in inflammatory bowel disease: a systematic review and meta-analysis. Eur J Nutr. 2021 Aug;60(5):2855-2875. doi: 10.1007/s00394-021-02503-5. Epub 2021 Feb 8. Erratum in: Eur J Nutr. 2021 Aug;60(5):2877. doi: 10.1007/s00394-021-02592-2. PMID: 33555375.

304. Ganji-Arjenaki M, Rafieian-Kopaei M. Probiotics are a good choice in remission of inflammatory bowel diseases: A meta analysis and systematic review. J Cell Physiol. 2018 Mar;233(3):2091-2103. doi: 10.1002/jcp.25911. Epub 2017 May 3. PMID: 28294322.

305. Aguilar-Toalá JE, Garcia-Varela R, Garcia HS, Mata-Haro V, González-Córdova AF, Vallejo-Cordoba B, et al. Postbiotics: An evolving term within the functional foods field. Trends Food Sci Technol. 2018;75:105–14. doi:10.1016/j.tifs.2018.03.009

306. Paramsothy S, Paramsothy R, Rubin DT, Kamm MA, Kaakoush NO, Mitchell HM, Castaño-Rodríguez N. Faecal Microbiota Transplantation for Inflammatory Bowel Disease: A Systematic Review and Meta-analysis. J Crohns Colitis. 2017 Oct 1;11(10):1180-1199. doi: 10.1093/ecco-jcc/jjx063. PMID: 28486648.

307. Samal B, Sun Y, Stearns G, Xie C, Suggs S, McNiece I. Cloning and characterization of the cDNA encoding a novel human pre-B-cell colony-enhancing factor. Mol Cell Biol. 1994 Feb;14(2):1431-7. doi: 10.1128/mcb.14.2.1431-1437.1994. PMID: 8289818; PMCID: PMC358498.

308. Fukuhara A, Matsuda M, Nishizawa M, Segawa K, Tanaka M, Kishimoto K, Matsuki Y, Murakami M, Ichisaka T, Murakami H, Watanabe E, Takagi T, Akiyoshi M, Ohtsubo T, Kihara S, Yamashita S, Makishima M, Funahashi T, Yamanaka S, Hiramatsu R, Matsuzawa Y, Shimomura I. Visfatin: a protein secreted by visceral fat that mimics the effects of insulin. Science. 2005 Jan 21;307(5708):426-30. doi: 10.1126/science.1097243. Epub 2004 Dec 16. Retraction in: Science. 2007 Oct 26;318(5850):565. doi: 10.1126/science.318.5850.565b. PMID: 15604363.

309. Wen F, Gui G, Wang X, Ye L, Qin A, Zhou C, Zha X. Drug discovery targeting nicotinamide phosphoribosyltransferase (NAMPT): Updated progress and perspectives. Bioorg Med Chem. 2024 Feb 1;99:117595. doi: 10.1016/j.bmc.2024.117595. Epub 2024 Jan 11. PMID: 38244254.

310. Sun Z, Lei H, Zhang Z. Pre-B cell colony enhancing factor (PBEF), a cytokine with multiple physiological functions. Cytokine Growth Factor Rev. 2013 Oct;24(5):433-42. doi: 10.1016/j.cytogfr.2013.05.006. Epub 2013 Jun 17. PMID: 23787158; PMCID: PMC3791181.

311. Kim MK, Lee JH, Kim H, Park SJ, Kim SH, Kang GB, Lee YS, Kim JB, Kim KK, Suh SW, Eom SH. (2006) Crystal structure of visfatin/pre-B cell colony-enhancing factor 1/nicotinamide phosphoribosyltransferase (PDB ID: 2G95) [Data set]. RCSB Protein Data Bank.

312. Wang T, Zhang X, Bheda P, Revollo JR, Imai S, Wolberger C. Structure of Nampt/PBEF/visfatin, a mammalian NAD+ biosynthetic enzyme. Nat Struct Mol Biol. 2006 Jul;13(7):661-2. doi: 10.1038/nsmb1114. Epub 2006 Jun 18. PMID: 16783373

313. Chen X, Zhao S, Song Y, Shi Y, Leak RK, Cao G. The Role of Nicotinamide Phosphoribosyltransferase in Cerebral Ischemia. Curr Top Med Chem. 2015;15(21):2211-21. doi: 10.2174/1568026615666150610142234. PMID: 26059356; PMCID: PMC5644507.

314. Liu J, Che X, You J, Zhang G, Zhao R, Fu J, Li H. Intracellular Nampt impairs esophageal squamous cell carcinoma neo-adjuvant chemotherapy response independent of eNampt. Am J Transl Res. 2021 Mar 15;13(3):1411-1421. PMID: 33841666; PMCID: PMC8014354.

315. Garten A, Schuster S, Penke M, Gorski T, de Giorgis T, Kiess W. Physiological and pathophysiological roles of NAMPT and NAD metabolism. Nat Rev Endocrinol. 2015 Sep;11(9):535-46. doi: 10.1038/nrendo.2015.117. Epub 2015 Jul 28. PMID: 26215259.

316. Travelli C, Colombo G, Mola S, Genazzani AA, Porta C. NAMPT: A pleiotropic modulator of monocytes and macrophages. Pharmacol Res. 2018 Sep;135:25-36. doi: 10.1016/j.phrs.2018.06.022. Epub 2018 Jul 18. PMID: 30031171.

317. Zhang, L. Q., Van Haandel, L., Xiong, M., Huang, P., Heruth, D. P., Bi, C., Gaedigk, R., Jiang, X., Li, D.-Y., Wyckoff, G., Grigoryev, D. N., Gao, L., Li, L., Wu, M., Leeder, J. S., & Ye, S. Q. (2017). Metabolic and molecular insights into an essential role of nicotinamide phosphoribosyltransferase. Cell Death & Disease, 8(3), e2705.

318. Siyuan Tang, Miguel Garzon Sanz, Oliver Smith, Andreas Krämer, Daniel Egbase, Paul W. Caton, Stefan Knapp, Sam Butterworth, Chemistry-led investigations into the mode of action of NAMPT activators, resulting in the discovery of non-pyridyl class NAMPT activators, Acta Pharmaceutica Sinica B, Volume 13, Issue 2, 2023, Pages 709-721, ISSN 2211-3835, https://doi.org/10.1016/j.apsb.2022.07.016.

319. Peng A, Li J, Xing J, Yao Y, Niu X, Zhang K. The function of nicotinamide phosphoribosyl transferase (NAMPT) and its role in diseases. Front Mol Biosci. 2024 Oct 24;11:1480617. doi: 10.3389/fmolb.2024.1480617. PMID: 39513038; PMCID: PMC11540786.

320. Bogan KL, Brenner C. Nicotinic acid, nicotinamide, and nicotinamide riboside: a molecular evaluation of NAD+ precursor vitamins in human nutrition. Annu Rev Nutr. 2008;28:115-30. doi: 10.1146/annurev.nutr.28.061807.155443. PMID: 18429699.

321. Zhang, M., & Ying, W. (2019). NAD+ Deficiency Is a Common Central Pathological Factor of a Number of Diseases and Aging: Mechanisms and Therapeutic Implications. Antioxidants & Redox Signaling, 30(6), 890–905.

322. Khaidizar, F. D., Bessho, Y., & Nakahata, Y. (2021). Nicotinamide Phosphoribosyltransferase as a Key Molecule of the Aging/Senescence Process. International Journal of Molecular Sciences, 22(7), 3709.

323. Semerena E, Nencioni A, Masternak K. Extracellular nicotinamide phosphoribosyltransferase: role in disease pathophysiology and as a biomarker. Front Immunol. 2023 Oct 17;14:1268756. doi: 10.3389/fimmu.2023.1268756. PMID: 37915565; PMCID: PMC10616597.

324. Cheng Q, Dong W, Qian L, Wu J, Peng Y. Visfatin inhibits apoptosis of pancreatic β-cell line, MIN6, via the mitogen-activated protein kinase/phosphoinositide 3-kinase pathway. J Mol Endocrinol. 2011 Jul 4;47(1):13-21. doi: 10.1530/JME-10-0106. PMID: 21471274.

325. Revollo JR, Körner A, Mills KF, Satoh A, Wang T, Garten A, Dasgupta B, Sasaki Y, Wolberger C, Townsend RR, Milbrandt J, Kiess W, Imai S. Nampt/PBEF/Visfatin regulates insulin secretion in beta cells as a systemic NAD biosynthetic enzyme. Cell Metab. 2007 Nov;6(5):363-75. doi: 10.1016/j.cmet.2007.09.003. PMID: 17983582; PMCID: PMC2098698.

326. Xiao J, Xiao ZJ, Liu ZG, Gong HY, Yuan Q, Wang S, Li YJ, Jiang DJ. Involvement of dimethylarginine dimethylaminohydrolase-2 in visfatin-enhanced angiogenic function of endothelial cells. Diabetes Metab Res Rev. 2009 Mar;25(3):242-9. doi: 10.1002/dmrr.939. PMID: 19229883.

327. Kim SR, Bae SK, Choi KS, Park SY, Jun HO, Lee JY, Jang HO, Yun I, Yoon KH, Kim YJ, Yoo MA, Kim KW, Bae MK. Visfatin promotes angiogenesis by activation of extracellular signal-regulated kinase 1/2. Biochem Biophys Res Commun. 2007 May 25;357(1):150-6. doi: 10.1016/j.bbrc.2007.03.105. Epub 2007 Mar 28. PMID: 17408594.

328. Adya R, Tan BK, Punn A, Chen J, Randeva HS. Visfatin induces human endothelial VEGF and MMP-2/9 production via MAPK and PI3K/Akt signalling pathways: novel insights into visfatin-induced angiogenesis. Cardiovasc Res. 2008 May 1;78(2):356-65. doi: 10.1093/cvr/cvm111. Epub 2007 Dec 18. PMID: 18093986.

329. Adya R, Tan BK, Chen J, Randeva HS. Pre-B cell colony enhancing factor (PBEF)/visfatin induces secretion of MCP-1 in human endothelial cells: role in visfatin-induced angiogenesis. Atherosclerosis. 2009 Jul;205(1):113-9. doi: 10.1016/j.atherosclerosis.2008.11.024. Epub 2008 Dec 3. PMID: 19166999.

330. Fan Y, Meng S, Wang Y, Cao J, Wang C. Visfatin/PBEF/Nampt induces EMMPRIN and MMP-9 production in macrophages via the NAMPT-MAPK (p38, ERK1/2)-NF-κB signaling pathway. Int J Mol Med. 2011 Apr;27(4):607-15. doi: 10.3892/ijmm.2011.621. Epub 2011 Feb 15. PMID: 21327328.

331. Colombo G, Travelli C, Porta C, Genazzani AA. Extracellular nicotinamide phosphoribosyltransferase boosts IFNγ-induced macrophage polarization independently of TLR4. iScience. 2022 Mar 23;25(4):104147. doi: 10.1016/j.isci.2022.104147. PMID: 35402885; PMCID: PMC8990213.

332. Moschen AR, Kaser A, Enrich B, Mosheimer B, Theurl M, Niederegger H, Tilg H. Visfatin, an adipocytokine with proinflammatory and immunomodulating properties. J Immunol. 2007 Feb 1;178(3):1748-58. doi: 10.4049/jimmunol.178.3.1748. PMID: 17237424.

333. Li Y, Zhang Y, Dorweiler B, Cui D, Wang T, Woo CW, Brunkan CS, Wolberger C, Imai S, Tabas I. Extracellular Nampt promotes macrophage survival via a nonenzymatic interleukin-6/STAT3 signaling mechanism. J Biol Chem. 2008 Dec 12;283(50):34833-43. doi: 10.1074/jbc.M805866200. Epub 2008 Oct 21. PMID: 18945671; PMCID: PMC2596403.

334. Kim SR, Bae YH, Bae SK, Choi KS, Yoon KH, Koo TH, Jang HO, Yun I, Kim KW, Kwon YG, Yoo MA, Bae MK. Visfatin enhances ICAM-1 and VCAM-1 expression through ROS-dependent NF-kappaB activation in endothelial cells. Biochim Biophys Acta. 2008 May;1783(5):886-95. doi: 10.1016/j.bbamcr.2008.01.004. Epub 2008 Jan 16. PMID: 18241674.

335. Romacho T, Valencia I, Ramos-González M, Vallejo S, López-Esteban M, Lorenzo O, Cannata P, Romero A, San Hipólito-Luengo A, Gómez-Cerezo JF, Peiró C, Sánchez-Ferrer CF. Visfatin/eNampt induces endothelial dysfunction in vivo: a role for Toll-Like Receptor 4 and NLRP3 inflammasome. Sci Rep. 2020 Mar 25;10(1):5386. doi: 10.1038/s41598-020-62190-w. PMID: 32214150; PMCID: PMC7096459.

336. Grolla AA, Torretta S, Gnemmi I, Amoruso A, Orsomando G, Gatti M, Caldarelli A, Lim D, Penengo L, Brunelleschi S, Genazzani AA, Travelli C. Nicotinamide phosphoribosyltransferase (NAMPT/PBEF/visfatin) is a tumoural cytokine released from melanoma. Pigment Cell Melanoma Res. 2015 Nov;28(6):718-29. doi: 10.1111/pcmr.12420. PMID: 26358657.

337. Rongvaux A, Shea RJ, Mulks MH, Gigot D, Urbain J, Leo O, Andris F. Pre-B-cell colony-enhancing factor, whose expression is up-regulated in activated lymphocytes, is a nicotinamide phosphoribosyltransferase, a cytosolic enzyme involved in NAD biosynthesis. Eur J Immunol. 2002 Nov;32(11):3225-34. doi: 10.1002/1521-4141(200211)32:11<3225::AID-IMMU3225>3.0.CO;2-L. PMID: 12555668.

338. Tanaka M, Nozaki M, Fukuhara A, Segawa K, Aoki N, Matsuda M, Komuro R, Shimomura I. Visfatin is released from 3T3-L1 adipocytes via a non-classical pathway. Biochem Biophys Res Commun. 2007 Jul 27;359(2):194-201. doi: 10.1016/j.bbrc.2007.05.096. Epub 2007 May 25. PMID: 17543285.

339. Jing Z, Xing J, Chen X, Stetler RA, Weng Z, Gan Y, Zhang F, Gao Y, Chen J, Leak RK, Cao G. Neuronal NAMPT is released after cerebral ischemia and protects against white matter injury. J Cereb Blood Flow Metab. 2014 Oct;34(10):1613-21. doi: 10.1038/jcbfm.2014.119. Epub 2014 Jul 9. PMID: 25005877; PMCID: PMC4269719.

340. Zhao Y, Liu XZ, Tian WW, Guan YF, Wang P, Miao CY. Extracellular visfatin has nicotinamide phosphoribosyltransferase enzymatic activity and is neuroprotective against ischemic injury. CNS Neurosci Ther. 2014 Jun;20(6):539-47. doi: 10.1111/cns.12273. Epub 2014 Apr 21. PMID: 24750959; PMCID: PMC6493111.

341. Pillai VB, Sundaresan NR, Kim G, Samant S, Moreno-Vinasco L, Garcia JG, Gupta MP. Nampt secreted from cardiomyocytes promotes development of cardiac hypertrophy and adverse ventricular remodeling. Am J Physiol Heart Circ Physiol. 2013 Feb 1;304(3):H415-26. doi: 10.1152/ajpheart.00468.2012. Epub 2012 Nov 30. PMID: 23203961; PMCID: PMC3774498.

342. Lin YC, Wu HC, Liao CC, Chou YC, Pan SF, Chiu CM. Secretion of one adipokine Nampt/Visfatin suppresses the inflammatory stress-induced NF-κB activity and affects Nampt-dependent cell viability in Huh-7 cells. Mediators Inflamm. 2015;2015:392471. doi: 10.1155/2015/392471. Epub 2015 Feb 26. PMID: 25814788; PMCID: PMC4357042.

343. Ognjanovic S, Bao S, Yamamoto SY, Garibay-Tupas J, Samal B, Bryant-Greenwood GD. Genomic organization of the gene coding for human pre-B-cell colony enhancing factor and expression in human fetal membranes. J Mol Endocrinol. 2001 Apr;26(2):107-17. doi: 10.1677/jme.0.0260107. PMID: 11241162.

344. Yoon MJ, Yoshida M, Johnson S, Takikawa A, Usui I, Tobe K, Nakagawa T, Yoshino J, Imai S. SIRT1-Mediated eNAMPT Secretion from Adipose Tissue Regulates Hypothalamic NAD+ and Function in Mice. Cell Metab. 2015 May 5;21(5):706-17. doi: 10.1016/j.cmet.2015.04.002. Epub 2015 Apr 23. PMID: 25921090; PMCID: PMC4426056.

345. Martínez-Morcillo, F. J., Cantón-Sandoval, J., Martínez-Menchón, T., Corbalán-Vélez, R., Mesa-del-Castillo, P., Pérez-Oliva, A. B., García-Moreno, D.,& Mulero, V. (2021). Non-canonical roles of NAMPT and PARP in inflammation. Developmental & Comparative Immunology, 115, 103881.

346. Carbone, F., Liberale, L., Bonaventura, A., Vecchiè, A., Casula, M., Cea, M., Monacelli, F., Caffa, I., Bruzzone, S., Montecucco, F., & Nencioni, A. (2017). Regulation and Function of Extracellular Nicotinamide Phosphoribosyltransferase/Visfatin. Comprehensive Physiology, 7(2), 603–621.

347. Dalamaga, M., Christodoulatos, G. S., & Mantzoros, C. S. (2018). The role of extracellular and intracellular Nicotinamide phosphoribosyl-transferase in cancer: Diagnostic and therapeutic perspectives and challenges. Metabolism, 82, 72–87.

348. Burgos, E. S. (2011). NAMPT in regulated NAD biosynthesis and its pivotal role in human metabolism. Current Medicinal Chemistry, 18(13), 1947–1961.

349. Burgos, E. S., Ho, M.-C., Almo, S. C., & Schramm, V. L. (2009). A phosphoenzyme mimic, overlapping catalytic sites and reaction coordinate motion for human NAMPT. Proceedings of the National Academy of Sciences, 106(33), 13748–13753.

350. Hara N, Yamada K, Shibata T, Osago H, Tsuchiya M. Nicotinamide phosphoribosyltransferase/visfatin does not catalyze nicotinamide mononucleotide formation in blood plasma. PLoS One. 2011;6(8):e22781. doi: 10.1371/journal.pone.0022781. Epub 2011 Aug 3. PMID: 21826208; PMCID: PMC3149623.

351. Torretta S, Colombo G, Travelli C, Boumya S, Lim D, Genazzani AA, Grolla AA. The Cytokine Nicotinamide Phosphoribosyltransferase (eNAMPT; PBEF; Visfatin) Acts as a Natural Antagonist of C-C Chemokine Receptor Type 5 (CCR5). Cells. 2020 Feb 21;9(2):496. doi: 10.3390/cells9020496. PMID: 32098202; PMCID: PMC7072806.

352. Camp SM, Ceco E, Evenoski CL, Danilov SM, Zhou T, Chiang ET, Moreno-Vinasco L, Mapes B, Zhao J, Gursoy G, Brown ME, Adyshev DM, Siddiqui SS, Quijada H, Sammani S, Letsiou E, Saadat L, Yousef M, Wang T, Liang J, Garcia JG. Unique Toll-Like Receptor 4 Activation by NAMPT/PBEF Induces NFκB Signaling and Inflammatory Lung Injury. Sci Rep. 2015 Aug 14;5:13135. doi:

10.1038/srep13135. PMID: 26272519; PMCID: PMC4536637.

353. Philp AM, Butterworth S, Davis ET, Jones SW. eNAMPT Is Localised to Areas of Cartilage Damage in Patients with Hip Osteoarthritis and Promotes Cartilage Catabolism and Inflammation. Int J Mol Sci. 2021 Jun 23;22(13):6719. doi: 10.3390/ijms22136719. PMID: 34201564; PMCID: PMC8269388.

354. Garcia AN, Casanova NG, Kempf CL, Bermudez T, Valera DG, Song JH, Sun X, Cai H, Moreno-Vinasco L, Gregory T, Oita RC, Hernon VR, Camp SM, Rogers C, Kyubwa EM, Menon N, Axtelle J, Rappaport J, Bime C, Sammani S, Cress AE, Garcia JGN. eNAMPT Is a Novel Damage-associated Molecular Pattern Protein That Contributes to the Severity of Radiation-induced Lung Fibrosis. Am J Respir Cell Mol Biol. 2022 May;66(5):497-509. doi: 10.1165/rcmb.2021-0357OC. PMID: 35167418; PMCID: PMC9116358.

355. Colombo G, Clemente N, Zito A, Bracci C, Colombo FS, Sangaletti S, Jachetti E, Ribaldone DG, Caviglia GP, Pastorelli L, De Andrea M, Naviglio S, Lucafò M, Stocco G, Grolla AA, Campolo M, Casili G, Cuzzocrea S, Esposito E, Malavasi F, Genazzani AA, Porta C, Travelli C. Neutralization of extracellular NAMPT (nicotinamide phosphoribosyltransferase) ameliorates experimental murine colitis. J Mol Med (Berl). 2020 Apr;98(4):595-612. doi: 10.1007/s00109-020-01892-0. Epub 2020 Apr 27. PMID: 32338310.

356. Neubauer K, Bednarz-Misa I, Walecka-Zacharska E, Wierzbicki J, Agrawal A, Gamian A, Krzystek-Korpacka M. Oversecretion and Overexpression of Nicotinamide Phosphoribosyltransferase/Pre-B Colony-Enhancing Factor/Visfatin in Inflammatory Bowel Disease Reflects the Disease Activity, Severity of Inflammatory Response and Hypoxia. Int J Mol Sci. 2019 Jan 4;20(1):166. doi: 10.3390/ijms20010166. PMID: 30621173; PMCID: PMC6337260.

357. Saadoun MM, Nosair NAE, Abdel-Azeez HA, Sharaf SM, Ahmed MH. Serum Visfatin as a Diagnostic Marker of Active Inflammatory Bowel Disease. J Gastrointestin Liver Dis. 2021 Sep 21;30(3):339-345. doi: 10.15403/jgld-3504. PMID: 34551033.

358. Colombo G, Caviglia GP, Ravera A, Tribocco E, Frara S, Rosso C, Travelli C, Genazzani AA, Ribaldone DG. NAMPT and NAPRT serum levels predict response to anti-TNF therapy in inflammatory bowel disease. Front Med (Lausanne). 2023 Feb 1;10:1116862. doi: 10.3389/fmed.2023.1116862. PMID: 36817780; PMCID: PMC9928959.

359. Galli U, Colombo G, Travelli C, Tron GC, Genazzani AA, Grolla AA. Recent Advances in NAMPT Inhibitors: A Novel Immunotherapic Strategy. Front Pharmacol. 2020 May 12;11:656. doi: 10.3389/fphar.2020.00656. PMID: 32477131; PMCID: PMC7235340.

360. Hasmann M, Schemainda I. FK866, a highly specific noncompetitive inhibitor of nicotinamide phosphoribosyltransferase, represents a novel mechanism for induction of tumor cell apoptosis. Cancer Res. 2003 Nov 1;63(21):7436-42. PMID: 14612543.

361. Olesen UH, Thougaard AV, Jensen PB, Sehested M. A preclinical study on the rescue of normal tissue by nicotinic acid in high-dose treatment with APO866, a specific nicotinamide phosphoribosyltransferase inhibitor. Mol Cancer Ther. 2010 Jun;9(6):1609-17. doi: 10.1158/1535-7163.MCT-09-1130. Epub 2010 Jun 1. PMID: 20515945.

362. Tarrant JM, Dhawan P, Singh J, Zabka TS, Clarke E, DosSantos G, Dragovich PS, Sampath D, Lin T, McCray B, La N, Nguyen T, Kauss A, Dambach D, Misner DL, Diaz D, Uppal H. Preclinical models of nicotinamide phosphoribosyltransferase inhibitor-mediated hematotoxicity and mitigation by co-treatment with nicotinic acid. Toxicol Mech Methods. 2015 Mar;25(3):201-11. doi: 10.3109/15376516.2015.1014080. Epub 2015 Apr 20. PMID: 25894564.

363. Misner DL, Kauss MA, Singh J, Uppal H, Bruening-Wright A, Liederer BM, Lin T, McCray B, La N, Nguyen T, Sampath D, Dragovich PS, O'Brien T, Zabka TS. Cardiotoxicity Associated with Nicotinamide Phosphoribosyltransferase Inhibitors in Rodents and in Rat and Human-Derived Cells Lines. Cardiovasc Toxicol. 2017 Jul;17(3):307-318. doi: 10.1007/s12012-016-9387-6. PMID: 27783203.

364. Cassar S, Dunn C, Olson A, Buck W, Fossey S, Ramos MF, Sancheti P, Stolarik D, Britton H, Cole T, Bratcher N, Huang X, Peterson R, Longenecker K, LeRoy B. From the Cover: Inhibitors of Nicotinamide Phosphoribosyltransferase Cause Retinal Damage in Larval Zebrafish. Toxicol Sci. 2018 Feb 1;161(2):300-309. doi: 10.1093/toxsci/kfx212. PMID: 29378070.

365. Olesen UH, Christensen MK, Björkling F, Jäättelä M, Jensen PB, Sehested M, Nielsen SJ. Anticancer agent CHS-828 inhibits cellular synthesis of NAD. Biochem Biophys Res Commun. 2008 Mar 21;367(4):799-804. doi: 10.1016/j.bbrc.2008.01.019. Epub 2008 Jan 15. PMID: 18201551.

366. von Heideman A, Berglund A, Larsson R, Nygren P. Safety and efficacy of NAD depleting cancer drugs: results of a phase I clinical trial of CHS 828 and overview of published data. Cancer Chemother Pharmacol. 2010 May;65(6):1165-72. doi: 10.1007/s00280-009-1125-3. Epub 2009 Sep 30. PMID: 19789873.

367. Ravaud A, Cerny T, Terret C, Wanders J, Bui BN, Hess D, Droz JP, Fumoleau P, Twelves C. Phase I study and pharmacokinetic of CHS-828, a guanidino-containing compound, administered orally as a single dose every 3 weeks in solid tumours: an ECSG/EORTC study. Eur J Cancer. 2005 Mar;41(5):702-7. doi: 10.1016/j.ejca.2004.12.023. PMID: 15763645.

368. Zak M, Liederer BM, Sampath D, Yuen PW, Bair KW, Baumeister T, Buckmelter AJ, Clodfelter KH, Cheng E, Crocker L, Fu B, Han B, Li G, Ho YC, Lin J, Liu X, Ly J, O'Brien T, Reynolds DJ, Skelton N, Smith CC, Tay S, Wang W, Wang Z, Xiao Y, Zhang L, Zhao G, Zheng X, Dragovich PS. Identification of nicotinamide phosphoribosyltransferase (NAMPT) inhibitors with no evidence of CYP3A4 time-dependent inhibition and improved aqueous solubility. Bioorg Med Chem Lett. 2015 Feb 1;25(3):529-41. doi: 10.1016/j.bmcl.2014.12.026. Epub 2014 Dec 17. PMID: 25556090.

369. Korotchkina L, Kazyulkin D, Komarov PG, Polinsky A, Andrianova EL, Joshi S, Gupta M, Vujcic S, Kononov E, Toshkov I, Tian Y, Krasnov P, Chernov MV, Veith J, Antoch MP, Middlemiss S, Somers K, Lock RB, Norris MD, Henderson MJ, Haber M, Chernova OB, Gudkov AV. OT-82, a novel anticancer drug candidate that targets the strong dependence of hematological malignancies on NAD biosynthesis. Leukemia. 2020 Jul;34(7):1828-1839. doi: 10.1038/s41375-019-0692-5. Epub 2020 Jan 2. PMID: 31896781; PMCID: PMC7326709.

370. Conforti I, Benzi A, Caffa I, Bruzzone S, Nencioni A, Marra A. Iminosugar-Based Nicotinamide Phosphoribosyltransferase (NAMPT) Inhibitors as Potential Anti-Pancreatic Cancer Agents. Pharmaceutics. 2023 May 11;15(5):1472. doi: 10.3390/pharmaceutics15051472. PMID: 37242714; PMCID: PMC10222582.

371. Travelli C, Aprile S, Rahimian R, Grolla AA, Rogati F, Bertolotti M, Malagnino F, di Paola R, Impellizzeri D, Fusco R, Mercalli V, Massarotti A, Stortini G, Terrazzino S, Del Grosso E, Fakhfouri G, Troiani MP, Alisi MA, Grosa G, Sorba G, Canonico PL, Orsomando G, Cuzzocrea S, Genazzani AA, Galli U, Tron GC. Identification of Novel Triazole-Based Nicotinamide Phosphoribosyltransferase (NAMPT) Inhibitors Endowed with Antiproliferative and Antiinflammatory Activity. J Med Chem. 2017 Mar 9;60(5):1768-1792. doi: 10.1021/acs.jmedchem.6b01392. Epub 2017 Feb 22. PMID: 28165742.

372. Travelli C, Aprile S, Mattoteia D, Colombo G, Clemente N, Scanziani E, Terrazzino S, Alisi MA, Polenzani L, Grosa G, Genazzani AA, Tron GC, Galli U. Identification of potent triazolylpyridine nicotinamide phosphoribosyltransferase (NAMPT) inhibitors bearing a 1,2,3-triazole tail group. Eur J Med Chem. 2019 Nov 1;181:111576. doi: 10.1016/j.ejmech.2019.111576. Epub 2019 Aug 1. PMID: 31400709.

373. Grolla AA, Travelli C, Genazzani AA, Sethi JK. Extracellular nicotinamide phosphoribosyltransferase, a new cancer metabokine. Br J Pharmacol. 2016 Jul;173(14):2182-94. doi: 10.1111/bph.13505. Epub 2016 Jun 2. PMID: 27128025; PMCID: PMC4919578.

374. Chiarugi A, Dölle C, Felici R, Ziegler M. The NAD metabolome--a key determinant of cancer cell biology. Nat Rev Cancer. 2012 Nov;12(11):741-52. doi: 10.1038/nrc3340. Epub 2012 Sep 28. PMID: 23018234.

375. Zabka TS, Singh J, Dhawan P, Liederer BM, Oeh J, Kauss MA, Xiao Y, Zak M, Lin T, McCray B, La N, Nguyen T, Beyer J, Farman C, Uppal H, Dragovich PS, O'Brien T, Sampath D, Misner DL. Retinal toxicity, in vivo and in vitro, associated with inhibition of nicotinamide phosphoribosyltransferase. Toxicol Sci. 2015 Mar;144(1):163-72. doi: 10.1093/toxsci/kfu268. Epub 2014 Dec 11. PMID: 25505128.

376. Békés M, Langley DR, Crews CM. PROTAC targeted protein degraders: the past is prologue. Nat Rev Drug Discov. 2022 Mar;21(3):181-200. doi: 10.1038/s41573-021-00371-6. Epub 2022 Jan 18. PMID: 35042991; PMCID: PMC8765495.

377. Zhu X, Liu H, Chen L, Wu C, Liu X, Cang Y, Jiang B, Yang X, Fan G. Addressing the Enzyme-independent tumor-promoting function of NAMPT via PROTAC-mediated degradation. Cell Chem Biol. 2022 Nov 17;29(11):1616-1629.e12. doi: 10.1016/j.chembiol.2022.10.007. Epub 2022 Nov 1. PMID: 36323324.

378. Wu Y, Pu C, Fu Y, Dong G, Huang M, Sheng C. NAMPT-targeting PROTAC promotes antitumor immunity via suppressing myeloid-derived suppressor cell expansion. Acta Pharm Sin B. 2022 Jun;12(6):2859-2868. doi: 10.1016/j.apsb.2021.12.017. Epub 2021 Dec 31. PMID: 35755293; PMCID: PMC9214341.

379. Sun BL, Tang L, Sun X, Garcia AN, Camp SM, Posadas E, Cress AE, Garcia JGN. A Humanized Monoclonal Antibody Targeting Extracellular Nicotinamide Phosphoribosyltransferase Prevents Aggressive Prostate Cancer Progression. Pharmaceuticals (Basel). 2021 Dec 17;14(12):1322. doi: 10.3390/ph14121322. PMID: 34959723; PMCID: PMC8706080.

380. Quijada H, Bermudez T, Kempf CL, Valera DG, Garcia AN, Camp SM, Song JH, Franco E, Burt JK, Sun B, Mascarenhas JB, Burns K, Gaber A, Oita RC, Reyes Hernon V, Barber C, Moreno-Vinasco L, Sun X, Cress AE, Martin D, Liu Z, Desai AA, Natarajan V, Jacobson JR, Dudek SM, Bime C, Sammani S, Garcia JGN. Endothelial eNAMPT amplifies pre-clinical acute lung injury: efficacy of an eNAMPT-neutralising monoclonal antibody. Eur Respir J. 2021 May 6;57(5):2002536. doi: 10.1183/13993003.02536-2020. PMID: 33243842; PMCID: PMC8100338.

381. Sammani S, Bermudez T, Kempf CL, Song JH, Fleming JC, Reyes Hernon V, Hufford M, Tang L, Cai H, Camp SM, Natarajan V, Jacobson JR, Dudek SM, Martin DR, Karmonik C, Sun X, Sun B, Casanova NG, Bime C, Garcia JGN. eNAMPT Neutralization Preserves Lung Fluid Balance and Reduces Acute Renal Injury in Porcine Sepsis/VILI-Induced Inflammatory Lung Injury. Front Physiol. 2022 Jun 22;13:916159. doi: 10.3389/fphys.2022.916159. PMID: 35812318; PMCID: PMC9257134.

382. Ahmed M, Zaghloul N, Zimmerman P, Casanova NG, Sun X, Song JH, Hernon VR, Sammani S, Rischard F, Rafikova O, Rafikov R, Makino A, Kempf CL, Camp SM, Wang J, Desai AA, Lussier Y, Yuan JX, Garcia JGN. Endothelial eNAMPT drives EndMT and preclinical PH: rescue by an eNAMPT-neutralizing mAb. Pulm Circ. 2021 Nov 12;11(4):20458940211059712. doi: 10.1177/20458940211059712. PMID: 34790349; PMCID: PMC8591779.

383. Garcia AN, Casanova NG, Kempf CL, Bermudez T, Valera DG, Song JH, Sun X, Cai H, Moreno-Vinasco L, Gregory T, Oita RC, Hernon VR, Camp SM, Rogers C, Kyubwa EM, Menon N, Axtelle J, Rappaport J, Bime C, Sammani S, Cress AE, Garcia JGN. eNAMPT Is a Novel Damage-associated Molecular Pattern Protein That Contributes to the Severity of Radiation-induced Lung Fibrosis. Am J Respir Cell Mol Biol. 2022 May;66(5):497-509. doi: 10.1165/rcmb.2021-0357OC. PMID: 35167418; PMCID: PMC9116358.

384. Liu Z, Sammani S, Barber CJ, Kempf CL, Li F, Yang Z, Bermudez RT, Camp SM, Herndon VR, Furenlid LR, Martin DR, Garcia JGN. An eNAMPT-neutralizing mAb reduces post-infarct myocardial fibrosis and left ventricular dysfunction. Biomed Pharmacother. 2024 Jan;170:116103. doi: 10.1016/j.biopha.2023.116103. Epub 2023 Dec 30. PMID: 38160623; PMCID: PMC10872269.

385. Sun BL, Tang L, Sun X, Garcia AN, Camp SM, Posadas E, Cress AE, Garcia JGN. A Humanized Monoclonal Antibody Targeting Extracellular Nicotinamide Phosphoribosyltransferase Prevents Aggressive Prostate Cancer Progression. Pharmaceuticals (Basel). 2021 Dec 17;14(12):1322. doi: 10.3390/ph14121322. PMID: 34959723; PMCID: PMC8706080.

386. Miele S, Polasek T, Mantovani S, Camp SM, Garcia JGN. Safety, Tolerability and Pharmacokinetics of the eNAMPT-Neutralizing ALT-100 Mab in Healthy Volunteers. J Clin Res Clin Trials. 2024 Sep;3(3):https://bioresscientia.com/article/safety-tolerability-and-pharmacokinetics-of-the-enampt-neutralizing-alt-100-mab-in-healthy-volunteers. Epub 2024 Sep 18. PMID: 39950187; PMCID: PMC11823460.